Università degli studi dell'Aquila

Dipartimento di Scienze Cliniche Applicate e Biotecnologiche

Doctoral school in

EXPERIMENTAL MEDICINE

"Biotechnology and biochemical sciences"

XXXVII *cycle*

BIOS-09A

Doctoral Thesis

"The SOS response in bacteria and the LexA transcriptional repressor: withstanding infections by inhibiting bacterial adhesion and biofilm formation"

PhD Candidate

Dott.ssa Lisaurora Nazzicone

Coordinator

Prof.ssa Mariagrazia Perilli

Tutor

Prof. Giuseppe Celenza

Co-tutor

Dott. Pierangelo Bellio

Academic year 2023/2024

Summary

ABSTRACT 7
CHAPTER I 8
The Antimicrobial resistance 8
1.1 How antibiotics work 8
1.1.1 Inhibition of bacterial cell wall synthesis 9
1.1.2 Disruption of cell membrane function 10
1.1.3 Inhibition of protein synthesis 11
1.1.4 Inhibition of nucleic acid synthesis 13
1.1.5 Inhibition of metabolic pathways 14
1.2 Microbial resistance mechanisms 15
1.2.1 Enzyme production 16
1.2.2 Changes in target sites 17
1.2.3 Reduce permeability 17
1.2.4 Efflux pumps 18
1.3 Resistance Mechanisms in *E. coli* 20
1.4 Strategies to bypass antimicrobial resistance 22
CHAPTER II 25
The SOS response in bacteria and the LexA transcriptional repressor 25
2.1 The SOS response and its role in mutagenesis 25
2.2 The DNA damage sensor: the recombinase RecA 28
2.3 The LexA transcriptional repressor: an overall 31
2.4 Dimerization of LexA 33
2.5 The LexA binding box and the interaction with the DNA 34
2.6 LexA catalytic site 37
2.7 Interaction between RecA and LexA and RecA-stimulated LexA self-cleavage 40
CHAPTER III 45
Boron Compounds: natural distribution, chemical properties, and pharmaceutical potentialities 45
3.1 Natural distribution and physiological role of boron 45
3.1.1 Boron's role in plants 46
3.1.2 Boron in bacteria 47

3.1.3 Boron and human health 48
3.2 Chemistry of boron 51
3.3 Boronic acids as a serine-enzyme inhibitors 52
3.4 Boronic acid in medical applications 54
CHAPTER IV 57
Aim of the work 57
CHAPTER V 58
Materials and methods 58
5.1 Organisms 58
5.2 Antibiotic and boron compounds 58
5.3 Reagents 58
5.4 RecA and LexA cloning and purification 61
5.5 *In vitro* susceptibility test 61
5.6 Filamentation assay 62
5.7 Inhibition assay of LexA by alkaline-induced autohydrolysis 62
5.8 Co-protease activity and determination of half-maximal inhibitory concentrations 63
5.9 Biofilm assay 64
5.10 Biofilm assay: inhibition and eradication 64
5.11 Biofilm assay: SEM visualization 65
5.12 Molecular docking 65
5.13 Software and data analysis 65
CHAPTER VI 66
Results 66
6.1 Boron compounds selected by drug repurposing approach 66
6.1.1 Determination of the Minimum Inhibitory Concentrations (MICs) 66
6.1.2 Filamentation assay 67
6.1.3 Inhibition assay of LexA by alkaline-induced autohydrolysis 84
6.1.4 Co-protease activity and determination of half-maximal inhibitory concentration (IC_{50}) 85
6.1.5 Biofilm assay: inhibition and eradication 86
6.1.6 Biofilm inhibition assay: SEM visualization 91
6.1.7 Molecular docking 95
6.2 Benzoxaboroles 98

6.2.1 Co-protease activity and determination of half-maximal inhibitory concentration (IC_{50})..... 98
6.2.2 Determination of the Minimum Inhibitory Concentrations (MICs) 100
6.2.3 Filamentation assay..... 100
CHAPTER VII 119
Discussion..... 119
CHAPTER VIII 133
Conclusions..... 133
References:..... 134

ABSTRACT

The ever-increasing urgency of addressing the growing phenomenon of antimicrobial resistance is driving the scientific community to explore new strategies to combat what could soon represent the greatest threat to human health. The synthesis of new pharmacologically active molecules is not the most viable path due to the need for rapid intervention and the tendency of microorganisms to quickly develop resistance. Searching for alternative microbial targets distinct from those targeted by traditional antibiotics represents one of the most promising strategies, particularly in terms of not relying solely on antibiotic therapy. From this perspective, the SOS pathway is an excellent target since modulating this response essentially means modulating microbial pathogenicity mechanisms. Blocking the activation of the SOS response does not lead to microbial death; instead, it could enhance antibiotic therapy by preventing the activation of mechanisms to counteract the antibiotic's activity.

The RecA/LexA pathway modulates the SOS response, where both proteins represent excellent targets for blocking the SOS response. RecA is the sensor for DNA damage, which activates LexA, the transcriptional repressor responsible for repressing about 60 genes in the SOS regulon. Of the two, LexA is the least explored target but is, in fact, the most promising. LexA is a protein that undergoes self-cleavage, a reaction induced by RecA. This reaction is facilitated by the catalytic dyad Ser119/Lys156. If LexA were treated as a serine enzyme, it would be possible to use serine protease inhibitors to block LexA and disrupt the cascade of events it initiates. Among the most promising serine protease inhibitors are boronic acid-based compounds, particularly notable for their low toxicity, making them safe for pharmaceutical application.

As part of this research, we explored potential inhibitors of the LexA transcriptional repressor within a pool of boron-containing molecules by a drug-repurposing approach. This investigation confirmed the promising and versatile properties of boron-based compounds and demonstrated that these molecules can effectively interact with LexA, interfering with processes associated with its self-cleavage. In particular, we identified promising inhibitors belonging to the benzoxaborole category, which are already commercially available for treating various conditions.

CHAPTER I

The Antimicrobial resistance

Antimicrobial resistance (AMR) indeed poses one of the greatest threats to global health, comparable to cancer and cardiovascular disease, with alarming predictions that by 2050, AMR could become the leading cause of death globally, according to the O'Neill report (2016). The problem of bacterial resistance emerged soon after the introduction of antibiotics. However, the issue is not simply the use of antibiotics but rather their misuse and overuse, significantly contributing to the rise of resistant microorganisms. Antibiotics are often administered beyond the necessary scope, both in human medicine and animal husbandry. This includes their use in livestock and aquaculture not only for treating infections but also for promoting growth and preventing disease in unsanitary conditions. This excessive usage is problematic because it leads to prolonged bacteria exposure to antibiotics, allowing them to evolve resistance mechanisms. Human pathogens have shown significant resistance, with multidrug-resistant bacteria (MDR) becoming more prevalent.

1.1 How antibiotics work

Antimicrobial resistance occurs when microorganisms such as bacteria, viruses, fungi, and parasites survive and continue growing despite exposure to drugs intended to eliminate them. Infections caused by these resistant organisms are not only harder to treat but can also result in severe illness or death. Antimicrobials encompass a diverse range of substances, including antibiotics, antivirals, antifungals, and pesticides, all of which are critical tools in combating infectious diseases. These compounds kill or inhibit the growth of microorganisms such as bacteria, viruses, fungi, and parasites (Kresge N. *et al.*, 2004; Pieren M. *et al.*, 2012). An antibiotic is a natural substance, often produced by microorganisms such as bacteria or fungi, that can inhibit or completely block the growth of other microorganisms. The discovery of the first antibiotic dates to 1928, when Alexander Fleming observed that the mold *Penicillium notatum* could inhibit the growth of *Staphylococcus aureus*, leading to the development of penicillin, the first widely used antibiotic (Tan S.Y. and Tatsumura Y. 2015). Antibiotics have been crucial in reducing the spread of bacterial infections and mitigating the severe complications they can cause. Before their introduction, bacterial infections often led to high mortality rates. The ability of antibiotics to target and kill or suppress bacteria made them a key health resource, transforming medical treatments and saving countless lives. The activity of an antibiotic generally revolves around five key mechanisms:

- ***inhibition of bacterial cell wall synthesis;***
- ***disruption of cell membrane function;***
- ***inhibition of protein synthesis;***
- ***inhibition of nucleic acid synthesis;***
- ***inhibition of metabolic pathways.***

1.1.1 Inhibition of bacterial cell wall synthesis

The inhibitors of the bacterial cell wall interfere with the peptidoglycan synthesis. Biosynthesis of the cell wall is a complex process involving multiple proteins in three stages: cytoplasmic, membrane-associated, and exocytoplasmic (Garde S. *et al.*, 2021). Antibiotics targeting the cytoplasmic stage include **inhibitors** of enzymes such as D-Ala-D-Ala ligase and D-Ala racemase, like D-cycloserine (also known as Seromycin), which is produced by *Streptomyces* (Prosser G.A. et al, 2013). The D-Ala-D-Ala dipeptide is synthesized in the final steps of peptidoglycan formation, involving two key enzymes: first, alanine racemase, which converts L-alanine to D-alanine, and second, D-alanyl-D-alanine ligase (Ddl), which facilitates the formation of the D-Ala-D-Ala dipeptide (Barreteau H. *et al.*, 2008) Currently, the antibiotic **fosfomycin** is in use, and it works by inhibiting the MurA enzyme, which is responsible for the first step in bacterial cell wall synthesis (Kahan F.M. *et al.*,1974). Molecules that target the membrane-associated stage include uridylyl peptidase inhibitors, such as **tunicamycin**, **liposidomycins**, and **mureidomycin**. These molecules act as competitive inhibitors of MraY, a key membrane enzyme essential for bacterial cell wall biosynthesis. Unfortunately, none of these inhibitors are approved for clinical use (Brandish P.E. *et al.*, 1996). Another crucial target in the bacterial cell wall biosynthetic pathway is Lipid II, the fully formed peptidoglycan precursor. Four classes of antibiotics, including **mannopeptimycins**, **lantibiotics**, **defensins**, and **glycopeptides**, specifically target Lipid II to disrupt cell wall synthesis. The molecules interfering with the last stage are **β-lactam antibiotics**. β-lactam antibiotics work by inhibiting bacterial cell wall synthesis through binding to penicillin-binding proteins (PBPs) (Bush K. *et al.*, 2016), which play key roles in the cross-linking of peptidoglycan bot in Gram-positive and Gram-negative bacteria. These antibiotics include penicillins, cephalosporins, carbapenems, and monobactams, all characterized by a β-lactam ring structure (Bush K. *et al.*, 2016). Their effectiveness varies based on factors like PBP binding affinity, resistance to β-lactamases, and the ability to penetrate the outer membrane of Gram-negative bacteria. Monobactams differ structurally from other β-lactams as they lack a secondary ring attached to the lactam ring (Sarkar P. *et al.*, 2017).

1.1.2 Disruption of cell membrane function

The antibiotics that target the bacterial cell membrane compromise its integrity, disrupt its typical function, and ultimately lead to lysis and bacterial death. Several antibiotics, such as **polymyxins**, **daptomycin**, and **ionophores**, perform this function. Polymyxins are a large group of antibiotics comprising fifteen varieties of compounds discovered in 1947 and produced by *Paenibacillus* polymixa (Storm D.R., Rosenthal K.S., Swanson P.E. 1977; Ash C., Priest F.G., Collins M.D. 1994). Structurally, polymyxins are small lipopeptides characterized by a polycationic peptide ring that enables their solubility in aqueous environments and a short protruding peptide attached to a hydrophobic fatty acid tail, allowing the antibiotic to interact with the bacterial cell membrane, causing their disintegration (Newton B.A. 1956; Nation R.L. *et al*., 2014); however, this same feature is also linked to the nephrotoxicity observed in humans: the drug permeabilizes eukaryotic membranes, causing swelling and lysis (Falagas M.E. *et al*., 2006). Due to toxicity concerns, polymyxins were initially reserved for treating persistent infections in cystic fibrosis, ophthalmic conjunctivitis, and topical antibiotic ointments. However, their use has surged recently due to rising antibiotic resistance. Today, polymyxins are the last-line treatment for serious multidrug-resistant (MDR) Gram-negative infections, especially those caused by MDR *Pseudomonas aeruginosa*, *Acinetobacter baumannii*, and *Klebsiella pneumoniae* (Trimble M.J. *et al*., 2016). Daptomycin is a cyclic lipopeptide antibiotic derived from the fermentation of *Streptomyces roseosporus*. *It is used in severe Gram-positive infections and is* ineffective against Gram-negative bacteria. This antibiotic finds application in severe skin infections caused by methicillin-susceptibility and methicillin-resistant *Staphylococcus aureus, Streptococcus pyogenes, Streptococcus agalactiae, Streptococcus dysgalactiae,* and vancomycin-susceptible *Enterococcus faecalis* (Scott D. *et al*., 2016). Daptomycin's activity targets the cytoplasmic membrane in a calcium-dependent manner and permeabilizes them, causing a rapid membrane depolarization, resulting in loss of cell function and cell death. In addition, evidence suggests that daptomycin can bind lipid II of the bacterial cell wall, interfering with its biosynthesis (Patel S. *et al*., 2024). Ionophores are naturally occurring compounds produced by bacteria, mainly by spore-forming species, *Streptomyces* genus, and exhibit antibiotic properties. They are specifically active against Gram-positive bacteria by disrupting the function of the cell membrane. This disruption impairs the membrane's ability to maintain ion gradients, crucial for cellular function. Normally, the membrane acts as a barrier, requiring significant activation energy for ion transport. Ionophores reduce this energy barrier, allowing ions to cross freely, thus collapsing the ion gradient and compromising membrane integrity. They disrupt the ionic balance inside bacterial cells, often leading to cell death (Bakker E.P. 1979). An example is Salomycin. Salinomycin is a monocarboxylic polyether antibiotic produced by the fermentation of Streptomyces

albus and is active against mycobacteria and filamentous fungi; it is inactive against gram-negative bacteria. Salinomycin can reduce mortality and increase the weight in chickens infected with *Eimeria tenella* (Miyazaki Y. *et al.*, 1974). Salinomycin shows an affinity for alkali metals, particularly potassium ions and facilitates ion flux across the bacterial membrane; it would appear promising as an antineoplastic drug (Dewangan J. *et al.*, 2017). Another example is Valinomycin, a cyclic-depsipeptide specific for alkali metal ions, K^+ in particular. It is composed of both hydrophobic and hydrophilic regions, structures that facilitate the transport of ions across the lipophilic membranes of cells. This ion transport not only interferes with osmoregulatory processes but can also lead to cellular toxicity, potentially resulting in cell death. Due to these properties, valinomycin exhibits other properties besides antibacterial, such as antitumor, antifungal, and antibabesial effects (Wibowo J.T. *et al.,* 2021).

1.1.3 Inhibition of protein synthesis

Antibiotics that interfere with bacterial protein synthesis specifically target the bacterial ribosome by binding to either the 30S or 50S ribosomal subunits, disrupting critical steps in protein translation, such as initiation, elongation, and termination: this binding prevents any cellular events, interfering with bacterial survival. There are indeed several classes of antibiotics that block bacterial protein synthesis: **aminoglycosides** and **tetracyclines** that act binding the 30s subunit, **macrolides**, **oxazolidinones**, **chloramphenicol**, **lincosamides** and **streptogramins** that bind the 50s subunit. Aminoglycosides are natural, or semisynthetic, broad-spectrum antibiotics, first isolated by *Streptomyces griseud* and introduced in clinical practice in 1944; of this class, we can mention kanamycin, gentamicin, netilmicin, tobramycin, and amikacin. Aminoglycosides are active against Gram-positive and Gram-negative bacteria and are particularly potent against *Escherichia coli*, *Klebsiella pneumoniae*, *Enterobacter cloacae*, and other members of the *Enterobacteriaceae* family (Landman D. *et al.*, 2010). The antibiotics are also good activity against *Staphylococcus aureus*, methicillin-resistant and vancomycin-resistant, *Pseudomonas aeruginosa*, *Acinetobacter baumanii*, and many *Mycobacterium* spp. (Ristuccia A.M. *et al.*, 1985; Landman D. *et al.*, 2011; Ho Y.I. *et al.*, 1977). Aminoglycosides inhibit bacterial protein synthesis by binding to the A-site on the 16S rRNA of the 30S ribosomal subunit (Kotra L.P. *et al.*, 2000). This binding alters the ribosome's conformation, causing codon misreading and incorrect amino acid incorporation. The resulting faulty proteins disrupt cellular functions, particularly damaging the cell membrane and contributing to the antibiotic's bactericidal effect. This mechanism makes aminoglycosides highly effective against severe bacterial infections (Krause K.M. *et al.*, 2016).

Tetracyclines were discovered for the first time in 1940 and produced by *Streptomyces aerofacensis, S. rimosus* and *S. viridofacensis*, and more of these were produced by a semi-synthetic approach. Likewise, aminoglycosides and tetracyclines inhibit the protein synthesis by targeting the ribosomal 30S subunit, preventing the attachment of aminoacyl-tRNA to the acceptor A-site. Tetracyclines are versatile antibiotics active against a large range of Gram-positive and Gram-negative bacteria, but their efficacy is also found against *Chlamydia, Mycoplasma, Rickettsia*, and protozoa and also used for preventing *Plasmodium falciparum* malaria (Grossman T.H. *et al.,* 2016; Chopra I. and Roberts M 2001). Macrolides are a large group of natural or synthetic, hydrophobic compounds characterized by a macrocyclic lactone ring and variable chains. Macrolides block the protein synthesis by interaction with the subunit 50S of the bacterial ribosome: they bind the ribosomal RNA 23s and block the protein elongation. These molecules show different pharmaceutical properties, such as antibacterial, antiviral, antimycotic and antiparasitic, which makes them highly versatile in treating infections (Lenz K.D. *et al.,* 2021): they are used in the treatment of infection sustained by *Streptococcus pneumoniae, S. pyogenes, Staphylococcus aureus, Mycoplasma pneumoniae, Legionella pneumophila, Chalamidia pneumoniae*. Macrolides are synthetized by *Steptomyces*, like *S. venezuelae, S. eurocidicus, S. albus, S. erythreus, S. antibioticus, S. felleus* and others; an example is Erythromycin A, the first macrolide discovered and used in clinical practice, but its instability determined the necessity to obtained new macrolides by semi-synthetic, or synthetic reactions (Zhanel G.G. *et al.,* 2001; Gaynor M. & Mankin A.S. 2005). Oxazolidinones are a synthetic bacteriostatic antibiotic, synthesized in the 1980s and used in treating multi-drug-resistant bacteria, such as MRSA, penicillin-resistant streptococci, and vancomycin-resistant enterococci. They work by inhibiting protein synthesis, through binding to the P site of the 50S ribosomal subunit (Bozdogan B. *et al.,* 2004). The first FDA-approved oxazolidinose was Linezoned and used since 2000 for treating skin and soft tissue infections sustained by Gram-positive bacteria (Aksoy D.Y. and Unal S. 2008). We also mention Tedizolin and Radezolid, used, respectively, for skin infections and for strains resistant to Linezolid (Foti C. *et al.,* 2021) Chloramphenicol is a bacteriostatic agent that reversibly binds 50S subunit; it was isolated in 1949 from *Streptomyces venezuelae* and is a broad-spectrum antibiotic, used in Gram-positive and gram-negative infections, but also used against *Rickettsiae*, spirochetes, several *Salmonella* species and pathogen responsible for respiratory infections (Purmina K. 2017). Lincosamides are natural compounds identified for the first time in 1962 from *Stremptomyces lincolnensis*, and used from 1967 for Gram-positive bacterial infections, not only in humans but also in veterinary medicine. Lincomycin was the first lincosamide antibiotic to be used, but its effectiveness was enhanced through specific modifications, leading to the development of clindamycin. Clindamycin

has a broad spectrum of activity, is effective against a range of bacteria from staphylococci to streptococci, as well as certain protozoa, and exhibits moderate activity against some Gram-negative bacilli (Schwarz S. *et al.,* 2016). Streptogramins were produced by *Streptomyces*, such as *S. pristinaespiralis, S. virginiae* and *S. mitakaensis,* and are active only against Gram-positive bacteria: they found application for treatment of infections sustained by Staphylococci. Lincosamides and streptogramins act causing the dissociation of peptidyl-tRNA by the ribosome (Tanel T. *et al.,* 2003).

1.1.4 Inhibition of nucleic acid synthesis

Bacterial nucleic acid synthesis inhibitors act either by inhibiting DNA replication or by interfering with its transcription, which results in the cell's inability to complete growth and cell division. These antibiotics can be divided into four groups based on their inhibiting mechanism: **quinolones** and their derivatives **fluoroquinolones**, **rifamycins** and **metronidazole**. Quinolones are antibiotics that bind two different bacterial targets: DNA gyrase, an enzyme that controls the topological transition of DNA during its replication, which reduces supercoiling tension, and Topoisomerase IV, which only resolves DNA interlinking to enable chromosome segregation. Quinolone compounds with medicinal properties, including antiallergenic, anticancer, and antimicrobial effects, have been identified in animals, plants, and microorganisms. These natural compounds have inspired the development of synthetic drugs, notably fluoroquinolone antibiotics. For instance, *Pseudomonas aeruginosa* produces 2-alkyl-4(1H)-quinolones, some of which possess antimicrobial properties (Heeb S. *et al.,* 2011). **Nalidixic acid** was the first quinolone used in clinical practice for infection sustained by Gram-negative bacteria, especially for treating urinary tract infection sustained by *E. coli*, with low activity towards Gram-positive. In 1978 was introduced fluoroquinolone **norfloxacin**, with activity also against Gram-positive bacteria, but the real breakthrough in the treatment of Gram-positive infections came with the introduction of ciprofloxacin and levofloxacin (Millanao A.R. *et al.,* 2021). **Rifamycins** are a group of antibiotics produced by *Streptomyces mediterranei* discovered in 1957, whose antimicrobial activity is linked to its ability to inhibit bacterial RNA polymerase through binding its β-subunit (Campell E.A. *et al.,* 2001); at the same time, they don’t interact with mammalian RNA polymerase (Wehrli W. *et al.,* 1983). A variety of biologically active molecules belong to this group, categorized as A, B, C, D, E and also, there are several rifamycin analogous, such as rifampicin, rifabutin, rifapentine and rifamixin used in clinical practice. Rifamycins possess broad-spectrum antimicrobial activity against Gram-positive and Gram-negative bacteria and are used to treat various infections. Notably, they are essential in the treatment of pulmonary tuberculosis (Munsiff S.S. *et al.,* 2006) and

are also effective against severe staphylococcal infections, particularly those complicated by biofilm formation (Zimmerli W. *et al.,* 2019; Adams R.A. *et al.,* 2021). **Metronidazole** is an antibiotic belonging to the nitroimidazoles class, a large group of organic compounds consisting of an imidazole ring with different substituents bonded on the same nitrogen atom; metronidazole was initially identified as a drug useful in the treatment of infections sustained by protozoa, such as *Trichomonas vaginalis*, *Entamoeba histolytica*, and *Giardia lamblia*. This drug is also effective against Gram-negative anaerobes belonging to the *Bacteroides* and *Fusobacterium* spp. and Gram-positive anaerobic bacteria. Metronidazole is also used in combination with other antibiotics, e.g. with amoxicillin for the treatment of *Helicobacter pylori* and with vancomycin for the treatment of *Clostridium difficile (*Mégraud F. *et al.,* 2008*;* Freeman C.D. *et al.,* 1997). Metronidazole and other related compounds such as tinidazole and nimorazole, enter microbial cells and here they are reduced to obtain the active form of the drug; the reduction process converts nitroimidazoles into highly reactive nitrogen-based free radicals, which interact with intracellular components, mainly targeting DNA causing strand breaks, inhibiting DNA synthesis, and preventing repair processes, but also RNA and protein This results in lethal damage to the microbial cells, ultimately causing cell death (Freeman C.D. *et al.*, 1997).

1.1.5 Inhibition of metabolic pathways

Antibiotics that target metabolic bacterial pathways are a class of drugs that interfere with essential biochemical processes within bacterial cells. Disrupting these pathways can inhibit bacterial growth or kill the bacteria outright. This category includes **sulfonamides**, **dapsone**, **trimethoprim** and **isoniazid**. Sulfonamides, a class of synthetic antibiotics, are characterized by a sulfur atom linked to an amide nitrogen; these compounds have proven effective against a wide range of bacterial infections. Pioneered by sulfanilamide in the 1930s, sulfonamides have evolved into a diverse group, including sulfamethazine, sulfadiazine, sulfamethoxazole, sulfasalazine, sulfisoxazole, sulfamerazine, sulfadimethoxine, sulfafurazole, and others. Their mechanism of action involves interfering with bacterial folic acid synthesis, a crucial step in bacterial growth and replication. While sulfonamides are particularly effective against Gram-negative bacteria like *Klebsiella*, *Salmonella*, *E. coli*, and *Enterobacter*, they also exhibit activity against certain Gram-positive bacteria and even some fungal and protozoal infections (Ovung A. *et al.,* 2021). Sulfonamides act as competitive inhibitors of the enzyme dihydropteroate synthase (DHPS); by blocking DHPS, sulfonamides prevent the formation of dihydropteroate, leading to a decrease in the production of folic acid. Folic acid is essential for bacteria as it is needed to synthesize nucleotides for DNA and RNA. Since bacteria cannot obtain folic acid from their environment and must

synthesize it, inhibiting this pathway effectively stunts bacterial growth (Sköld O. 2010). Because sulfonamides do not kill bacteria directly but rather inhibit their growth by depriving them of necessary components, they are considered bacteriostatic agents. Mention should also be made of **dapsone**, a sulfone-derivative that, like sulfonamides, inhibits folic acid synthesis by competing with para-aminobenzoate for binding by dihydropteroate synthase (Zhu Y.I. *et al.,* 2001). **Trimethoprim** is another antibiotic that targets bacterial folic acid production. Trimethoprim blocks the bacterial enzyme dihydrofolate reductase (DHFR), which is essential for converting dihydrofolic acid to tetrahydrofolic acid (Huoviven P. *et al.,* 1995). This step is crucial for creating folic acid derivatives needed in DNA and RNA building blocks; because of its activity, trimethoprim is often paired with sulfamethoxazole (Goodman and Gilman 2016; Huovinen P. *et al.,* 1995). This double-action approach amplifies its effectiveness, making it difficult for bacteria to produce folic acid, growing slowly. Isoniazid, a synthetic antibiotic introduced in 1952, is a cornerstone in the fight against tuberculosis (TB). It exhibits a targeted bactericidal effect, specifically eliminating *Mycobacteria*, particularly *M. tuberculosis*, *M. bovis*, and *M. Kansai*, but is ineffective against other microorganisms. Isoniazid employs a two-pronged attack. It enters the mycobacterium cell through passive diffusion. Once inside, a unique enzyme exclusive to *Mycobacteria* activates Isoniazid, transforming it into its potent form. This activated form disrupts the bacterium's internal defenses by generating reactive oxygen species (ROS). These ROS wreak havoc by forming adducts, which cripple a critical enzyme called InhA reductase. InhA reductase is crucial in mycolic acid biosynthesis, a key component of the *Mycobacterium* cell wall. By inhibiting this enzyme, Isoniazid disrupts cell wall formation, ultimately leading to the death of the bacteria (Fernandes G.F. *et al.,* 2017).

1.2 Microbial resistance mechanisms

Drug resistance development is a direct result of evolutionary pressure. When exposed to antibiotics, microorganisms are driven to survive, adapting through various mechanisms. Initially, a few bacteria may acquire mutations or gene variations that confer resistance, enabling them to withstand the antibiotic's effects. These surviving individuals then pass these advantageous traits to their offspring, through reproduction or horizontal gene transfer, leading to the gradual spread of resistance within the population. Antibiotics catalyze these resistance mechanisms, exerting selective pressure that promotes resistant strains over susceptible ones. As antibiotics eliminate vulnerable bacteria, the resistant variants thrive, proliferate, and eventually dominate. This cycle accelerates with repeated or inappropriate antibiotic use, as each exposure to the drug heightens the evolutionary pressure, allowing bacteria to refine and reinforce their resistance

strategies. This process underscores the critical need for prudent antibiotic use and developing alternative strategies to control bacterial infections and mitigate resistance spread. In some instances, the microorganism has an **intrinsic** ability to resist certain drugs due to its genetic predisposition: for example, *Enterococci* have an innate resistance to β-lactam because of their penicillin-binding protein (Urban-Chmiel R. *et al.,* 2022); in other circumstances, this resistance is **acquired**, through the acquisition of resistance genes, by Horizontal Gene Transfer (HGT), namely the movement of genetic elements, pieces of information, between bacteria (Burmeister A.R. *et al.,* 2015). **Adaptive resistance** is another phenomenon driven by environmental conditions surrounding the bacterial population. A resistant sub-population rapidly emerges when bacteria are exposed to sub-inhibitory antibiotic concentrations. The key feature of adaptive resistance is its reversibility; once the stimulus is removed, bacteria revert to their original, non-resistant state. Though the mechanisms governing adaptive resistance remain poorly understood, several factors are implicated, including high mutation rates, gene amplification, efflux pump activity, biofilm formation, and other adaptive responses (Motta S.S. *et al.,* 2015; Salam M.A. *et al.,* 2023). In general, four main mechanisms are put in place to counteract antibiotic activity:

- ***enzyme production***;
- ***changes in target sites***;
- ***reduce permeability;***
- ***efflux pumps*.**

However, the already mentioned **Horizontal Gene Transfer** and the microbial **biofilm** formation must also be added, as the biofilm community drastically reduces antibiotic susceptibility.

1.2.1 Enzyme production

By producing enzymes that can modify or degrade the antibiotic, microorganisms can render it harmless, as it can no longer interact with its target. Gram-positive and gram-negative bacteria implemented this strategy, and many enzymes are known to date. The best example of an enzyme that degrades the target is certainly β-lactamases, enzymes capable of cleaving the amide bond of the β-lactam ring, thus deactivating the molecule; the first β-lactamase was identified in *E. coli*, not long after penicillin began to be used in the clinical setting (Abraham E.P. et al, 1940) and such enzymes are also produced by *S. aureus* (Zygmunt D.J. *et al.,* 1992). An alternative mechanism is the production of enzymes that do not degrade the antibiotic but modify its base structure by adding covalently bound substituent groups through acetylation, phosphorylation, and adenylation. The result, however, is an inability to interact with the target. One example is enzymes that confer

resistance to aminoglycosides through modification of the amine or hydroxyl group. Such enzymes are often found as an integral part of the bacterial genome, as in the case of *Serratia marcescens* and *Enterococcus faecium*, and, in general, are commonly found among both Gram-positive and Gram-negative (Ramirez M.S. *et al.,* 2010).

1.2.2 Changes in target sites

Bacteria can prevent the interaction between the antibiotic and the target through two possible strategies: protect the target or modify it. Concerning target protection, the typical example is represented by tetracyclines through the resistance determinants Tet(M) and Tet(O). These are genes that are widespread among different bacterial species, which encode for proteins called ribosome protection proteins (RPPs); these proteins act similarly to the elongation factors involved in the process of protein synthesis: these displace the tetracycline from binding to its target, the 16s rRNA (Dönhöfer A. *et al.,* 2012). Target modification involves three different mechanisms: mutation of its gene, modification by enzymatic reactions, and replacement or bypass of the original target. Regarding mutation of the target gene, the typical case is rifampicin resistance, in which a mutation occurs in the gene encoding RNA polymerase (Floss H.G. *et al.,* 2005); alteration of the target by enzymatic modification is well characterized in the case of resistance to antibiotics that bind the 50S subunit. This is due to the presence of enzymes encoded by the *erm* (erythromycin ribosome methylation) genes, capable of methylation on the adenines of the 23s rRNA (Weisblum B. 1995). Finally, through the replacement or bypass of the target site, bacteria can develop alternative targets to bypass antimicrobial inhibition, as seen in methicillin-resistant *S. aureus* via the acquisition of an exogenous penicillin-binding protein (PBP2a), or by overproduction of the target site for bypass the antibiotic activity, like of trimethoprim resistance, where there is an overexpression of DHFR enzyme (Fishovitz J. *et al.,* 2014; Huovinen P. *et al.,* 1987).

1.2.3 Reduce permeability

This resistance mechanism limits the intracellular concentration of antibiotics by impeding their entry, mainly targeting drugs that need to cross the outer and, potentially, the cytoplasmic membranes to reach their intracellular targets. This is a common strategy among Gram-negative bacteria, as their antibiotic targets are frequently located within the cell (Pagès *et al.,* 1994). Gram-negative bacteria are distinguished by an additional membrane layer known as the outer membrane. This membrane primarily functions as a permeability barrier, blocking the entry of

harmful compounds while permitting the influx of essential nutrients. The outer membrane acts as a selective barrier, especially against hydrophilic substances; these drugs must use specific channels, known as porins, to penetrate the membrane. Alterations in porin expression can decrease a drug's ability to bind and traverse the membrane, as seen with β-lactams in *Pseudomonas* species (Hancock R.E. and Brinkman F.S. 2002). There are different types of porins, categorized by their structure, selectivity, and expression levels. Generally, changes in membrane permeability through porins alone do not constitute a primary resistance mechanism. Still, they are often combined with other factors, such as efflux pumps, to enhance drug elimination from the cell (Nikidao H. 2003).

1.2.4 Efflux pumps

Membrane systems, known as efflux pumps, actively expel toxic compounds from bacterial cells, contributing to antimicrobial resistance. The first of these systems, identified in *E. coli* in 1980, was plasmid-encoded and provided resistance to tetracyclines (McMurray *et al.,* 1980). Efflux pumps may be either substrate-specific or broadly active, capable of ejecting a range of substances. Generally, substrate-specific pumps are acquired via mobile genetic elements, whereas broad-spectrum pumps are chromosomally encoded, often expressed at low basal levels, and can be activated by regulatory gene mutations or environmental stimuli (Poole, 2005; Blanco *et al.,* 2016). At least five families of efflux pumps are known, which differ in conformation, energy source, substrates they can transport, and the microorganisms in which they are found (Piddock L.J. *et al.,* 2006). The tetracycline-specific efflux pump, which confers bacterial resistance, uses exchanged protons as an energy source; such systems are prevalent in Gram-negative, with a few exceptions for Gram-positive (Grossman T.H. 2016; Munita J.M. and Arias C.A. 2016).

As already mentioned, two other mechanisms determine microbial resistance, in addition to the classical ones just discussed, which are horizontal gene transfer and biofilm formation. **Horizontal gene transfer (HGT)** enables the movement of genetic material between organisms via three main mechanisms: **transformation**, where exogenous DNA is taken up from the environment; **transduction**, mediated by bacteriophages (viruses specific to bacteria); and **conjugation**, where genetic material is directly transferred from one bacterial cell to another. When the transferred genetic material includes genes encoding drug-degrading enzymes or efflux pumps, it spreads antibiotic-resistance genes (ARGs), fostering the development of multidrug-resistant (MDR) bacteria (Burmeister A.R. 2015). These MDR plasmids can transfer within the same species and across species boundaries, facilitating the emergence of so-called "superbugs" in various

environmental niches, spanning humans, animals, and plants (Sun D. *et al.,* 2019). *Acinetobacter baumannii* poses a significant threat to human health due to its multidrug-resistant (MDR) profile, which results from its remarkable capacity to acquire foreign genetic material via horizontal gene transfer. This adaptability enables *A. baumannii* to rapidly accumulate resistance genes, making infections difficult to treat and control (Cooper R.M. *et al.,* 2017). Notably, *Staphylococcus aureus* is a pathogen responsible for human and animal infections. The highest risk arises from methicillin-resistant *S. aureus* (MRSA) and vancomycin-resistant *S. aureus* (VRSA). MRSA evolved through interspecies gene transfer from an ancestral *Staphylococcus* species, while VRSA acquired its resistance via horizontal gene transfer from *Enterococcus*, illustrating the adaptive potential of *S. aureus* to gain multidrug resistance traits (Hiramatsu K. *et al.,* 2014). **Biofilm** formation is a key microbial survival strategy characterized by a community of bacteria nearby embedded within a self-produced extracellular matrix that protects against hostile external conditions (Carey D. *et al.,* 2009; Flemming H.C. *et al.,* 2007). Biofilms significantly contribute to antibiotic resistance and are a leading cause of medical device failures, including catheter and prosthesis rejection, due to their reduced sensitivity to antibiotics compared to free-floating (planktonic) bacteria. The extracellular polymeric substance (EPS) matrix within biofilms acts as a formidable barrier against antibiotic penetration. It creates an ideal environment for plasmid DNA exchange, especially through conjugation (HGT), given the physical closeness of bacteria. When biofilms consist of multiple species, they further facilitate the horizontal transfer of resistance elements, promoting the spread of multidrug resistance (MDR) phenotypes (McCarty S. *et al.,* 2014).

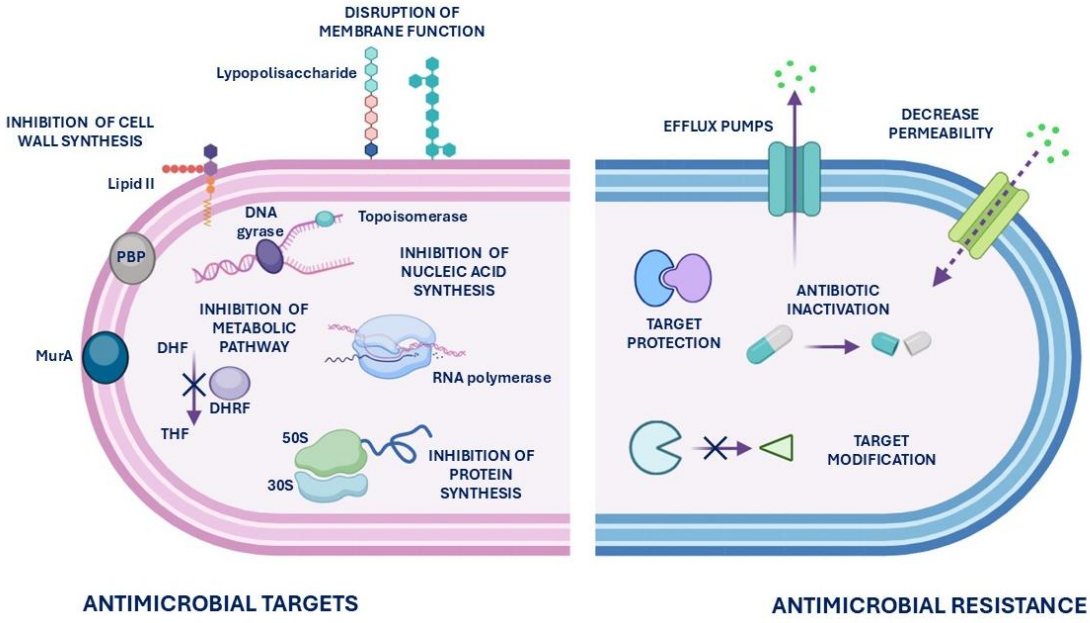


Figure 1. Typical antibiotic targets (left) and antibiotic resistance (right) mechanisms. The image was made using BioRender and PowerPoint.

1.3 Resistance Mechanisms in *E. coli*

Escherichia coli is a diverse group of Gram-negative bacteria that usually function as commensals in the gastrointestinal tract of healthy individuals. However, under specific circumstances, *E. coli* can become pathogenic, leading to gastrointestinal and urinary tract infections. While *E. coli* is initially susceptible to a range of antibiotics, its remarkable ability to acquire resistance genes through horizontal gene transfer presents a major clinical challenge. This adaptability enables *E. coli* to develop multidrug resistance rapidly and complicates treatment strategies, significantly contributing to the global antimicrobial resistance crisis. Currently, *Escherichia coli* harbors numerous genes that can confer resistance to nearly all major antibiotic classes available on the market. Of particular concern is its capacity to acquire genes encoding extended-spectrum β-lactamases (ESBLs). ESBLs are enzymes belonging to different classes that grant resistance to a wide range of beta-lactam antibiotics, including penicillins and cephalosporins (especially third-generation cephalosporins like ceftriaxone, cefotaxime, and ceftazidime), rendering these treatments ineffective. ESBLs are usually plasmid-encoded, allowing them to spread easily across bacterial populations. The first ESBL identified was TEM-1, discovered in the 1960s in *E. coli*. This enzyme provides resistance to both penicillins and cephalosporins, and to date, over 170 variants have been isolated in clinical settings (Salverda M.L. *et al.*, 2010). Another key ESBL,

SHV-1, was identified in *Klebsiella pneumoniae* in 1972 and is commonly found across various Enterobacteriaceae (Chaves J. *et al.,* 2001). The most recent major ESBL to be identified is CTX-M, discovered in the 1980s and widespread across Enterobacteriaceae. TEM-1, SHV-1 and CTX-M are class A of ESBLs. Over 50 CTX-M allotypes have been documented (Rossolini G.M *et al.,* 2008). ESBL genes are typically labeled with the prefix "*bla*," followed by the enzyme family (e.g., bla_{TEM}, bla_{SHV}, bla_{CTX-M}) and a number that specifies the variant. For instance, $bla_{CTX-M-15}$, the most prevalent ESBL in *E. coli*, is associated with the highly virulent O25:H4ST131 clone (Pitout G. and Peirano J.D. 2010). Class C ESBLs, also known as AmpC β-lactamases, are a common group of enzymes that confer resistance specifically to cephalosporins. These β-lactamases are often plasmid-encoded, with the CMY, DHA, and ACC types being the most prevalent. Among these, CMY-type AmpC β-lactamases are the most widespread, appearing in both human and animal populations (Börjesson S. *et al.,* 2016). Carbapenemases, enzymes that can degrade carbapenems, were initially identified in animals. The first, VIM-1, was isolated from mammals on a farm in Germany (Fischer J. *et al.,* 2016). Other notable carbapenemases include NDM-1 and NDM-5, discovered in the United States and China, and IMP-1, OXA-48, and its variant OXA-181, found in humans. KPC, a prominent carbapenemase, is also commonly identified in humans but has not been found in animals. In addition to β-lactamase-mediated resistance, *E. coli* has developed resistance to quinolones and fluoroquinolones, another class of antimicrobials targeting DNA gyrase. Mutations in the gene encoding this enzyme can confer resistance (Hopkins K.L. *et al.,* 2005). Resistance to these antimicrobials can also arise by acquiring plasmid-mediated quinolone resistance (PMQR) genes in humans and animals. This acquisition reduces the microorganism's susceptibility via target protection, efflux pumps, or drug modification (Rodríguez-Martínez J.M. *et al.,* 2016). About aminoglycosides, the most common resistance mechanism involves modification of the target site, specifically the 16s ribosomal rRNA. This modification is often achieved through methylation by various methylases, including ArmA, an enzyme produced by *Streptomyces*, a natural producer of aminoglycosides. The spread of ArmA is accelerated by the transposon Tn1548, facilitating its dissemination across bacterial populations (Galimand M. *et al.,* 2005). Resistance to fosfomycin is also mediated by plasmid-encoded genes, known as *fos* genes. These plasmids frequently carry additional resistance genes; for instance, the *fosA3* gene is often found alongside ESBL genes like $bla_{CTX-M-55}$ and other resistance determinants (Lupo A. *et al.,* 2018). This clustering of resistance genes poses an added risk due to the potential of these plasmids to promote the emergence of multidrug-resistant (MDR) phenotypes. Tetracyclines, widely used in veterinary medicine, have led to selective pressure and subsequent resistance in various microorganisms, including *E. coli*. Resistance to tetracyclines can arise through several mechanisms, generally encoded by *tet* genes. The *tet(A)* and *tet(B)*

genes are the most common in *E. coli* of animal origin, and they are part of the non-conjugative transposons Tn1721 and Tn10, respectively (Allmeier H. *et al.,* 1992; Chalmers R. *et al.,* 2000). Resistance to sulphonamides is mediated by the *sul1*, *sul2*, and *sul3* genes, with *sul1* being the most widespread due to its presence on integrons, which facilitate gene transfer (Recchia G.D. *et al.,* 1995). Resistance to trimethoprim is conferred by *dfr* genes, which are prevalent among Enterobacteriaceae and other Gram-negative bacteria. These *dfr* genes are categorized into two major groups, *dfrA* and *dfrB* (Pattishall K.H. *et al.,* 1977). Additionally, the *mcr-1* gene, responsible for polymyxins resistance, was identified in 2016. This gene has been detected not only in *E. coli* and other Enterobacteriaceae but also in *Salmonella*, *Shigella*, *Klebsiella*, and *Enterobacter* species (Schwarz S. *et al.,* 2016; Poirel L. *et al.,* 2017). In summary, *E. coli* resistance to antimicrobials poses a significant concern for both human and animal health due to the bacteria's ability to acquire and spread multiple resistance genes across species. Consequently, it is increasingly challenging to identify bactericidal agents to which *E. coli* and similar pathogens have not already developed resistance.

1.4 Strategies to bypass antimicrobial resistance

Antimicrobial resistance (AMR) has emerged as one of the most pressing health challenges of the 21st century. It could become the leading cause of mortality worldwide, even in industrialized nations, if effective control strategies are not implemented. The misuse and overuse of antibiotics have accelerated the selection of multidrug-resistant (MDR) strains, like the ESKAPE pathogens. The acronym **ESKAPE** refers to a group of bacterial pathogens known for their ability to "escape" the effects of most conventional antibiotics (***E****nterococcus faecium;* ***S****taphylococcus aureus;* ***K****lebsiella pneumoniae;* ***A****cinetobacter baumannii;* ***P****seudomonas aeruginosa;* ***E****nterobacter* species) against which many current drug therapies are now largely ineffective (Mulani M.S. *et al.,* 2019). A striking example of this is the case of carbapenems. Once considered a last-resort treatment for infections caused by Gram-negative MDR organisms, the increased reliance on carbapenems in clinical settings has led to the selection of carbapenem-resistant strains, especially carbapenem-resistant *Enterobacteriaceae* (CRE) (Sheu C.C. *et al.,* 2019). This shift has significantly limited the effectiveness of these critical drugs and underscored the urgent need for alternative treatment approaches and improved antimicrobial stewardship. Given the complexity and limitations of developing new antibiotics, particularly due to the rapid emergence of resistance, alternative strategies must be employed to curb or control the spread of MDR strains.

One highly effective approach is **combination therapy**, which involves simultaneously administering two antibiotics or an antibiotic with another type of molecule, aiming to create a synergistic effect between them. The underlying principle is that the two molecules target distinct sites within the bacterial cell, each amplifying the efficacy of the other. For instance, β-lactam antibiotics are frequently paired with aminoglycosides to treat infections caused by Gram-negative bacteria. By disrupting peptidoglycan synthesis, β-lactams improve the cell's permeability, thereby facilitating aminoglycoside entry and enhancing overall antimicrobial efficacy (Tamma P.D. *et al.,* 2012). This approach often allows for the "revival" of older antibiotics largely set aside due to their ineffectiveness when used alone. Fagnani L. *et al.,* evaluated the adjuvant capacities of newly synthesized cyclic *N*-oxides combined with oxacillin against methicillin-resistant *Staphylococcus aureus* (MRSA). The surfactants demonstrated intrinsic antimicrobial activity and, notably, showed a synergistic effect when paired with oxacillin. This combination significantly reduced oxacillin's minimum inhibitory concentration (MIC), lowering it below the resistance breakpoint and effectively reversing MRSA resistance to the tested β-lactam antibiotic (Fagnani L. *et al.,* 2021).

Another applicable approach is the **drug delivery system**, which can significantly enhance and support the activity of antimicrobial agents. This approach helps to overcome numerous limitations, such as poor solubility, challenges in reaching the target site, and rapid drug degradation. Drug delivery systems can improve therapeutic effectiveness by optimizing drug stability, targeting accuracy, and controlled release while reducing side effects and dosing frequency (Săndulescu O. *et al*., 2022). Exploring **alternative microbial targets** represents a promising strategy to curb the spread of antimicrobial-resistant (AMR) strains. This approach should focus on identifying targets involved in essential pathways critical for bacterial survival. Ideally, these targets should be conserved across several microbial species and evolutionary scales to enable broad-spectrum applicability.

The bacterial **SOS response**, which plays a key role in bacterial pathogenicity and stress adaptation, is particularly compelling as a potential target due to its involvement in resistance and survival mechanisms. To tackle antimicrobial resistance (AMR) effectively, containment strategies must extend well beyond drug research and target discovery. A multifaceted approach is essential, emphasizing comprehensive education on the responsible use of antimicrobials, focusing primarily on healthcare professionals and extending to the public to build a coordinated, community-wide commitment to AMR containment. Antibiotic stewardship should also be rigorously applied in veterinary care, encompassing pets, livestock, and agricultural practices, acknowledging AMR’s far-reaching impact on human, animal, and environmental health.

This vision aligns with the **One Health** approach, a comprehensive framework linking human, animal, and environmental health to address complex public health issues. By recognizing the interconnectedness of these domains, One Health addresses the root causes through interdisciplinary collaboration among medicine, veterinary science, ecology, and public health fields. This approach strengthens capacities to detect, prevent, and respond to health threats, reducing pandemic risks, combating AMR, and preserving biodiversity. Initially introduced in the 19th century, One Health now provides a sustainable, integrative framework for tackling global health challenges more holistically and coordinatedly (Velazquez-Meza M.E. *et al.,* 2011; Manyi-Loh C. *et al.,* 2018).



Figure 2. One Health Approach: the interconnection and interdependence among the three dimensions: human, animal, and environmental health. The image was obtained by BioRender.

CHAPTER II

The SOS response in bacteria and the LexA transcriptional repressor

As antimicrobial resistance (AMR) reaches crisis levels worldwide, developing effective containment and countermeasures has become an urgent global health priority. A pivotal approach to controlling and potentially reversing AMR is unraveling how bacteria evolve to acquire multidrug resistance (MDR) phenotypes. Given the natural propensity of bacteria to mutate as a survival tactic, a deeper understanding of these resistance pathways could be crucial in limiting AMR's progression and restoring the effectiveness of existing treatments. In this context, the bacterial SOS response emerges as a promising target. This global regulatory system, triggered by DNA damage, is central to bacterial survival under severe stress conditions. By activating DNA repair mechanisms, the SOS response helps maintain genetic integrity. However, it also introduces mutations, accelerating bacterial evolution and potentially driving antibiotic resistance when these mutations enhance survival. Targeting the SOS pathway could provide a novel strategy to impede bacterial adaptation, offering a new avenue for addressing the root mechanisms of multidrug resistance and enhancing the durability of antibiotic therapies.

2.1 The SOS response and its role in mutagenesis

First described and hypothesized in 1975 by Miroslav Radman, the SOS response is how bacteria aim to ensure survival under DNA damage and stress conditions (Radman M. 1975). In his work, we find written:

"A hypothesis was proposed several years ago that Escherichia coli possesses an inducible DNA repair system ("SOS repair") which is also responsible for induced mutagenesis."

Bacteria are continuously subjected to a multitude of damaging stimuli that can lead to various types of damage, including damage to genetic material, which can impair their viability. They are equipped with an inducible DNA damage response system called the **SOS response** to respond to these insults. The SOS response is responsible for controlling phenomena that go far beyond just maintaining the integrity of genetic material; its activation is linked to bacterial pathogenicity phenomena such as dissemination and acquisition of drug tolerance genes (Beaber J.W. *et al.* 2004), adhesion and biofilm formation (Gotoh H. *et al.,* 2010; Walter B.M. *et al.*, 2015), filamentation (Trusca D. *et al.,* 1998; Bellio P. *et al.,* 2020), sporulation

and bacterial motility (Walter B.M. *et al*., 2015), the appearance of the subpopulation with drug tolerance characteristics (Podlesek Z. *et al*. 2020).

The key stimulus for the activation of the SOS response is the formation of single-stranded DNA; this is formed when DNA damage is detected, and thus the double helix must be opened for the damage to be processed or due to a replicative fork stall when DNA polymerase blocks and at the same time DNA helicase continues to unfold the double-strand (Maslowska KH *et al.,* 2019; McKenzie GJ *et al.,* 2000). The regulation of the SOS response occurs via the RecA/LexA pathway: RecA is the DNA damage sensor, and LexA is the transcriptional repressor that regulates the expression of approximately 60 genes, denominated *din*, DNA-inducible genes (Oh T.J *et al.,* 1999). When DNA damage occurs, RecA binds ssDNA and, through an ATP-dependent reaction, causes LexA to self-cleavage, resulting in gene transcription. Activation of the SOS response is directly linked to DNA damage repair, and the genes under the control of LexA are not all activated simultaneously but at different times.

Following the activation of the SOS response, the expression of the inhibitor of cell division *sulA* and *uvrA, uvrB,* and *uvrC* genes occurs immediately, which regulates DNA repair by the Nucleotide Excision Repair (NER) mechanism (Van Houten B. *et al.,* 2005). This is followed by the expression of *polB* and *dinB* genes encoded for DNA polymerase II and IV. DNA polymerase II is a high-fidelity enzyme with 3'→5' exonuclease activity; it is constitutively expressed, with approximately 30 molecules present per cell. However, its expression can increase up to sevenfold following activation of the SOS response. Its primary role is repairing DNA damage caused by UV radiation and oxidative stress (Banach-Orlowska M. *et al.*, 2005; Masker W. *et al.,* 1973; Escarceller M. *et al.,* 1994). DNA polymerase IV is an error-prone polymerase that, when overexpressed, induces frameshift mutations. This protein belongs to the Y family polymerase, the main expressed polymerase in *E. coli* after DNA damage (Kim S.R. *et al.,* 200; Henrikus S.S. *et al.,* 2018).

Finally, 45 minutes after the SOS response activation, the last polymerase to be expressed is polymerase V, codified by *umuC* and *umuD* genes. Polymerase V is a specialized DNA polymerase in *E. coli*, critical for translesion DNA synthesis (TLS) within the bacterial SOS response to DNA damage. Polymerase V, another member of the Y-family polymerases, is characterized by its high error rate during DNA synthesis. Due to its mutagenic potential, its activity is tightly regulated. Its expression is induced only after the self-cleavage of LexA, which ensures that Pol V is synthesized exclusively under conditions of severe DNA damage. Additionally, Pol V is rapidly degraded by the Lon protease to prevent prolonged activity, thereby limiting its mutagenic effects and maintaining genomic integrity once DNA repair is complete (Frank E.G. *et al.,* 1996). Structurally, Pol V is a heterotrimeric complex consisting of two UmuD' subunits and one UmuC subunit, collectively known as

UmuD'$_2$C. Its activation requires the formation of an active mutasome complex, Pol V Mut (UmuD'$_2$C-RecA-ATP), facilitated by RecA and ATP. This complex allows Pol V to bypass replication-blocking DNA lesions, enabling survival under genotoxic stress, though at the expense of replication fidelity, often introducing mutations (Jaszczur M.M. *et al.,* 2019). This mutagenic TLS mechanism, while error-prone, is essential for overcoming replication roadblocks and contributes to bacterial adaptability under environmental stresses. Pol V's role in balancing survival and mutagenesis underscores its importance in bacterial evolution and antibiotic resistance mechanisms.

The first identification of this event was found in a culture of UV-irradiated *E. coli,* a phenomenon that causes direct DNA damage, and several antibiotics act by inducing DNA damage, like fluoroquinolones levofloxacin and ciprofloxacin. The SOS response is also activated by several external inducers like high pH, which can determine LexA activation in a RecA-independent way (Smith M.H. *et al.*,1991), acoustic cavitation, high pressure, chromate shock, oxidative stress, and alkylating agents (Erill I. *et al.,* 2007).

Although initially described in *E. coli*, the key feature of the SOS response is its dispersion among various bacterial species: it is a universal response. The LexA sequence is broadly conserved across bacterial genomes, spanning multiple *phyla*, which indicates a likely common evolutionary origin for the SOS response system. LexA homologues have been identified *Firmicutes bacillus subtilis* (Wojciechowski M.F. *et al.*, 1991), in *Micobacterium tubercolosis (*Movahedzadeh F. *et al.*, 1997), *Thermotoga naepolitana* (Zverlov V.V. & Schwarz W.H. 1999), *Rhodobacter sphaeroides* (Fernandez de Henestrosa A.R. *et al.*, 1998), *Cyanobacterium Anabaena* sp. (Mazon G. *et al.,* 2004). In many human pathogens, such as *Pseudomonas aeruginosa* and *Staphylococcus aureus*, the presence of the SOS system contributes to biofilm formation and facilitates horizontal gene transfer, processes that enhance bacterial virulence and adaptability, especially in environments exposed to antibiotics or other stressors (Gotoh H. *et al.,* 2010; Maiques E. *et al.,* 2006). However, there are notable exceptions where certain bacterial species lack this system. In such cases, the absence of LexA homologs is often attributed to evolutionary pressures that lead to genome reduction, as observed in bacteria like *Epsilonproteobacteria*. These dynamics underline the evolutionary versatility of the SOS system, shaping bacterial survival strategies and their interactions with hosts. The system's dual role in repair and mutation makes it a key target in studying bacterial resistance and pathogenicity.

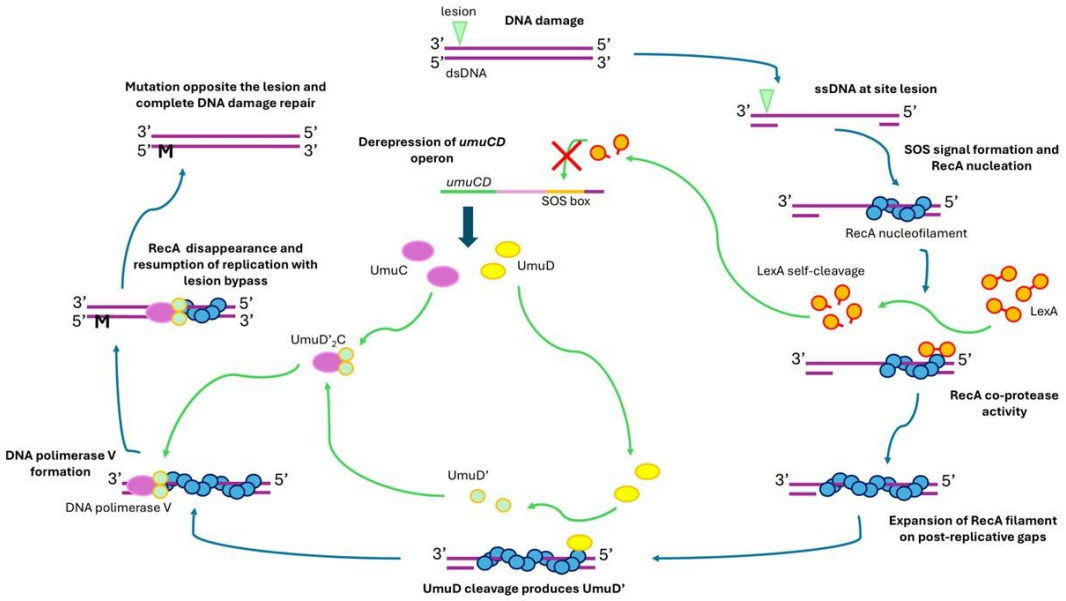


Figure 3. Schematic representation of SOS response activation made using PowerPoint.

2.2 The DNA damage sensor: the recombinase RecA

RecA is a recombinase protein consisting of 352 amino acids, with a molecular weight of approximately 38 kDa. This protein functions as a sensor of DNA damage, initiating the SOS response. Additionally, it plays an essential role in DNA repair through homologous recombination (HR). The gene encoding RecA was first identified in *Escherichia coli* in 1965, and homologs have since been discovered in bacteriophages, archaea, and eukaryotic cells (Story R. *et al.,* 1992).

The RecA monomer consists of a large central core flanked by two smaller domains at the N-terminal and C-terminal ends. The central core, residues 34–269, comprises β-sheets and α-helices, representing the most conserved region of the protein across different bacterial species. Additionally, the core features two highly conserved regions called loops, which are crucial for DNA binding. These are loop L1, spanning residues 157–164 and loop L2, spanning residues 195–209. These loops play a vital role in interacting with the DNA strand during processes like homologous recombination and the formation of the RecA-DNA filament (Bellio P. *et al.,* 2017). Both the recombinase and co-protease functions of RecA require the binding of two effector species: ssDNA and a nucleoside triphosphate (NTP), but the co-protease activity does not require NTP hydrolysis. However, RecA protein is a DNA-dependent ATPase (Maslowska K.H. *et al.,* 2019). The nucleotide-binding site of a RecA is located at the interface of two RecA monomers; therefore, a dimer of RecA is required for RecA filament assembly on ssDNA (Chen Z. *et al*., 2008). Six RecA monomers polymerize around DNA in the presence of ATP, covering

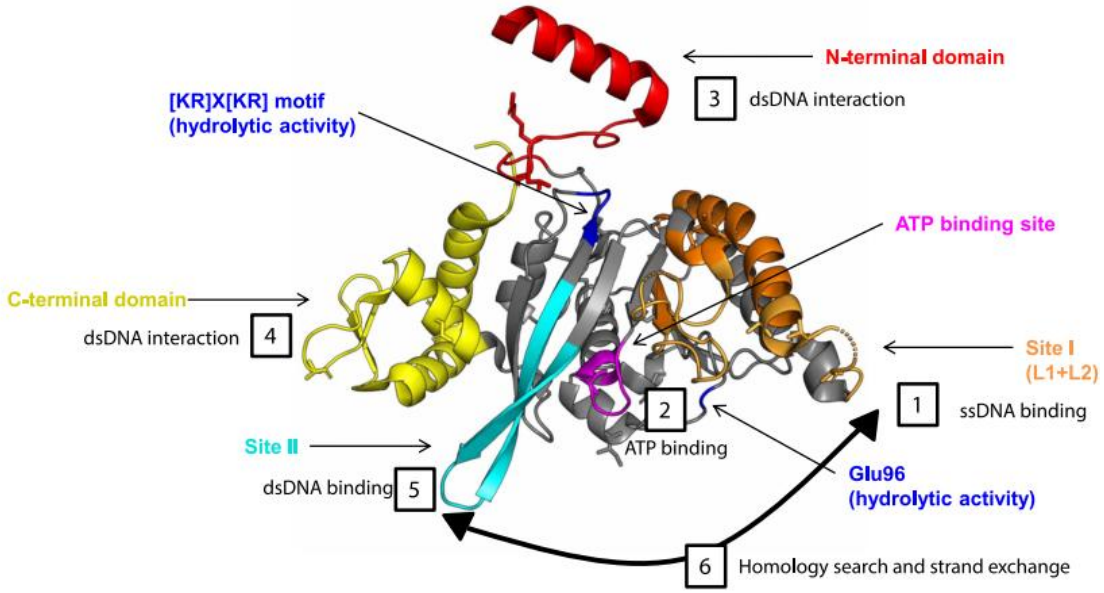
approximately 18 DNA base pairs. This binding facilitates the formation of a nucleofilament, a structure necessary for either DNA repair via homologous recombination (HR) or activation of the SOS response.

During homologous recombination, the DNA exchange mediated by RecA occurs in four steps; the first step is **nucleation**: RecA binds to single-stranded DNA (ssDNA) in the presence of ATP, forming an initial complex. The filaments are extended in the 5'-3' direction in the second step. Follow the **Homologous Alignment** where the nucleoprotein filament aligns with homologous double-stranded DNA (dsDNA). The last step is **DNA Duplex Formation and Extension**: A hybrid DNA structure (duplex DNA) forms, followed by a unidirectional extension of the hybrid DNA in the 5'-3' direction. This process requires ATP hydrolysis to ensure unidirectional DNA exchange, overcome structural barriers, and facilitate the final exchange step. ATP hydrolysis rates differ depending on the DNA substrate: ~30 ATP molecules per minute when bound to ssDNA and ~20 ATP molecules per minute when bound to dsDNA. RecA's function is tightly regulated at multiple levels:

- ***Transcriptional Regulation***: Its expression is controlled by the LexA transcriptional repressor, as it is part of the SOS response gene network.
- ***C-terminal Domain***: The C-terminal region, consisting of 25 hydroxyl-rich amino acids, is crucial for RecA functionality. Mutations or deletions in this region impair RecA activity.
- ***Protein Interactions***: RecA interacts with several regulatory proteins, including RecF, RecO, and RecR, which facilitate RecA loading onto DNA; DinI, RecX, RdgC, and Psi, which modulate RecA filament stability and dynamics; Uvr proteins, which indirectly affect its function in repair processes; and SSB proteins, which compete with RecA for ssDNA binding, indirectly regulating its activity.

This multi-layered regulation ensures that RecA's activity is finely tuned to cellular needs, preventing unnecessary DNA recombination or repair. (Cox M.M 2007a; Cox M.M. 2007b). Finally, the eukaryotic analog of RecA is the Rad51 protein, which is also capable of catalyzing homologous recombination. This protein is found in simpler eukaryotes, such as *Saccharomyces cerevisiae*, and in mammals. However, Rad51 does not hydrolyze ATP at the same rate as its prokaryotic counterpart (Shinohara A. *et al.,* 1992; Vispé S. *et al.,* 1997).

A



B

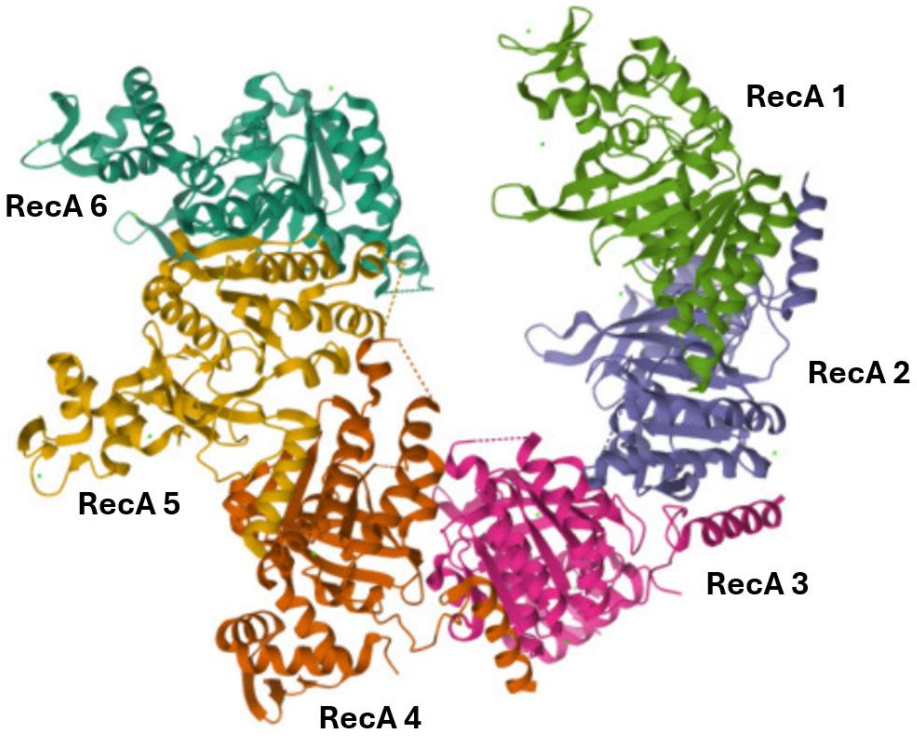


***Figure 4*. (A)** 3D structure of RecA monomer. The different domains of the protein and the various steps of the recombination are indicated by numbers. (Del Val E. *et al.,* 2019); **(B)** 3D structure of RecA assembly for the DNA binding, obtained by PDB (ID:1U94) and modified with PowerPoint.

2.3 The LexA transcriptional repressor: an overall

The LexA protein is the leading player in the SOS response, responsible for initiating the cascade of events leading to the resolution of DNA damage. It is a 202-amino-acid protein organized into two distinct domains connected by a flexible linker region, known as the "hinge" region. This is a hydrophilic and solvent-exposed region, spanning residues Gln70 to Gln74, crucial in stabilizing LexA's interactions with DNA as a transcriptional repressor (Luo Y. *et al.*, 2001). This region separates the protein into amino-terminal (NTD) and carboxy-terminal (CTD) portions.

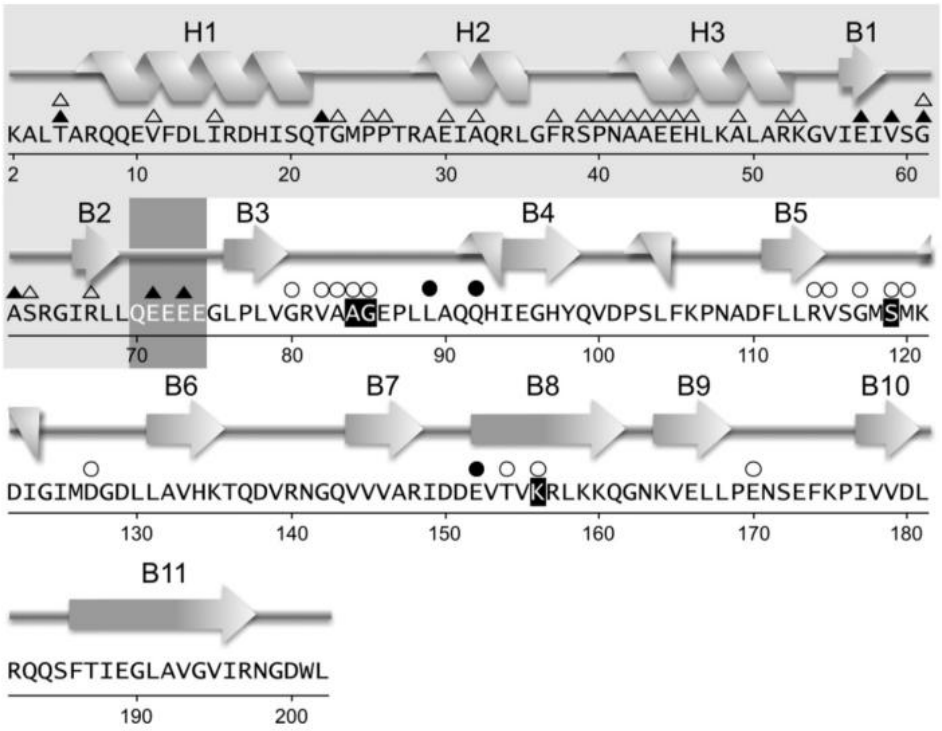


Figure 5. Sequence and secondary structure of LexA transcriptional repressor. Light grey evidence the NTD domain; the dark grey is for the hinge region, followed by the CTD region. Black shading highlights residues Ser119 and Lys156 of the catalytic dyad, and Ala84 and Gly85, the peptide bond cleaved. The triangles indicate positions of substitutions that enhance (solid symbols) or prevent (open symbols) DNA binding. The circles indicate positions of substitutions in hypercleavable LexA mutants (solid symbols) or non-cleavable mutants (open symbols) (Butala M. *et al.,* 2009).

The **NTD** comprises α-helices and β-sheets and is responsible for DNA interactions via a helix-turn-helix motif (Luo Y. *et al.,* 2001). It includes three α-helices, Helix I (residues 6–21), Helix II (28–35), and Helix III (41–52), followed by two β-sheets. Helices II and III form the helix-turn-helix motif critical for DNA binding. The NTD extends to residue Leu69 and interacts with the CTD through minimal contact, hidden between the two domains. The **CTD** spans residues Gly75 to Asn198 and is

composed solely of β-sheets. It harbours the protein's autocatalytic activity and is responsible for dimerization. The CTD is organized into three regions: the **cleavage site region** (Gly75–Tyr98), which includes the cleavage site (Ala84–Gly85), **intervening linker** (Gln99–Asp110) and the **catalytic core** (Phe111–Asn198), containing the catalytic dyad Ser119/Lys156 responsible for LexA self-cleavage. The cleavage site region exists in two conformations, cleavable (**C**) and non-cleavable (**NC**), which alternate to control LexA's self-cleavage; both are intimately associated with the catalytic core through hydrogen bonds between β-sheet b3 and b5. Notably, the catalytic core and CTD share structural homology with proteins like UmuD and various CI repressors from bacteriophages, collectively forming the *LexA superfamily*. This structural similarity is evident in β-sheet b3, which contains the cleavage site region and the conserved Ser119/Lys156 catalytic dyad, along with a similar catalytic mechanism (Sauer R.T. *et al.,* 1982; Perry *K.L*. et al., 1985). These proteins interact with RecA-ssDNA-ATP filaments and function in oligomeric forms. Despite shared features, there are significant differences in their self-cleavage reactions; for example, LexA undergoes intramolecular cleavage, whereas UmuD involves intermolecular cleavage. Additionally, the cleavage rates for CI and UmuD are slower compared to RecA-induced LexA self-cleavage (Butala M. *et al.,* 2009).

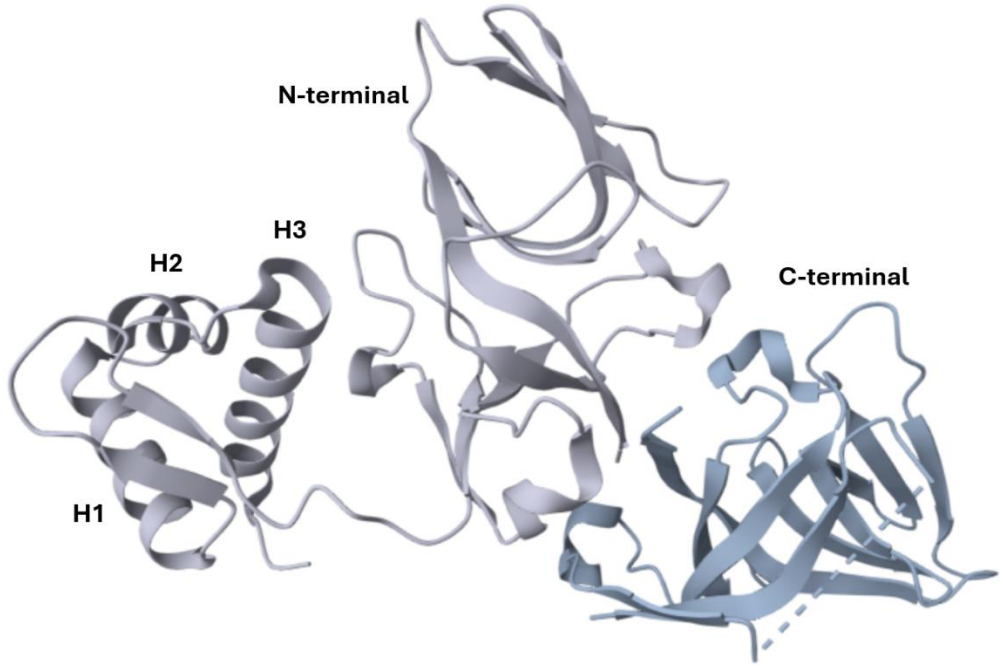


Figure 6. 3D structure of LexA monomer obtained by PDB (ID: 1JHH). The NTD (light purple) is composed of α-helix and β-strand; the CTD region (light blue) is composed exclusively of β-strands.

2.4 Dimerization of LexA

The concentration of LexA *in vivo* is approximately 2 μM in cells without DNA damage, dropping to approximately 0.2 μM in cells with activated RecA (Griese K.C. *et al.,* 2007). Generally, a bacterial cell contains about 7200 molecules of RecA and 1300 molecules of LexA, of which only 20% is free, while the rest is bound to DNA. For most DNA-binding proteins, cooperative interaction is often crucial for proper function: typically, a first monomer binds DNA with relatively low specificity, facilitating the binding of a second monomer. However, this is not true for the LexA transcriptional repressor (Mohana-Borges R. *et al.,* 2001).

Free LexA predominantly exists as a dimer, significantly reducing the monomeric form. Therefore, LexA recognizes its binding site in dimeric form. LexA binds DNA at a specific, symmetrical, and conserved sequence known as the ***LexA binding box*** through interactions mediated by its N-terminal domain (NTD). Each subunit can bind DNA, recognizing the same sequence but in an inverted orientation. The dimerization process is mediated by the protein's C-terminal domain (Schnarr M. *et al.,* 1988). The dimerization interface covers a surface area of approximately 1380 $Å^2$ and involves residues located within the β-11 strand distributed across two loops: from Gln99 to Asp110 and from Ser116 to Gly128. *In vitro* studies report a dimerization constant K_d of approximately 50 μM (Schnarr M. *et al.,* 1985; Kim B. and Little J.W. 1992). Similarities in the dimerization process have also been observed for UmuD and the CI repressor (Luo Y. *et al.,* 2001).

The *E. coli* LexA repressor forms higher-order aggregates under acidic conditions, reducing its ability to bind DNA specifically. This pH-dependent behavior is crucial during the SOS response, which can activate independently of RecA in acidic environments, such as exposure to gastric acid. *In vitro*, LexA exhibits its strongest DNA-binding affinity near neutral pH. At pH 4.0, aggregation impairs its specific DNA-binding capability, while at pH 2.5, tetramer formation and unfolding of the DNA-binding domain led to a complete loss of specificity. Near its isoelectric point (pH 6.5), LexA precipitates in low-salt conditions due to interactions involving its C-terminal domain (CTD). So, pH and ionic strength are essential in regulating LexA stability and function (Butala M. *et al.,* 2009).

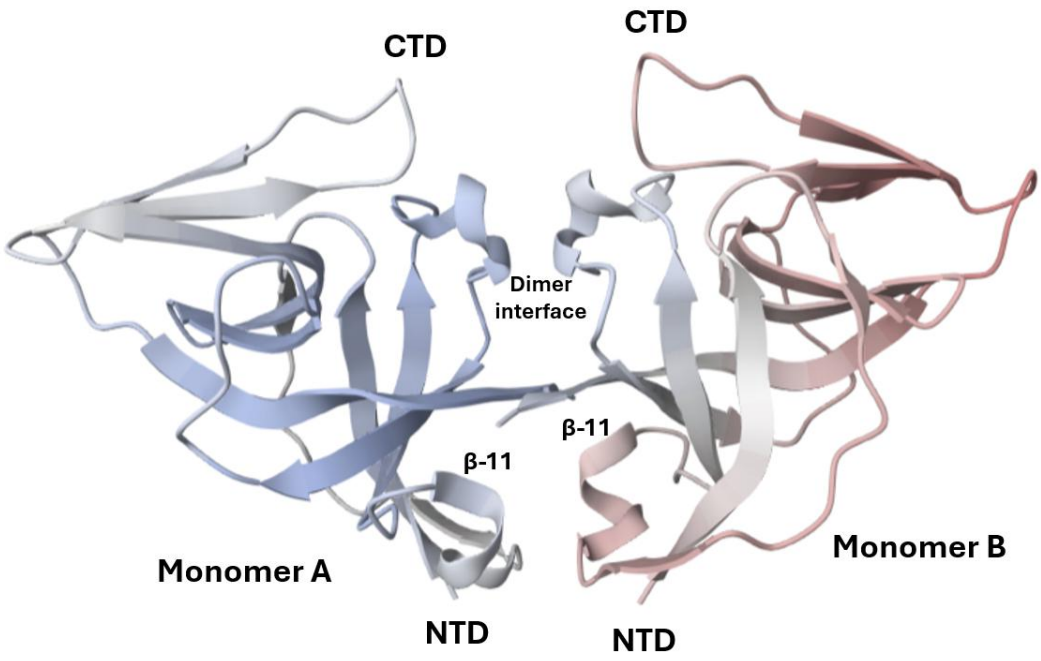


Figure 7. 3D structure of LexA dimer obtained by PDB (ID: 1JHE). The dimerization is obtained by interactions between residues located in the strands β-11 of the CTD portions; when the dimer is formed, the two monomers are positioned specularly to each other.

2.5 The LexA binding box and the interaction with the DNA

LexA binds to DNA at a specific sequence called the LexA binding box. Generally, DNA-binding proteins attach non-specifically to DNA through electrostatic interactions and then search for their specific target (von Hippel P.H. *et al.,* 1986). This process ensures accurate target binding. However, LexA does not follow this mechanism. ChiP and microarray analyses have shown that the *E. coli* genome is "permissive", allowing equal accessibility for protein binding across its entire genome, unlike eukaryotic genomes organized into chromatin that restrict accessibility (Wade J.T. *et al.,* 2005). Thus, LexA can access any part of the *E. coli* genome. The LexA transcriptional repressor binds to a specific sequence in the prokaryotic genome, referred to as the LexA binding box or SOS box. This sequence is a 16–20 bp palindromic motif located upstream of or within the RNA polymerase binding site. Gram-negative bacteria typically follow the $CTGTN_8ACAG$ pattern, with the 8 bp spacer being variable. In *E. coli*, the sequence is 16 bp long: CTGTATATATATACAG, characterized by an AT-rich content. At least 30 LexA binding boxes have been identified in *E. coli*. However, other sequences may also interact with LexA *in vivo*, potentially requiring co-factors for binding, as these interactions

are not observed *in vitro* (Wade et al., 2005). As the SOS response is conserved across bacterial species, so is the consensus sequence of the LexA box. In Gram-positive bacteria the LexA box was first identified in *Bacillus subtilis*, called the Cheo box and has the $GAACN_4GTTC$ motif (Cheo D.L. *et al.,* 1991). This motif is also found in *Clostridium perfringens* (Nuyts S. *et al.,* 2001), *Staphylococcus aureus* (Bisognano C. *et al.,* 2004), and *Streptomyces* spp. (Vierling S. *et al.,* 2001). However, to these two sequences, which we could then associate with gram-negatives or gram-positives, new LexA boxes must be added: in the *Alphaproteobacteria Rhizobium etli* and *R. sphaeroides*, the sequence is $GTTCN_7GTTC$, and has an odd spacer (N7) and a repeat motif, a structure very different from those just described (Fernández de Henestrosa A. R. *et al,* 1998); in 2002, the sequence was identified in *Xanthomonas campestris* and *Xylella fastidiosa*, corresponding to $TTAGN_6TACTA$ (Campoy S. et al, 2002; Yang M.K. *et al.,* 2002); a few years later, the SOS box was described in *Mycoccus xanths*: $CTAN_6GTTCAGG$ (Campoy S. *et al.,* 2003); in *Proteobacteria*, the sequence is $CCTN_{10}AGG$ (Fernández de Henestrosa A.R. *et al.,* 2003); the LexA box in *Petrotoga myotherma* has been reported as $GANTN_6GANNAC$ (Mazón G. *et al.,* 2006), while the SOS box in *Leptospira interrogans* is $TTTGN_5CAAA$ (Cuñé J. *et al.,* 2005) and in *Acidovacterium capsulatum* it is $GTTCN_7GTTC$ (Erill L. *et al.,* 2007).

Regardless of the specific sequence of the LexA binding box, the interaction between LexA and its target occurs through residues located in the NTD portion of the protein in a helix-turn-helix motif. The α-helices of this portion all participate in the interaction with DNA: helix III contains residues that insert into the major groove of DNA, forming interactions with all four bases, while the shorter portion of helix II, while contacting the major groove, forms interactions with the phosphate skeleton. The N-terminal residue of helix I also forms contacts with the target bases, together with the ring region connecting the β-strands, forming hydrogen bonds with the sugars and phosphates of the DNA (Butala M. *et al.,* 2008).

In a study by Zhang *et al.*, 2010, crystallographic studies assess the specific interaction of LexA (mutant for K156) with the SOS box and find that the helix III residues Glu45, Asn41 and Ala42 are key residues in interactions with DNA: Glu45 forms hydrogen bonds with cytosine, and a mutation of it results in lower binding specificity, while Asn41 is essential in the formation of hydrogen bonds with thymine and the next GC base pair; Ala42 forms a hydrophobic contact with the before mentioned thymine, and guanine also forms a hydroxyl bond with Ser39.

Binding to the target sequence occurs when LexA is in dimeric form, to allow for stabilization in interactions with the duplex DNA; moreover, in the dimeric form, the NTD portion is not able to bind its target, but a reorientation in the NTD relative to the CTD portion is required; this phenomenon is not exclusive to *E. coli*, but is also

observed in *B. subtilis*. An interesting aspect is the different affinity that LexA can have for different operators; first, in some cases we have that the same regulon possesses several LexA binding boxes, resulting in a more intense degree of regulation of gene expression. This is the case with the *lexA* gene promoter, which undergoes a feedback regulation process in the cell. It carries several sequences in tandem to be able to respond promptly to any variation in signal, however small (Brent R. 1982). Furthermore, the SOS response's level, duration, and intensity depend on differences related to the strength of the different LexA boxes, their position relative to the promoter, and the strength of the promoter itself. Thus, based on these differences, since LexA binds some operons weakly, transcription for these genes could occur following even weak signals, in contrast to those genes of those operons bound more strongly, whose expression is subject to tighter control, a typical example being translesion DNA polymerases, which are only expressed as a last resort, and very late in the onset of SOS response activation (Butala M. *et al.,* 2008).

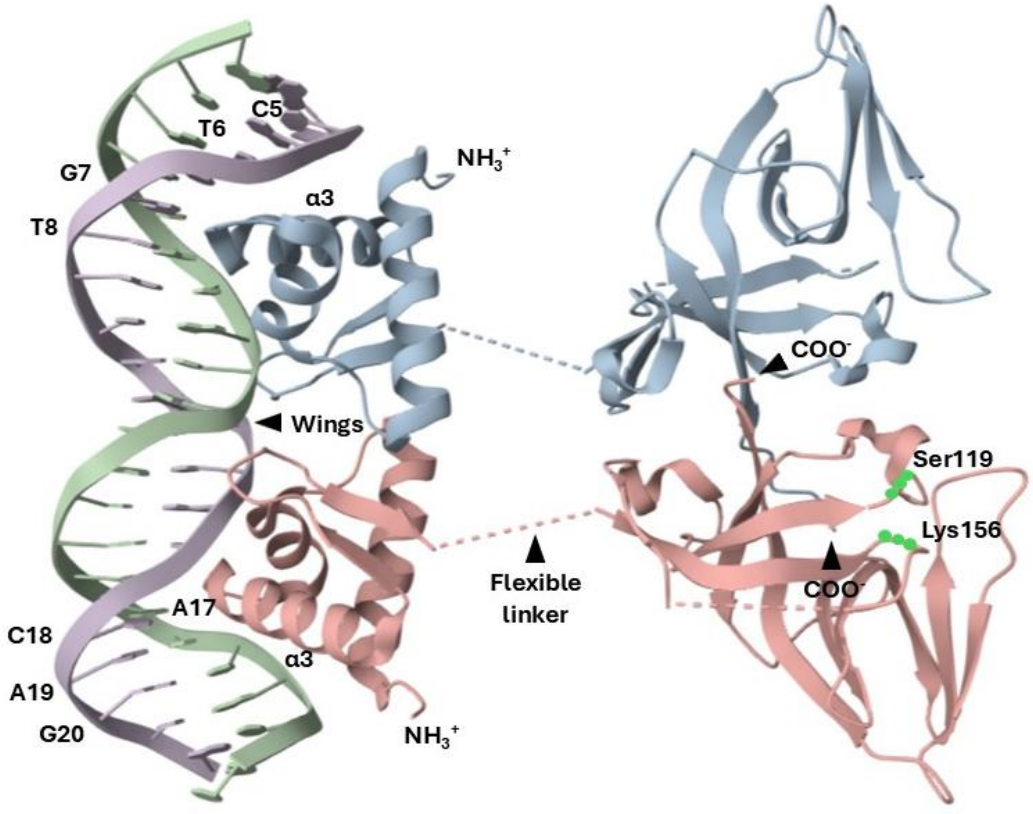


Figure 8. The overall structure of the E. coli LexA-DNA complex. The image was obtained by PDB (ID: 3JSO). Individual subunits are colored in light blue and pink. Green balls represent the catalytic residues S119 (nucleophile) and K156 (general base).

2.6 LexA catalytic site

As mentioned, the active site of LexA, known as the cleavage site region, is in the CTD portion and is organized into three parts. This region includes the cleavage site Ala84-Gly85 and the catalytic core containing the catalytic dyad Ser119/Lys156, which is responsible for the cleavage of the molecule and the loss of its repressive activity. Deprotonation of Lys156 is required for LexA self-cleavage since autocleavage is efficient only at a high pH. The β-hydroxyl group of the nucleophile Ser119 establishes a strong hydrogen bond with the ε-amino group of Lys156, which acts as a general base. In the cleavable conformation of LexA, the Oγ of Ser119 is positioned about 2.7 Å from the carbon atom of Ala84, with which it interacts during the cleavage process. The C form is characterized by a significantly lowered pK_a for Lys156 (~5–6), aligning with its catalytic role. This reduced pK_a may result from charge repulsion caused by nearby positive charges; however, no charged amino acids are found within 8 Å of Lys156's ε-amino group. In the non-cleavable form, the Nε of Lys156 is partially exposed to the solvent, with a solvent-accessible surface area of approximately 11 $Å^2$ (compared to 40–50 $Å^2$ for full exposure). Conversely, in the C form, this group is completely buried. Lys156's side chain forms strong van der Waals interactions with hydrophobic residues Met120 and Ile177, which are part of the active site and are further enclosed by residues from the cleavage site (Ala84 to Pro87). The nearest charged residue to Lys156's ε-amino group is the γ-carboxylate of a conserved Glu152, located about 8 Å away. In Ser-His-Asp proteases like chymotrypsin, a tetrahedral oxyanion intermediate is stabilized by a structural feature known as the "oxyanion hole" (Kraut J. 1977). The structure of LexA with its substrate in the cleavage site region reveals a similar oxyanion hole. In LexA's C form, the backbone oxygen of Ala84 is within the hydrogen-bonding distance of the backbone amide nitrogen of Ser119 (2.8 Å) and Met118 (3.2 Å), defining the oxyanion hole of LexA. The oxyanion hole's stability is supported by hydrogen bonds between adjacent backbone atoms of Gly117 and a solvent molecule, as well as interactions with the side chain of Asp127. Mutations in Gly117 or Asp127 disrupt the cleavage process, highlighting their critical roles in the reaction mechanism.

LexA exhibits substrate specificity, as evidenced by the structure of its active site in the cleavable conformation, a hallmark feature of serine enzymes. The catalytic dyad is situated at the end of an extended hydrophobic pocket. The cleavage site region resides within this pocket, with the β-sheet b3 intercalated between b5 and b8 of the catalytic core. Members of the LexA superfamily cleave the Ala-Gly bond, and in the cleavable form, substrate residues Arg81 and Ala84 fit into the active site pocket. The side chains of Val82 and Ala84 are well-positioned within the hydrophobic pocket. Alterations in these amino acids could cause steric clashes

with atoms at the substrate interface, destabilizing the cleavable conformation. The selectivity for Gly85, a universally conserved residue, is likely due to its unusual conformation, which is unfavourable for other amino acids (ϕ = +163°, ψ = −142°). Gly85 resides at the tip of a type IV turn, with its nitrogen atom forming a hydrogen bond with the N-ε of Lys156. This conformation is critical for positioning the glycine leaving group near Lys156, a potential proton donor, during the cleavage reaction (Luo Y. *et al.,* 2001).

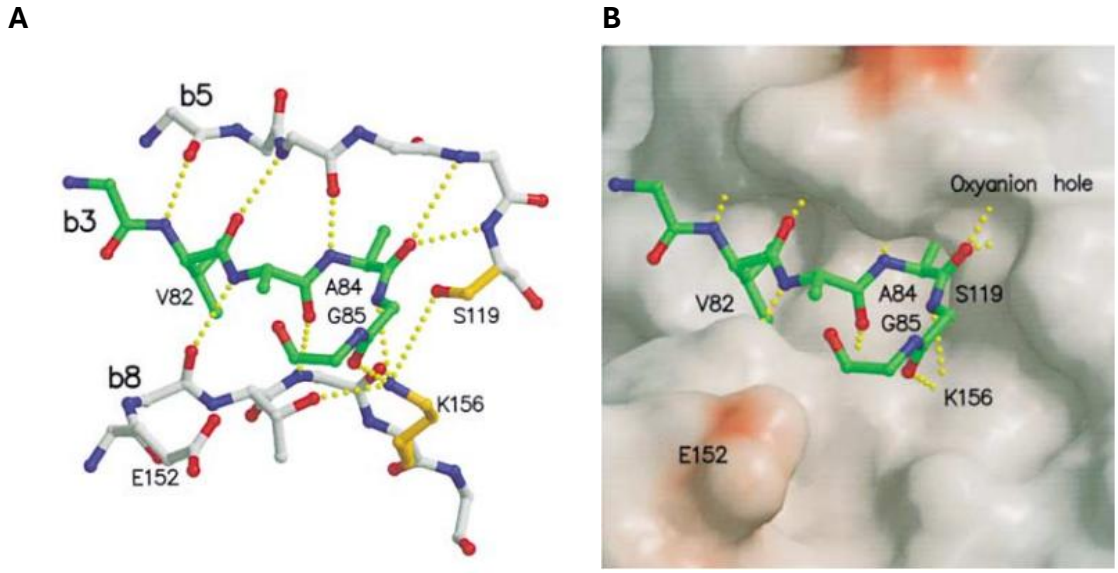


Figure 9. Active site geometry of LexA. **(A)** A ball and stick model for the active site in the C form. The dashed lines indicate hydrogen bonds. **(B)** the same view of A, with added the electrostatic surface (Luo Y. *et al.,* 2001).

The cleavage site region alternates between two conformations: cleavable (C) and non-cleavable (NC). The C form of LexA is rare, constituting less than 0.1% of the bacterial cell population (Luo Y. *et al.,* 2001); the alternation between these two states is the key mechanism regulating LexA's self-cleavage. In the **C** state, the cleavage site is in close contact with the catalytic core: the scissile bond Ala84-Gly85 is directly adjacent to Ser119/Lys156 dyad, whereas, in the **NC** state, the two regions are approximately 20 Å apart (Luo Y. *et al.,* 2001; Butala M. *et al.,* 2009). These conformations are stabilized by hydrogen bonds between the cleavage site and the catalytic core. Conformational switching between C and NC involves localized changes in the cleavage site region, including four consecutive bond rotations (ψ of V79, ψ and Φ of G80, and Φ of R81) and significant rearrangements in residues from Gly85 to Glu95. The forces driving this interconversion include hydrophobic interactions, differences in solvent distribution, and protonation of Lys156; indeed, protonation of the ε-amino group of Lys156 destabilizes the C

conformation in favour of the NC conformation. In the NC state, this group is partially exposed to the solvent, whereas the bound substrate completely shields it in the C conformation. A significant amount of energy is likely required to convert the protonated lysine in the NC form to the neutral form necessary for catalysis in the cleavable conformation.

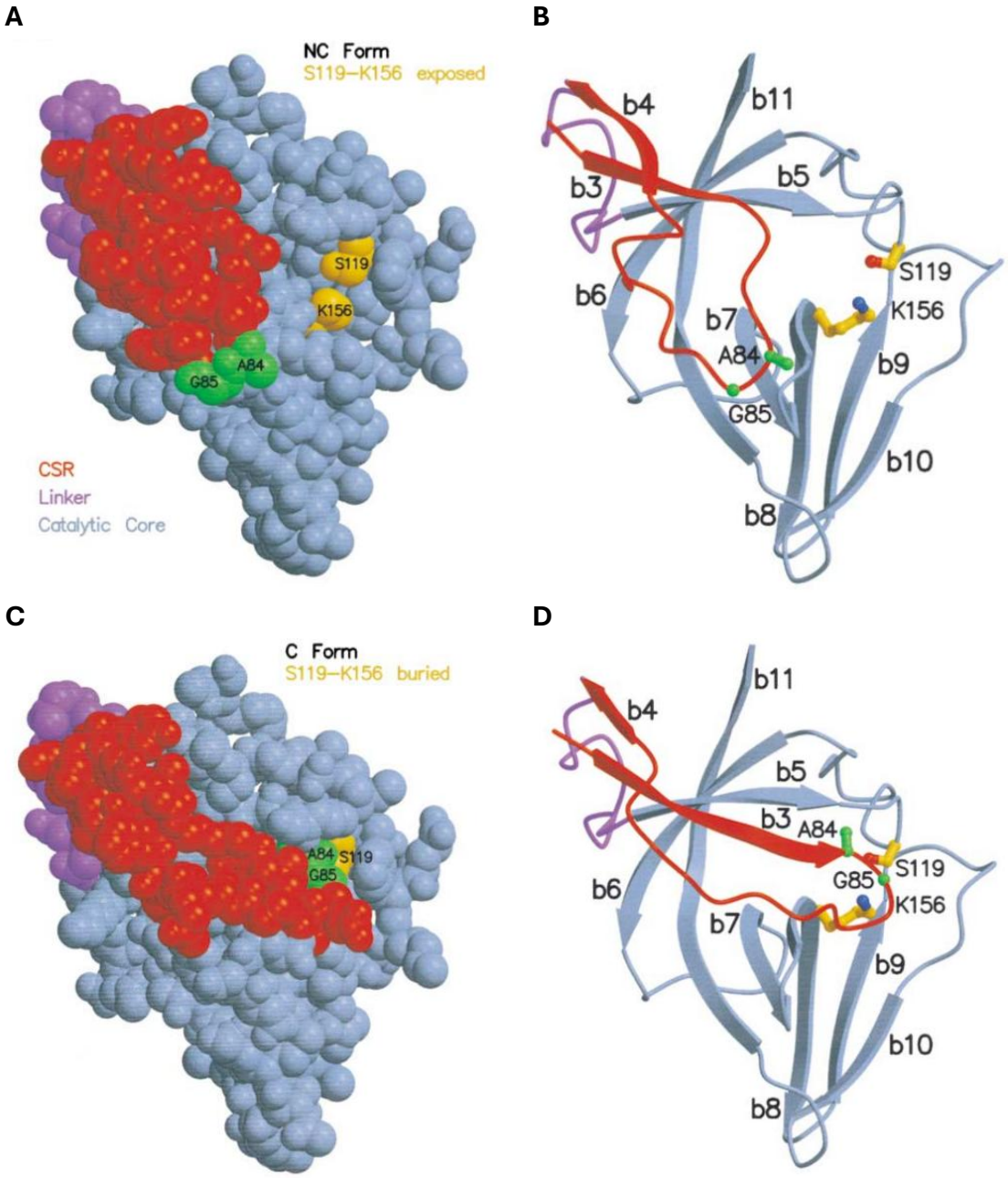


Figure 10. **(A)-(B)** Spacefully and representation and ribbon representation of LexA $\Delta_{1\text{-}67}$ S119A mutant with the CSR in NC conformation; **(C)-(D)** Spacefully and ribbon representation of LexA Δ1-67 QM with the CRS in the C conformation (Luo Y. *et al.,* 2001).

2.7 Interaction between RecA and LexA and RecA-stimulated LexA self-cleavage

The accumulation of ssDNA is first required to activate the SOS response. This can occur due to double-strand breaks or replication fork stalling. At this point, ssDNA serves as a template for the ATP-dependent polymerization of the RecA protein. By polymerizing around the DNA, RecA forms the active ssDNA-ATP-RecA* complex. This active form can interact with the transcriptional repressor LexA. Under normal conditions, LexA adopts a conformation with its active site in a non-cleavable state. The transition to a cleavable state is triggered by interaction with RecA*. This interaction induces a conformational change in the CTD of LexA, where its catalytic activity resides. The catalytic core, which includes the catalytic dyad Ser119/Lys156, is brought closer to the cleavage site region at Ala84-Gly85. Following autoproteolysis, the NTD and CTD domains of LexA dissociate, destabilizing the interaction of the LexA box on DNA. This dissociation allows LexA to detach from the nucleotide sequence, initiating transcriptional activation of SOS genes. The formation of the ternary complex RecA*-ssDNA-LexA, known as the "SOS signal complex," is thus the critical step for activating the SOS response. When LexA is unbound, it adopts a non-cleavable conformation. However, upon activation of the SOS response, LexA is rapidly degraded within minutes, and its self-cleavage rate increases by 50-fold.

The interaction with RecA triggers a conformational change in LexA, stimulating its self-cleavage (Little JW. 1983). In a 2024 study by Cory M.B. *et al.,* the specific interactions between two proteins are thoroughly described, revealing a mechanism known as the “lock and key” model. This work represents the first observation of the SOS signal complex model with a full-LexA. In the proposed model, it is observed that RecA and LexA monomers, when bound, are held together by numerous van der Waals interactions across the entire surface of LexA and within the groove of the nucleoprotein filament. Additionally, multiple sites could facilitate charge-charge interactions. A LexA monomer interacts with three RecA subunits (RecA1-2-3), interacting with residues in the L2 loop (192-212). Furthermore, the L2 loops appear to support both the NTD and CTD portions of LexA (RecA1 and RecA3). RecA2, on the other hand, participates in specific interactions with LexA through residue F203 in the L2 loop. Residue F203 is deeply buried in a hydrophobic pocket on LexA, formed by residues V79, V82, F111, L113, V146, and V153. This pocket exists only when LexA is in its “cleavable” conformation. This allosteric pocket of LexA is located opposite the active site. The insertion of F203 appears to stabilize the β-sheets of the portion containing the cleavage site, specifically the CSR. This residue is involved in promoting the hydrolysis of LexA. Experiments conducted with mutants of F203 in all three RecA monomers revealed

that LexA hydrolysis was abolished, as this variant could not bind the transcriptional repressor. However, hydrolysis occurred when at least one of the three RecA monomers contained the wild-type residue, indicating that only one is specifically involved in interaction with LexA and its hydrolysis. Thus, the minimum requirement for forming the "SOS signal complex" is the interaction of LexA with three RecA monomers, specifically binding the F203 residue of the central RecA monomer (RecA2).

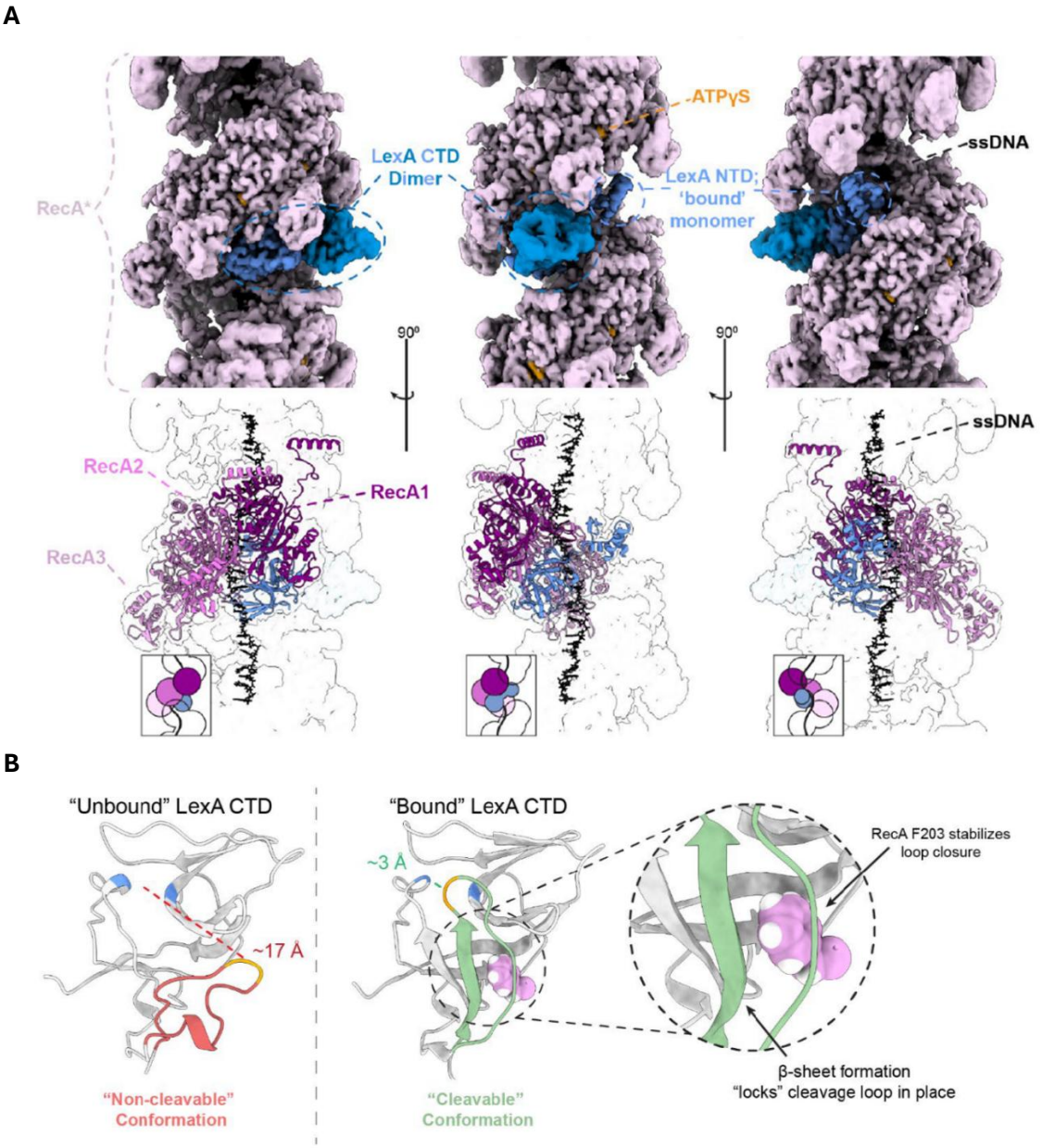


Figure 11. Structure of the SOS signal complex. **(A)** At the top, the density of the SOS signal complex shows a solid structure; at the bottom, the map density is shown as a contour, and the black filament is the ssDNA. **(B)** Comparison between the unbonded and bonded LexA CTD within the dimer. The cleavage loop is coloured in red or green, with the scissile bond in orange and the Ser119 in blue. RecA F203 is represented in pink and is associated with the bound LexA monomer (Cory M.B. *et al.*, 2024).

This residue functions like a key in a lock, stabilizing LexA in its cleavable "C configuration." Moreover, while all F203 variants can produce RecA* filaments, they cannot bind LexA or trigger its cleavage, explaining the tolerance observed for mutations at this residue. The F203 residue in the L2 loop fits into a critical allosteric pocket located at a distance from the active site and the scissile bond. Like a key fitting into a lock, F203 inserts into this pocket, present only in the cleavable variant of LexA, thus stabilizing its cleavable conformation. While all F203 variants have been able to produce RecA* filaments in our mutational studies, the substitutions of this critical residue led to impaired binding with LexA, which directly correlates with an alteration in the cleavage kinetics of LexA. This observation may help explain previously reported tolerance models in vivo to substitutions at the F203 position (Hörtnagel K. *et al.,* 1999).

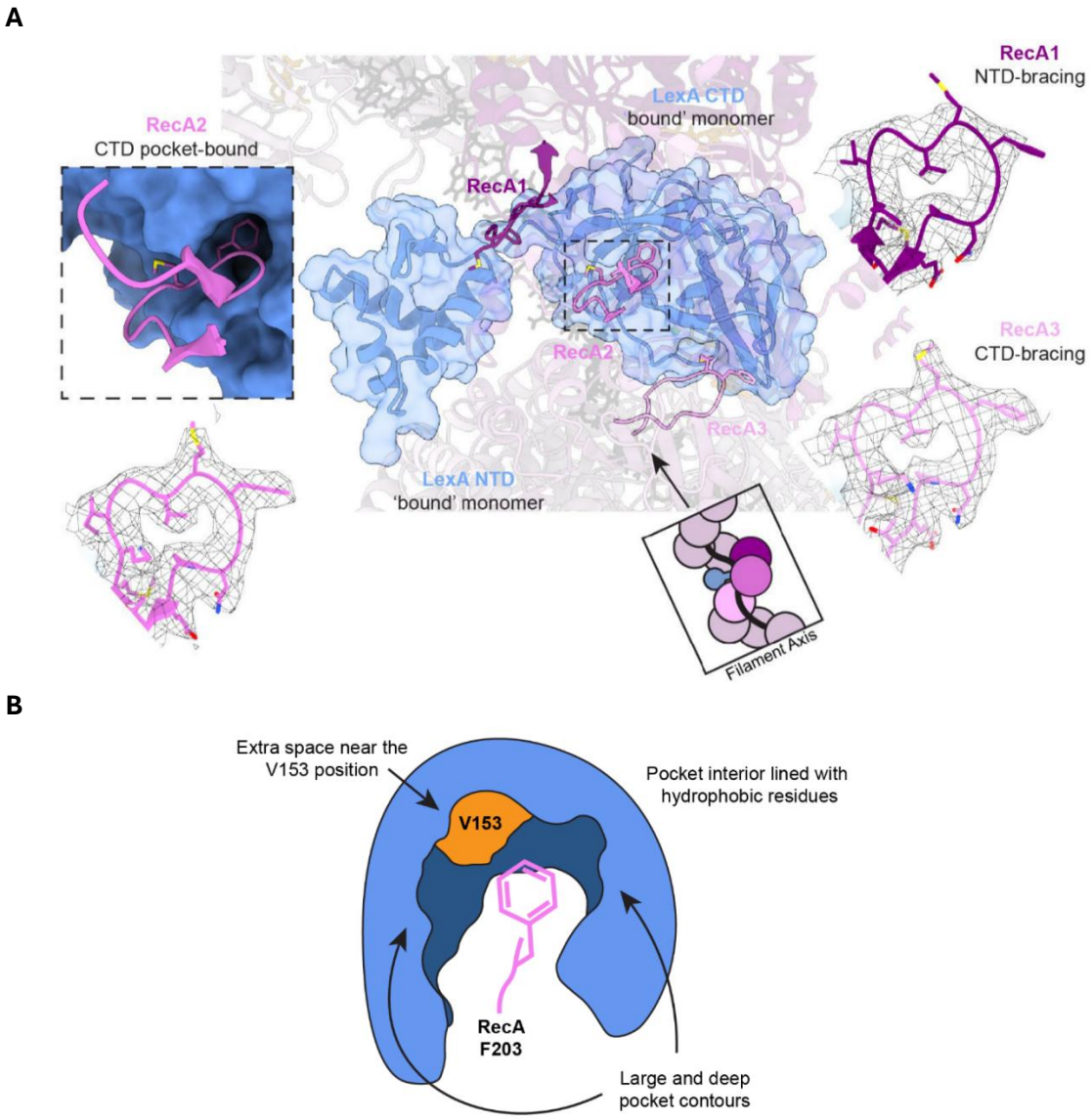


Figure 12. The role of RecA L2 loop in complex formation. **(A)** L2 loop region (residues 197-212) of the three RecA units, with a zoom of the L2 loop from RecA2, with F203 binding in a deep allosteric pocket within LexA. **(B)** Cartoon representation of the F203-binding pocket, highlighting different pocket features (Cory M.B. *et al.,* 20214).

LexA remains in the non-cleavable conformation until it binds to RecA, with the ε-amino group of Lys156 in its protonated form, exposed to the aqueous environment. In this state, Lys156 cannot serve as a base for activating the catalytic serine (Ser119), preventing LexA from undergoing self-cleavage. Binding to RecA induces a conformational change to the cleavable form, creating a hydrophobic pocket where the neutralization of the ε-amino group occurs. In this new conformation, Lys156 is deprotonated and can act as a general base, facilitating the activation of Ser119. This transition leads to a 100-fold increase in the self-cleavage rate at neutral pH. Lys156 removes a proton from Ser119, making it nucleophilic and

allowing it to attack the Ala84-Gly85 bond, thereby cleaving the bond (Luo Y. *et al.*, 2001; Slilaty S.N. and Little J.W. 1987; Little J.W. *et al.*, 1991).

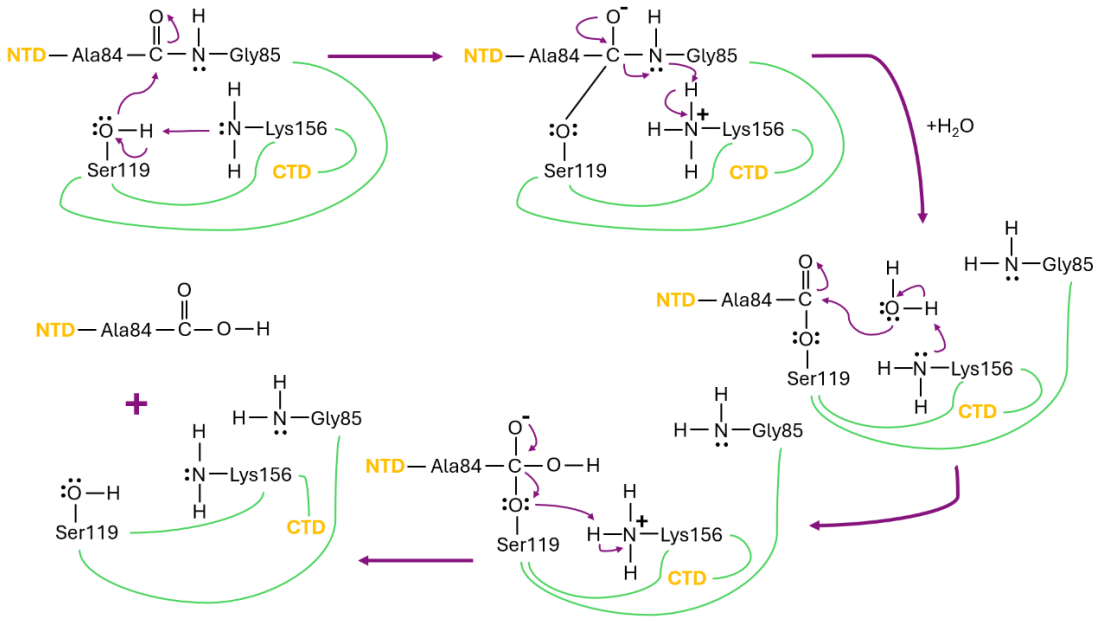


Figure 13. Cartoon drawing of LexA self-cleavage catalysis mechanism. The uncharged Lys156 extracts a proton from the hydroxyl group of Ser119, increasing its nucleophilicity. The nucleophilic oxygen of Ser119 then attacks the carbonyl carbon of Ala84, forming a transient bond between Ser119 and Ala84. In the subsequent step, the nitrogen from the α-amino group of Gly85 accepts a proton from the ε-amino group of Lys156, leading to the cleavage of the peptide bond between Ala84 and Gly85. The hydrolysis of the transient bond between Ala84 and Ser119 occurs in the following step, facilitated by an incoming water molecule. As a result, the reaction produces two fragments of LexA: an N-terminal fragment and a C-terminal fragment. The thin purple arrows indicate the direction of electron transfer. This figure was inspired by Osman K.T. 2010, and made using PowerPoint.

CHAPTER III

Boron Compounds: natural distribution, chemical properties, and pharmaceutical potentialities

Boronic acids are highly versatile and potent compounds in medicinal chemistry, with significant applications in cancer therapy, diabetes management, and developing antiviral and antibacterial agents. Their unique ability to interact with diverse biological molecules and regulate key enzymatic pathways positions them as invaluable tools in pursuing innovative treatments for a broad spectrum of diseases. While boronic acids are relatively scarce, they occur in certain natural products and biological systems, particularly within specific biosynthetic pathways found in microorganisms and plants. Boronic acids often play critical roles in these organisms' defense mechanisms or metabolic processes. This natural occurrence underscores their biological relevance and highlights their potential for developing targeted therapies that leverage their inherent bioactivity, further enhancing their promise in developing next-generation pharmaceuticals.

3.1 Natural distribution and physiological role of boron

Boron is a metalloid element that shares several chemical characteristics with carbon, such as its tendency to form covalent bonds, valence, and position in the periodic table. These similarities make it an essential element in the chemical industry, particularly for synthesizing organic compounds. Boron is especially valuable in introducing specific functionalities into molecules. In nature, boron is not found as a free element but rather is complex with other elements to form borates. As an element, boron is primarily present in water and soil, and its primary dietary source comes from plant-based products, especially fruits and nuts (Hunt C.D. *et al.,* 1991). Boron was isolated by Joseph Louis Gay-Lussac, Louis Thénard, and Humphry Davy in 1808, and its earliest uses date back over 4.000 years. Like other elements, boron is found in the atmosphere, hydrosphere, lithosphere, and biosphere. Still, it is particularly abundant in seawater, with a concentration of approximately 0.4 mM, suggesting its key role in marine life. The accumulation of boron in seawater is due to flows between the atmosphere, hydrosphere, and lithosphere, and it is present in the forms of $B(OH)_3$ and $B(OH)_4$. Furthermore, boron has gained significant attention as a pH surrogate in paleoclimate studies, particularly in the context of climate change, but the interest in boron is primarily attributed to its pharmacological properties, which make it highly versatile. It has shown significant potential in antimicrobial therapy and cancer treatment. Boron's

unique chemical behavior enables it to interact with biological systems in ways that are being explored for their therapeutic benefits. This versatility underscores its growing importance in modern medicine and pharmaceutical research.

3.1.1 Boron's role in plants

Boron is a vital element for all unicellular and multicellular organisms, playing a key role in various essential biological functions. As an indispensable micronutrient in algae and plants, boron deficiency can lead to significant growth defects. These deficiencies typically result from inadequate boron levels in the soil, posing significant challenges in agriculture. The role of boron in plant physiology was only fully understood in recent decades, particularly its involvement in the formation of esters with alcohols in a pH-dependent manner. Boron is crucial for cross-linking rhamnogalacturonan II, a pectic polysaccharide found in primary cell walls, providing structural strength and facilitating cell adhesion. Additionally, boron appears essential for maintaining cytoskeletal functions within plant cells. However, excessive boron concentrations can be toxic to plants. To regulate this, plants employ specific transport mechanisms to control boron uptake and retention. One of the most well-characterized transporters is NIP5-1, which belongs to the major intrinsic protein (MIP) family, also known for including aquaporins. The expression of NIP5-1 is inducible and increases in response to higher external boron concentrations. In contrast, the BOR1 transporter extrudes excess boron from plant cells. This transporter shares significant similarities with anion exchange proteins, and its accumulation within cells decreases as external boron concentrations rise. Boron is then incorporated into endosomes, where it is degraded, maintaining proper cellular balance and preventing toxicity (Miwa K. *et al.,* 2010).

Boron's role in plants is also expressed through its interaction with macronutrients. It is essential to assimilate nitrogen, a fundamental element for plant growth, photosynthesis, and various metabolic processes. Interestingly, nitrogen also regulates boron absorption, especially when boron levels are excessive, thus helping to limit its toxicity. Another significant interaction occurs between boron and phosphorus, as the absorption and transport of boron in plants are closely related to phosphorus absorption. This synergistic relationship improves the photosynthesis rate and supports overall plant growth. Boron also interacts with calcium, influencing the cross-linking of pectin polysaccharides in the cell wall, which is crucial for cell integrity. Furthermore, the interaction between boron and zinc plays a key role in regulating the plant's metabolic processes, affecting the absorption of other nutrients. Combining boron, zinc, and manganese stimulates the concentration of polyphenols and enhances lignin production, making the plant more damage-resistant. Finally, boron directly affects iron absorption and its chelation in the cell wall, improving overall nutrient management (Vera-Maldonado

P. *et al.,* 2024). Boron is essential in several symbioses between plants and bacteria. It is involved in the formation of symbiotic interactions between legumes and nitrogen-fixing bacteria, such as *Rhizobium*, *Azorhizobium*, and *Bradyrhizobium*; in fact, when boron concentration is deficient, these bacteria become pathogenic to the plant. The accumulation of boron in certain parts of the plant is also directly regulated by the presence of mycorrhizal and saprotrophic species, which in turn regulate nutrient acquisition from the soil. Another type of symbiosis is actinorhizal, a form of nitrogen-fixing bacteria, where boron appears to be necessary to maintain the envelope of the heterocyst of cyanobacteria (Biţă A. *et al.,* 2022).

3.1.2 Boron in bacteria

Boron plays a very interesting role in bacteria; as already mentioned, it is important to establish symbiotic mechanisms with plants. Furthermore, it is a structural component in several antibiotic-active molecules and is used as a means of bacterial communication in quorum sensing. Cyanobacteria produce many biologically active molecules, including peptides with highly modified amino acid residues and cyclic hexapeptides. These are unique antibiotics due to their structural characteristics, as they bind boron in their structure. Among them is borophicyn, isolated from *Nostoc spongiaeforme* and *N. linckia*. Boromycin, first isolated from an african soil sample, is produced by *Streptomyces antibioticus*. Aplasmomycin, originally isolated from *Streptomyces griseus* from marine sediments, differs from boromycin by having two identical subunits surrounding the borate complex. Several variants of aplasmomycin exist, labeled A, B, and C, all produced by *S. griseus*. Aplasmomycin is also produced by the actinomycete *Plasmodium berghei*. In addition, other natural boron-containing molecules have been isolated, known as tartrolones A and B, produced by Gram-negative eubacteria *Sorangium cellulosum*. The biosynthesis of tartrolones is closely linked to boromycin and aplasmomycin: they share the same boron-binding substructure C_1-C_7 in each half of the symmetric molecules (Dembitsky V.M. *et al.,* 2002).

A very interesting role that boron plays in bacteria is as a signalling molecule. Specifically, bacteria do not live in isolation but in communities, and they must communicate with each other. To do this, they use signalling molecules and a specific system called Quorum Sensing, which is the basis for forming microbial biofilms. The best-known signalling molecule is acyl-homoserine lactones, primarily used in Gram-negative bacteria. However, some bacteria, such as cyanobacteria and *E. coli*, use a molecule called Auto-inducer-2. This is a small boron-containing molecule first identified in the bioluminescent marine bacterium *Vibrio harveyi*, which is associated with bioluminescence in this bacterium. The name "autoinducer" comes from its accumulation “autoinduces” phenotypic changes in the studied strains: it accumulates extracellularly until a threshold concentration is reached, which is critical for phenotypic induction. For AI-2 to be

produced, the cell must possess the enzyme LuxS. This enzyme is an integral part of the activated methyl cycle (AMC), the system through which cells recycle S-adenosyl-L-methionine (SAM), the primary methyl group donor in bacteria, archaebacteria, and eukaryotic cells. AI-2 is therefore produced from SAM, which is first converted into S-adenosyl-L-homocysteine (SAH), rapidly detoxified to produce S-ribosylhomocysteine (SRH), and then, through the action of the LuxS enzyme, converted into pro-AI-2, namely 4,5-dihydroxy-2,3-pentadione (DPD). This molecule reacts with boron to form the active form of AI-2. This molecule is associated with bacterial pathogenicity phenomena, including virulence and biofilm formation. The LuxS/AI-2 system is not only linked to biofilm formation but also virulence, making it a system generally associated with microbial pathogenicity and essential for intra- and inter-species communication (Dembitsky V.M. *et al.,* 2002; Vendeville A. *et al.,* 2005).

3.1.3 Boron and human health

Boron plays a crucial role in humans and animals in general. In humans, Boron is essential for bone health, as it plays a crucial role in osteogenesis, and its deficiency impacts bone development and regeneration. Its activity is linked to the production of steroid hormones and is involved in preventing calcium (Ca^{++}) loss and bone demineralization: the introduction of boron into the diet reduces calcium excretion through urine, promotes its absorption, and increases serum estradiol levels (Beattie J.H. *et al.,* 1993). Studies conducted on animals have shown that growth observed during the healing process can be inhibited when animals are boron-deficient compared to controls with normal levels, resulting in osteogenesis defects (Gorustovich A.A. *et al.,* 2008). Boron seems to influence gene expression related to tissue mineralization in osteoblasts (Hakki S.S. *et al.,* 2010), which is also associated with promoting wound healing. 3% boron solutions are used for the treatment of deep wounds. Its activity occurs at the extracellular matrix level, enhancing the activity of enzymes such as elastase, collagenase, and alkaline phosphatase and the release of protein, collagen, and proteoglycan synthesis (Nzietchueng R.M. *et al.,* 2002).

It also regulates serum levels of sex hormones, increasing these levels in conjunction with higher boron intake by affecting the half-life of estradiol. This is also observed with vitamin D, whose levels rise with increased dietary boron intake, again increasing its half-life. This probably involves the increasing level of 25-hydroxyvitamin D in serum. Boron has an anti-inflammatory role in osteoarthritis (Travers R.L. *et al.,* 1990), reducing pain, likely by acting on leukocytes and neutrophil activity and promoting the scavenging of free radicals by increasing levels of SOD, catalase, and glutathione peroxidase. Its role is also crucial for ensuring cognitive and psychological well-being, as boron deprivation impairs attention and

short-term memory and negatively affects brain functions and cognitive activities (Penland J.G. *et al.,* 1998).

Boron also plays a protective role against the liver, the organ responsible for detoxifying drugs and toxins. Animal studies have shown that liver damage is reduced through its action on the mitochondria, particularly acting at the level of the Krebs cycle, methionine metabolism, and overall oxidative stress (Khaliq H. *et al.,* 2018). Its protective role is further demonstrated through anti-tumour effects: generally, boron-rich diets are linked to a lower incidence of prostate, cervical, and lung cancers. The action seems to occur through the inhibition of serine proteases, NAD-dehydrogenases, mRNA splicing, and cell division (Scorei R.I. *et al.,* 2010), and it also induces apoptosis in cancer cells (Pizzorno L. 2015). Boron limits lipid accumulation, facilitating cholesterol elimination, thereby reducing the risk of stroke and ischemia and further contributing to maintaining heart health (Shatha R.M. 2015). Due to their complex structure, borates are involved in inhibiting various biologically active enzymes, such as aldehyde dehydrogenase, nitric oxide synthetase, peptidases, xanthine oxidase, and proteases. They actively protect rat liver against ethanol (Sogut I. *et al.,* 2017).

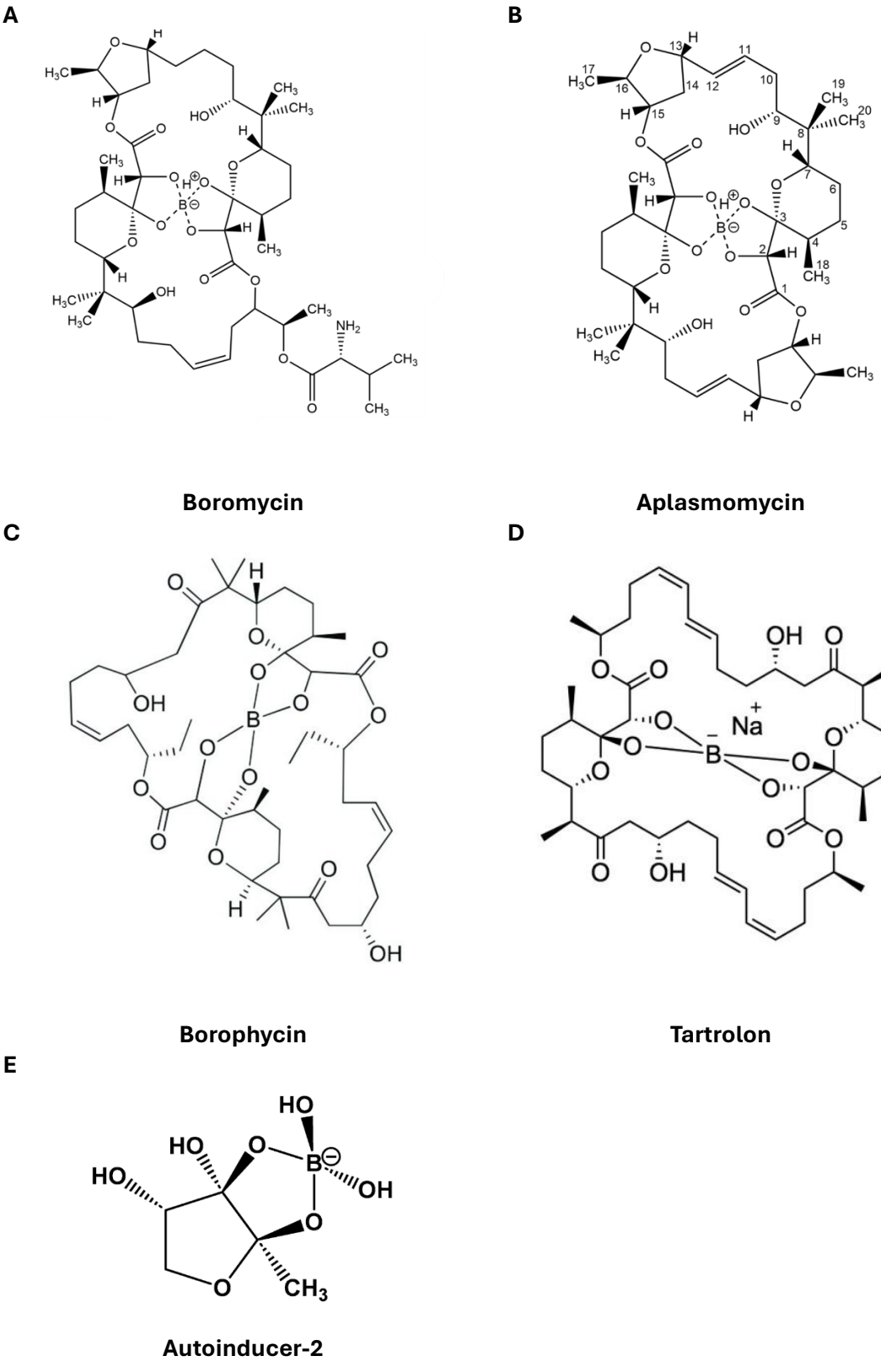


Figure 14. Natural boron compounds product by bacteria.

3.2 Chemistry of boron

Boron typically exists in the planar trigonal form BX3, with an electronic configuration $2s^2p^1$. It, therefore, has three valence electrons and tends to form neutral trivalent compounds. Being an element with an empty p orbital, boron is characterized by electronic deficiency. It often reacts with electron-pair donors to fill its p orbital, forming tetrahedral adducts with a negative charge (Carrano C.J. *et al.,* 2009). Boron shares many similarities with carbon, though it has a greater electronic deficiency, and because of these similarities, the compounds it forms are considered bioisosteres of carboxylic acids. Boron tends to react with both carbon and oxygen, forming a wide variety of compounds, the classification of which varies significantly in the literature. When it reacts with carbon, the resulting compounds are generically called boranes. The C-B bond is longer than the typical C-C bond and is characterized by considerable reactivity, making it of pharmacological interest. Boron has a high tendency to react with oxygen, and such molecules are classified as borates, which are oxyanions containing boron. When oxygen is also bonded to a generic group R, we get borate esters, and if the bond is with at least one hydroxyl group, we get a boronic acid. Boronic acid B(OH)3 is a molecule known for its extremely low toxicity in humans, with levels comparable to NaCl (De Francesco H. *et al.,* 2005).

Boronic acids were first synthesized in 1860 by Edward Frankland. They are particularly useful as intermediates in synthesis reactions due to their high reactivity and relatively non-toxic degradation products. Boronic acids are considered Lewis acids, as they have a pK_a between 4 and 10. Changes in pK_a values result from the presence of substituents: boronic acids with alkyl substituents are less acidic than those with aryl substituents. At physiological pH, boronic acids are present in a non-charged protonated trigonal form, but in aqueous environments where the pH is higher than their pK_a, they are converted into the tetrahedral anionic form. Only in rare cases do they behave as Brønsted-Lowry acids, when the formation of the tetrahedral anionic intermediate is unfavourable. Being Lewis acids, boronic acids tend to react with electron-donating groups, such as nitrogen or oxygen, which are electrophilic centres. This characteristic is manifested in their ability to interact with nucleophilic centres in biological molecules, such as carbohydrates, proteins, and nucleic acids. This gives boronic acids high reactivity towards biological targets. In addition to their relatively low toxicity, this makes them excellent candidates for use in synthetic reactions, such as the metal-catalyzed Suzuki-Miyaura cross-coupling reaction, one of the most widely used reactions in synthetic organic chemistry. It is a highly complex reaction involving oxidation, substitution, transmetallation, and elimination steps to create new C-C bonds (Molander G.A. *et al.*, 2012).

3.3 Boronic acids as a serine-enzyme inhibitors

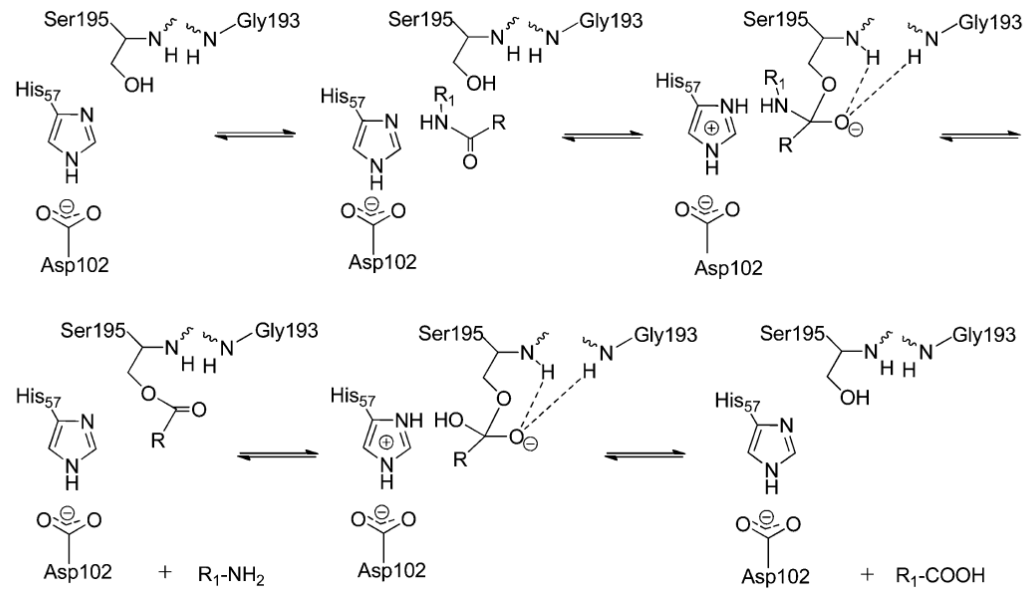
As previously discussed, boronic acids are Lewis acids that can interact with nucleophilic centres, a property that makes them highly versatile in biological systems. Their ability to bind to various biological molecules, such as enzymes and nucleic acids, renders them valuable as pharmacological tools. An interesting application of boronic acids is their role as inhibitors of serine proteases, a class of enzymes involved in numerous vital physiological processes, including digestion, coagulation, and immune response. Serine proteases are also implicated in several pathological conditions, such as viral infections and cancer. Over 800 structures of these enzymes have been deposited in the Protein Data Bank (PDB), demonstrating their extensive biological relevance.

The active site of serine proteases consists of a catalytic triad comprising Ser195, His57, and Asp102, along with an oxyanion hole that stabilizes reaction intermediates. In the context of serine protease catalysis, a tetrahedral intermediate is formed during the nucleophilic attack of the hydroxyl group of Ser195 on the carbonyl carbon of the substrate. This intermediate is a crucial step in the enzyme's mechanism. A high-energy state characterizes the tetrahedral structure because the bond angles and electron distribution are distorted compared to a stable, lower-energy configuration. The formation of the tetrahedral intermediate involves the nucleophilic attack of Ser195 on the carbonyl carbon of the substrate, which leads to the breaking of the peptide bond. The intermediate has four bonds around the central carbon, which creates significant electronic strain due to the forced angles and electron repulsion between the atoms. This results in a relatively high-energy transition state. However, this intermediate is stabilized by the oxyanion hole, a structural feature in the enzyme's active site. The oxyanion hole stabilizes the negatively charged oxygen in the intermediate, which helps to lower the energy of the transition state and thus facilitates the reaction. Despite this stabilization, the tetrahedral intermediate remains a transient high-energy state, quickly proceeding to the breakdown stage via proton transfer from His57 to release the cleaved peptide and regenerate the serine residue.

Boronic acids can interfere with this catalytic mechanism due to their Lewis acid properties, which enable them to interact with nucleophilic centres, particularly the hydroxyl group of Ser195. When boronic acids are used as inhibitors, they can form a stable, high-energy tetrahedral adduct with the serine residue in the active site, preventing the enzyme from progressing through the catalytic cycle. The boronic acid traps the hydroxyl group of Ser195 in the tetrahedral configuration, preventing it from attacking the substrate. This inhibition halts the enzymatic cleavage of the peptide bond, effectively blocking the protease activity. Thus, while the high-energy tetrahedral intermediate formed during normal catalysis, the boronic acid-

mediated adduct prevents the enzyme from reaching the transition state required for peptide bond cleavage, leading to enzyme inhibition (Smoun R. *et al.,* 2012). This ability of boronic acids to inhibit serine proteases has vast therapeutic potential, particularly in the treatment of viral infections, cancers, and inflammatory diseases where serine proteases play crucial roles in disease progression. Moreover, the specificity of boronic acids for the catalytic serine hydroxyl group ensures that they can selectively modulate enzyme activity without causing widespread disruption to other biological processes.

A



B

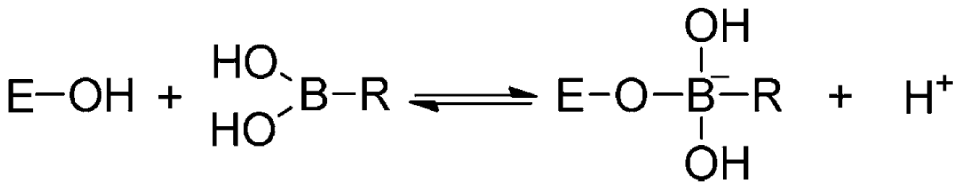


Figure 15. **(A)** General mechanism of reaction for serine proteases; **(B)** Reaction of the transition state analog inhibitors (boronic acids) with serine peptidase (Smoun R. *et al.,* 2012).

3.4 Boronic acid in medical applications

The ability of boron to interfere with serine proteases makes it highly interesting in pharmacological applications. Rather than focusing solely on its activity against serine proteases, the discussion should be expanded to include proteases in general, as well as the broad range of applications resulting from this activity. This could manifest in pharmacological effects applicable to various diseases, including chemotherapy and treatments for microbial infections. Beyond proteases, boronic acids also demonstrate activity against other types of targets, such as transcription factors, receptors, and other proteins. This expanded view reveals a wide range of potential pharmacological applications, offering therapeutic possibilities for diverse conditions. These include chemotherapy and treatments for microbial infections and other pathologies, positioning boron-based compounds as versatile tools in developing novel treatments across multiple medical fields.

Interest in boron for pharmacological purposes has grown since the 1970s, but it was only in the early 2000s that the first boron-based drug was approved. Specifically, bortezomib, approved in 2004, became the first boron-based compound approved for medical use. Bortezomib (or Velcade) is a proteasome inhibitor used in the treatment of multiple myeloma. The development of this molecule was based on the structure of the first synthetic proteasome inhibitor, the aldehyde proteasome inhibitor, where the aldehyde group was replaced with a boronic acid. This substitution enhances the molecule's activity, improving selectivity and low dissociation rates from the proteasome's active site. In this case, the boronic acid is responsible for destroying the NF-κB protein complex, promoting apoptosis in tumor cells.

Several years after the introduction of bortezomib, other boron-based molecules were approved: Ixazomib in 2016, with the exact mechanism of action as bortezomib, and Vaborbactam in 2017. Vaborbactam, however, is used in antimicrobial therapy. It is a cyclic boronic acid that inhibits β-lactamases, often used in combination with antibiotics to treat urinary and abdominal infections. Boronic acids inhibit these enzymes by interfering with their catalytic activity through interaction with the serine residue in the active site. Since β-lactamases open the β-lactam ring of antibiotics, combining these antibiotics with inhibitors like Vaborbactam restores the antibiotic's effectiveness, even against microorganisms resistant to β-lactams due to the expression of these enzymes.

Boronic acids also exhibit activity against penicillin-binding proteins (PBPs), transpeptidases involved in bacterial cell wall synthesis. Inhibiting these enzymes interferes with the synthesis and integrity of the bacterial cell wall (Zervosen A. *et al.,* 2012). Another interesting bacterial target is *Staphylococcus aureus*'s

chromosomal NorA efflux pump, which is part of the drug resistance mechanisms. Pyridine-3-boronic acid derivatives have shown promise as inhibitors of this efflux pump (Fontaine F. *et al.,* 2015). In the field of antimicrobial therapy, Tavaborole is another notable compound. Tavaborole is an inhibitor of leucyl-tRNA synthetase, used explicitly for treating onychomycosis. This drug, classified as a benzoxaborole with a fluorine atom in position 5, was approved by the FDA and EMA and has been in use since 2014 in the USA (Gupta G. *et al.,* 2015).

Boron derivatives are also being explored in antiviral therapy, proving promising for treating infections caused by viruses such as HIV. Boronic compounds show potential on two distinct viral targets: the Rev protein and the HIV-1 protease. The Rev protein, necessary for viral genome replication, can be inhibited through small molecules known as branched peptides, with boronic acids enhancing their activity (Wynn J.E. *et al.,* 2016). The HIV-1 protease, involved in viral replication, catalyzes a reaction involving Asp30, and boronic acid derivatives show competitive inhibition with K_i values in the picomolar range, much lower than those of approved antiviral drugs (Windsor I.W. *et al.,* 2018). Another significant target is the N63 protease of the Hepatitis C virus (HCV), which plays a role in mature virus formation. The most well-known inhibitor of this enzyme is boceprevir. Researchers have synthesized new N63 inhibitors by modifying boceprevir with boronic acid derivatives, achieving highly active compounds with Ki values in the nanomolar range (Venkatraman S. *et al.,* 2009).

Boron also reacts with diols, forming covalent but reversible bonds, a property that can be leveraged to create sensors, such as those for carbohydrates, helpful in monitoring diseases like diabetes. This is achieved by complexing phenylboronic acid with poly (L- and D-lysine) to create a glucose sensor that functions optically. Boronic acid sensors may also be employed in diabetic patients for insulin delivery (Brooks W.L. *et al.,* 2016). These sensors are incorporated into hydrogels, which trap and release insulin in response to increased glucose concentrations. Another boron-based drug in therapeutic use is Crisaborole. This drug shares the same core structure as Tavaborole and is used for treating atopic dermatitis due to its role as a phosphodiesterase 4 (PDE4) inhibitor (Jarnagin K. *et al.,* 2016; Silva M.P. *et al.,* 2020).

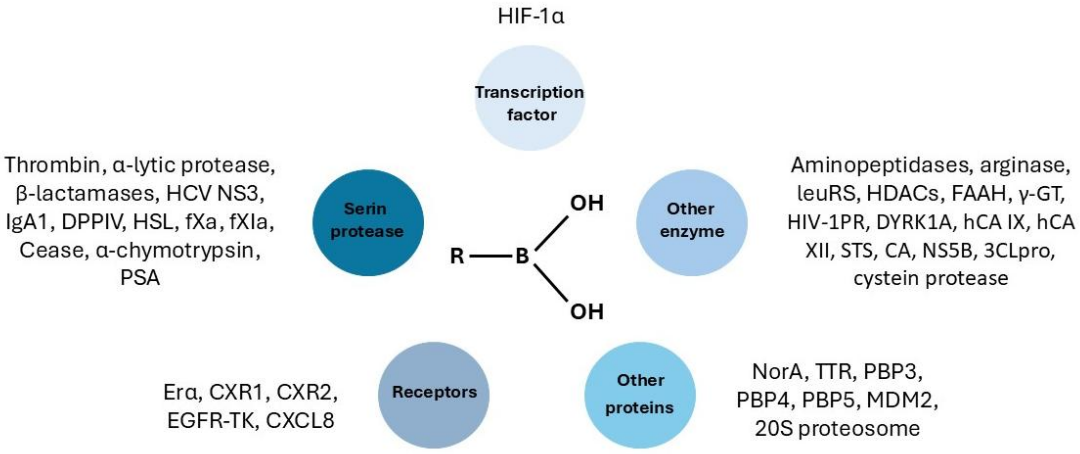


Figure 16. Molecular targets of boronic acids. The image was inspired by Silva M.P. *et al.*, 2020 and made using PowerPoint.

CHAPTER IV

Aim of the work

Given LexA's pivotal role in the SOS response and, more generally, in regulating bacterial pathogenicity mechanisms, this protein emerges as a promising therapeutic target for combating the ongoing evolution of antimicrobial resistance (AMR).

From a biochemical perspective, LexA exhibits significant similarities with serine proteases, as it uses the catalytic dyad Ser119/Lys156 for its self-cleavage. The concept of treating LexA like serine proteases has been explored, and its inhibition potential through boronic acids has been successfully demonstrated.

Boron is a metalloid characterized by an electronic deficiency that explains its remarkable reactivity and tendency to form bonds with atoms capable of donating electron pairs. Physiologically, boron behaves as a Lewis acid, tending to form tetrahedral anionic intermediates and demonstrating the ability to react with the nucleophilic centres of biological macromolecules. These tetrahedral anions have a structure like the high-energy tetrahedral intermediate formed during reactions catalyzed by serine proteases. Consequently, boronic acids are excellent inhibitors of such enzymes and, by structural analogy, of LexA.

The potential of boron to inhibit LexA has already been adequately demonstrated. Based on this premise, this study aimed to identify new boron-containing molecules capable of interfering with LexA hydrolysis using a drug-repurposing approach.

To achieve this, the assays employed were not limited to understanding the biochemical aspects; they also, and perhaps more importantly, focused on the phenomenon from a phenotypic perspective, assessing the inhibition of two critical processes associated with the SOS response: filamentation and biofilm formation.

CHAPTER V

Materials and methods

5.1 Organisms

For this study, two strains of *E. coli* were used: *E. coli* BL21(DE3) with genotype F- *ompT gal dcm lon hsdS*$_b$(*r*$_b^-$*m*$_b^-$) *λ*(DE3 [*lacI lacUV5-t7p07 ind1 sam7 nin5*]) [*malB*$^+$]$_{k\text{-}12}$(λ^s) was purchased from Sigma-Aldrich (Milan, Italy), and *E. coli* ATCC® 25922 came from stock we had collected in our laboratory.

5.2 Antibiotic and boron compounds

We used one antibiotic, levofloxacin (LVX), purchased from Sigma-Aldrich, and a total of 21 boron-containing drugs: a first group of 8 compounds selected through a drug repurposing approach and a second group of 13 benzoxaboroles. The first group belonged to: 1-Hydroxy-3H-2,1-benzoxaborole was from Sial (Roma); Tavaborole, Crisaborole, Talabostat, Ixazomib, Vaborbactam, Delanzomib and Bortezomib were from Vinci-Biochem (Firenze) (**Table 1**). The second group belonged to: 6-amino benzo[c][1,2]oxaborol-1(3H)-ol; 6-nitrobenzo[c][1,2]oxaborol-1(3H)-ol; 6-amino-3,3-dimethylbenzo[c][1,2]oxaborol-1(3H)-ol; 3,3-dimethyl-6-nitrobenzo[c][1,2]oxaborol-1(3H)-ol; 3,3-dimethylbenzo[c][1,2]oxaborol-1(3H)-ol; 1-hydroxy-1,3-dihydrobenzo[c][1,2]oxaborole-5-carboxylic acid; 1-hydroxy-1,3-dihydro-2,1-benzoxaborole-6-carboxylic acid; 1,3-dihydro-1-hydroxy-2,1-benzoxaborol-5-ol; 7-metoxybenzo[c][1,2]oxaborol-1(3H)-ol; 3-vinylbenzo[c][1,2]oxaborol-1(3H)-ol; 5-chloro-1,3-dihydro-1-hydroxy-2,1-benzoxaborole; 4-((1-hydroxy-1,3-dihydrobenzo[c][1,2]oxaborol-5yl)oxy) phthalonitrile and benzo[b]thiophen -2-yl boronic acid. All these compounds were purchased from Molport (Latvia) (**Table 2**). For simplicity, a specific nomenclature will be used to name compounds in the relative tables.

5.3 Reagents

Luria-Bertani broth (LB), Tryptic Soy Broth (TSB), and Muller-Hinton broth (MH) were purchased from Lickson (Palermo); Dulbeccos' Phosphate Buffered saline (DPBS), Trizma, Magnesium Clorure ($MgCl_2$), Dimethyl Sulfoxide (DMSO), β-Mercaptoethanol, Fluoroshield with DAPI (4'-6-diamidino-2-phenylindole), p-formaldehyde (powder), Glutaraldehyde 25%, Hexamethyldisilazane (HMDS),

Ethanol absolute, Methanol absolute, Acetic Acid absolute, Acetone absolute, Crystal Violet (CV, powder) were purchased from Sial (Roma). Glycerole, Potassium monobasic phosphate, Potassium dibasic phosphate, Ferrous sulfate heptahydrate ($FeSO_4$ ×$7H_2O$), Magnesium sulfate ($MgSO_4$), Ammonium sulfate ($(NH_4)_2SO_4$), Dithiothreitol (DTT), were purchased from Merck, Sigma-Aldrich (Milano); Blue Coomassie R250 (powder), Mini-PROTEAN® Precast Gel, Tris-Glycine running buffer 10x, 4× Leammli Sample Buffer, poly(dt)36, ATP (powder) Sodium Dodecyl Sulfate (SDS, powder) were purchased from Bio-Rad (Milano).

Table 1. Boronic compounds selected by drug repurposing approach.

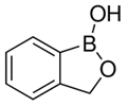
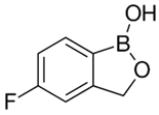
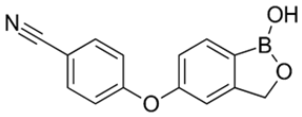
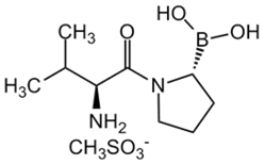
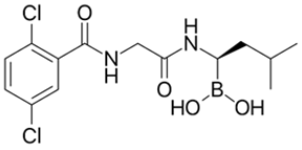
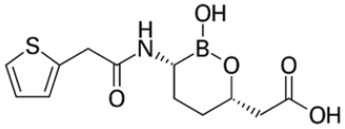
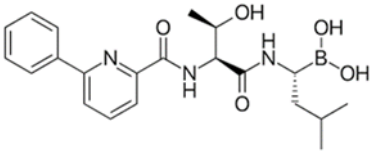
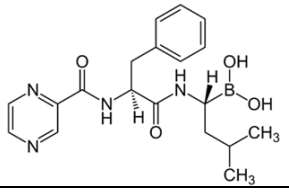
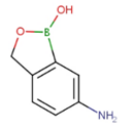
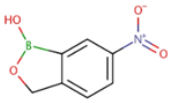
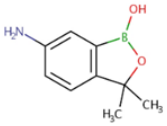
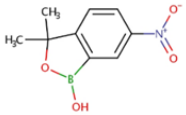
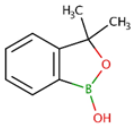
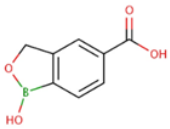
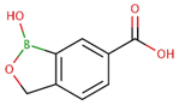
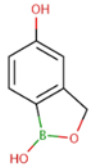
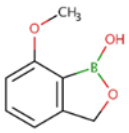
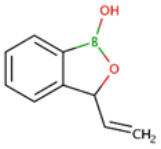
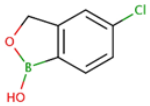
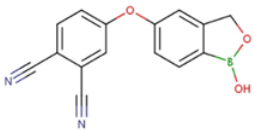
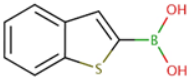
Boronic compounds		
Structure	**Name**	**Code**
	1-hydroxy-3H-2,1-benzoxaborole	**1**
	Tavaborole	**2**
	Crisaborole	**3**
	Talabostat	**4**
	Ixazomib	**5**
	Vaborbactam	**6**
	Delanzomib	**7**
	Bortezomib	**8**

Table 2. Benzoxaboroles selected to evaluate the effect of different substituents on the same scaffold.

Benzoxaboroles		
Structure	**Name**	**Code**
	6-amino benzo[c][1,2]oxaborol-1(3H)-ol	**A**
	6-nitrobenzo[c][1,2]oxaborol-1(3H)-ol	**B**
	6-amino-3,3-dimethylbenzo[c][1,2]oxaborol-1(3H)-ol	**C**
	3,3-dimethyl-6-nitrobenzo[c][1,2]oxaborol-1(3H)-ol	**D**
	3,3-dimethylbenzo[c][1,2]oxaborol-1(3H)-ol	**E**
	1-hydroxy-1,3-dihydrobenzo[c][1,2]oxaborole-5-carboxylic acid	**F**
	1-hydroxy-1,3-dihydro-2,1-benzoxaborole-6-carboxylic acid	**G**
	1,3-dihydro-1-hydroxy-2,1-benzoxaborol-5-ol	**H**
	7-metoxybenzo[c][1,2]oxaborol-1(3H)-ol	**I**
	3-vinylbenzo[c][1,2]oxaborol-1(3H)-ol	**J**
	5-chloro-1,3-dihydro-1-hydroxy-2,1-benzoxaborole	**K**
	4-((1-hydroxy-1,3-dihydrobenzo[c][1,2]oxaborol-5yl)oxy) phthalonitrile	**L**
	Benzo[b]thiophen -2-yl boronic acid	**M**

5.4 RecA and LexA cloning and purification

RecA and LexA proteins were previously cloned and purified in our laboratory (Bellio *et al.,* 2017; Bellio *et al.,* 2020). Briefly, genes *recA* and *lexA*, encoding respectively for RecA and LexA proteins, were cloned separately, into pET28b(+) expression vector and were used *E. coli* JM109 (DE3) competent cells with genotype *endA1, recA1, gyrA96, thi, hsdR17 (rk^-, mk^+), relA1, supE44, λ–, Δ(lac-proAB), [F´, traD36, proAB, $lacI^qZ\Delta M15$],* λDE3, for proteins expression.
RecA protein purification was obtained with two His Trap FF 1 ml columns in series, and LexA protein purification was performed in HiTrap FF column. The proteins were quantified using Bradford assay, and their pureness was estimated using SDS-Page.

5.5 *In vitro* susceptibility test

The microdilution method was used to determine MIC values of LVX and boronic derivatives in a U-bottom 96-well polystyrene microtiter plate. Levofloxacin was dissolved in distilled water, and boronic acids were dissolved in DMSO. *E. coli* BL21 (DE3) and *E. coli* ATCC® 25922 were grown in MH at 37°C overnight in an orbital shaker. The O/N culture was diluted in 0.9% NaCl. 100µL of bacterial suspension was added to a plate already containing 100 µL of antibiotic or boron compound to reach a final concentration of 5×10^5 CFU/mL, for a final volume of 200 µL. Every compound was tested by serial double dilution in MH cation adjusted broth at concentrations ranging from 8 µg/mL to 3.9×10^{-3} µg/mL for LVX, from 1024 µg/mL to 0.5 µg/mL for **1** and compounds from **A** to **M**, and from 128 µg/mL to 0.0625 µg/mL for compounds from **2** to **8**. Positive control and negative control are also added. The plates were incubated for 18h at 37°C in static conditions. The growth in each well was quantified spectrophotometrically at $\lambda\ 595_{nm}$ by a microplate reader Beckman Coulter DTX-880 (Multimode Detector), and the percentage growth was calculated as:

$$\frac{OD_{drug\ containing\ well} - OD_{background}}{OD_{drug\ free\ well} - OD_{background}}$$

The microorganisms-free wells represented the background. The MIC value for the tested compounds is the concentration of the drug at which an 80% reduction in microbial growth occurs, compared to the growth of microorganisms in the absence of the drug (drug-free wells). The MIC value for every compound was reported by the median of three independent experiments.

5.6 Filamentation assay

The filamentation assay was performed following the indications of Bellio P. *et al.,* 2020. First of all, it was determined which of the two strains was best to use for this purpose. LVX was used as a filamentation inducer, testing it at concentrations ranging from its MIC value down to 0.0313×MIC. Incubation times were varied, with samples incubated for 3, 4, and 5 hours. After this evaluation, *E. coli* BL21(DE3) was selected for the whole filamentation assay, and LVX at 9.75×10^{-4} µg/mL value was used as a filamentation inductor. Bacteria were cultured in LB and incubated at 37°C overnight in an orbital shaker in anaerobic conditions; the O/N culture was diluted in fresh LB to reach a final concentration of 10^6 CFU/mL and dispensed in glass tubes. A combination of the boron compounds, at concentrations ranging from MIC to 0.0313×MIC value, and LVX was added to 800 µL of culture, reaching a final volume of 1 mL. LVX at 9.75×10^{-4} µg/mL, boronic compounds alone at various concentrations, and drug-free control were included. After 3h at 37°C of incubation in an orbital shaker, the cultures were transferred in 1.5 mL microtubes, centrifugated at 14,000 rpm for 10 min at 4°C, and then washed with PBS. These steps were repeated three times. The pellets were resuspended in 4% p-formaldehyde (in PBS) and incubated in ice for 30 min. After this step, the p-formaldehyde was removed by washing it in PBS. Finally, the pellets were resuspended in 100 µL of PBS, spotted in polylysine glass slides, and air-dried overnight at room temperature. Fluoroshield with DAPI is added, and a fluorescence microscope is used to observe the filamentation. The filaments were measured, and the results were expressed, such as the % of reduction of filament length compared to the filament length obtained with levofloxacin alone. The experiments were repeated three times.

5.7 Inhibition assay of LexA by alkaline-induced autohydrolysis

LexA autoproteolysis has been obtained following the indication by Mo C.Y. *et al.,* 2014, with some modifications. The self-cleavage was performed by adding cleavage buffer (100 mM Tris-Glycine; 300 mM NaCl; pH=10.6) to 7.5 µg of LexA protein. To evaluate the inhibitor potentialities, LexA concentration was fixed at 12.4 µM, corresponding to 7.5 µg of protein, and it was estimated the 1000:1 [Bor]:[LexA] ratio. The reactions were conducted at 37°C for 30 minutes. After a preliminary evaluation of the inhibitor potentialities, the same reaction was performed with a previous incubation between LexA and the boron compounds at 30°C for 15 minutes, followed by adding the buffer. The reactions were stopped by adding 4× Laemmli Sample Buffer, with β-Mercaptoethanol at a final concentration of 2.36 M; the samples were boiled at 100°C for 7 min to get the denaturation and transferred

onto Mini-PROTEAN® Precast Gel and resolved on SDS-page. The running buffer was 10X Tris/Glycine/SDS electrophoresis buffer, and the runner condition was 50 mA, with variable voltage, for 40 minutes. The gels were stained with staining solution (Coomassie Blue R250 0.1% (w/v); 45% methanol and 10% acetic acid) for 1.5 minutes in a microwave and de-stained with destaining solution (40% ethanol and 10% acetic acid) for 3h in shaker condition. The gels were visualized by ChemyDoc XRS+ System (*Bio Rad*). The uncleaved LexA is reported as the mean of residual fraction obtained in three independent experiments.

5.8 Co-protease activity and determination of half-maximal inhibitory concentrations

The IC_{50} values for the selected boron compounds were determined by evaluating the co-protease activity RecA/LexA. Set the LexA concentration at 12.4 μM, several [Bor]:[LexA] ratios were evaluated, such as 0:1, 100:1, 250:1, 500:1, 750:1, and 1000:1. To trigger the activation of RecA (1.29 μM), and thus the subsequent self-cleavage of LexA, the reaction requires the presence of 5.74 μM poly(dt)36 and 500 μM ATP. A mix containing LexA, RecA, poly(dt)36 and Assay Buffer (20 mM Tris HCl pH 7.5; 8 mM MgCl2; 1 mM DTT) was prepared. Firstly, the inhibitors were incubated with LexA at 30°C for 15 min, and subsequently, the reaction was activated by adding ATP and conducted at 30°C for 10 minutes. Negative and positive controls are also added. The reactions were stopped with 4× Laemmli Sample Buffer with β-Mercaptoethanol, at a final concentration of 2.36 M, and followed the same conditions as above (**5.7**). The IC_{50} values were calculated by the residual fraction of uncleaved LexA obtained in three independent experiments. The residual fraction of uncleaved LexA (***Fu***) was calculated using the following formula:

$$Fu = \frac{\frac{LexA_I}{RecA_I} - \frac{LexA_{C+}}{RecA_{C+}}}{\frac{LexA_{C-}}{RecA_{C-}} - \frac{LexA_{C+}}{RecA_{C+}}}$$

$\boldsymbol{LexA_I}$ is the residual LexA in the treated samples; $\boldsymbol{LexA_{C+}}$ is the residual LexA in the positive control sample; $\boldsymbol{LexA_{C-}}$ is the residual fraction in the negative control sample; $\boldsymbol{RecA_I}$ is the RecA in the treated sample; $\boldsymbol{RecA_{C+}}$ is the RecA in the positive control sample and $\boldsymbol{RecA_{C-}}$ is the RecA in the negative control sample.

5.9 Biofilm assay

The indication by Merritt J.H. *et al.,* 2005 was used for performing the biofilm assay with some modifications. Initially, it was determined which between *E. coli* ATCC® 25922 and *E. coli* BL21(DE3) was better for conducting biofilm experiments. Bacteria were cultured in LB and incubated at 37°C overnight in an orbital shaker in aerobic conditions, followed by a refresh for approximately 2h at the same conditions. When the culture has achieved an optical density at 600nm (OD_{600nm}) around 0.4, it is diluted 1:10 in M63 minimum broth ($(NH_4)_2SO_4$ 15 mM; KH_2PO_4 100 mM; $FeSO_4(\times 7H_2O)$ 1.8 µM) and subsequently dispensed into a 96-well polystyrene flat-bottomed microtiter plate, when it reached a final concentration of around 3×10^7 CFU/mL. After 24h of incubation at 26°C and 37°C in static conditions, the OD_{595nm} was measured to verify the microbial growth with a microplate reader Beckman Coulter DTX-880 Multimode Detector; after, the non-adherent cells were removed, and the plate was gently washed in dH_2O. The biofilm was fixed at 60°C for 1 h, stained with Crystal Violet 0.1%, washed with dH_2O, and air-dried overnight. For the quantitative assay, the CV was solubilized with 80% Ethanol and 20% Acetone for 15 minutes, and then the OD_{595nm} was measured. The quantification of the biofilm formed was determined by applying the following formula:

$$BF = AB - CW$$

$\boldsymbol{BF}$ is biofilm formation, $\boldsymbol{AB}$ is the OD_{595nm} of stained attached bacteria, and $\boldsymbol{CW}$ is the OD_{595nm} of stained control wells containing medium only (Kadurugamuwa J.L *et al.,* 2003). *E. coli* ATCC® 25922 was then selected to conduct the subsequent biofilm experiments.

5.10 Biofilm assay: inhibition and eradication

For the inhibition assay, every compound was tested at a concentration ranging from 128 µg/mL to 0.0625 µg/mL, with six replicates for every concentration. After the culture was dispensed, the boronic compounds were added and incubated at 37°C for 24h in static conditions. Following the same conditions as above. After the 24h-incubation, the biofilm formed in the control and treated wells was quantified, and the results were expressed as the % of reduction of biofilm formation, compared to the inhibitor-free biofilm. The experiments were repeated three times.

For the eradication assay, the boronic compounds were added to a 24-hour mature biofilm and incubated for 96h at 37°C in static conditions (Zhu X. *et al.,* 2022). Every compound was tested at a concentration ranging from 128 µg/mL to 0.0625 µg/mL with six replicates for every concentration. Following the same conditions as above. The results were expressed as the % of eradication of preformed biofilm, compared to the inhibitor-free biofilm. The experiments were repeated three times.

5.11 Biofilm assay: SEM visualization

The sample preparation for visualization at scanning electronic microscopy was performed by using the indication of Marcellini L. *et al*., 2010, with the necessary modifications to adapt the protocol to our needs. Biofilm was cultured in a 24-well polystyrene plate, using a 13mm cover glass as a support for the bacterial adhesion, and incubated at 37°C for 24 hours with the boron compounds. The day after, the medium was eliminated, and the samples were washed twice with KPB 0.1 M and fixed with Glutaraldehyde 2.5 % in KPB 0.1 M at 4 °C for 2 hours. The samples were washed with KPB to eliminate the fixative agent, at 4° C for 10 minutes, four times. The dehydration was obtained by grated ethanol series 30%, 50%, 70%, 80%, 95%, and 100%; in the final step, for full dehydration and drying, we used HMDS, which dried overnight. The cover glasses are mounted on a specific support, stub, and coated with a thin layer of chrome (Cr) using a high vacuum chrome coated and visualized at SEM.

5.12 Molecular docking

The docking between the LexA protein and the boronic compounds under examination was performed using Autodock 4.0 software (https://autodock.scripps.edu/; Morris G.M. *et al.,* 2009). For LexA, the crystallographic structure 1JHF from the Protein Data Bank, G85D mutant, at 1.80 Å resolution (https://www.rcsb.org/structure/1JHF) deposited by Luo, Y., was used. Fifty possible interactions between LexA and each of the candidate boron compounds were simulated. This resulted in the clusters formation, grouped based on the binding energy. The results were visualized using Pymol 3.1 software (https://www.pymol.org/; Schrödinger L. *et al.,* 2020), and the final structure was selected based on the lowest binding energy.

5.13 Software and data analysis

Gels acquisition and bands quantification were obtained with ImageLab™ 6.1 software. Filament lengths were measured with ImageJ 1.53t. Data analysis and non-linear fitting were performed with OriginPro 2018 SR1 (OriginLab).

CHAPTER VI

Results

6.1 Boron compounds selected by drug repurposing approach

6.1.1 Determination of the Minimum Inhibitory Concentrations (MICs)

The microdilution method estimated the susceptibility of *E. coli* BL21(DE3) and *E. coli* ATCC® 25922 to the selected boron compounds. The MIC values for both microorganisms are reported in **Table 3**. The MIC values for LVX are also determined. Among the compounds under examination, except for **1** and **2**, all others had MIC values higher than 128 μg/mL for *E. coli* BL21(DE3) and ATCC® 25922; compound **2** had the lowest MIC value. It should be emphasized that for compounds **3** to **8**, determining values above 128μg/mL was not feasible due to issues with solubility and the concentration of DMSO.

Table 3. MICs value for the boronic compounds selected by drug repurposing approach.

Compound(s)	**MIC value (μg/mL)**	
	***E. coli* BL21 (DE3)**	***E. coli* ATCC® 25922**
levofloxacin	7.8×10^{-3}	3.13×10^{-2}
1	16	8
2	8	8
3	>128	>128
4	>128	>128
5	>128	>128
6	>128	>128
7	>128	>128
8	>128	>128

6.1.2 Filamentation assay

Both *E. coli* ATCC® 25922 and *E. coli* BL21 DE3 were evaluated for their ability to form filaments in the presence of levofloxacin, at various concentrations and incubation times. Six concentrations, from MIC value to 0.0313×MIC, and incubation times of 3, 4 and 5 hours were tested. The results for *E. coli* BL21 DE3 are shown in **Figures 17 and 18**: a 3-hour incubation period is optimal (**Fig.17-A**), as longer incubation leads to increased spontaneous filamentation in the control (**Fig.17**-**B**-**C**). The concentrations of 1.95×10^{-3} µg/mL (**Fig.17**-**J**-**K**-**L**) and 9.75×10^{-4} µg/mL (**Fig.18**-**A**-**B**-**C**) are the concentrations that allow the highest degree of filamentation, and they always yield comparable filamentation results. The ideal concentration of levofloxacin was determined to be 9.75×10^{-4} µg/mL, equivalent to 0.125×MIC value, as it is the lower of the two. The results for *E. coli* ATCC® 25922 are reported in **Figure 19**.

In contrast, achieving comparable filamentation levels in *E. coli* ATCC® 25922 required a higher levofloxacin concentration of 1.56×10^{-2} µg/mL, 0.5×MIC, with a 5-hour incubation period (**Fig.19**-**I**). However, this concentration led to excessive cell death, making it impractical for further analysis. The results for the 0.125×MIC, 0.0625×MIC, and 0.0313×MIC concentrations are not reported, as any of these concentrations, at the various incubation times, could induce filamentation. Consequently, *E. coli* BL21 DE3 was chosen for continued studies, with conditions set at a 3-hour incubation and a concentration of 9.75×10^{-4} µg/mL.

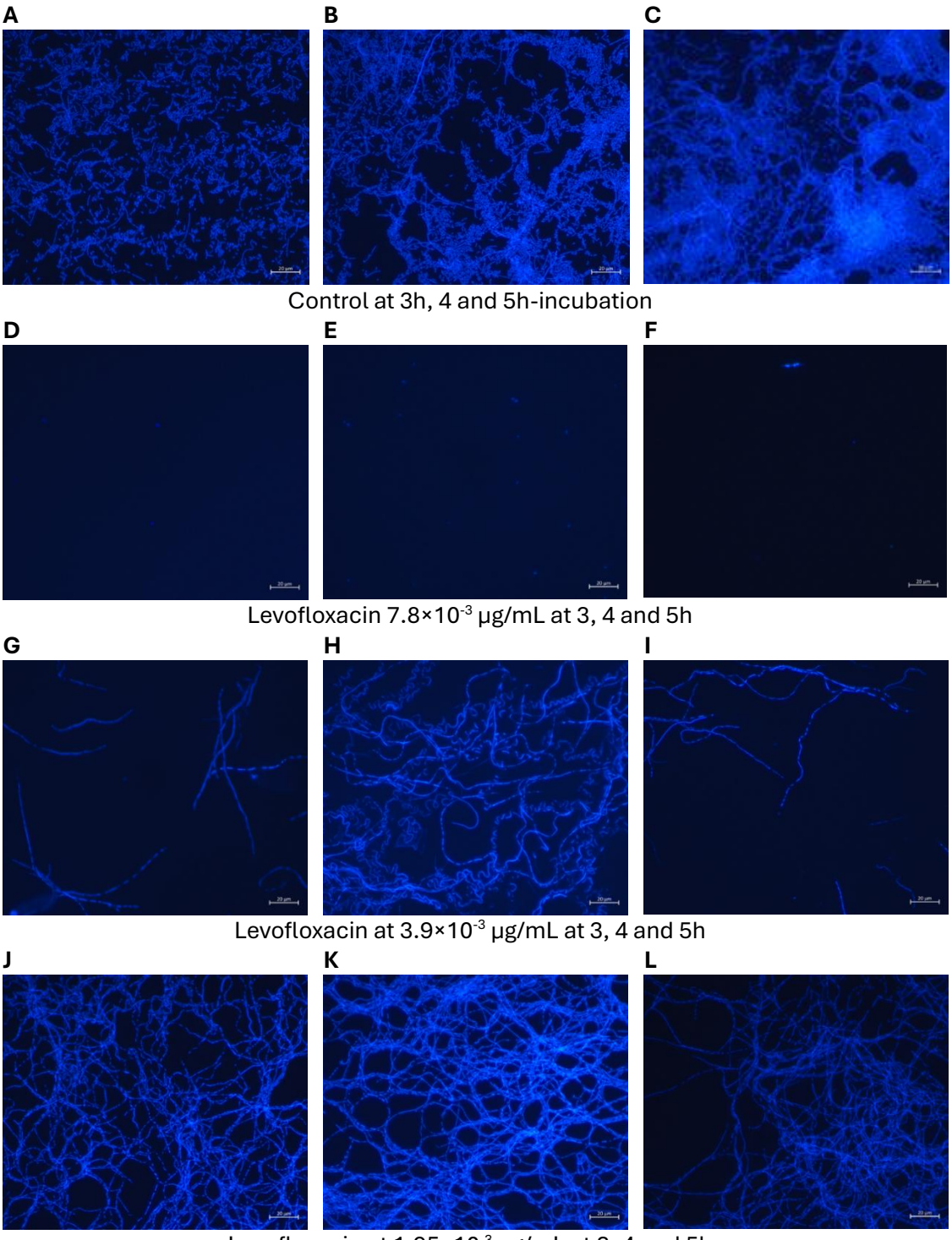


Figure 17. Fluorescence microscopy of *E. coli* BL21 (DE3) at 40x.

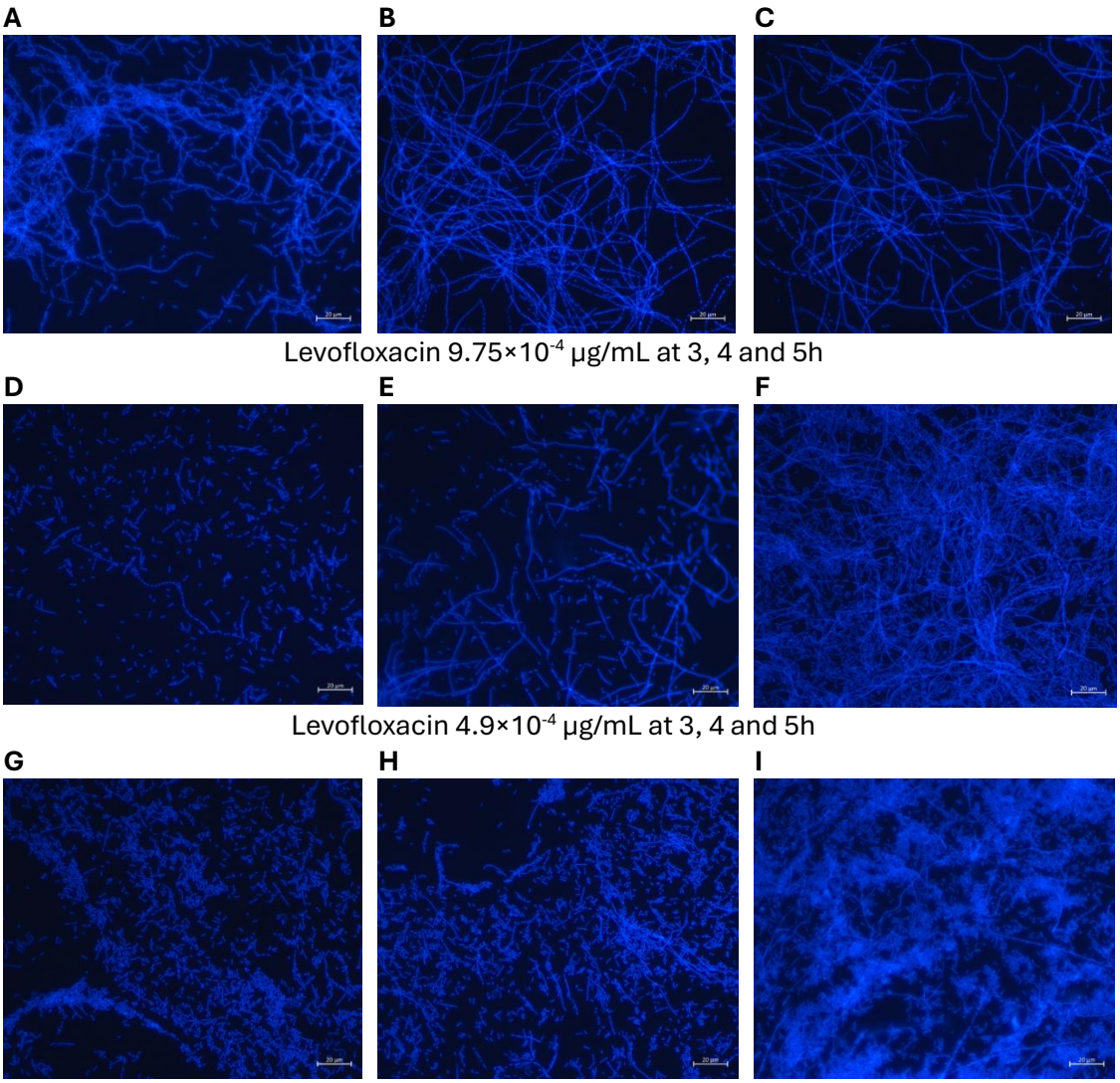


Figure 18. Fluorescence microscopy of *E. coli* BL21 (DE3) at 40x.

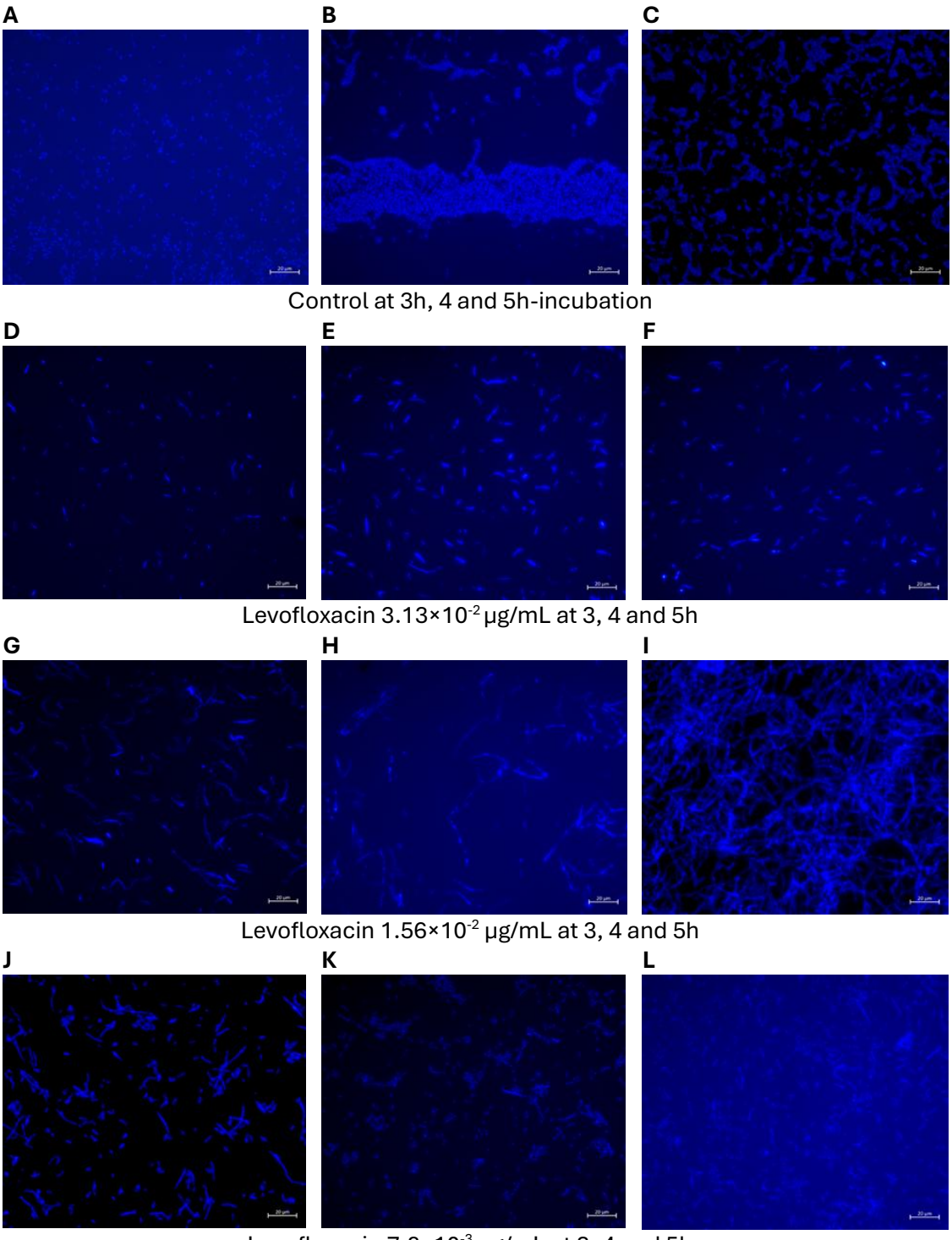


Figure 19. Fluorescence microscopy of *E. coli* BL21 (DE3) at 40x.

The whole filamentation assay was performed in *E. coli* BL21(DE3). The filamentation was induced by a subinhibitory concentration of levofloxacin, corresponding at 9.75×10^{-4} µg/mL. Boron compounds were tested at concentrations corresponding to their MIC values. Every compound was also tested alone, to exclude their ability to induce the phenomenon under examination. In **Figures 20, 21 and 22** we reported the images obtained by fluorescence microscopy: the filamentation was observed when the culture was treated with levofloxacin (**Fig. 20-B**) concerning the untreated control (**Fig.20**-**A**). When boronic is alone, it does not lead to bacterial filamentation (**Fig.20 C-E**; **Fig. 21 A**-**C**; **Fig. 22 A**-**C**-**E**), except for compound **5** (**Fig. 21 E**). When combined with levofloxacin, it was observed a drastic filamentation reduction for compounds **1** and **2** (**Fig. 20 D**-**F**) and for compound **3** the observed reduction was moderate (**Fig. 21 B**). Finally, for compounds **4** to **8**, no reducing capacity is observed in the filamentation process (**Fig. 21 D**-**F**; **Fig. 22 B**-**D**-**F**).

The filamentation assay was further explored for compounds **1**, **2** and **3** by evaluating six concentrations, alone and with levofloxacin combination, from their MIC value up to 1/32.

Figures 23 and **24** report data for **1**, **figures 25** and **26** for **2** and **figures 27** and **28** for **3**. For each of the three compounds, a concentration-dependent effect was found. Whereas for **1** and **2** the reduction in filament length was observed for every concentration tested, for **3** this phenomenon is related to the three higher concentrations. Furthermore, the effect remains moderate in comparison to **1** and **2**.

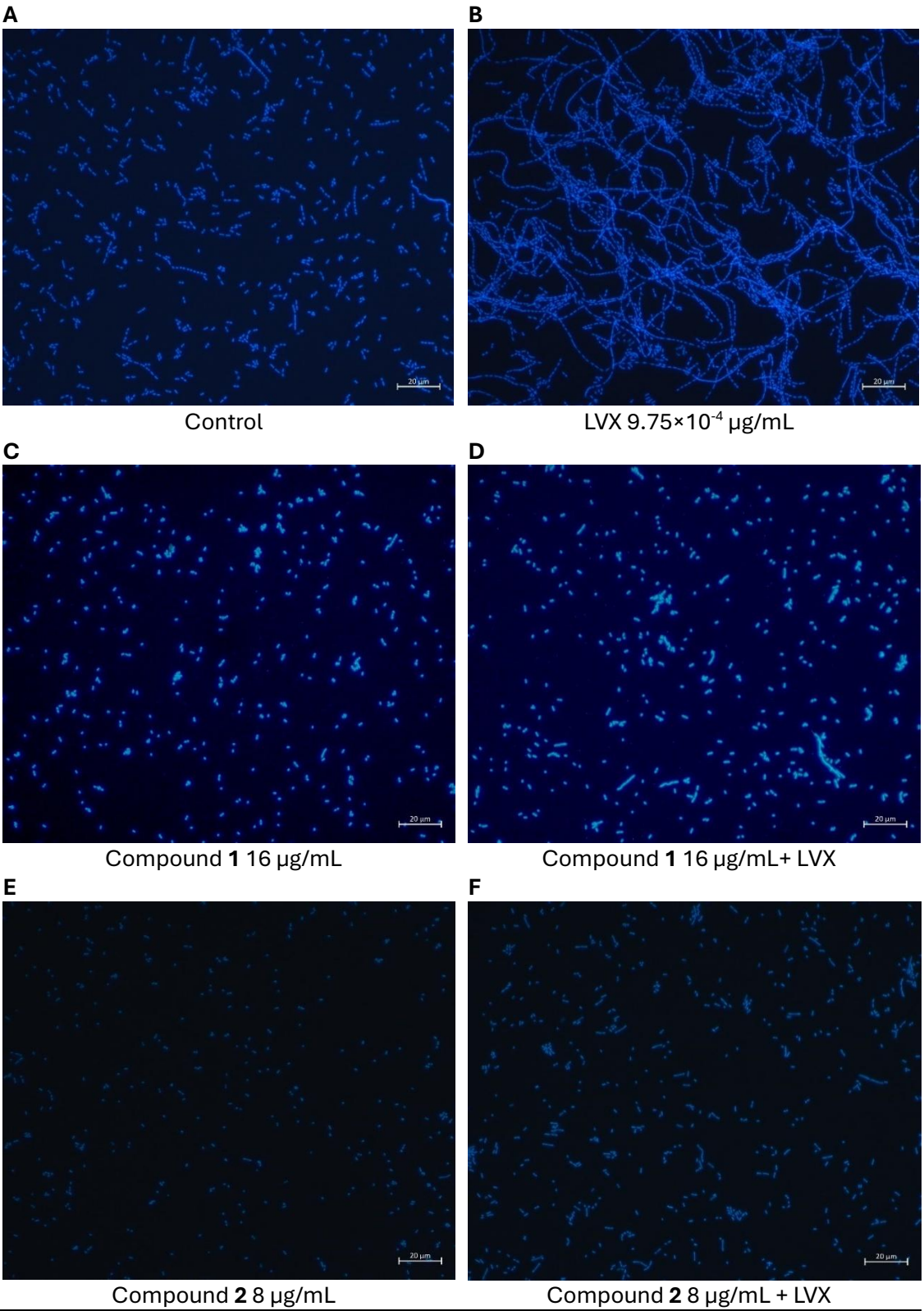


Figure 20. Fluorescence microscopy of *E. coli* BL21(DE3) with DAPI at 40×.

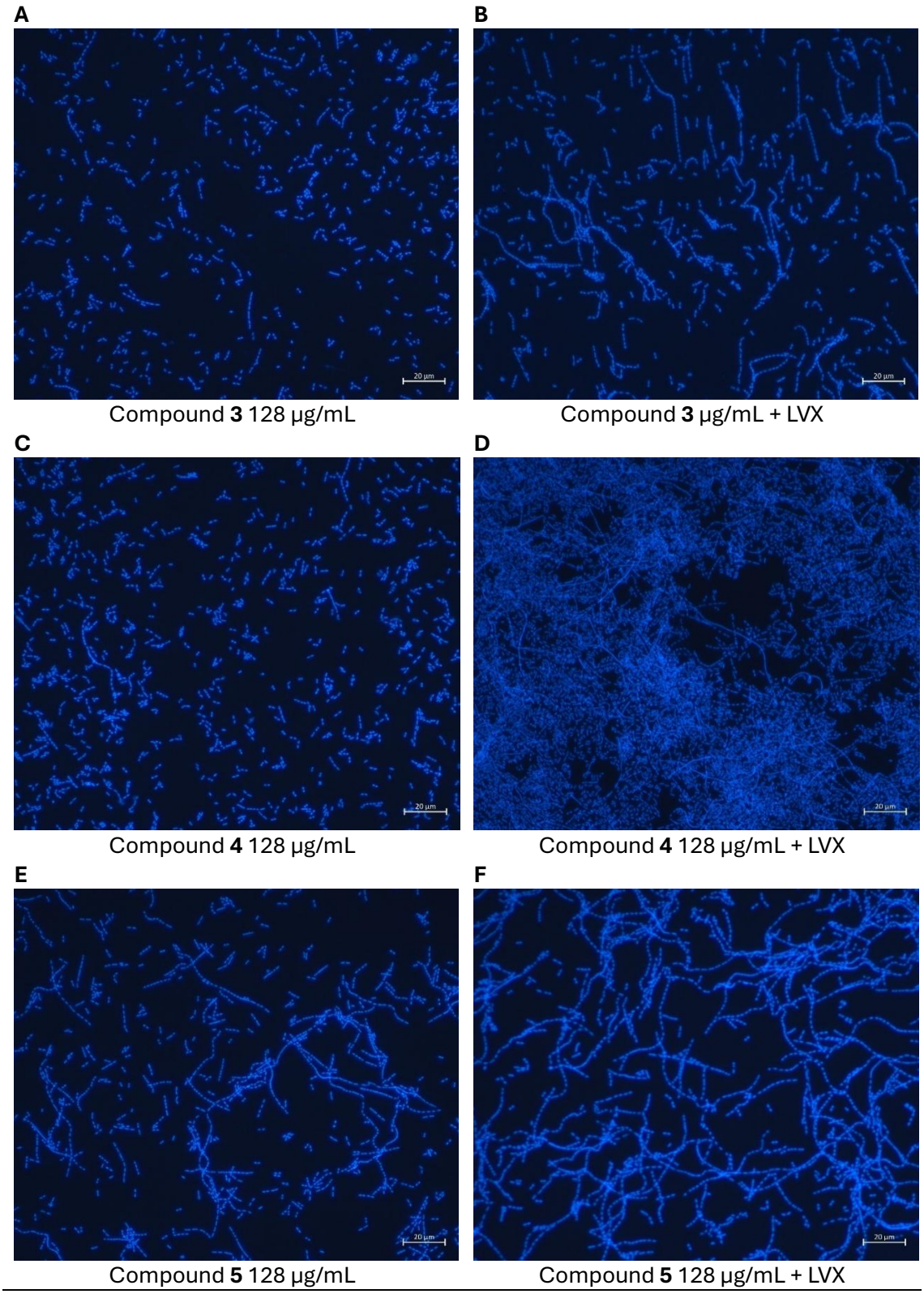


Figure 21. Fluorescence microscopy of *E. coli* BL21(DE3) with DAPI at 40×.

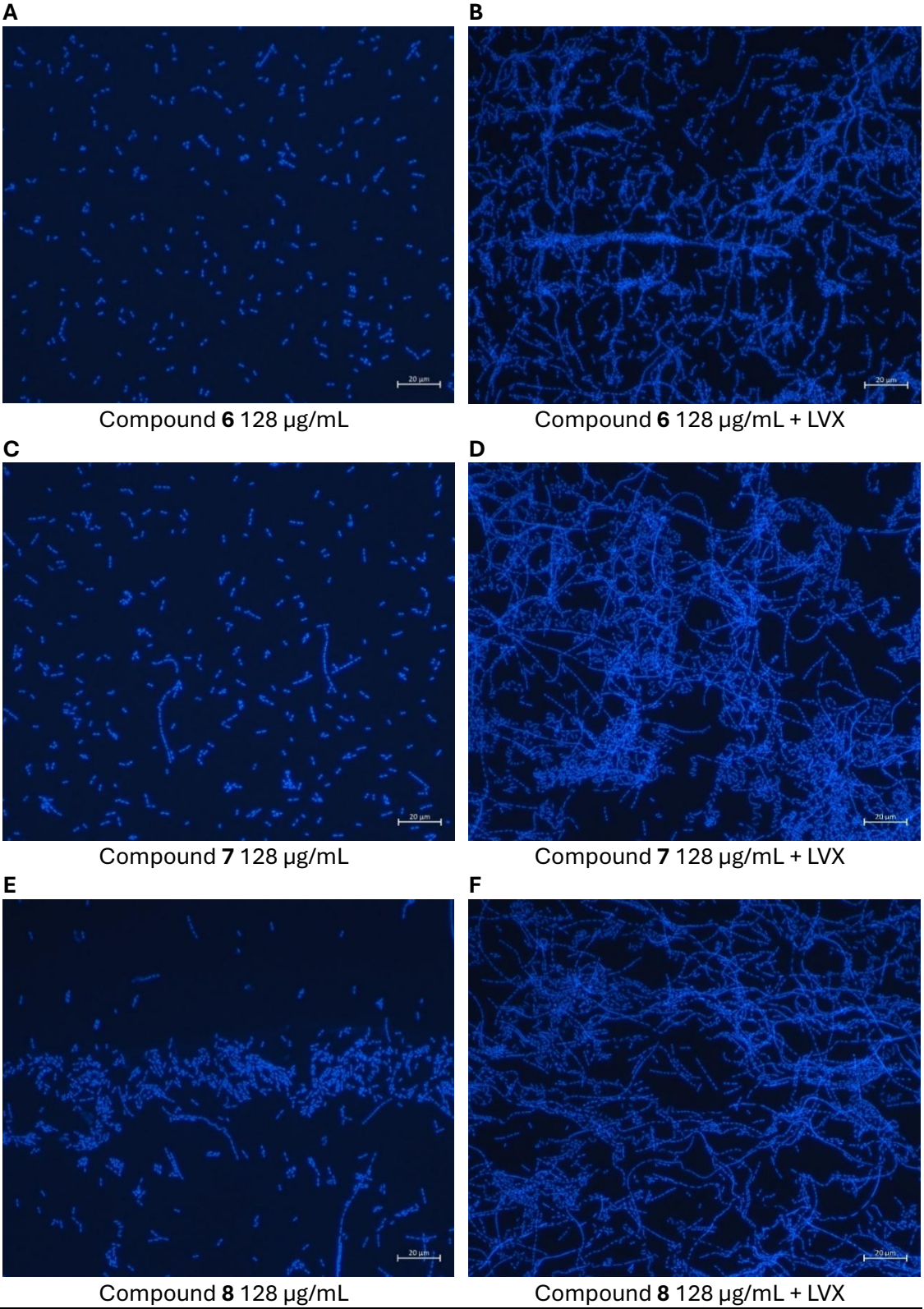


Figure 22. Fluorescence microscopy of *E. coli* BL21(DE3) with DAPI at 40×.

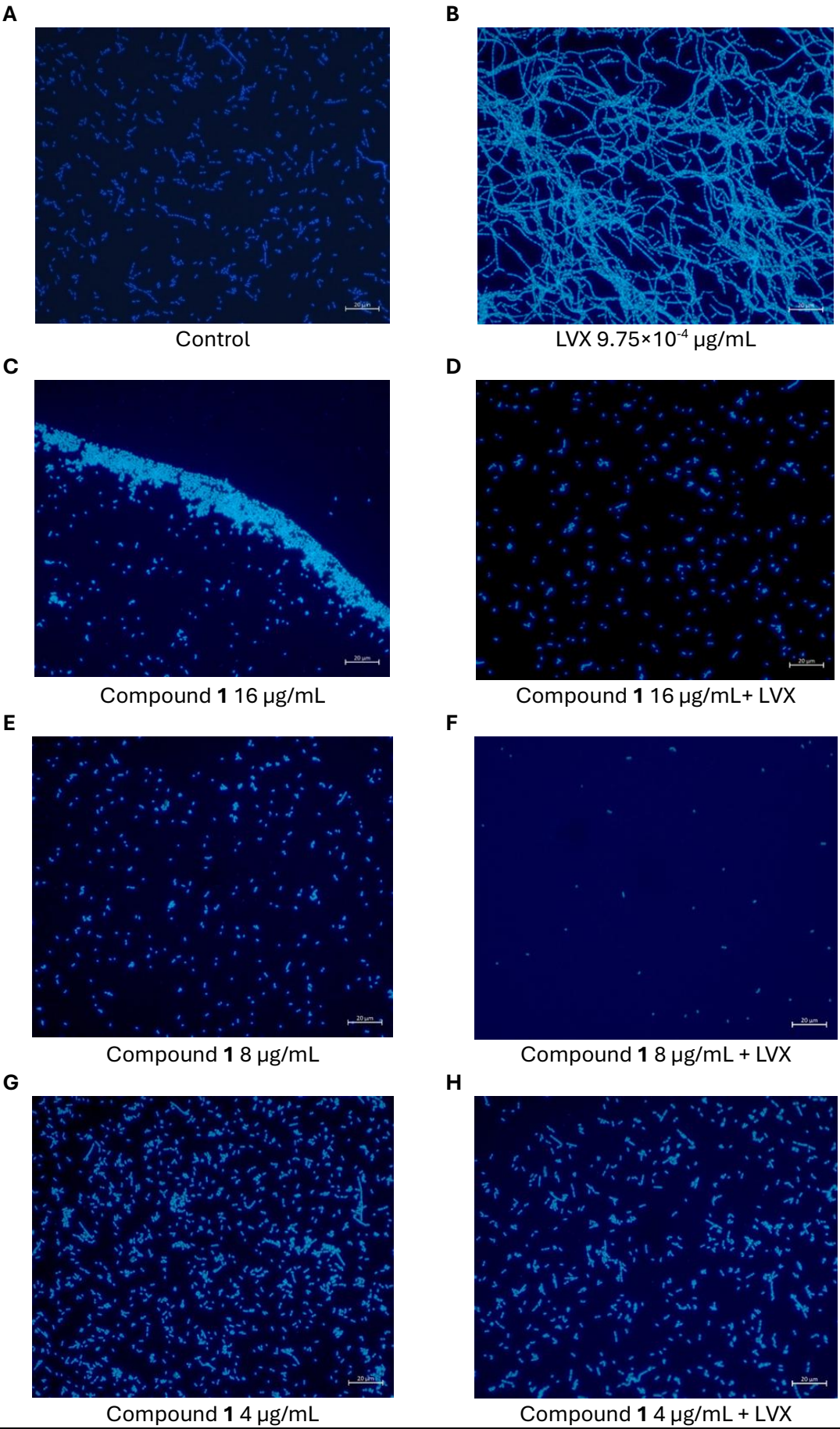


Figure 23. Fluorescence microscopy of *E. coli* BL21(DE3) with DAPI at 40×.

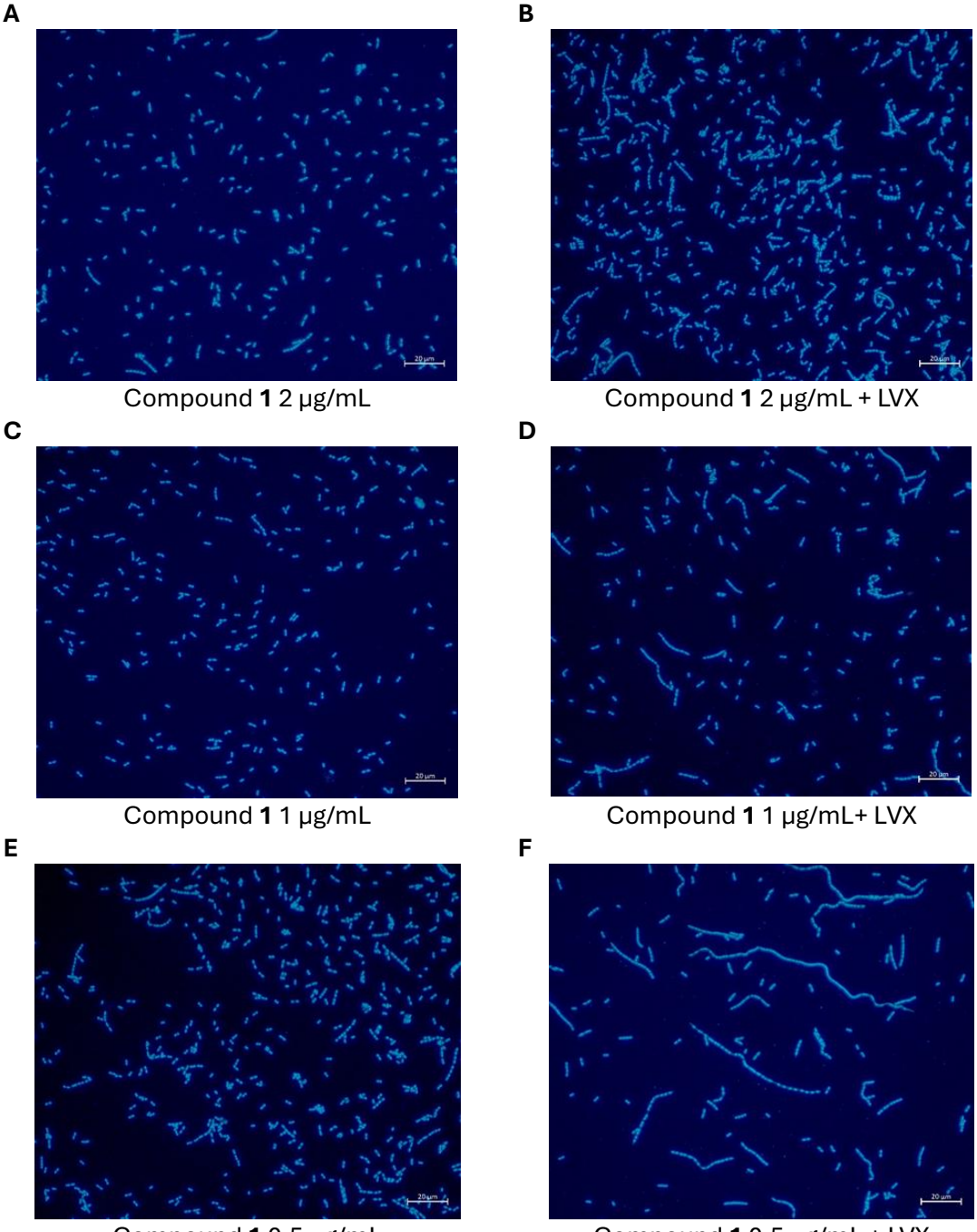


Figure 24. Fluorescence microscopy of *E. coli* BL21(DE3) with DAPI at 40×.

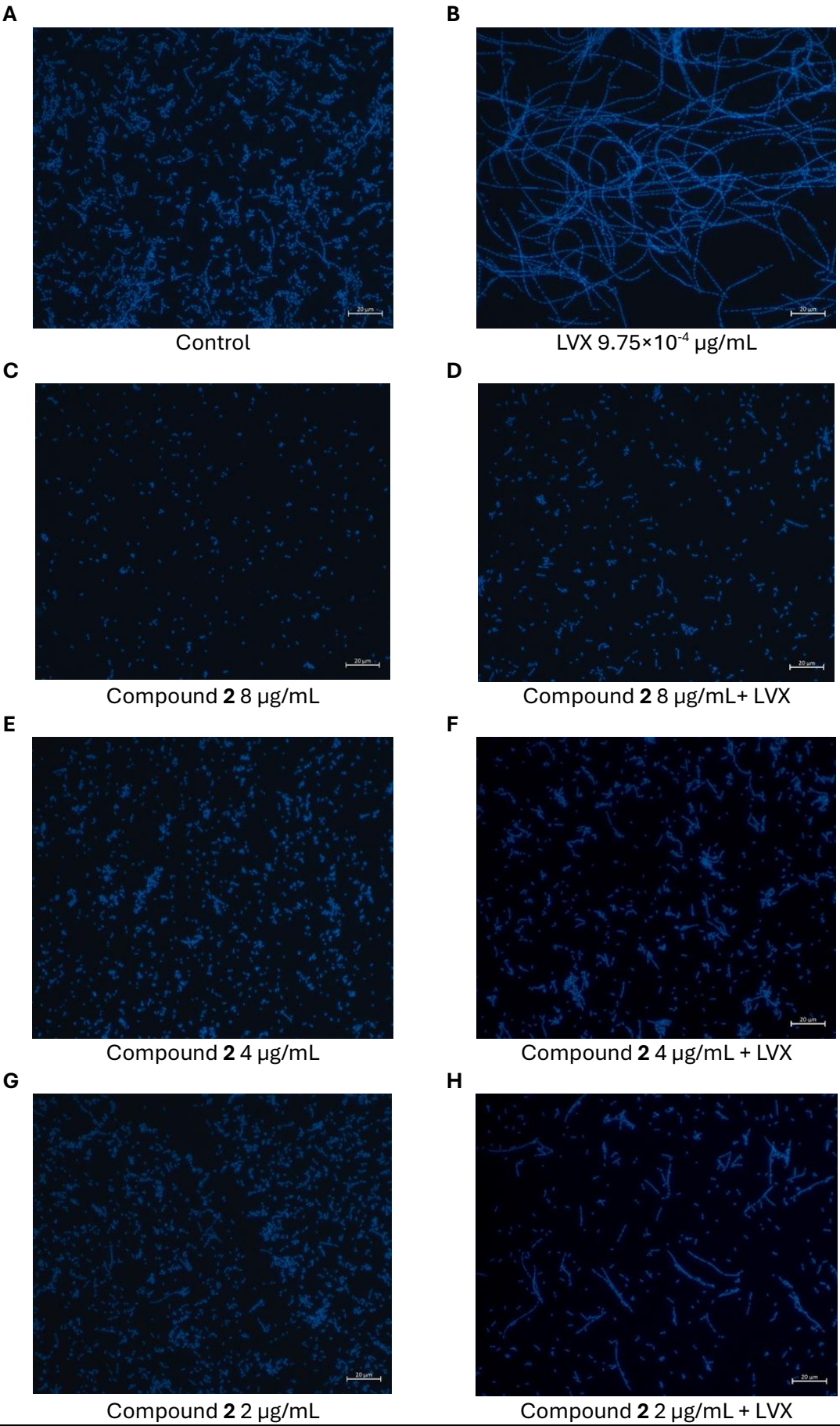


Figure 25. Fluorescence microscopy of *E. coli* BL21(DE3) with DAPI at 40×.

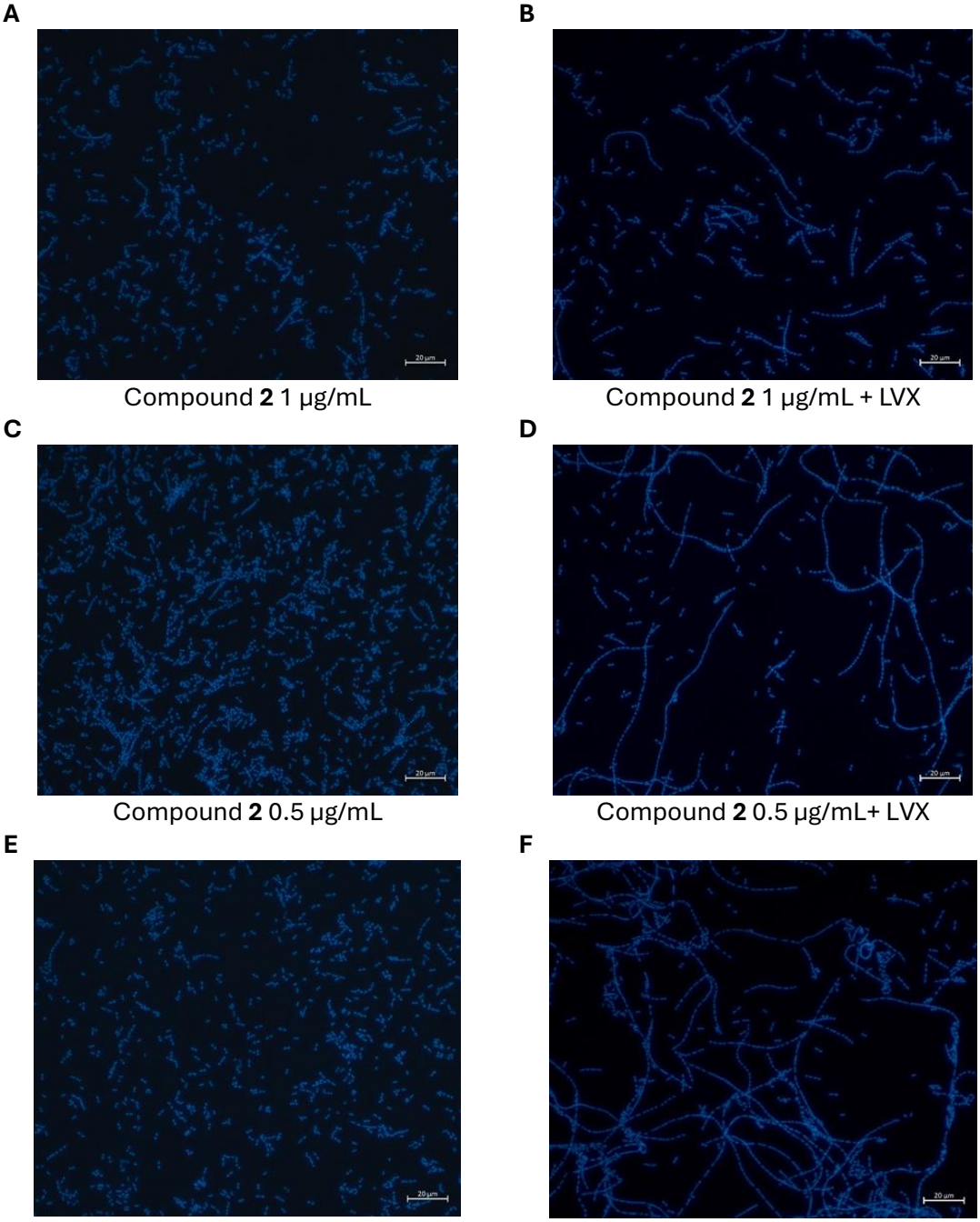


Figure 26. Fluorescence microscopy of *E. coli* BL21(DE3) with DAPI at 40×.

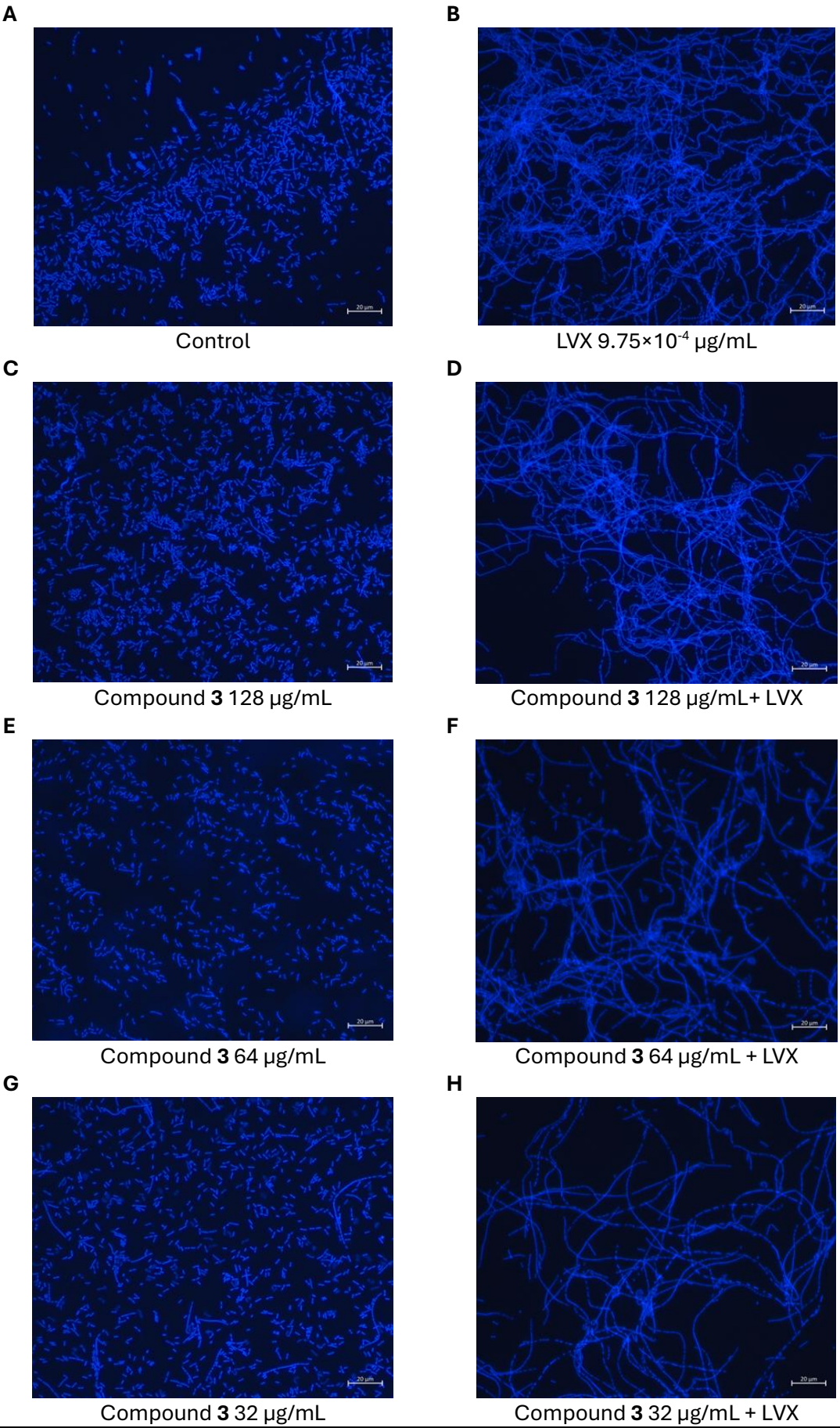


Figure 27. Fluorescence microscopy of *E. coli* BL21(DE3) with DAPI at 40×.

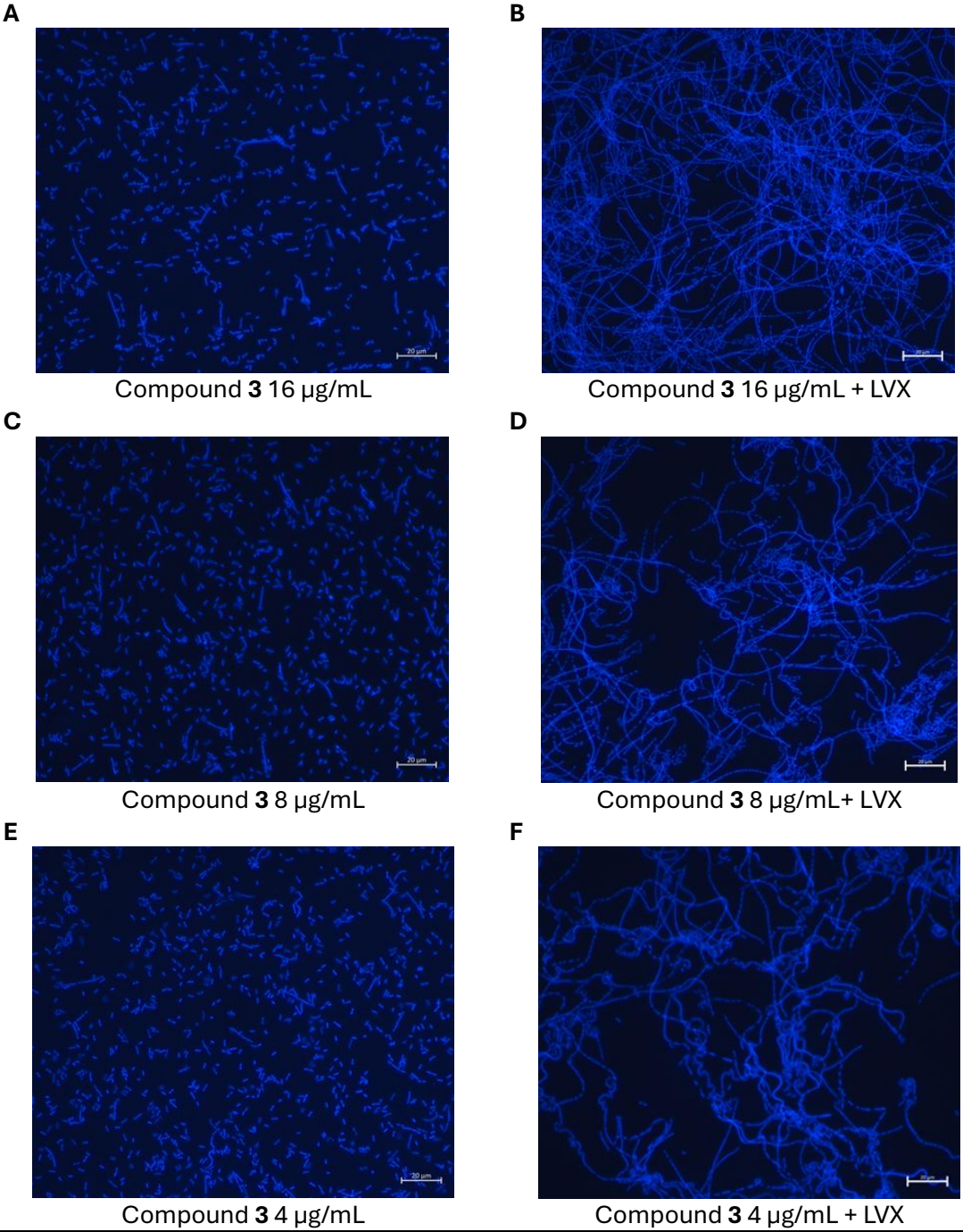


Figure 28. Fluorescence microscopy of *E. coli* BL21(DE3) with DAPI at 40×.

The filament length was measured by ImageJ, and the results were expressed as the percentage of reduction of filament length, compared to the filament length obtained through levofloxacin only. In **Figure 29** are reported the plots of the mean of filaments length for compound **1**, and in **Table 4** the percentage of reduction. Among the six concentrations tested, all demonstrated inhibitory capacity, with reduction rates spanning from 70% at the lowest concentration to 97% at the MIC value.

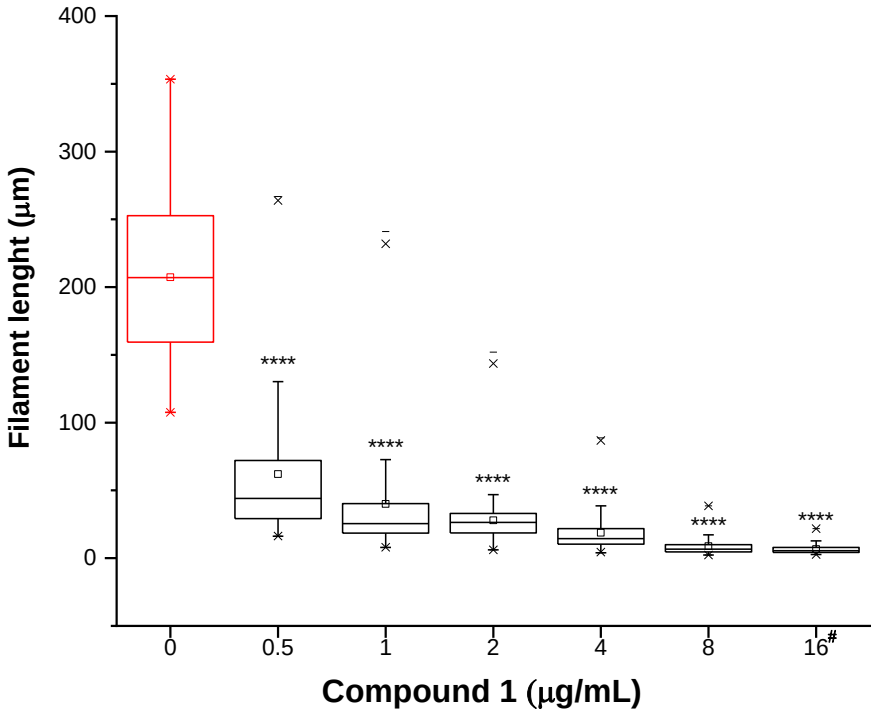


Figure 29. Plots of the mean of filaments length related to the compound **1** concentration; the concentrations tested range from the MIC value up to 1/32 of its value. (#) MIC value; **** p<0.001.

Table 4. Percentage of filament length reduction for compound **1**

Compound(s) (µg/mL)	Mean of filament length (µm)	SD	Percentage of reduction
LVX ($9.75x10^{-4}$)	207.29	59.06	-
LVX+ **1** (0.5)	61.97	51.19	70%
LVX + **1** (1)	40.01	42.68	81%
LVX + **1** (2)	27.89	16.97	87%
LVX + **1** (4)	18.75	14.29	91%
LVX + **1** (8)	8.76	6.26	96%
LVX + **1** (16)#	6.59	3.48	97%

(#)MIC value

In **Figure 30** are reported the plots of the mean filament length for compound **2**, and the percentage of reduction in **Table 5**. All six concentrations exhibited inhibitory capacity, with reduction rates starting at a minimum of 32% for the lowest concentration tested, and up to 97% for the MIC value.

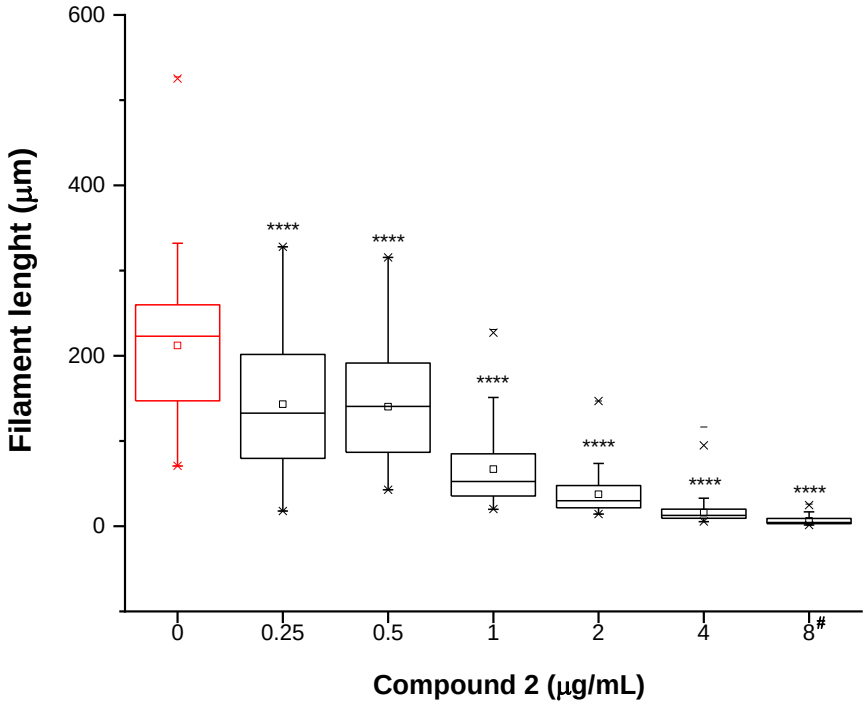


Figure 30. Plots of the mean of filaments length related to the compound **2** concentration; the concentrations tested range from the MIC value up to 1/32 of its value. (#) MIC value; **** p<0.001.

Table 5. Percentage of filament length reduction for compound **2**

Compound(s) (µg/mL)	Mean of filament length (µm)	SD	Percentage of reduction
LVX ($9{,}75x10^{-4}$)	212.06	72.58	-
LVX+ **2** (0.25)	143.26	79.92	32%
LVX + **2** (0.5)	140.3	63.63	34%
LVX + **2** (1)	66.88	46.49	68%
LVX + **2** (2)	37.39	23.19	82%
LVX + **2** (4)	15.71	11.81	93%
LVX + **2** (8)#	6.1	4.39	97%

(#)MIC value

In **Figure 31** are reported the plots of the mean of filament length for compound **3**, and the percentage of reduction in **Table 6**. Among the concentrations evaluated, the three lowest displayed minimal inhibitory capacity, with negligible reduction percentages. In contrast, the three highest concentrations showed a concentration-dependent effect, with reduction rates ranging from 26% to 54%. However, these reductions remain more moderate compared to those observed with compounds **1** and **2**.

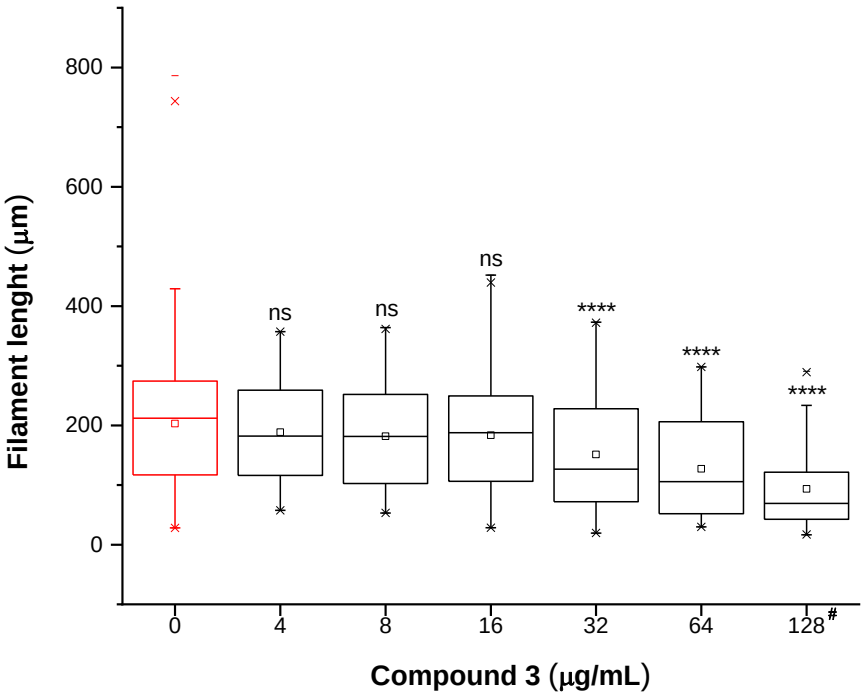


Figure 31. Plots of the mean of filaments length related to the compound **3** concentration; the concentrations tested range from the MIC value up to 1/32 of its value. (#) MIC value; **** p<0.001.

Table 6. Percentage of filament length reduction for compound **3**

Compound(s) (µg/mL)	Mean of filament length (µm)	SD	Percentage of reduction
LVX ($9{,}75 \times 10^{-4}$)	202.9	109.27	-
LVX+ **3** (4)	188.6	81.47	7%
LVX + **3** (8)	181.8	82.49	10%
LVX + **3** (16)	183.41	85.45	10%
LVX + **3** (32)	151.12	94.33	26%
LVX + **3** (64)	127.05	79.91	37%
LVX + **3** (128)#	93.58	69.45	54%

(#)The MIC value is higher than 128 µg/mL

6.1.3 Inhibition assay of LexA by alkaline-induced autohydrolysis

Self-cleavage of LexA can be achieved by alkalinization of the medium. The reaction was first conducted without preincubation between LexA protein and the boronics (**Figure 32-A**); subsequently, the same experiment was conducted with a preliminary 15-minute incubation (**Figure 32-B**) to verify a possible time-dependent effect on the activity of the compounds. As shown in **Figure 32**, the difference in the band intensity becomes much more evident when LexA and the benzoxaboroles were pre-incubated (**B**) compared to the reactions triggered without incubation (**A**). The fraction of uncleaved LexA supports this evidence reported in **Table 7.** After incubation, we observed an increase in the residual uncleaved LexA fraction for all compounds. Regardless of the boron under investigation, it is found that the residual fraction of LexA is inclined to almost double after incubation. Of the three, compounds **1** and **2** give fairly comparable results, except compound **3,** which shows a lower inhibitory capacity but still improved after incubation with our target. We can consequently conclude that the compounds act in a time-dependent way.

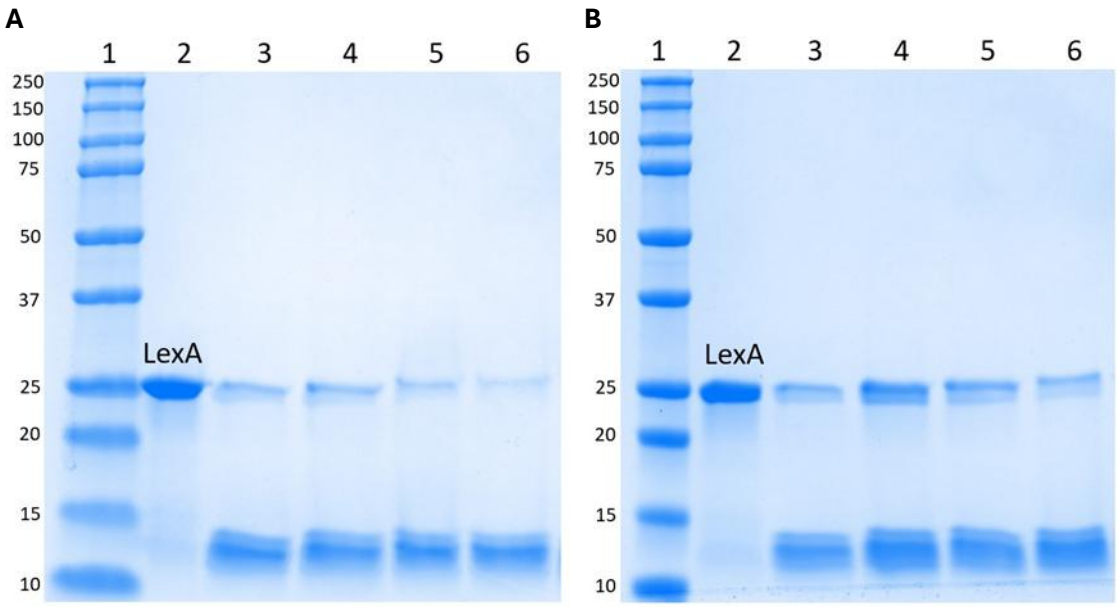


Figure 32. SDS-PAGE of uncleaved and self-cleaved LexA inducted by alkaline pH. (**A**)-(**B**) Lane 1, molecular weight marker; Lane 2, uncleaved LexA; Lane 3, self-cleaved LexA; Lane 4, self-cleavage of LexA with compound **1**; Lane 5, self-cleavage of LexA with compound **2**; Lane 6, self-cleavage of LexA with compound **3**. **(A)** The benzoxaboroles were added to the reaction with the alkaline buffer. **(B)** The compounds were previously incubated with LexA at 30°C for 15 minutes, followed by adding the buffer.

Table 7. Fraction of uncleaved LexA.

Compounds	Fraction of uncleaved LexA	
	No incubation	Incubation
1	0.33	0.58
2	0.21	0.49
3	0.13	0.27

6.1.4 Co-protease activity and determination of half-maximal inhibitory concentration (IC_{50})

The half-maximal inhibitory concentration for the three boron compounds was determined by evaluating the co-protease activity between RecA and LexA. In **Figure 33** we reported the plots of the fraction of uncleaved LexA, versus the inhibitor concentration, expressed like molar ratios ([I]:[LexA]); (**A**) compound **1**, (**B**) compound **2** and (**C**) compound **3**. The IC_{50} values correspond to 671.7 ± 48 for **1**, 313.07 ± 70.6 for **2**, and 538.8 ± 245.2 for **3**, when they are expressed such as molar ratio with LexA. The values expressed in mM corresponded at 8.33, 3.88, and 6.68, for **1**, **2** and **3**, respectively.

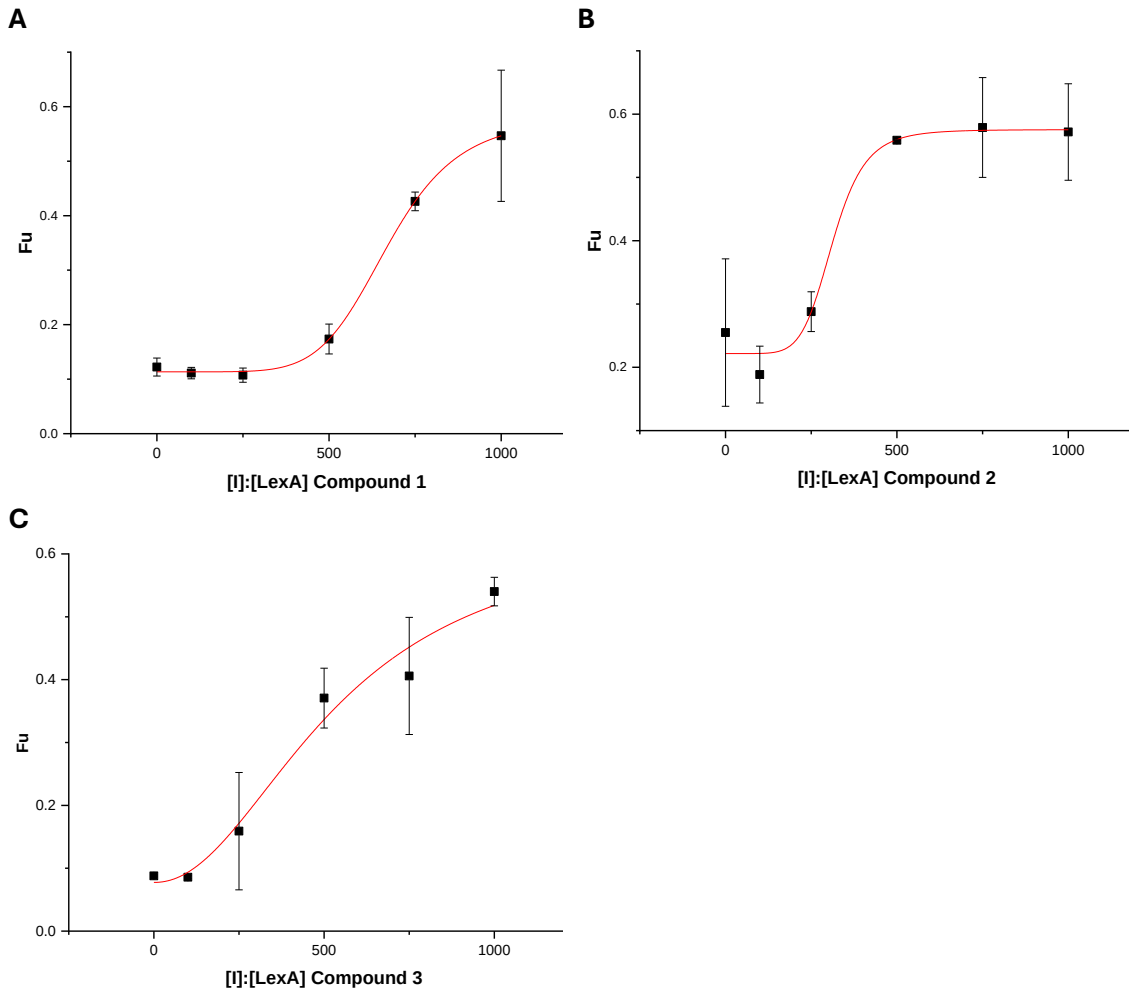


Figure 33. Plots of LexA fraction uncleaved versus the inhibitor concentration, expressed as molar ratios ([I]:[LexA]). (A) compound **1**; (B) compound **2**; (C) compound **3**.

6.1.5 Biofilm assay: inhibition and eradication

A preliminary test was used to identify the best biofilm producer between *E. coli* ATCC® 25922 and *E. coli* BL21 (DE3). The biofilm formation was induced by starvation, growing the bacteria in the minimum broth M63. The strains were incubated in 96-polystyrene plates for 24 hours at 26°C and 37°C in static conditions. **Figure 34** shows the results: *E. coli* ATCC® 25922 is the best biofilm producer, for both temperatures, with strong biofilm production for the highest temperature tested. Therefore, the subsequent biofilm experiments were conducted with *E. coli* ATCC® 25922 at 37°C.

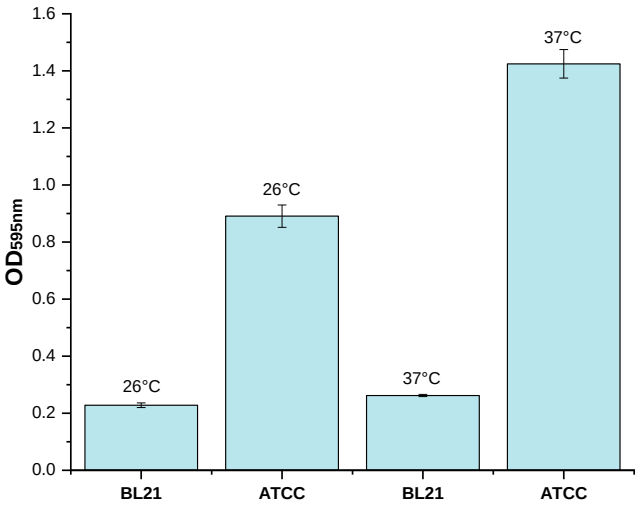


Figure 34. Biofilm formation for *E. coli* ATCC® 25922 and *E. coli* BL21(DE3) at 26°C and 37°C.

To estimate the potentiality of boronic acids to inhibit biofilm formation, the compounds were incubated with the culture at concentrations ranging from 128 µg/mL to 0.0625 µg/mL, corresponding to a range from 16×MIC to 7.8×10^{-3}×MIC value for compounds **1** and **2**, and a range from MIC to 4.8×10^{-4}×MIC value for compound **3**.

For compound **1**, the concentrations ranging from 2×MIC to 16×MIC, determine a substantial reduction in biofilm formation, as shown in **Figure 35**, with percentages of reduction ranging from 65% to 88% **(Table 8)**.

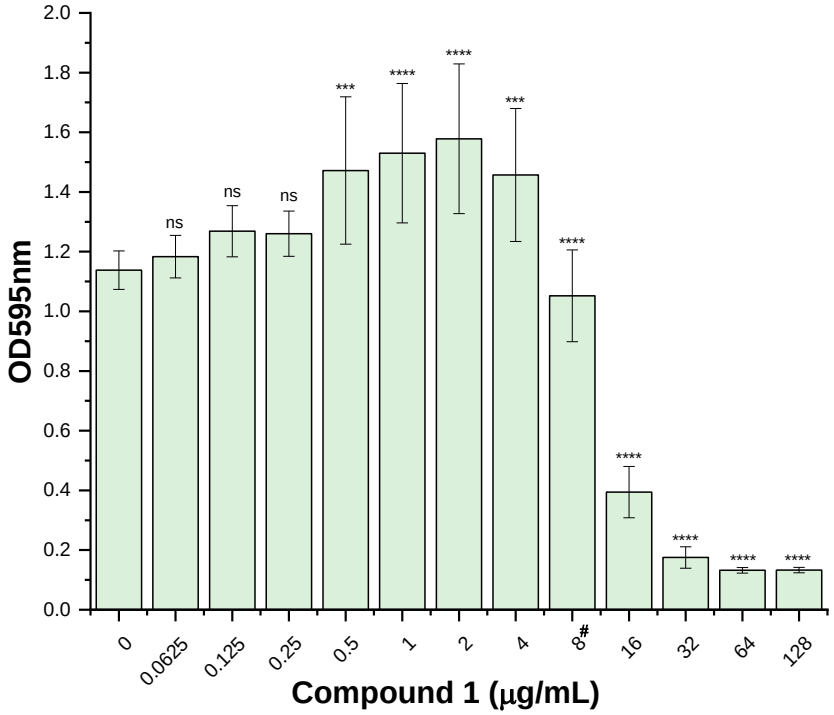


Figure 35. Plot of the mean of formed biofilm related to the compound **1** concentrations. The biofilm formation in *E. coli* ATCC® 25922 is obtained by M63 medium; the concentrations tested ranged from 16×MIC up to 7.8×10^{-3}×MIC value; (#) MIC value; * p<0.05; ** p<0.01; *** p<0.005; **** p<0.001.

Table 8. Percentage of reduction of biofilm formation for compound **1**

Compound concentration (μg/mL)	Mean of Biofilm biomass (OD_{595nm})	SD	Percentage of reduction
0	1.13637	0.06438	-
0.0625	1.18145	0.07131	-4%
0.125	1.26683	0.08569	-11%
0.25	1.25855	0.07576	-11%
0.5	1.47003	0.24699	-29%
1	1.52815	0.23336	-34%
2	1.57638	0.25092	-39%
4	1.4554	0.22292	-28%
8#	1.05042	0.15391	8%
16	0.39235	0.08591	65%
32	0.17327	0.03569	85%
64	0.1303	0.00924	89%
128	0.13117	0.00915	88%

(#)MIC value

For compound **2**, the concentration ranging from 0.5×MIC to 16×MIC can inhibit biofilm formation, **Figure 36,** with a percentage of reduction ranging from 47% to 90% (**Table 9**).

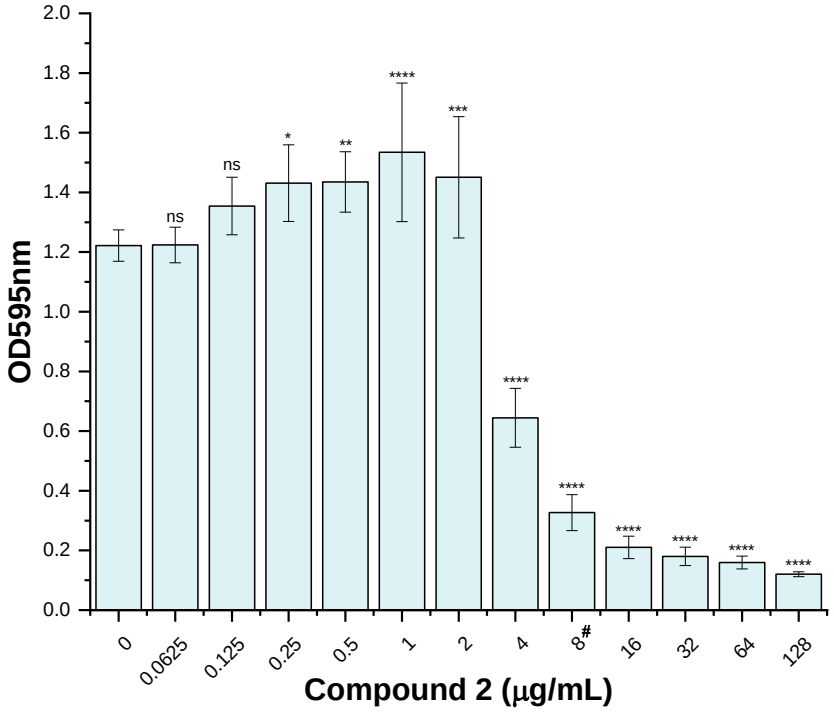


Figure 36. Plots of the mean of formed biofilm related to the compound **2** concentrations. The biofilm formation in *E. coli* ATCC® 25922 is obtained by M63 medium; the concentrations tested ranged from 16×MIC up to 7.8×10^{-3}×MIC value; (#) MIC value; * p<0.05; ** p<0.01; *** p<0.005; **** p<0.001.

Table 9. Percentage of reduction of biofilm formation for compound **2**

Compound concentration (μg/mL)	Mean of Biofilm biomass (OD_{595nm})	SD	Percentage of reduction
0	1.22433	0.0526	-
0.0625	1.22655	0.05946	0%
0.125	1.3571	0.09654	-11%
0.25	1.4338	0.12821	-17%
0.5	1.43752	0.10121	-17%
1	1.53717	0.23208	-26%
2	1.45342	0.20341	-19%
4	0.64717	0.0988	47%
8#	0.32948	0.06034	73%
16	0.21293	0.03742	83%
32	0.1827	0.03078	85%
64	0.1621	0.02146	87%
128	0.12298	0.00844	90%

(#)MIC value

In **Figure 37** and **Table 10** are reported the data about compound **3**. It was not possible to assess higher concentrations than the MIC value, and none of the concentrations evaluated was able to interfere with the biofilm formation.

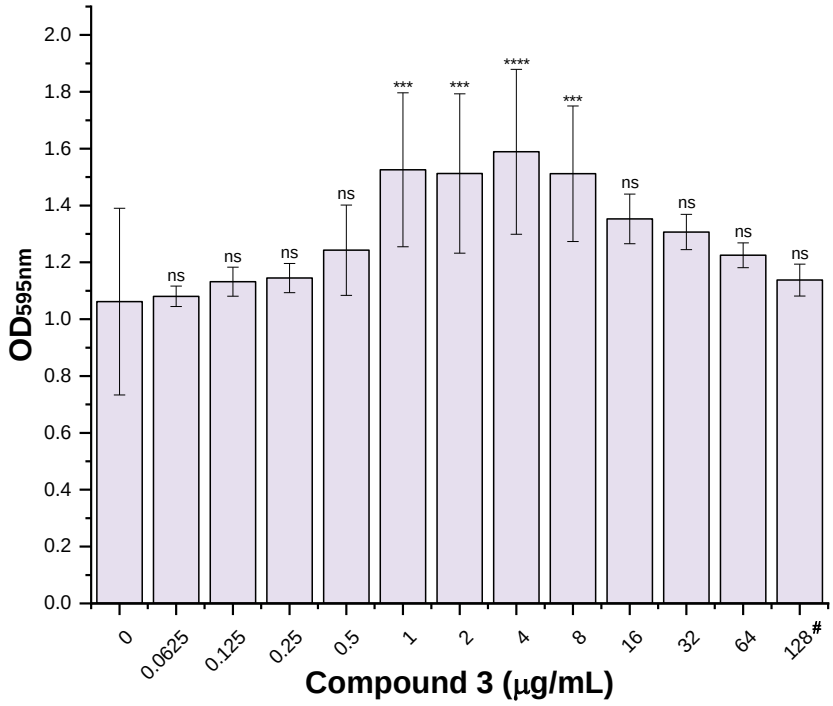


Figure 37. Plots of the mean of formed biofilm related to the compound **3** concentrations. The biofilm formation in *E. coli* ATCC® 25922 is obtained by M63 medium; the concentrations tested ranged from the MIC value up to 4.8×10^{-4}×MIC of its value; (#) MIC value; * p<0.05; ** p<0.01; *** p<0.005; **** p<0.001.

Table 10. Percentage of reduction of biofilm formation for compound **3**

Compound concentration (μg/mL)	Mean of Biofilm biomass (OD_{595nm})	SD	Percentage of reduction
0	1.06574	0.32841	-
0.0625	1.0842	0.03585	-2%
0.125	1.13553	0.05099	-7%
0.25	1.1487	0.05135	-8%
0.5	1.2465	0.15864	-17%
1	1.52947	0.27106	-44%
2	1.51643	0.28044	-42%
4	1.59282	0.29011	-49%
8	1.51575	0.23847	-42%
16	1.35645	0.08735	-27%
32	1.31055	0.06192	-23%
64	1.22877	0.04373	-15%
128#	1.14153	0.05606	-7%

(#)The MIC value is higher than 128 μg/mL

To estimate the eradication potential, the boron compounds, at the same concentration as above, were added to a mature 24h-biofilm, and incubated for 96h. None of the three showed eradication capacity (**Figure 38**).

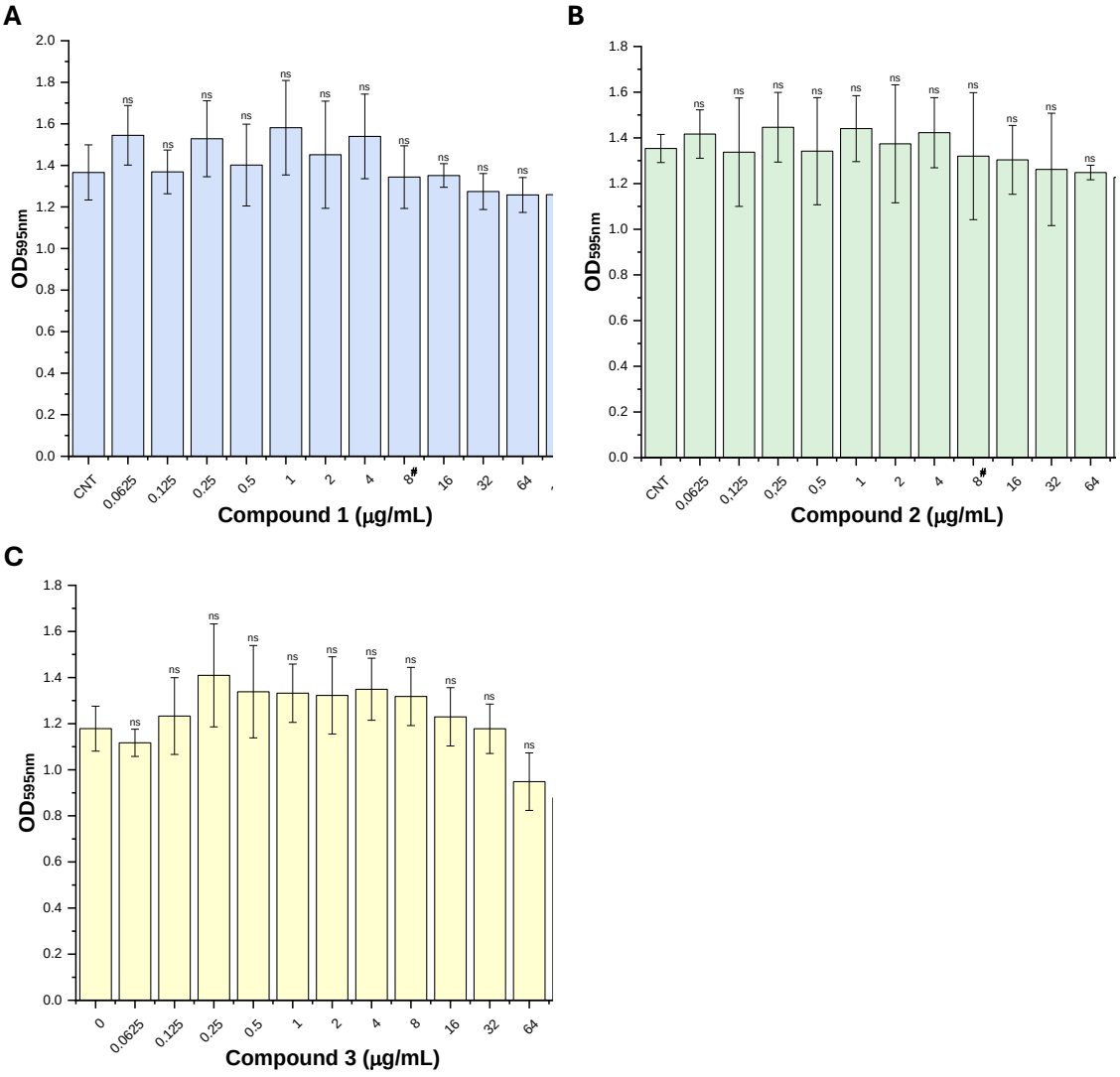


Figure 38. Plots of the mean of eradicated biofilm related to the boronic concentrations. The biofilm formation in *E. coli* ATCC® 25922 is obtained by M63 medium. (A)-(B) for **1** and **2**, the concentrations tested ranged from 16×MIC up to 7.8×10^{-3}×MIC value; (C) for **3**, the concentrations tested ranged from the MIC value up to 4.8×10^{-4}×MIC of its value; (#) MIC value; (ns) non-significant.

6.1.6 Biofilm inhibition assay: SEM visualization

Compound **3** was not evaluated for SEM visualization due to its inability to inhibit biofilm formation in *E. coli* ATCC® 25922. Compounds **1** and **2**, however, were assessed at a single concentration, the level at which biofilm formation is inhibited by at least 50%. For compound **1**, this concentration was 16 µg/mL, 2×MIC, while for compound **2**, it was 4 µg/mL, 0.5×MIC. In **Figure 39**, the images related to **1** are reported, and in **Figure 40**, for **2**.

In the control sample, **Figures 39 and 40 (A-C-E-G)** show clear evidence of biofilm formation, with bacterial cells embedded in an external polysaccharide matrix. This matrix forms a cohesive film that envelops the cells, often making individual bacterial cells difficult to distinguish. Additionally, unusually elongated cells are observed, indicating filamentation as a result of the activation of the SOS response **(A-C)**.

In the sample treated with **1**, **Figure 39 (B-D-F-H)** the typical matrix observed in the control is absent, indicating inhibited biofilm formation. A homogeneous bacterial surface is visible, with sparse connections between individual bacterial cells, likely representing portions of the extracellular matrix in early formation.

For **2**, **Figure 40** (**B**-**D**-**F**-**H**), the outer matrix surrounding the bacterial cells is again absent. A rough bacterial surface is observed, with connections indicative of partially formed polysaccharide matrix segments. Additionally, numerous channel-similar structures extending from the cell surface are visible.

In **Figure 41**, only control images are reported. In these images, nanochannels of considerable length that connect the bacterial cells to each other are visible (**C**-**D**-**E**-**F**). Biofilm is a condition that promotes the formation of these structures because such channels facilitate the exchange of nutrients and genetic material between cells, contributing to the overall resilience and adaptability of the microbial community.

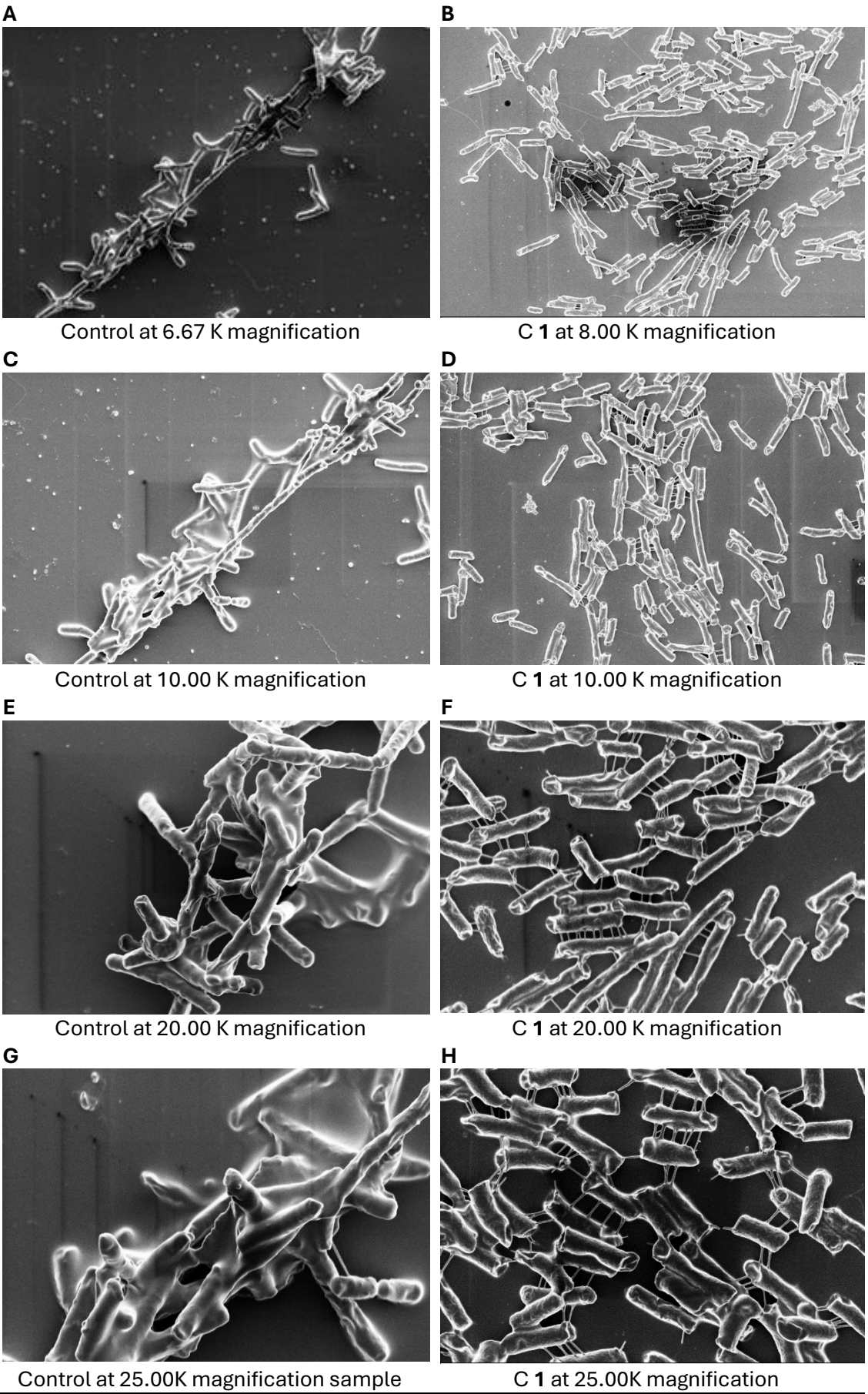


Figure 39. Biofilm of *E. coli* ATCC® 25922 visualized at scanning electron microscope.

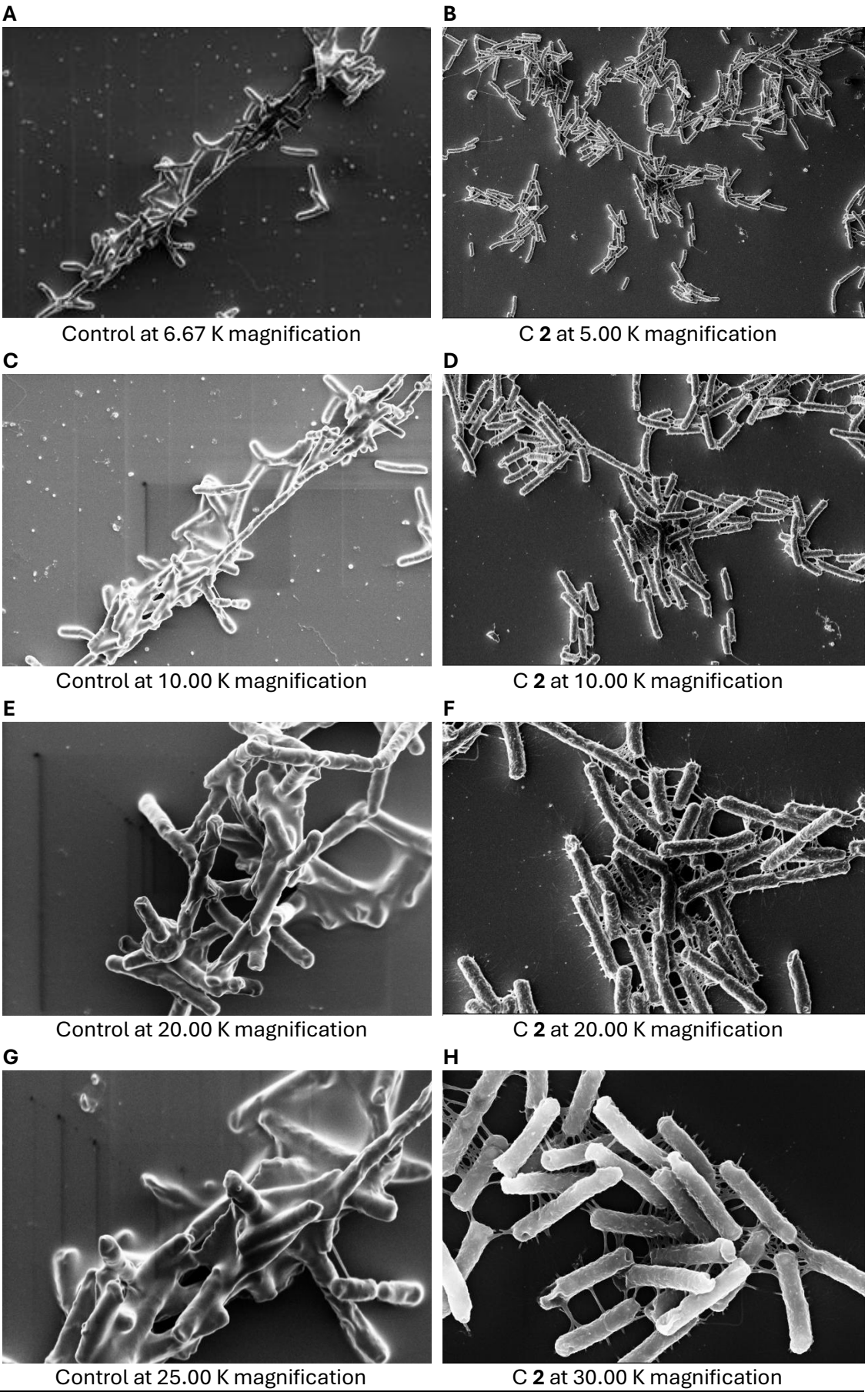


Figure 40. Biofilm of E. coli ATCC 25922 visualized at scanning electron microscope.

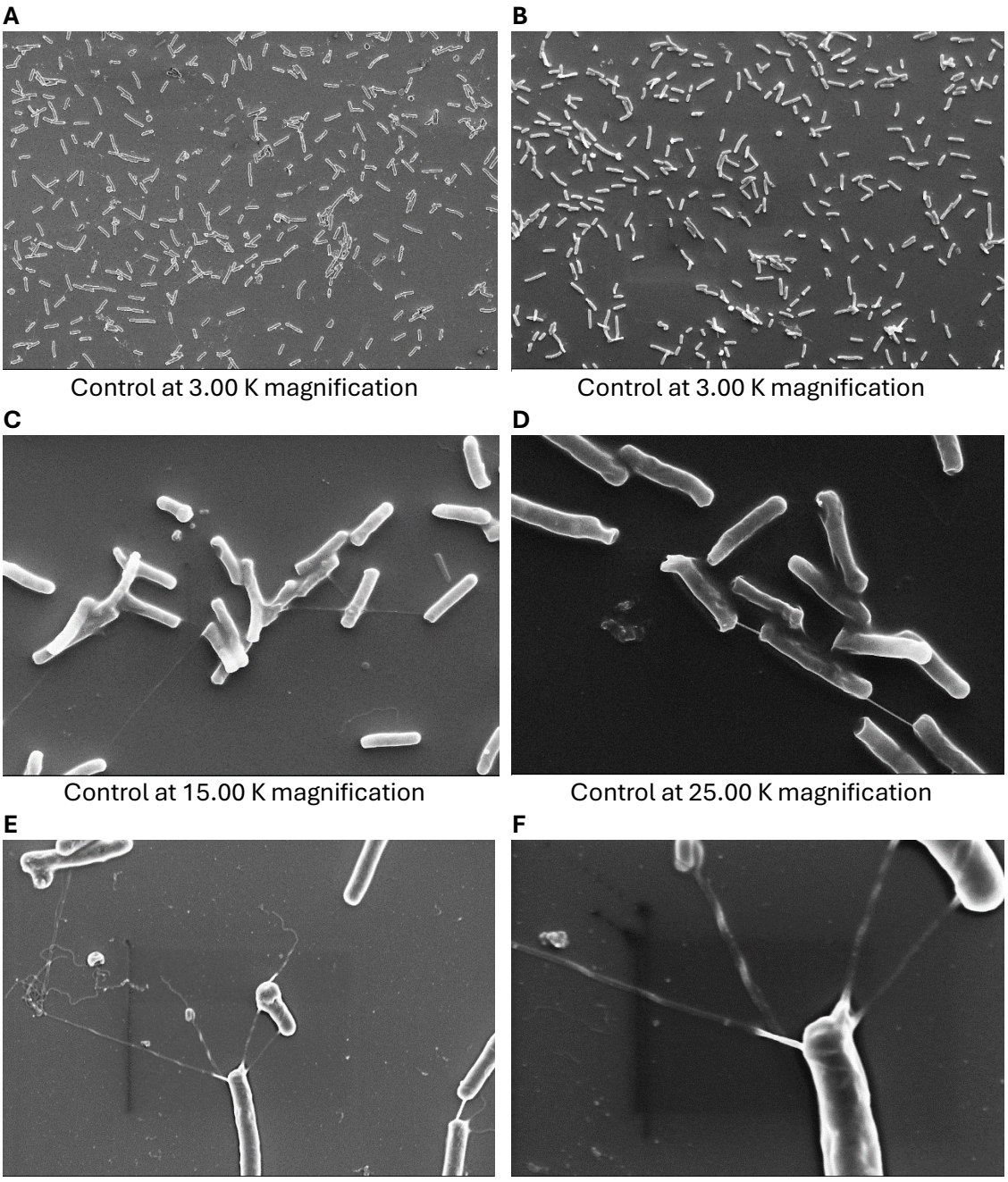


Figure 41. Biofilm of *E. coli* ATCC® 25922 visualized at scanning electron microscope.

6.1.7 Molecular docking

The docking was performed for each compound under examination by evaluating fifty possible interactions with the transcriptional repressor LexA, using the Autodock 4.0 software. The final structure was selected based on the lowest theoretical binding energy and visualized by Pymol 3.1. The results are shown in **Figure 42** (**A**-**B**-**C**). The images highlight only the portion of the protein that interacts with the boronic compounds.

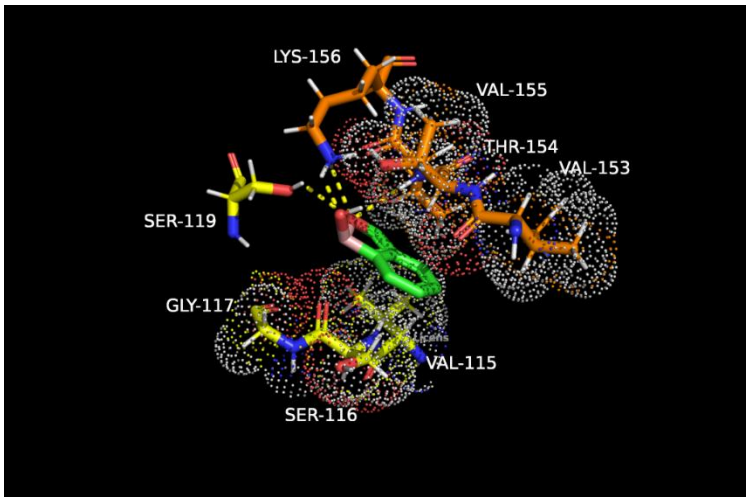
For compound **1** (**A**), the selected complex has a theoretical binding energy of -4.92 kcal/mol and a theoretical inhibition constant (K_i) of 248.47 μM. Compound **1** interacts with LexA by forming four hydrogen bonds and interacting with hydrophobic residues. Specifically, one hydrogen bond forms between the H of the ε-NH_2 group of Lys156 and the oxygen of the OH group attached to the boron. The remaining three hydrogen bonds all occur with the O in position 2 of compound **1**: the first bond forms with the H attached to the Oγ of Ser119; the second bond forms with the second H of the ε-NH_2 group of Lys156; the third bond forms with the H of the nitrogen in the Cα of Val155. Several hydrophobic interactions are observed with Gly117, Val153, Thr154, and Val155 residues.

For compound **2** (**B**), the selected interaction has a binding energy of -6.07 kcal/mol and a K_i of 35.36 μM. Compound **2** interacts with the transcriptional repressor by forming four hydrogen bonds and hydrophobic interactions. Specifically, for compound **2**, two hydrogen bonds are formed with the hydroxyl group attached to the boron, and two other bonds form with the O in position two of the boronic ring. The first hydrogen bond forms between the carbonyl oxygen of the Val155 backbone and the hydrogen of the hydroxyl group attached to the boron; the second bond forms between an hydrogen of the ε-NH_2 group of Lys156 and the O of the hydroxyl group of the boron. The third bond forms between the second hydrogen of the ε-NH_2 group of Lys156 and the O in position two, while the fourth bond forms between the same oxygen and the hydrogen attached to the Oγ of Ser119. Hydrophobic interactions occur with the amino acid residues Leu113, Val115, Gly117, Thr154, and Val155.

For compound **3** (**C**), the selected structure has a binding energy of -4.55 kcal/mol and a K_i of 458.63 μM. In this case, four hydrogen bonds are formed, along with hydrophobic interactions. As with the previous compounds, the hydrogen bonds form through the hydroxyl group attached to the boron and the oxygen in position two of the molecule's ring. Specifically, one bond forms between the α-NH_2 hydrogen of Ser119 and the hydroxyl oxygen of the boron; the second bond forms between the α-carbonyl oxygen of Ser116 and the hydroxyl hydrogen attached to the boron. The oxygen in position two forms a bond with an ε-NH_2 hydrogen of Lys156 and a second bond with the hydrogen attached to the Oγ of Ser119. The presence

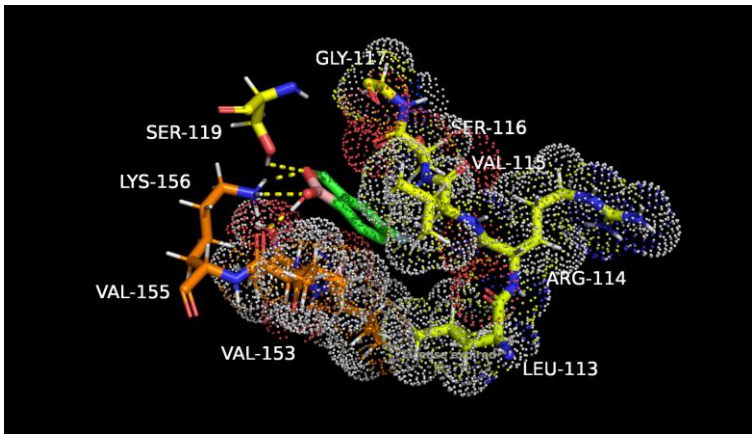
of the cyano-phenyl group at position 5 induces electrostatic interactions between the N of the cyano group, which carries a partial positive charge δ^+, and the Cδ oxygen of Glu173, which carries a partial negative charge δ^-. The structure is further stabilized by hydrophobic interactions between the scaffold of compound **3** and the residue Phe174. This interaction is particularly established by the cyanophenyl group of the benzoxaboroles.

A



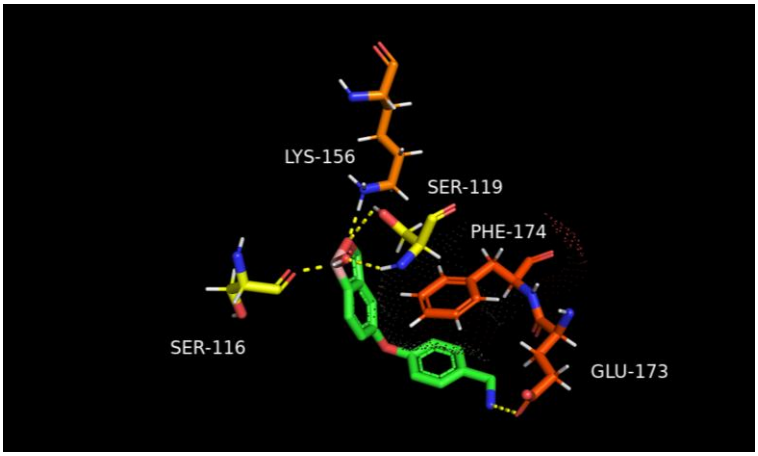
Interaction between LexA and compound **1**

B



Interaction between LexA and compound **2**

C



Interaction between LexA and compound **3**

Figure 42. Molecular docking was performed by Autodock 4.0, and results were visualized by Pymol 3.1.

6.2 Benzoxaboroles

6.2.1 Co-protease activity and determination of half-maximal inhibitory concentration (IC_{50})

The benzoxaboroles were first evaluated for their ability to inhibit LexA self-cleavage through RecA/LexA co-protease activity assay, using one concentration for every compound, 6.2 mM. LexA uncleaved fraction was determined and the data are reported in **Table 11**.

Table 11. LexA uncleaved fraction obtained after treatment with benzoxaboroles

Compound(s)	LexA uncleaved fraction
A	0.56
B	0.87
C	0.14
D	0.47
E	0.22
F	0.69*
G	0.76*
H	0.11
I	0.14
J	0.58
K	0.35*
L	0.66*
M	0.68

(*) these compounds showed precipitate formation under the conditions in use.

Following this initial evaluation, only benzoxaboroles with a non-hydrolyzed fraction around 0.5 were selected. Compounds marked with (*), **F, G**, **K**, and **L** were excluded due to solubility issues and precipitate formation under the experimental conditions. These compounds were discarded along with **C**, **E**, **H**, and **I**, due to their low LexA uncleaved fraction. For compounds **A**, **B**, **D**, **J** and **M** we determined the half-maximal inhibitory concentration. In **Figure 43** we reported the plots of the fraction of uncleaved LexA uncled, versus the inhibitor concentration, expressed like molar ratios ([I]:[LexA]): (**A**) compound **A**, (**B**) compound **B**, (**C**) compound **D**, (**D**) compound **J** and (**E**) compound **M**. The IC_{50} values correspond to 295.7±58 : 1 for **A**, 296.7±54 : 1 for **B**, 206.2±20 : 1 for **D**, 412.6±11 : 1 for **J** and 458.7±33 : 1 for **M** when they are expressed such as molar ratio with LexA. The values expressed in mM corresponded at 3.69 mM, 3.71 mM, 2.57 mM, 5.15 mM and 5.73 mM, respectively.

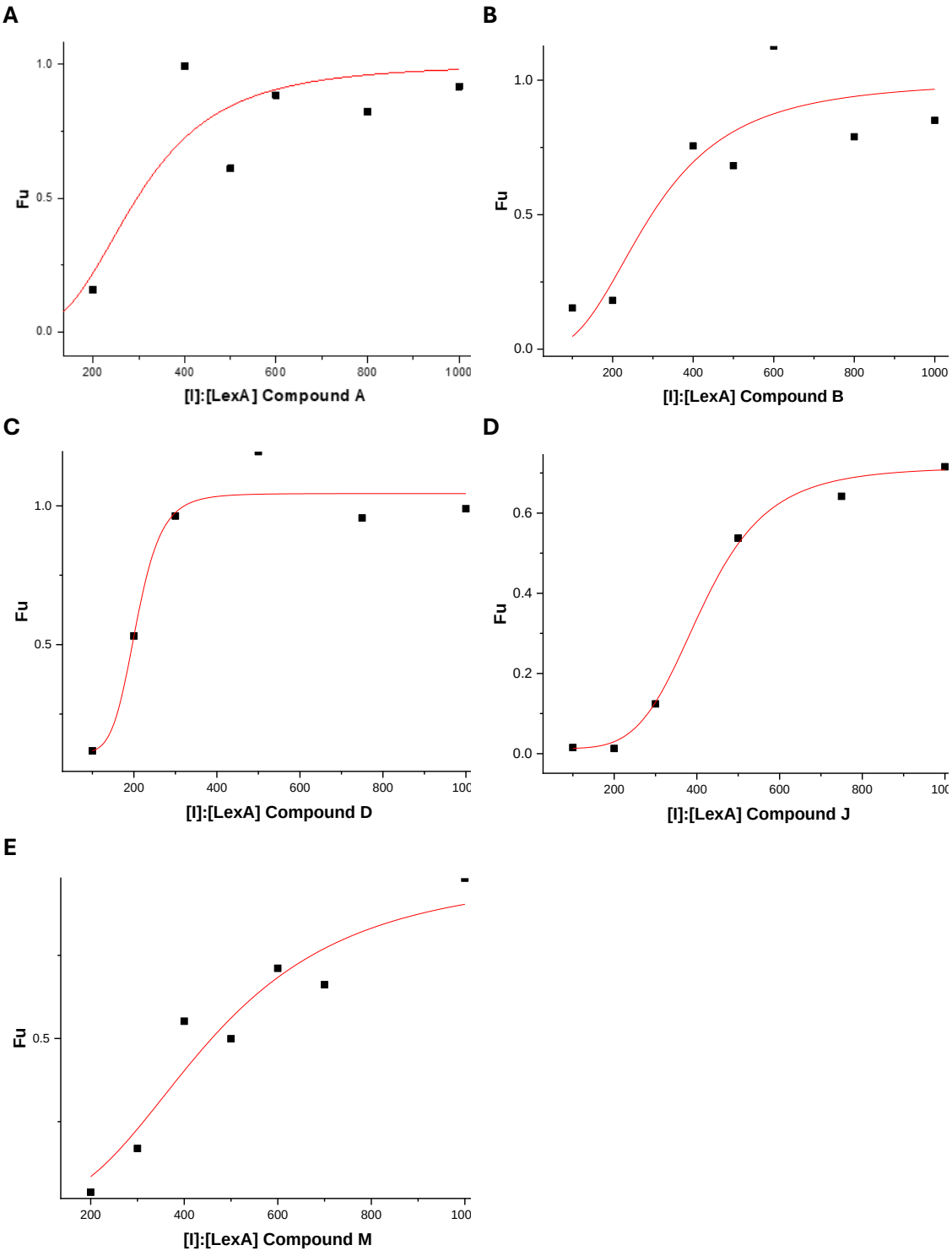


Figure 43. Plots of Fraction uncleaved of LexA versus the inhibitor concentration, expressed as molar ratios ([I]:[LexA]). **(A)** compound **A**; **(B)** compound **B**; **(C)** compound **D**; **(D)** compound **J**; **(E)** compound **M.**

6.2.2 Determination of the Minimum Inhibitory Concentrations (MICs)

The susceptibility of *E. coli* BL21(DE3) and *E. coli* ATCC® 25922 to the selected benzoxaboroles was established through the microdilution method. The MICs values are reported in **Table 12**. For most compounds, the MIC values are relatively high, ranging from 128 up to 1024 μg/mL. Notable exceptions are compounds **A**, **B**, and **K**. Compounds **K** and **L**, which are analogues of compounds **2** and **3**, respectively, already display solubility issues at this preliminary stage**.**

Table 12. MICs value for the new benzoxaboroles

Compound	MIC value (μg/mL)	
	***E. coli* BL 21(DE3)**	***E. coli* ATCC® 25922**
A	4	16
B	64	32
C	512	512
D	256	256
E	512	512
F	>1024	>1024
G	>1024	1024
H	>1024	128
I	128	128
J	128	64
K*	8	16
L*	>1024	>1024
M	256	128

(*) these compounds showed precipitate formation under the conditions in use.

6.2.3 Filamentation assay

The filamentation assay was performed on *E. coli* BL21 (DE3) using levofloxacin at 9.75×10^{-4} μg/mL. A concentration-dependent assessment was made for each, evaluating concentrations ranging from the MIC value up to 1/32 of its value alone and in combination with the filamentation inductor. A total of 7 benzoxaboroles were used: five of these compounds had previously been selected for IC_{50} determination, while the other two were included due to structural similarities with some of them.

The filamentation images were reported in **Figures 44-45**, **46-47**, **48-49**, **50-51**, **52-53**, **54-55** and **56-57**, for compounds **A**, **B**, **C**, **D**, **E**, **J** and **M**, respectively.

A concentration-dependent effect was found for compounds **A**, **B** and **M**: the reduction in filament length was found for every concentration tested, and every compound shows a good capacity to inhibit the phenome under investigation (**Fig. 44-45**, **46-47** and **56-57**). None of the 3, when alone, induces filamentation in *E. coli* BL21(DE3).

For compound **C**, the filamentation is observed at four tested concentrations when administered alone: MIC, 0.5×MIC, 0.25×MIC, and 0.125×MIC (**Fig. 48 C**-**E**-**G** and **Fig.49 A**). The reduction in filament length is observed only in **Fig. 48 D.**

Compound **D** is also capable of inducing filamentation when alone, as observed at MIC, 0.5×MIC, and 0.25×MIC concentrations **(Fig. 50 C**-**E**-**G)**. When combined with LVX, concentrations of MIC and 0.5×MIC reduced filament length **(Fig. 50 D**-**F)**.

Compound **E** also induces filamentation when used alone at concentrations of MIC, 0.5×MIC, 0.25×MIC, and 0.125×MIC **(Fig. 52 C**-**E**-**G** and **Fig. 53 A)**. When combined with LVX, an apparent reduction in filamentation is observed at MIC and 0.5×MIC concentrations **(Fig. 52 D**-**F)**.

Finally, compound **J** behaves like the previous ones: alone, it causes filament formation for concentrations of 0.5×MIC, 0.25×MIC, and 0.125×MIC **(Fig. 54 C**-**E**-**G** and **Fig. 55 A)**. When combined with levofloxacin, it can still inhibit its effect, although it can produce filaments of modest length **(Fig. 54 D-F-H** and **Fig.** 55 B). Note that in **Fig. 55 C**, no filamentation is observed, and in **D (Fig. 55)**, a good reduction in filament length is observed.

Overall, the benzoxaboroles under investigation have a basic ability to induce filamentation and, when combined with LVX, a reduction in filament length is only observed for the highest concentrations under investigation.

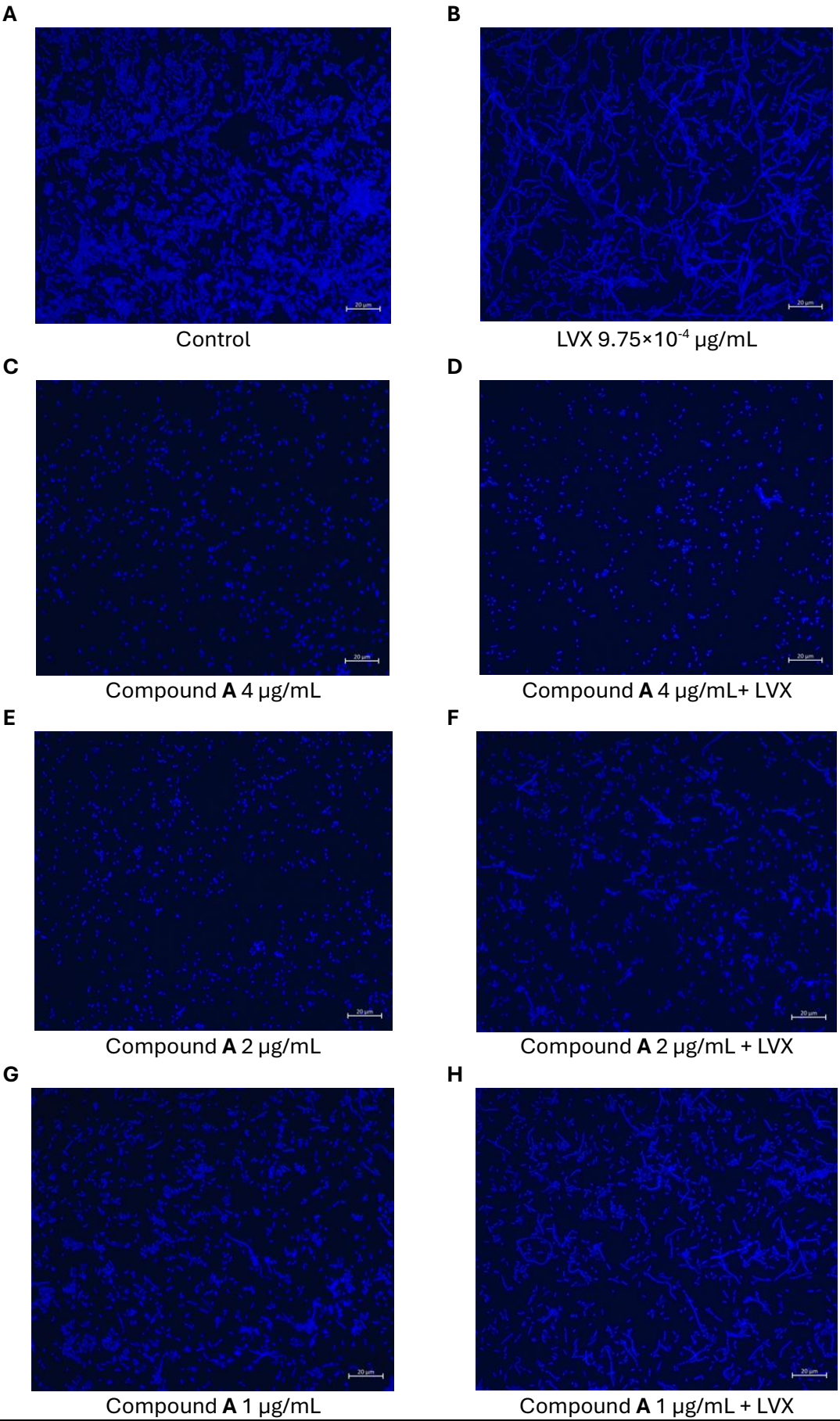


Figure 44. Fluorescence microscopy of *E. coli* BL21(DE3) with DAPI at 40×.

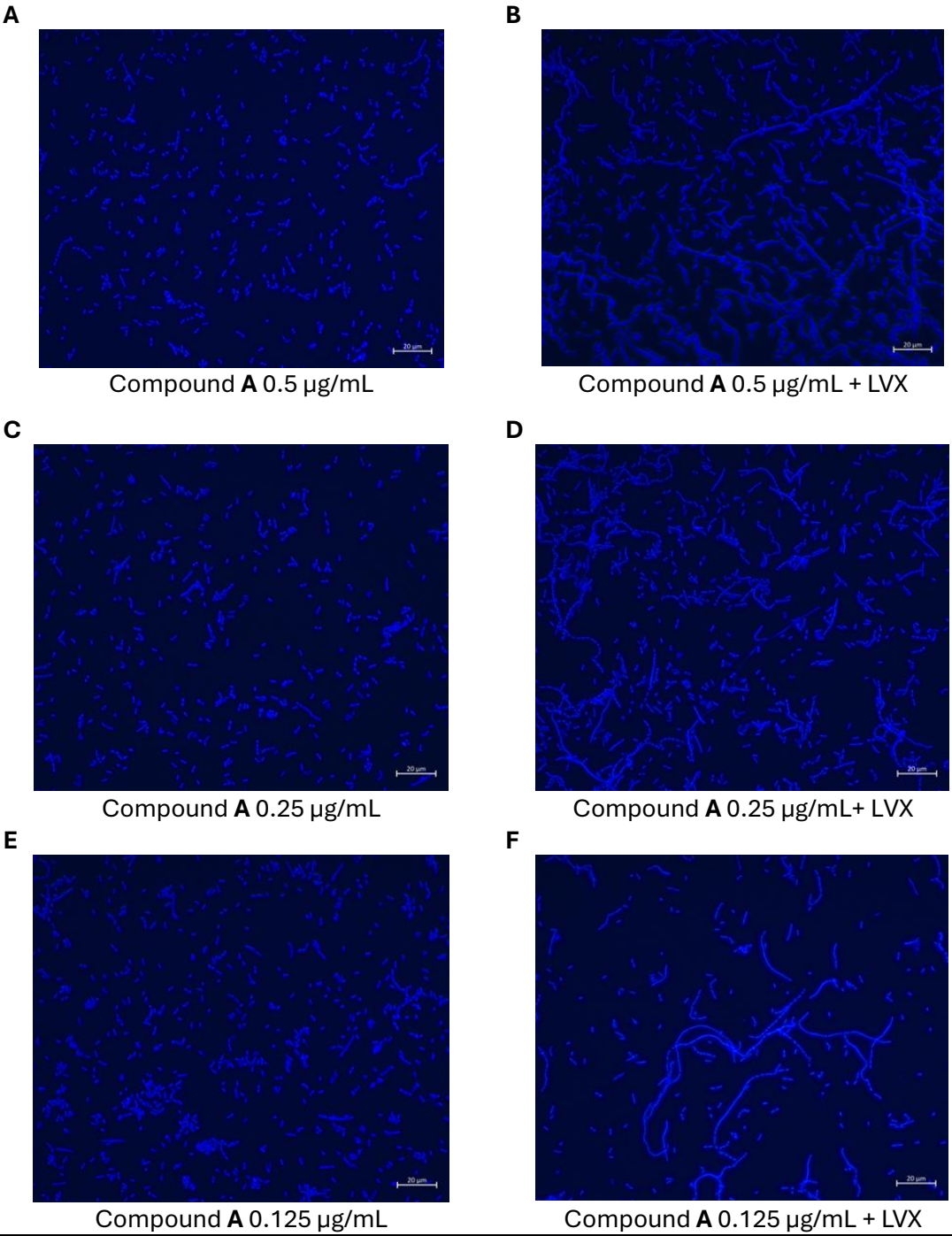


Figure 45. Fluorescence microscopy of *E. coli* BL21(DE3) with DAPI at 40×.

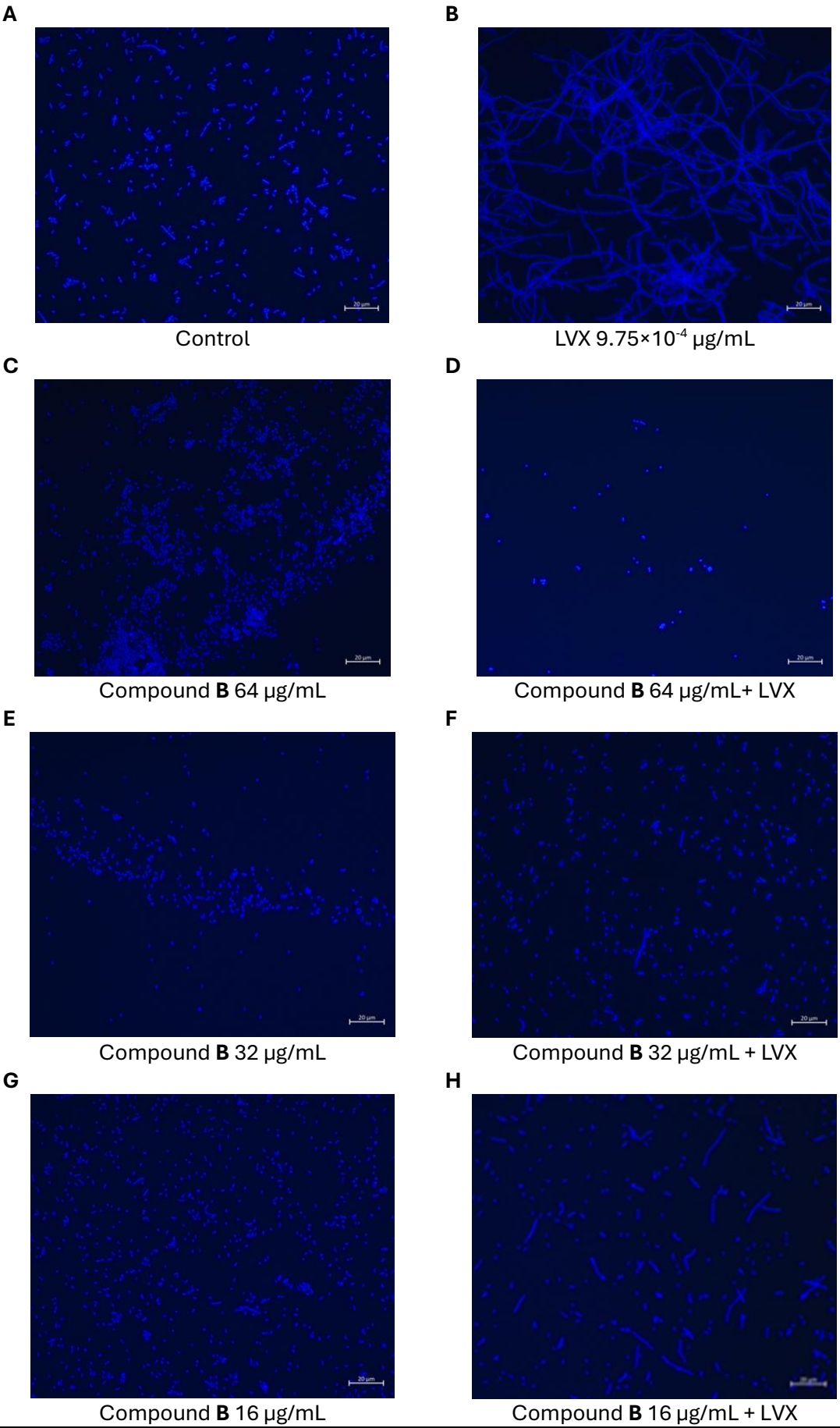


Figure 46. Fluorescence microscopy of *E. coli* BL21(DE3) with DAPI at 40×.

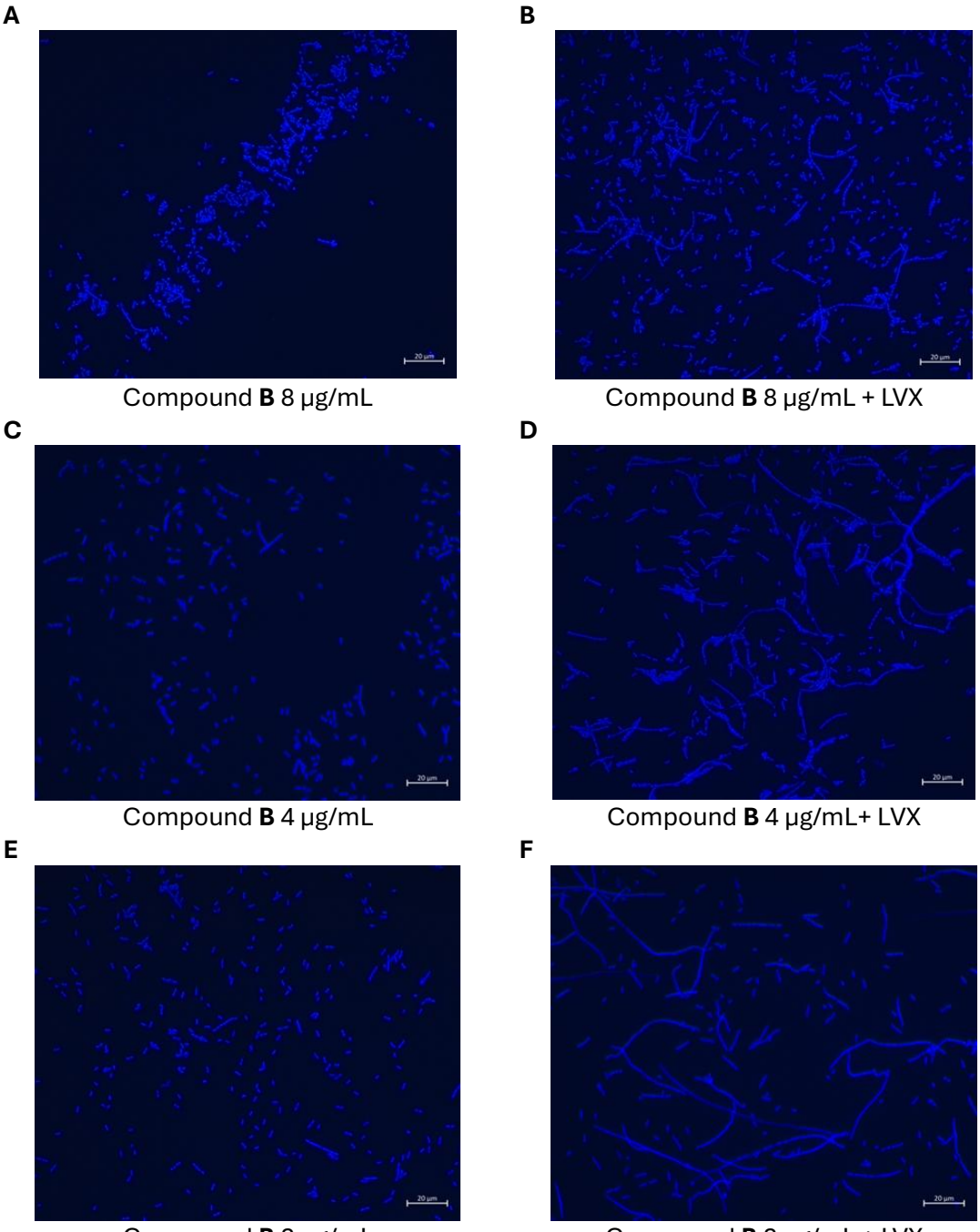


Figure 47. Fluorescence microscopy of *E. coli* BL21(DE3) with DAPI at 40×.

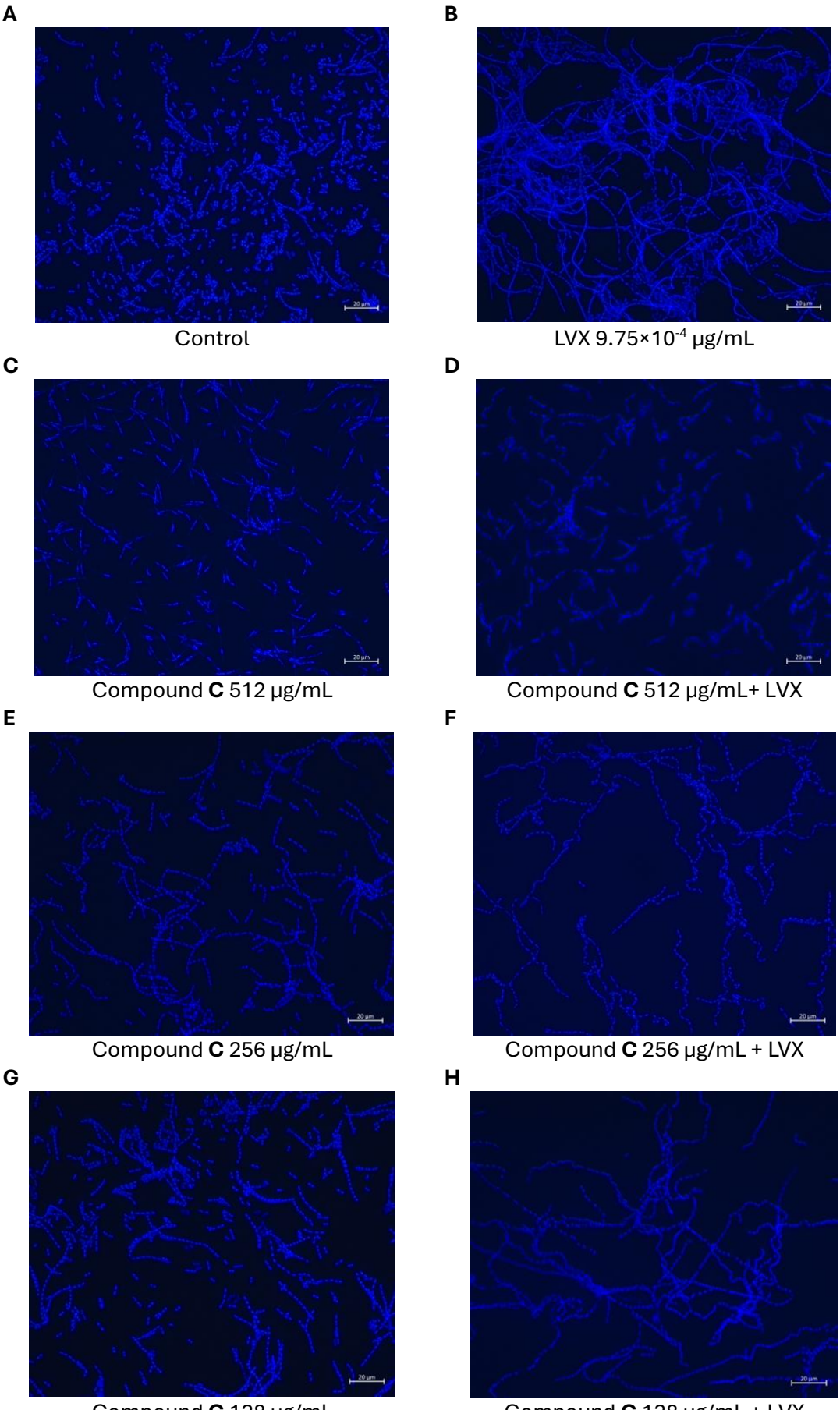


Figure 48. Fluorescence microscopy of *E. coli* BL21(DE3) with DAPI at 40×.

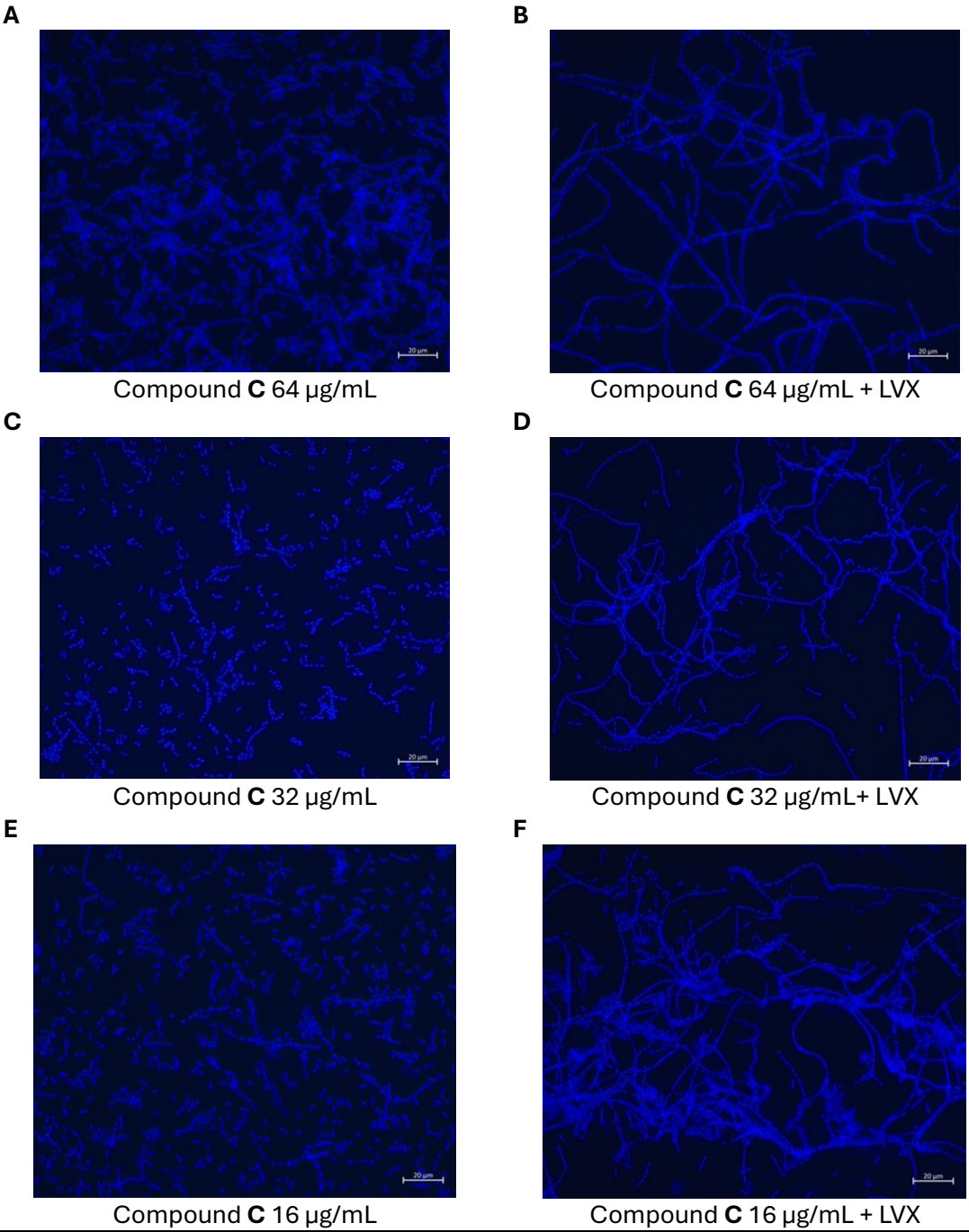


Figure 49. Fluorescence microscopy of *E. coli* BL21(DE3) with DAPI at 40×.

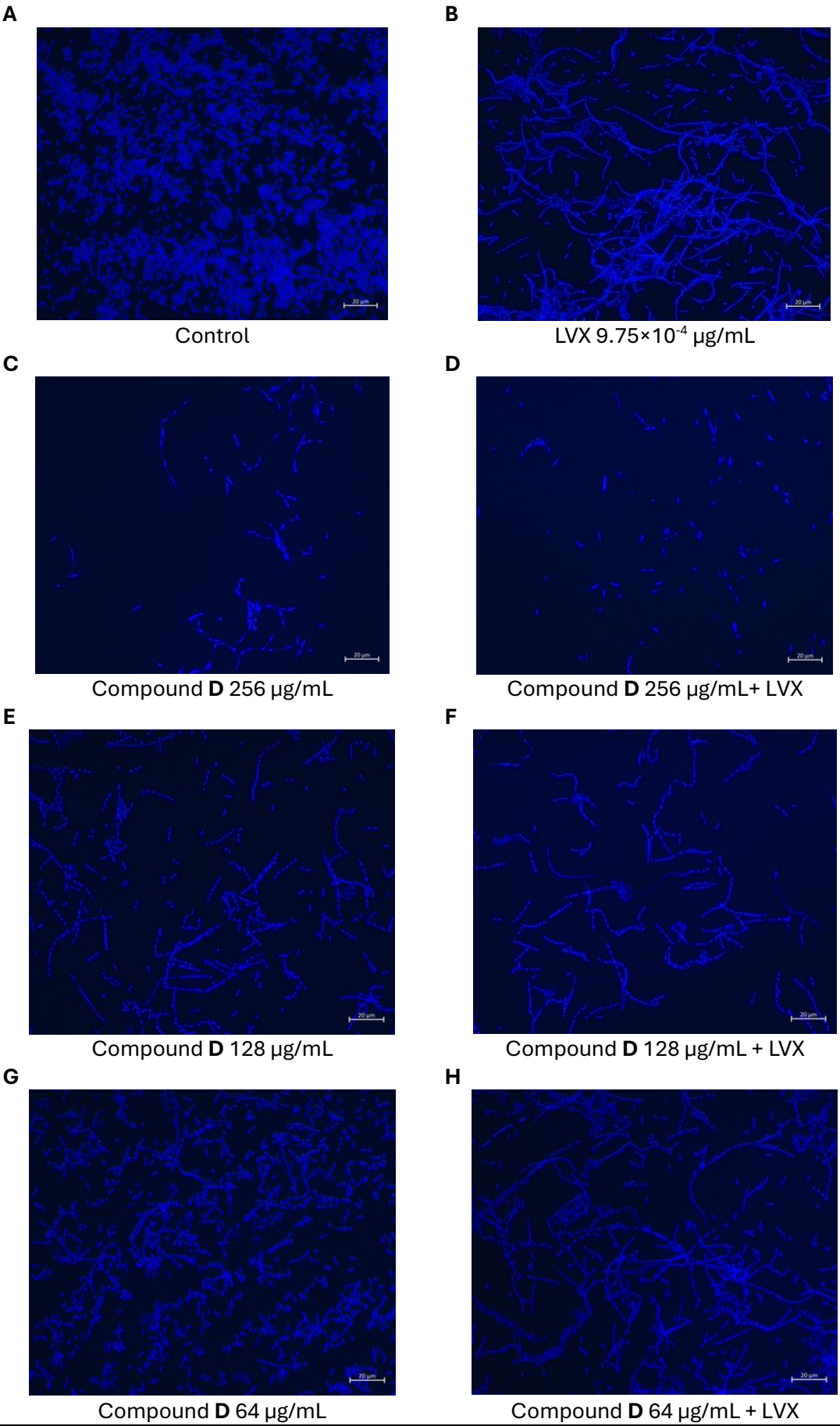


Figure 50. Fluorescence microscopy of *E. coli* BL21(DE3) with DAPI at 40×.

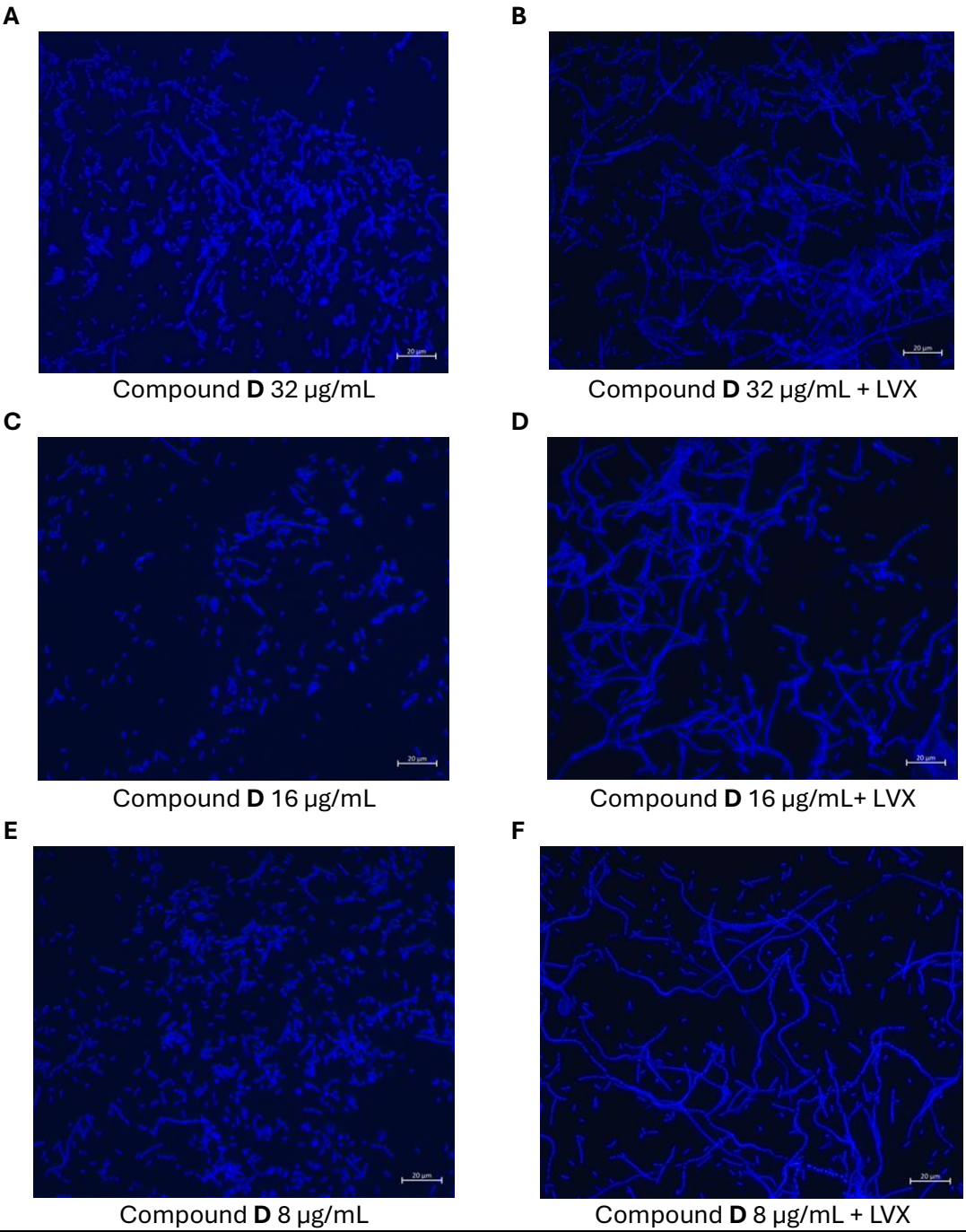


Figure 51. Fluorescence microscopy of *E. coli* BL21(DE3) with DAPI at 40×.

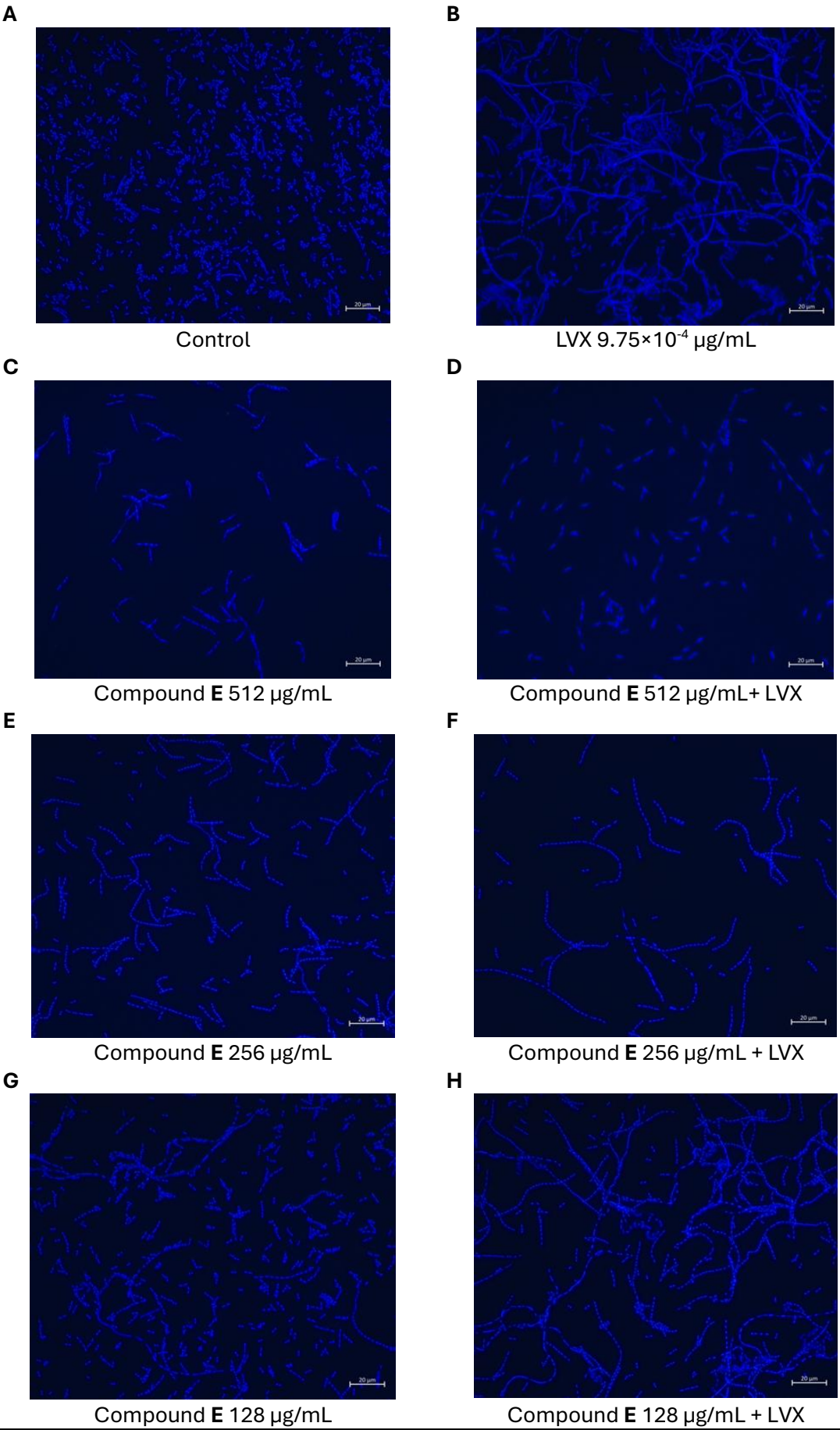


Figure 52. Fluorescence microscopy of *E. coli* BL21(DE3) with DAPI at 40×.

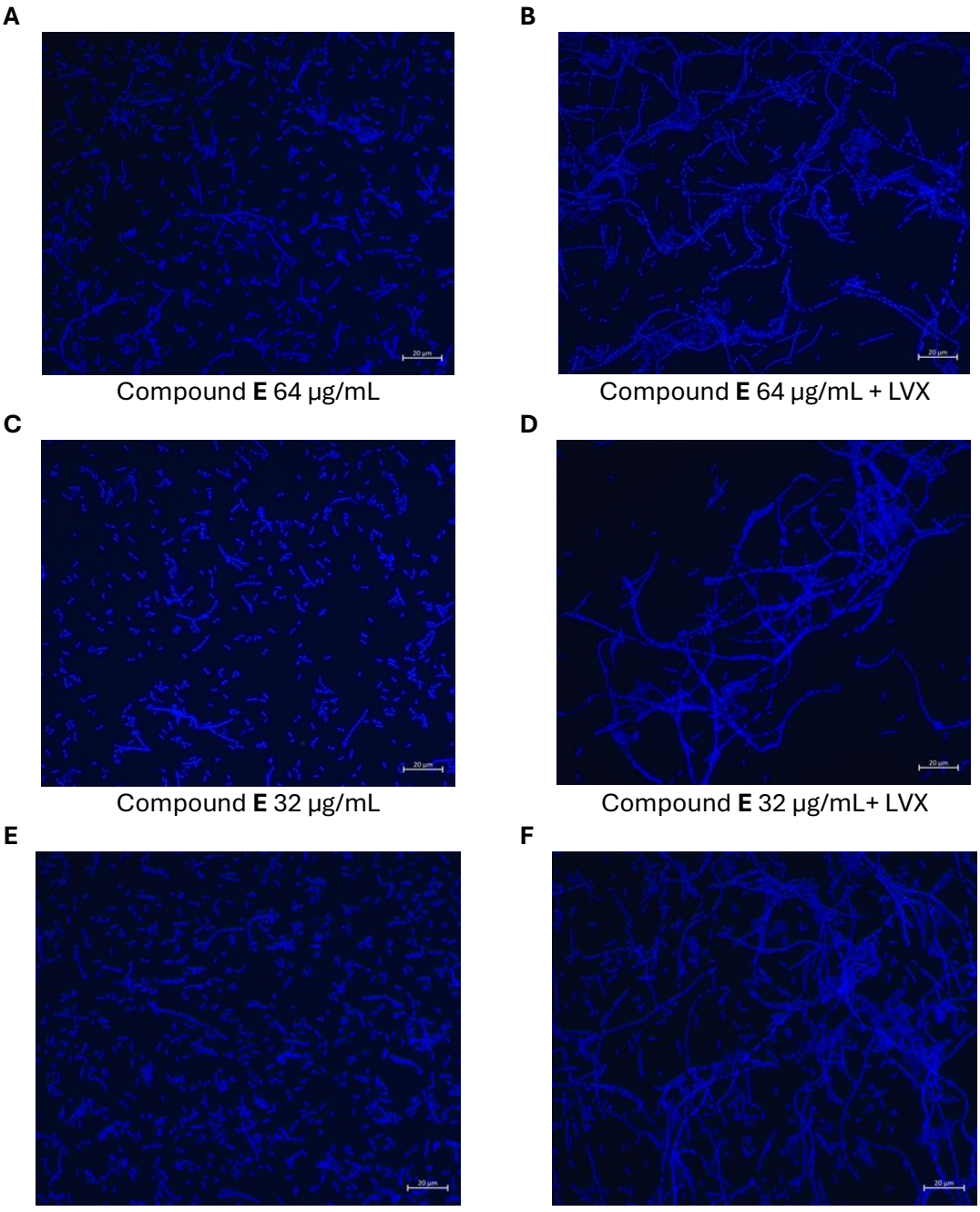


Figure 53. Fluorescence microscopy of *E. coli* BL21(DE3) with DAPI at 40×.

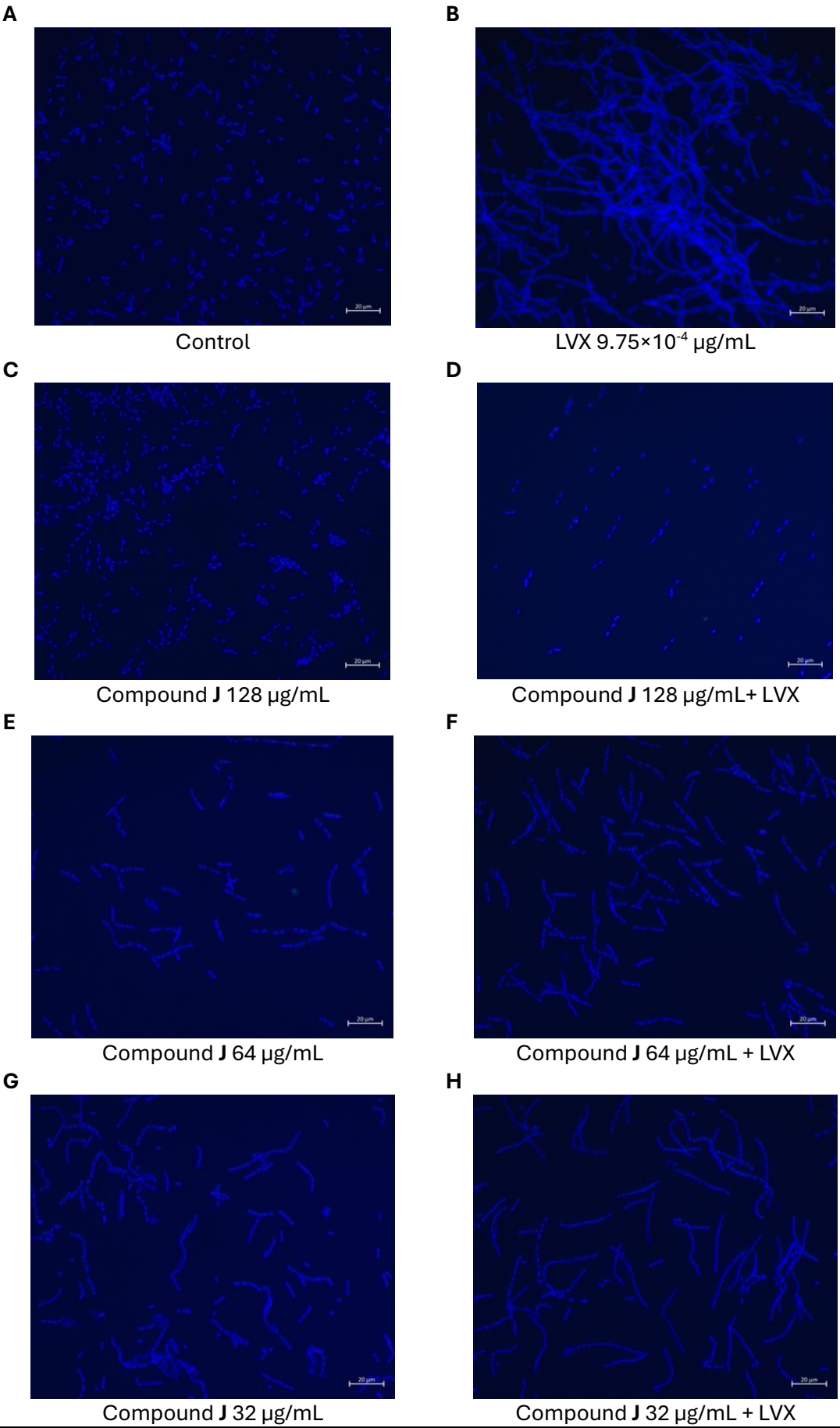


Figure 54. Fluorescence microscopy of *E. coli* BL21(DE3) with DAPI at 40×.

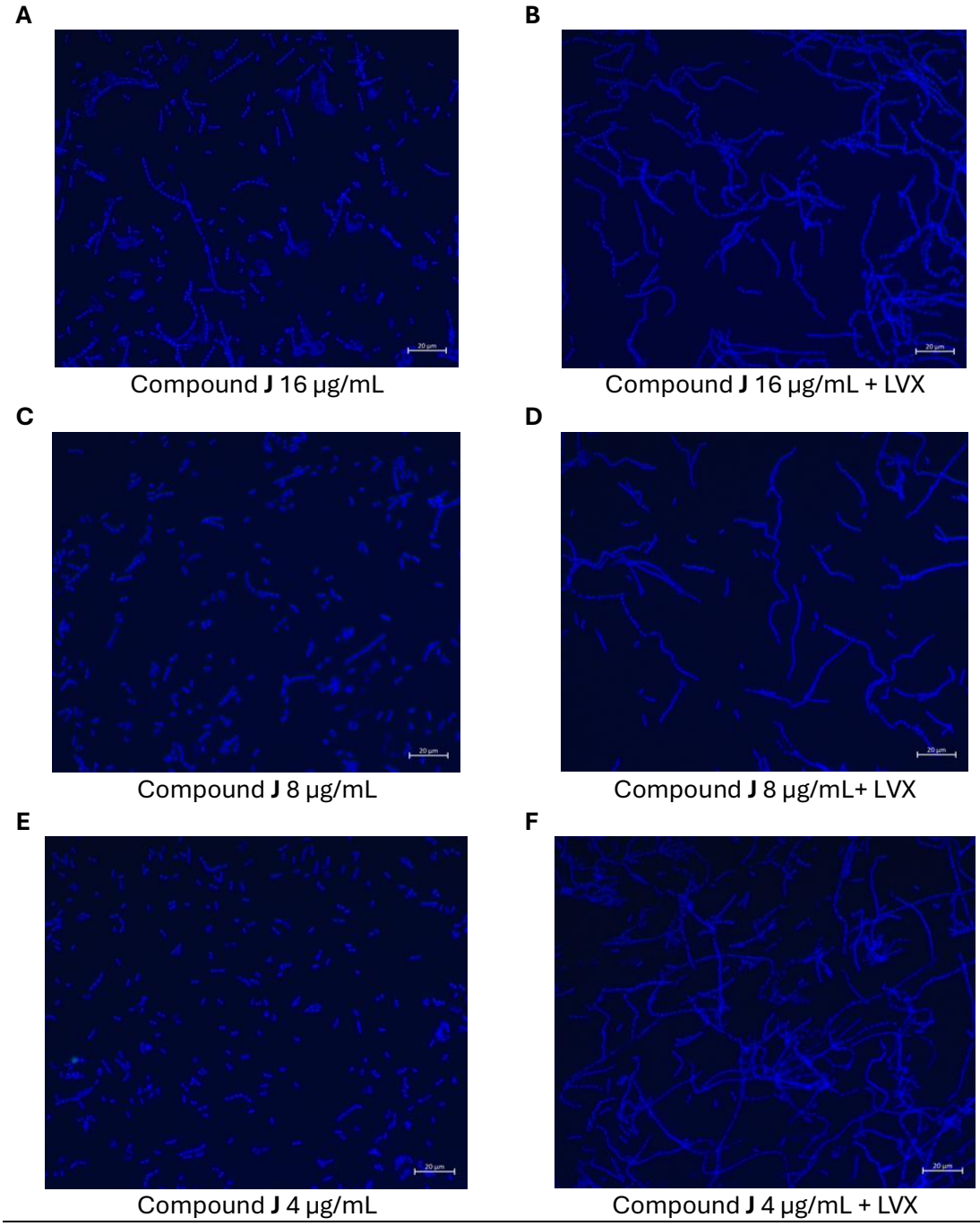


Figure 55. Fluorescence microscopy of *E. coli* BL21(DE3) with DAPI at 40×.

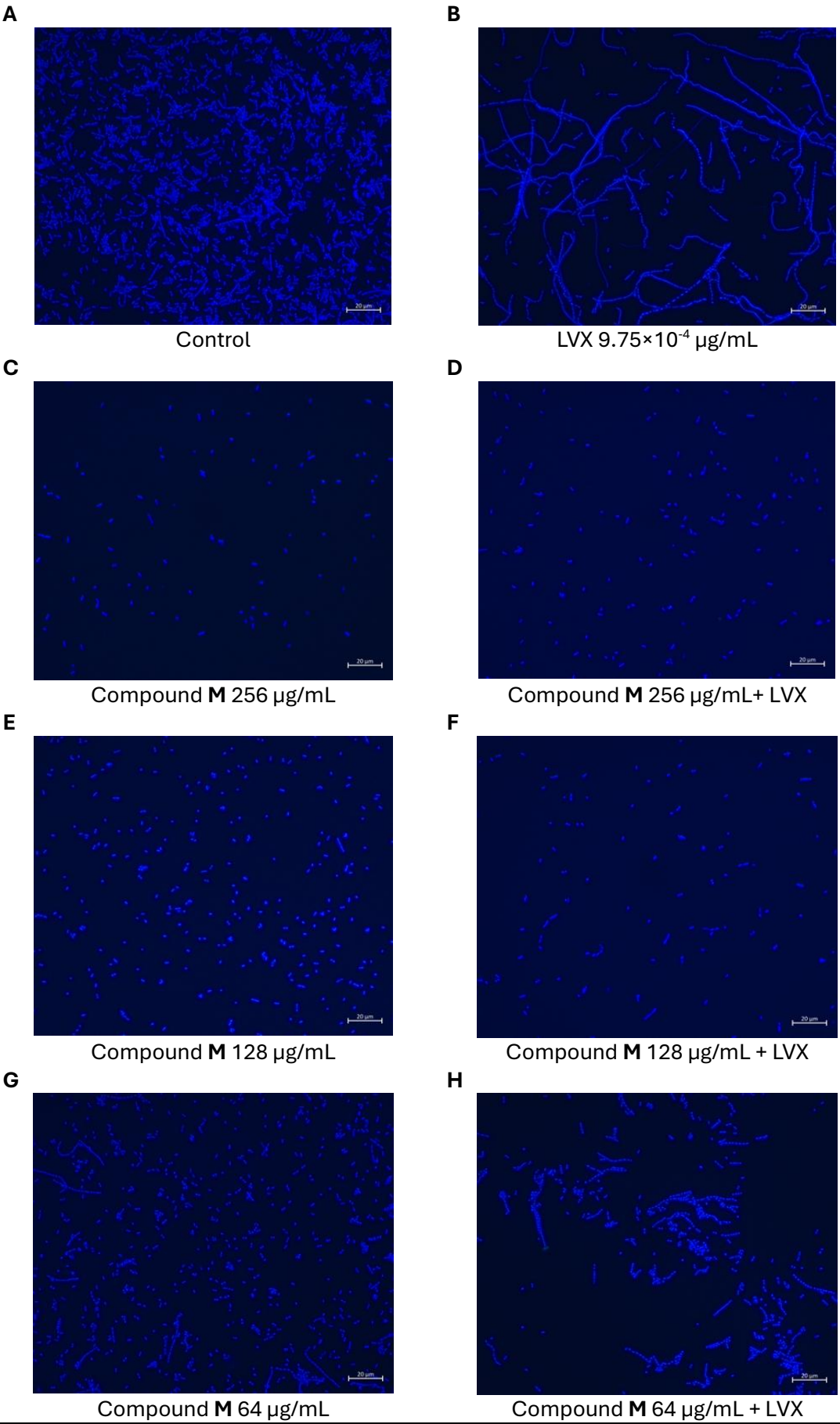


Figure 56. Fluorescence microscopy of *E. coli* BL21(DE3) with DAPI at 40×.

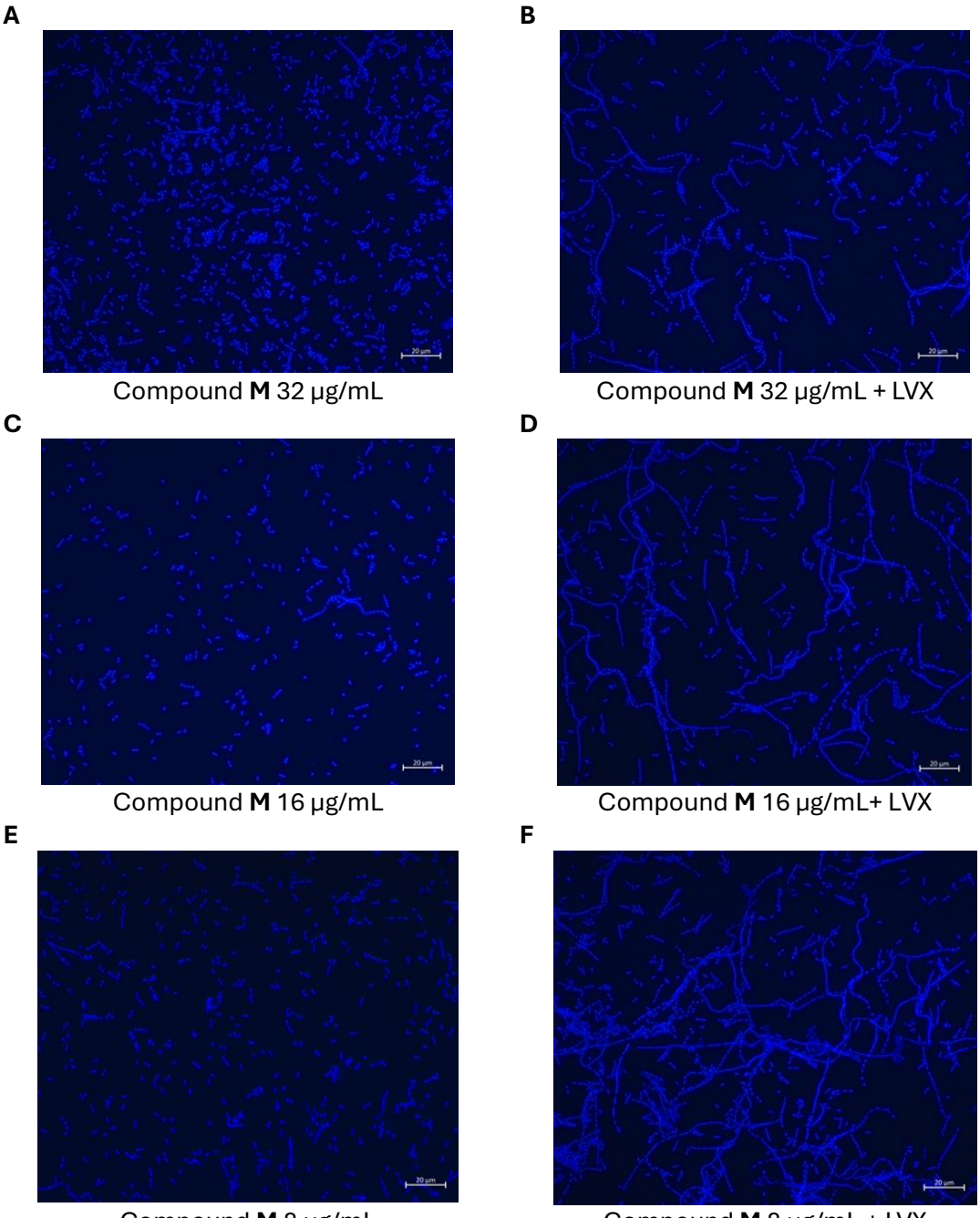


Figure 57. Fluorescence microscopy of *E. coli* BL21(DE3) with DAPI at 40×.

Figure 58 reports the plots of the mean filament length for compound A, and **Table 13** shows the percentage of reduction. All six concentrations exhibited inhibitory capacity, with a minimum percentage of reduction of 49% up to 94%.

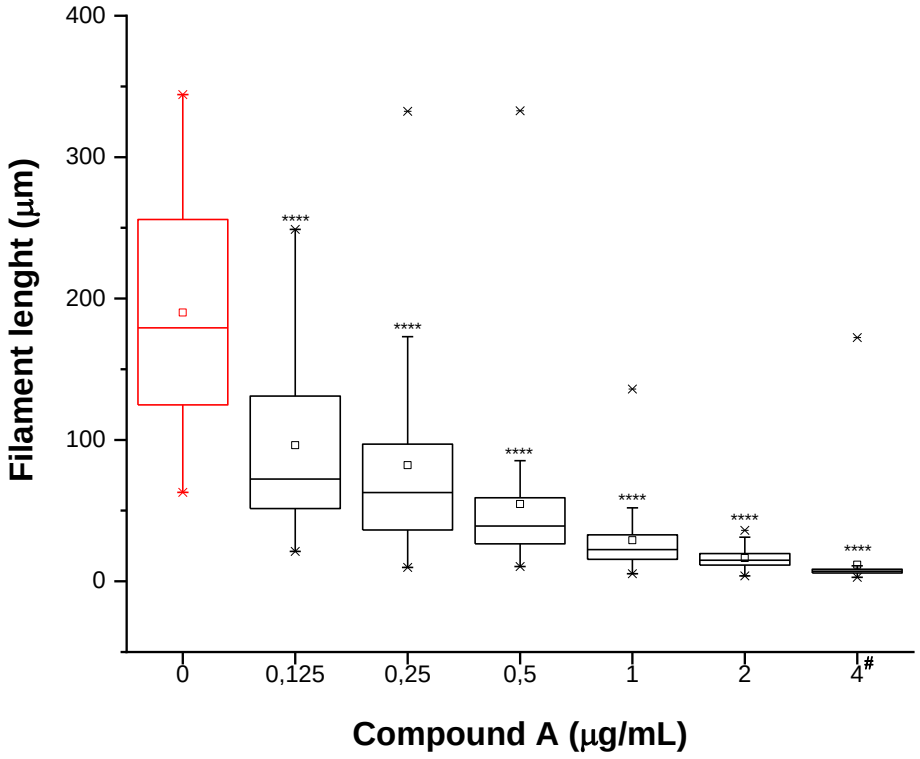


Figure 58. Plot of the mean of filament length related to the compound **A** concentration; the concentrations tested range from the MIC value up to 1/32 of its value. (#) MIC value; **** p<0.001.

Table 13. Percentage of filament length reduction for compound **A**

Compound(s) (µg/mL)	Mean of filament length (µm)	SD	Percentage of reduction
LVX ($9{,}75x10^{-4}$)	190.07	76.98	-
LVX+ **A** (0.125)	96.21	60.47	49%
LVX + **A** (0.25)	82.14	63.86	57%
LVX + **A** (0.5)	54.67	52.97	71%
LVX + **A** (1)	29.01	23.52	85%
LVX + **A** (2)	16.44	6.9	91%
LVX + **A** (4)#	11.7	22.45	94%

(#)MIC value

Figure 59 shows the trend of filament length reduction concerning the boron concentration in use, and **Table 14** shows the percentages of filament length reduction; these percentages, range from a minimum of 53% to a maximum of 97%. All six concentrations reduce filamentation.

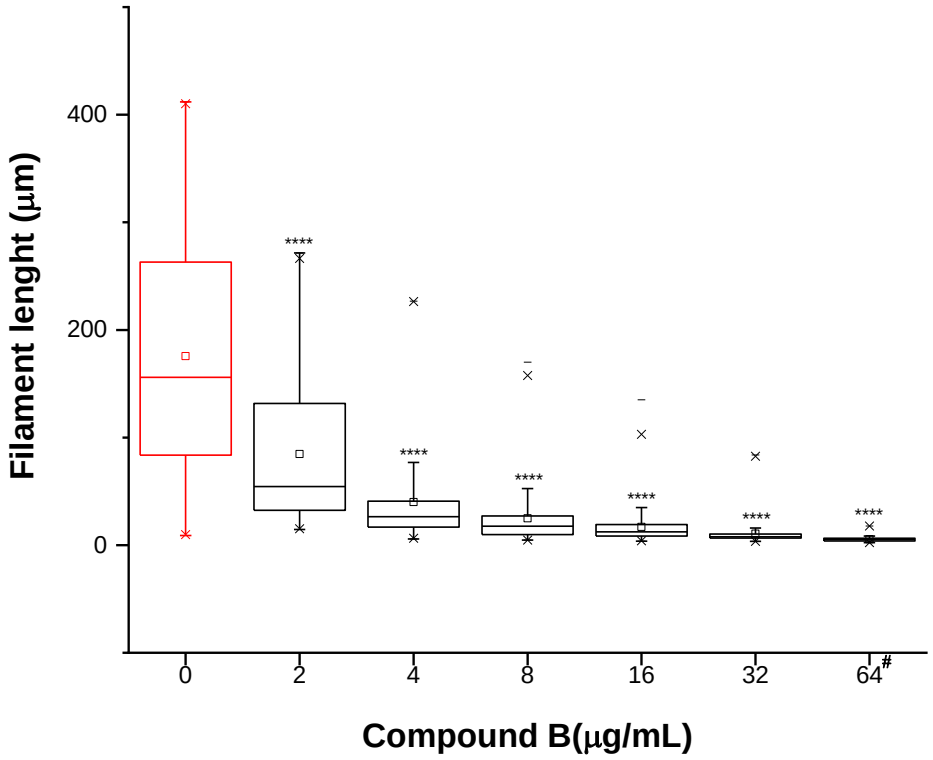


Figure 59. Plots of the mean of filament length related to the compound **B** concentration; the concentrations tested range from the MIC value up to 1/32 of its value. (#) MIC value; **** p<0.001.

Table 14. Percentage of filament length reduction for compound **B**

Compound(s) (µg/mL)	Mean of filament length (µm)	SD	Percentage of reduction
LVX ($9{,}75x10^{-4}$)	175.73	100.82	-
LVX+ **B** (2)	84.58	65.51	53%
LVX + **B** (4)	40.1	43.64	77%
LVX + **B** (8)	24.85	27.29	86%
LVX + **B** (16)	16.87	14.87	90%
LVX + **B** (32)	10.73	11.29	94%
LVX + **B** (64)#	5.54	2.73	97%

(#)MIC value

In **Figure 60** are reported the plots of the mean of filament length for compound **M**, and in **Table 15** the percentage of reduction. All six concentrations exhibited inhibitory capacity, with reduction rates starting at a minimum of 51% for the lowest concentration tested, and up to 91% for the MIC value. Compounds **A**, **B** and **M** show a very similar trend to that of compounds **1** and **2**.

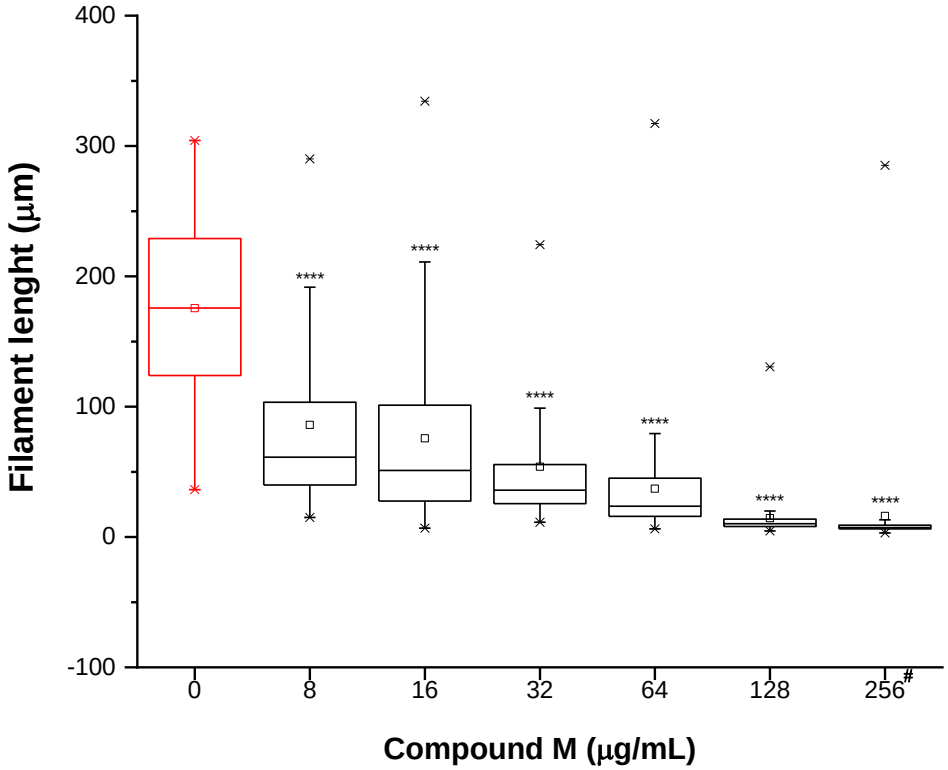


Figure 60. Plots of the mean of filament length related to the compound **M** concentration; the concentrations tested range from the MIC value up to 1/32 of its value. (#) MIC value; **** p<0.001.

Table 15. Percentage of filament length reduction for compound **M**

Compound(s) (μg/mL)	Mean of filament length (μm)	SD	Percentage of reduction
LVX ($9{,}75 \times 10^{-4}$)	175.46	68.6	-
LVX+ **M** (2)	86.01	66.35	51%
LVX + **M** (4)	75.63	70.15	57%
LVX + **M** (8)	53.89	48.13	69%
LVX + **M** (16)	37.05	44.05	79%
LVX + **M** (32)	14.46	18.39	92%
LVX + **M** (64)#	16.07	44.65	91%

(#)MIC value

CHAPTER VII

Discussion

In 1859, Charles Darwin proposed that organisms evolve through natural selection, favouring individuals possessing phenotypic traits advantageous to survival. This concept applies to multicellular organisms and can extend to unicellular organisms, including bacterial cells. In bacteria, natural selection works similarly to how it functions in other organisms: random genetic variations create traits that may be beneficial or detrimental in each environment. Bacteria with advantageous traits survive, reproduce, and pass these traits to subsequent generations, thereby evolving a population with specific genetic and phenotypic characteristics, such as the ability to survive in the presence of antimicrobial agents.

Although antimicrobial agents were one of the greatest medical discoveries of the last century, drastically reducing mortality from even trivial infections, we are now witnessing a downside to their use. The misuse of antibiotics and the evolutionary mechanisms that microorganisms employ to ensure their survival have led to the emergence of antimicrobial resistance (AMR). It is estimated that by 2050, AMR could become the leading cause of death, even in industrialized countries. To counter this phenomenon, the synthesis of new pharmacological molecules may not be the ideal solution in terms of time and cost. Once new drugs are introduced into clinical practice, regardless of their potency, resistance mechanisms will begin to develop shortly after that, and these mechanisms will rapidly spread within and between species.

Evolution drives the development of AMR, so addressing the root cause of resistance development might be the most effective strategy (Merrikh H. and Kholi R.M., 2020). This means researching and evaluating alternative antimicrobial targets, focusing on strategies that modulate microbial pathogenicity. The goal would be to "teach" microorganisms to become less virulent, making infections more straightforward to manage.

Specifically, the ideal strategy would involve finding an "antievolutionary" target, a highly conserved element across various bacterial species, irrespective of whether they are Gram-positive or Gram-negative, which also plays a role in establishing mutagenic mechanisms and, thus, resistance. In this context, the bacterial SOS response fits these criteria and would be an excellent candidate. This system is responsible for repairing DNA damage of any kind and is central to the onset of mutations, whether beneficial or not. Moreover, it regulates bacterial pathogenicity

mechanisms, including virulence and horizontal gene transfer, which explains why it is an interesting antimicrobial target.

Interfering with the activation of the SOS system would not directly kill the bacterial cell. Still, it would block processes that could either promote beneficial mutations, prevent the exchange of genetic material (including resistance genes), or interfere with other mechanisms related to pathogenicity. Modulating this response could enhance the effectiveness of currently used antibiotics, creating a synergistic effect.

The RecA/LexA pathway regulates the SOS response. RecA is an ATP-dependent recombinase that functions as a DNA damage sensor, while LexA is a transcriptional repressor that controls the expression of around 60 genes. An initial stimulus is required for the transcriptional process to begin, the formation of single-stranded DNA (ssDNA). RecA binds to this ssDNA, activates, and interacts physically with LexA, stimulating its self-cleavage. Inhibiting the activation of this system means either targeting the RecA/LexA axis or acting on one of the two proteins, RecA or LexA.

Targeting the RecA/LexA axis essentially means preventing the activation of the SOS response, regardless of whether this inhibition is achieved through blocking the damage sensor or the transcriptional repressor. In a study by Bellio P. *et al.,* 2014, the authors evaluated the ability of curcumin to inhibit the activation of this process, induced by the antibiotic levofloxacin, in various *E. coli* strains. These strains were made competent for the expression of the TEM-1 β-lactamase, with its gene under the control of the LexA box. The expression of TEM-1 was used to measure the SOS response activation, and the study found that curcumin effectively inhibited this phenomenon. Another study, conducted by Berger M. *et al.*, 2019, "measures" the activation of the SOS response in enterohemorrhagic *E. coli* by assessing Shiga toxin production. The study evaluates the potential for blocking this response, even after its initial induction, by examining the effects of transcriptional and translational inhibitors. It was found that even after activating the SOS response, the use of transcriptional inhibitors, particularly the antibiotic rifaximin, can still be effective in blocking the SOS response, as evidenced by a reduction in the production of Stx toxin.

In general, a direct approach targeting the axis may not be particularly effective, as it would require identifying molecules with the capacity to interact with RecA and LexA. On the other hand, a more selective approach, which discriminates between the two proteins involved, could prove far more promising. Of the two, RecA has certainly been more extensively explored. RecA is an attractive target because inhibiting it would prevent the activation of the SOS response at its onset, thereby blocking both DNA damage repair and the activation of other processes underlying

bacterial pathogenicity. To give some examples, we can cite a study by Yamikov A. *et al*., 2017, where synthetic peptides were developed based on the sequence of RecAX, a natural inhibitor of the RecA recombinase, capable of promoting the disassembly of the nucleofilament. Among the various synthesized peptides, one was shown to inhibit RecA *in vitro* effectively, and this inhibition translated into a blockage of SOS response activation *in vivo*. In another study by Bellio P. *et al.,* 2017, the inhibitory effects of secondary metabolites from lichens on *E. coli* RecA were explored. Of the 27 selected molecules representing different categories, 9 demonstrated approximately 80% inhibition of RecA at micromolar concentrations. These molecules acted as non-competitive inhibitors of the ATP binding site, with one molecule specifically interacting with the ssDNA binding site. Additionally, Alam M.K. *et al.,* (2016) synthesized RecA inhibitors based on the metatungstate molecule, a highly anionic compound known to inhibit RecA. These new inhibitors block the binding of ssDNA and, when combined with antibiotics, enhance both their bactericidal and bacteriostatic effects.

RecA serves as a DNA damage sensor and functions as a recombinase enzyme that promotes genome repair through homologous recombination. Importantly, RecA is not exclusive to bacterial cells. Its eukaryotic counterpart, Rad51, performs the same essential function in humans, ensuring the maintenance of genome integrity. The fact that Rad51 is also present in eukaryotic cells may pose challenges for targeted therapy, as its homology to bacterial RecA could hinder the development of highly specific pharmacological treatments.

In contrast, the transcriptional repressor LexA has been less explored as a target for the SOS response. Unlike RecA, it lacks eukaryotic homologs, and targeting a transcriptional repressor would represent an innovative approach. Traditional pharmacological strategies typically focus on inhibiting transcription through RNA polymerase blockers. Still, they do not specifically target the initial transcriptional repressor itself, making LexA inhibition a potentially novel and effective therapeutic strategy.

LexA prevents gene transcription functionally as long as it remains intact and bound to its specific sequence, the LexA box. For transcription of the SOS genes to begin, LexA must bind to RecA in its active form, which induces self-cleavage. This process is facilitated by RecA, which stabilizes LexA in its cleavable form, ensuring the protein is split into its N-terminal and C-terminal domains through an autolysis mechanism. Unlike an enzyme, once hydrolysis occurs, LexA irreversibly loses its function. Its catalytic mechanism involves the hydrolytic cleavage of the Ala84-Gly85 bond through a reaction involving the dyad Ser119-Lys156. Inhibiting the hydrolysis of LexA means preventing its cleavage and, therefore, the loss of function. To this end, a sustainable approach could involve targeting the blockage of the

cleavage reaction by aiming at the catalytic serine, treating LexA as if it were an enzyme.

An interesting strategy for the inhibition of LexA is described by Maso L. *et al.,* 2022. The basic idea is to use nanobodies (Nbs) derived from llamas against LexA. These nanobodies are distinguished by their ability to target unconventional epitopes inaccessible to traditional antibodies. In this specific case, they provide a larger interaction surface, capable of blocking LexA in the NC conformation, which is non-cleavable, with IC_{50} values in the μM range.

Since the 20th century, a new class of drugs characterized by boron in their structures has been introduced in medicine. Boron is an essential element in nature for plants and microorganisms, exhibiting many properties similar to carbon. Boron-based drugs are widely used in oncology, where they act as proteasome inhibitors. Still, they are also applied in treating other diseases, such as onychomycosis, atopic dermatitis, and diabetes mellitus.

The general mechanism of action of boron involves the inhibition of serine proteases, enzymes that use a serine residue in their active site. In this context, boron derivatives come into play: just as these molecules inhibit serine proteases, in a similar mechanism, they can bind to serine 119 of LexA, preventing its hydrolysis. This theory was initially developed and later confirmed by our research group, with the results published in 2020 (Bellio P. *et al.,* 2020). This study demonstrated the ability of small boron-based molecules to bind LexA of *E. coli* and interfere with its self-cleavage. Furthermore, a specific inhibitor of this transcriptional repressor was identified for the first time: 3-aminophenylboronic acid. This work was further validated by Chatterjee C. *et al.*, 2023, who evaluated the potential of the same boron compound on LexA of Mycobacteria.

Building on these findings, our approach has evolved, this time focusing on molecules that are either already in use in pharmacological treatments or in the pre-clinical phase, adopting a drug repurposing approach.

The core concept was to identify potential inhibitors of the LexA transcriptional repressor, by exploring a pool of molecules for which pharmacological data were either already available or actively being collected. This approach was chosen to streamline the process: once effective molecules were identified, there would be no need to initiate lengthy preclinical studies, thereby significantly reducing the time needed for potential approval for repurposing these compounds for a new therapeutic use.

Based on this assumption, an initial pool of molecules was selected (**Table 1**) for their status as either approved and marketed or in various stages of clinical experimentation. These molecules are used to treat diverse conditions but share the

common feature of incorporating boron, which is physically bound to the carbon backbone of the molecule. Specifically, 8 molecules were selected: Tavaborole (**2**), an antifungal compound used for treating onychomycosis (nail fungal infections). It acts by interacting with leucyl-tRNA synthetase, thereby inhibiting protein synthesis (Markham A. *et al.,* 2014). Marketed under the brand name Kerydin®, it has been available in the United States since July 2014. Crisaborole (**3**), which shares the same scaffold as Tavaborole, is used in atopic dermatitis treatment. It works by inhibiting phosphodiesterase 4 (PDE4), an enzyme involved in the proinflammatory cascade (Murrell D.H. *et al.,* 2015). Marketed as Eucrisa®, it has been used in the USA since December 2016. Talabostat (**4**) is currently in the investigational phase for the treatment of lymphoma (non-Hodgkin's), leukemia (lymphoid), lung cancer, melanoma, and pancreatic cancer. It is an inhibitor of human prolyl endopeptidase FAP, a cell surface glycoprotein serine protease involved in extracellular matrix degradation and numerous cellular processes (Narra K. *et al.,* 2007). Ixazomib (**5**) is a boron-based compound approved for cancer therapy. It became the first proteasome inhibitor approved in 2017, marketed under the name Ninlaro, for use in patients with relapsed or refractory multiple myeloma (Raedler L.A. *et al.,* 2016). Vaborbactam (**6**), a cyclic boronic acid β-lactamase inhibitor (BLI), exhibits a broad spectrum of activity against various serine β-lactamases, including KPC carbapenemases. The combination of Vaborbactam and meropenem is approved in the United States and Europe for treating various nosocomial infections (Tsivkovski R. *et al.,* 2020). Delanzomib (**7**), another proteasome inhibitor, is in phase II clinical trials for cancer treatment and immunological disorders (Wang M. *et al.,* 2019). Bortezomib (**8**) is a dipeptide boronic acid, approved as a proteasome inhibitor for treating multiple myeloma in patients who have failed at least two prior therapies (Curran M.P. *et al.,* 2009). Additionally, 1-hydroxy-(3H)-2,1-benzoxaborole (**1**) was included as a scaffold for compounds **2** and **3**.

The selected boron compounds were first evaluated for their ability to interfere with the microbial growth of *E. coli* BL21(DE3) and *E. coli* ATCC® 25922, by determining the MIC values for each compound. The corresponding MIC values are reported in **Table 3**. Only compounds **1** and **2** demonstrated the ability to interfere with microbial growth in both strains, showing similar values. All others, from **3** to **8**, did not exhibit this ability at the tested concentrations. It should be noted that for these compounds, concentrations higher than 128 μg/mL could not be evaluated due to issues related to product availability and DMSO concentration.

After completing this preliminary evaluation, in the next step, we focused on their ability to inhibit a well-known process correlated with the SOS response activation: filamentation. By assessing this process, we gain two essential insights: first, whether the molecule can penetrate the cell, effectively crossing the membrane

system of *E. coli*, and, more importantly, whether it can inhibit the SOS response by targeting the RecA/LexA pathway.

Filamentation is a cell division defect, where the cell does not divide despite genome replication. This results in the formation of cells with the genome replicated multiple times and with considerable lengths. SulA is responsible for the inhibition of cell division. SulA is expressed after the SOS response activation as part of the SOS checkpoint control system. SulA exerts its action through the binding with FtsZ, a tubulin-like protein with a GTPase activity, responsible for the Z-ring and septum formation for the completion of cell division (Trusca D. *et al.,* 1998). Fluoroquinolone levofloxacin was used to induce filamentation and activate the SOS response. This antibiotic inhibits genome replication, causing replication fork stalling and forming single-stranded DNA (ssDNA). Initially, we evaluated which strain, *E. coli* BL21 (DE3) or *E. coli* ATCC® 25922, would be most suitable for this assay by testing various inducer concentrations and incubation times, following the protocol established by Bellio P. *et al.,* 2020. The *E. coli* BL21 (DE3) and ATCC® 25922 results are presented in **Figures 17-18** and **19**, respectively.

From the filamentation images, it was clear that *E. coli* BL21 (DE3) is the optimal model for filamentation, particularly when exposed to a concentration of 9.75×10^{-4} µg/mL (0.125×MIC) for 3 hours (**Figure 17-A**). Longer incubation times resulted in filamentation in the control group, and higher inducer concentrations caused excessive cell death. For *E. coli* ATCC® 25922, to achieve a level of filamentation comparable to *E. coli* BL21, the microbial suspension needed to be exposed to 0.0156 µg/mL of LVX (0.5×MIC) for 5 hours (**Figure 19-I**). However, this concentration was too high, leading to excessive cell death at shorter incubation times, and the resulting filaments exhibited distinct morphological characteristics compared to those produced with lower antibiotic concentrations.

As a result, *E. coli* BL21 was chosen for further experimentation. This strain is more prone to filamentation due to carrying several mutations, including the mutation in the *lon* gene (Howard-Flanders P. *et al.,* 1964). In the filamentation process, the Lon protease plays a key role: it degrades various cellular proteins to maintain homeostasis, such as SulA. In *E. coli* BL21 (DE3), the accumulation of SulA, following SOS response activation, is not counteracted by Lon protease activity. As a result, filamentation is significantly more pronounced than the wild-type counterpart.

After identifying the most suitable *E. coli* strain for the filamentation assay, the compounds were tested at a single concentration corresponding to their MIC value, alone and in combination with LVX. The results are presented in **Figures 20**, **21**, and **22**. Only three of the eight boron compounds,**1**, **2**, and **3** (**Fig. 20 D-F**; **Fig. 21 B**) demonstrated a significant ability to interfere with filamentation, while the

remaining compounds were ineffective. This difference in activity is likely attributed to the molecular structure of the compounds; those that were ineffective are bulky and structurally complex, which could hinder their ability to cross the *E. coli* membranes system.

For this reason, the other compounds were excluded from the subsequent steps, and the decision was made to continue with compounds **1**, **2**, and **3**. These molecules share the same scaffold but differ in the substituents at position five: hydrogen in compound **1**, fluorine in compound **2**, and a cyanophenyl group in compound **3**. Filamentation was further investigated by testing six concentrations of each compound, ranging from MIC to 0.0313×MIC. The images for compounds **1**, **2**, and **3** are presented in **figures 23** and **24**, **25** and **26**, **27** and **28**, respectively. All three boron-based compounds clearly interfere with filamentation at each tested concentration, with more pronounced effects observed for compounds **1** and **2** compared to **3**. The length of the filaments generated by LVX alone was measured, and the length was also determined when combined with the different concentrations of boronic compounds. The resulting graphs demonstrate a concentration-dependent effect on filament length (**figures 29**, **30**, and **31**). The corresponding percentage reductions in filament length are shown in **tables 4**, **5**, and **6**.

For **1** and **2**, all concentrations tested significantly reduced filamentation, with reductions ranging from 70% to 97% for **1** and 32% to 97% for **2**. In contrast, compound **3** exhibits a less significant effect: three concentrations show no notable reduction, while the three highest concentrations (0.25×MIC, 0.5×MIC, and MIC) reduce filament length by 26% to 54%. The reason for this may be related to the nature of the substituent, which could result in a reduced ability to interact with the target.

Once it was demonstrated that the selected molecules could enter the cell and interact with the RecA/LexA pathway, the next step was to assess their actual interaction with our target, LexA protein. To achieve this, a biochemical assay on the protein was performed, which had been produced and purified previously in our laboratory. The inhibition assay of LexA by alkaline-induced autohydrolysis was assessed. At physiological pH, LexA is stabilized in its NC form; it is the interaction with RecA that triggers the switch to the C conformation, promoting self-cleavage. Although cleavage requires RecA *in vivo*, LexA can cleave itself *in vitro* without RecA, a reaction termed autocleavage. Autocleavage is relatively rapid at high pH and hydrolyzes the same bond as in RecA-stimulated cleavage (Luo Y. *et al.,* 2001). pH 10 promotes the hydrolysis of LexA by increasing the nucleophilicity of key residues involved in self-cleavage (Ser119/Lys156), destabilizing the NC form and enhancing the autocatalytic cleavage activity of LexA.

To achieve this, the reaction was carried out following the guidelines of Mo C.Y. *et al.,* 2014, and performed in two different conditions: one without incubation between LexA and the candidate boron compounds and another with a 15-minute incubation at 30°C. SDS-PAGE was used to resolve the samples. The gel images are shown in **Figure 32**. Panel **A** corresponds to the reaction without incubation, while panel **B** represents the experiment conducted after incubation. Visually, it is evident that the intensity of the LexA bands in the presence of the inhibitor is more intense in **B** compared to **A**, suggesting that the boron compounds have a time-dependent effect. **Table 7** displays the fraction of uncleaved LexA for both experiments. Regardless of the boron compound tested, the residual fraction of LexA nearly doubled after incubation. Among the three compounds, **1** and **2** show fairly similar results, while compound **3** demonstrates a lower inhibitory effect, though still enhanced after incubation with the LexA protein. This assay provides two key insights: first, the inhibition of filamentation is due to the ability to interfere with LexA self-cleavage; second, among the compounds tested, compound **3** is less effective. Specifically, in the filamentation assay, compounds **1** and **2** show a significantly stronger ability to reduce filament length at all tested concentrations, while compound **3** is less effective at lower concentrations. Even at higher concentrations, the reduction observed with compound **3** is modest when compared to compounds 1 and 2. The biochemical data reveal that compounds **1** and **2**, even without incubation, exhibit a notable ability to interfere with LexA, further enhancing this effect by incubation. In contrast, compound 3 demonstrates a weaker ability to interact with LexA, even after incubation. Therefore, the initial biochemical and microbiological data confirm that compounds **1** and **2** have a superior ability to interact with the LexA protein compared to compound **3**, a phenomenon always to be sought in the nature of the substituent, which bulky may not be able to establish interactions with LexA, unlike the substituents in **1** and **2**.

Having demonstrated that an interaction with LexA causes the observed inhibition of the SOS response activation, the subsequent step was to further validate this interaction through a biochemical assay that more accurately mimics the conditions for LexA hydrolysis induction: the RecA/LexA co-protease activity assay. This approach was not initially selected, as observing a lack of LexA hydrolysis could still have been attributed to an inhibition of RecA's activity. Fixed the LexA concentration, several [I]:[LexA] ratios were tested for determining the half-maximal inhibitory concentration for every compound, IC_{50}, which indicates the boron concentration at which 50% of LexA is uncleaved. In **figure 33** are reported the plots of the fraction of uncleaved LexA versus the inhibitor concentration, expressed as molar ratios. The IC_{50} value corresponded at 8.88 mM for **1**, 3.88 mM for **2** and 6.68 mM for **3**. In general, the lower the IC_{50} value, the greater the inhibitor's effectiveness. Therefore, based on the reported data, compound **2** shows the lower IC_{50} value, and exhibits the best activity in inhibiting the self-cleavage of LexA.

Another phenomenon associated with SOS response activation is microbial biofilm formation (Recacha E. *et al.,* 2019; Bernier S.P. *et al.,* 2013). Biofilm is a bacterial survival strategy primarily triggered by starvation, which occurs when nutrients are scarce, a stress condition that activates the SOS response. Bacteria form communities that adhere to surfaces or grow at air/liquid interfaces, embedded within a self-produced polysaccharide matrix. This matrix also confers resistance to antimicrobials by limiting access to antimicrobial agents, thereby reducing the effectiveness of antimicrobial therapies (Yang S. *et al.,* 2023). Biofilm, therefore, represents an additional strategy for antimicrobial resistance. The antibiofilm activity of boron-based compounds is still an underexplored area, but some recent studies demonstrate their effectiveness (Celebi O. *et al.,* 2024; Sayin Z. *et al.,* 2016). Given the general antibiofilm potential of boron, the fact that biofilm formation is associated with the bacterial SOS response, and the evidence that our candidates are well capable of interfering with one of the key players in this system, our further objective was to explore their potential antibiofilm properties, both in terms of inhibition and eradication (Konaklieva M.I. *et al.,* 2024).

As with the filamentation assay, a preliminary experiment was conducted to determine the best biofilm producer between *E. coli* BL21 (DE3) and *E. coli* ATCC® 25922, under starvation conditions and at two different incubation temperatures, 26°C and 37°C, for 24 hours. **Figure 34** presents the plot showing biofilm formation for both strains and at both temperatures. *E. coli* ATCC®25922 was identified as the best biofilm producer at both temperatures and was selected for further assay. Twelve concentrations were evaluated for each of the three compounds for both assays. The compounds were added to the bacterial suspension for the inhibition assay, followed by 24 hours of incubation. **Figures 35**, **36**, and **37** show compounds **1**, **2**, and **3** plots, respectively. For **1** and **2**, concentrations starting from 16×MIC were tested, and good inhibition was observed across various concentrations. For compound **3**, testing started at the MIC value, and none of the concentrations exhibited inhibitory activity. **Tables 8**, **9**, and **10** report the percentage reduction in biofilm formation for each of the three compounds. For compound **1**, concentrations ranging from 2×MIC to 16×MIC resulted in a significant reduction of biofilm formation, with reduction percentages ranging from 65% to 88%. For compound **2**, concentrations ranging from 0.5×MIC to 16×MIC effectively inhibited biofilm formation, with reduction percentages ranging from 47% to 90%. For **3**, none of the concentrations displayed inhibitory activity. This result further confirms that compound **3** exhibits more limited activity in direct interaction with LexA and cell entry during microbiological assays.

However, there is an important consideration to be made. For all three boronates, there is an increase in biofilm formation at specific concentrations. During biofilm formation, microorganisms communicate with each other through quorum sensing.

Quorum sensing regulates the metabolic activity of planktonic cells and can induce microbial biofilm formation and increased virulence (Preda V.G. *et al.,* 2019). Bacterial communication is mediated by specific signalling molecules known as autoinducers (AIs) (Song S. and Wood T.K. 2021). Specifically, AI-2 is a signalling molecule used by various bacteria, including *E. coli*, and it is a small boron-containing molecule that shares significant structural similarities with the boronates being studied. Therefore, the observed increase in biofilm formation could be explained by the fact that at sub-inhibitory concentrations, our compounds may promote Quorum Sensing through AI-2, stimulating biofilm formation (Chen H. *et al.,* 2022).

For the eradication assay, the boronic compounds were added to a mature 24-hour biofilm at the same concentrations as above, followed by 96 hours of incubation. None of the three compounds could eradicate the pre-formed biofilm (**Figure 38 A**-**B**-**C**). However, this result is noteworthy: since the activation of the SOS response sustains the biofilm, blocking its activation is essential to limit or inhibit biofilm formation. Once the biofilm is formed, its eradication does not require highly specific mechanisms. Instead, it involves the disruption of the pre-formed extracellular matrix (Jensen G.S. *et al.,* 2023), which also limits the access of the boronic compounds to the cell. Therefore, the lack of eradication capability does not indicate a lack of activity against the target, as eradication is a mechanism different from inhibition.

The latest evaluation of the biofilm focused on its observation using Scanning Electron Microscopy (SEM), performing a purely qualitative analysis. Compound **3** was not examined due to its inability to inhibit biofilm formation. A single concentration was chosen for compounds **1** and **2**, which was the one at which a 50% reduction in biofilm formation was observed. In **figures 39** and **40**, the images of **1** and **2** are shown, respectively. In the controls, a homogeneous EPS is observed, which engulfs the cells, making it difficult to distinguish individual bacteria from one another. This matrix is not present in the two treatments. For compound **1**, a homogeneous bacterial surface is visible, with sparse connections between individual bacterial cells, likely representing portions of the extracellular matrix in early formation. For compound **2**, a rough bacterial surface is observed, with connections indicative of partially formed polysaccharide matrix segments. Additionally, numerous channel-like structures extending from the cell surface are visible in both cases. These structures can be attributed to nanotubes formed under stress conditions and often before cell death. They are generally used to exchange proteins, DNA, and nutrients and are systems for intra-species and inter-species exchange (Pospíšil J. *et al.,* 2020). Their presence is more clearly visible in **figure 41**, where only images related to the control are shown. These channels/connections between the various bacterial cells, even of considerable lengths, are clearly seen.

Normally, bacteria exchange nutrients through diffusion, but using nanotubes/nanochannels minimizes the loss of substances that diffusion would cause. Therefore, this type of substance exchange is particularly advantageous in aquatic conditions or nutrient deprivation. In biofilm communities, starvation plays a role, and the close contact between cells also facilitates establishing such connections. The presence of these structures highlights a key aspect: the possibility for bacteria of different species to exchange enzymes, thus expanding their biochemical repertoire without the need for genetic adaptation (Pande S. *et al.*, 2015).

To confirm the biochemical and microbiological results obtained, the final step was to perform molecular docking between LexA and boron compounds **1**, **2**, and **3**. A total of 50 possible interactions between the transcriptional repressor and the boronic compounds were generated, selecting the interaction that showed the lowest theoretical binding energy. Based on the results shown in **Figure 42**, it was observed that for compounds **1** and **2**, very similar interactions are formed; the same number of hydrogen bonds is established, involving the same amino acid residues of the protein Ser119, Lys156, and Val155. While for Ser119 and Lys156, the established bonds are the same for both compounds, the difference is seen in the hydrogen bond with Val155. For compound **1**, the interaction occurs via the H of the nitrogen in Cα. In contrast, in compound **2**, this interaction with Val155 involves its carbonyl oxygen, which interacts with the hydrogen of the hydroxyl group attached to the boron. Hydrophobic interactions involve the same protein residues for both compounds, except for Leu113 and Val115, which are involved in interactions with compound **2**, and Val153, which participates in interactions with compound **1**.

For compound **3**, the hydrogen bonds formed always involve Ser119 and Lys156, in addition to Ser116. While this time, Lys156 participates by forming only one hydrogen bond between its ε-NH_2 group and the oxygen at position 2 of the boronic compound, Ser119 participates in the formation of two hydrogen bonds: one with the same oxygen that interacts with Lys156, and the other through an interaction with the hydroxyl group attached to the boron. Furthermore, the interaction is further stabilized by electrostatic interaction between the cyano group of the cyanophenyl group at position 5 and Glu173. Still, especially this substituent further stabilizes the structure by interacting with Phe174.

Regardless of the number of hydrogen bonds formed and the extent of hydrophobic interactions, the key point is that all three boron compounds interact with both amino acid residues that make up the catalytic dyad: Ser119 and Lys156. Both residues are engaged in forming at least two hydrogen bonds with the boronic compounds, which limits their ability to interact with each other, consequently blocking the self-hydrolysis reaction. Additionally, the binding energies for the three

compounds are consistent with each other. Significant differences are observed only in the theoretical K_i, where compound **2** shows the lowest value among the three molecules, while compound **3** corresponds to the highest value. However, this is still a purely theoretical parameter, which certainly does not consider the actual experimental conditions, such as working temperature and molecular solvation. Therefore, the docking data further supports the previous findings, confirming the ability of the boron compounds to interact with LexA, inhibiting self-cleavage and thus blocking the activation of the SOS response.

The combination of biochemical, microbiological, and docking data shows that the selected boronic compounds exhibit excellent inhibitory capability against our target, LexA. Based on this, a second set of molecules was selected, all sharing the same scaffold as the previous ones. These are molecules belonging to the benzoxaborole family, which differ from each other in the nature of the substituent and its position. The aim was to evaluate how different substituents might influence the activity of the individual molecules, using the same biochemical and microbiological assays once again. Thirteen molecules were selected from MolPort and are grouped in **Table 2**.

There is limited or no literature available for these molecules, except for few of them. Compound **G** has been shown to effectively interact with *P. aeruginosa* PBP3 (PaPBP3), forming trivalent interactions with Ser294, Ser349, and Lys484 (Newman H. *et al*., 2021). Additionally, these compounds are not currently in clinical use or undergoing trials, except for compounds **K**, **L**, and **M**. Compound **K** is an analogue of compound **2**, tavaborole, and differs by the presence of chlorine at position 5 instead of fluorine. It is under investigation for the treatment of Tinea pedis, a common fungal infection (https://go.drugbank.com/drugs/DB12810).

Compound **L** is an analogue of compound **3**, Crisaborole. The main difference is an additional cyano group in the cyanophenyl group. Like compound **3**, it works by inhibiting PDE4 and is under investigation for treating atopic dermatitis (https://go.drugbank.com/drugs/DB16039). Finally, compound **M** is distinct from the others in that the boron is not directly part of the cyclic structure but is externally attached, and it contains sulphur. This molecule and its derivatives are active against β-lactamases, making them a promising addition to pharmacological therapies (Minozzi M. *et al.,* 2011; Cendron L. *et al.,* 2019).

For this new group of molecules, the approach differed slightly from the previous one. Given the certainty that the base structure could interact with LexA, we began with an initial biochemical assessment aimed at identifying those molecules most capable of interfering with the self-cleavage of our target directly through the RecA/LexA co-protease activity assay. Only one concentration was tested, and the results are summarized in **Table 8**. This enabled an initial screening, allowing us to

select only those compounds that produced a fraction of uncleaved LexA of at least 0.5. As a result, compounds **C**, **E**, **H**, and I were discarded. Compounds **F**, **G**, **K**, and **L** were excluded due to significant solubility issues, rendering the results unreliable.

Thus, compounds **A**, **B**, **D**, **J**, and **M** proceeded to the determination of their IC_{50} values. The corresponding graphs are shown in **Figure 43**. The IC_{50} values are as follows: 295.7±58:1 for **A**, 296.7±54:1 for **B**, 206.2±20:1 for **D**, 412.6±11:1 for **J**, and 458.7±33:1 for **M** when expressed as a molar ratio with LexA. When expressed in mM, these values correspond to 3.69 mM, 3.71 mM, 2.57 mM, 5.15 mM, and 5.73 mM, respectively. As with the previous three boronic compounds, the values are in the mM range, with only minor differences likely attributable to the nature of the substituent. Among the five, the compounds with the lowest IC_{50} values are **A** and **B**, both characterized by a nitrogen atom at position 6. They differ in that, in **A**, nitrogen is attached as an amine group, while in **B**, it is attached as a nitro group. Nitrogen likely facilitates the formation of bonds that enhance the effectiveness of these molecules compared to the others.

After performing the biochemical assays, microbiological assays were carried out, initially by determining the MIC values for *E. coli* ATCC® 25922 and *E. coli* BL21 DE3. The data are presented in **Table 12**. The obtained values for the two strains are, in fact, perfectly overlapping. With few exceptions, most of the benzoxaboroles exhibit high MIC values. **A**, **B**, and **K** show relatively low values; for **C**, **D**, **E**, **I**, **J**, and **M**, the values are medium-high, while for the remaining ones, **F**, **G**, **H**, and **L**, the obtained values indicate an inability to inhibit growth even at the highest tested concentration (1024 µg/mL). It is worth noting that **K** and **L** showed solubility issues even during this preliminary assay.

The filamentation assay was performed on the compounds for which the IC_{50} value has previously been calculated, namely **A**, **B**, **D**, **J**, and **M**, with the addition of two other molecules based on structural analogy, **C** and **E**. Specifically, **A** and **C** are structural analogues: in **A**, the amino group is attached to C6, while in **C**, in addition to the amino group, there are two methyl groups at C3. **C** is also structurally analogous to **E**, as **E** contains the two methyl groups at C3. **B** and **D** are structural analogues as well: **B** has a nitro group attached to C6, while **D** has the same nitro group at the same position, plus two methyl groups at C3, making **D** structurally analogous to **E**. Lastly, **E** and **J** share similarities, as **J** has a vinyl group attached to C3.

Even in this case, six concentrations were tested, ranging from the MIC value down to 0.0313×MIC, for each compound, alone and in combination with LVX. The filamentation images are shown in **Figures 44-45**, **46-47**, **48-49**, **50-51**, **52-53**, **54-55**, and **56-57** for compounds **A**, **B**, **C**, **D**, **E**, **J**, and **M**, respectively. A concentration-dependent effect was observed for three of the compounds, particularly **A**, **B**, and

M. These three compounds show similar reduction trends, comparable to those obtained for **1** and **2**: each concentration, when combined with LVX, effectively limits filamentation and, when alone, none of these can induce filamentation. **Figure 58** shows the plot of mean filament length for compound **A**, and **Table 13** presents the percentage of reduction, which ranges from 49% at the lowest concentration evaluated, up to 94% at the highest concentration (the MIC value). **Figure 59** shows the plot for compound **B**, and **Table 14** presents the percentage of reduction, which ranges from 53% to 97%. Finally, for compound **M**, the plot is shown in **Figure 60**, and the percentage of reduction ranges from 51% to 91%, as shown in **Table 15**.

For the remaining molecules, **C**, **D**, **E**, and **J**, a different behaviour was observed compared to the previous compounds. In **C**, it was observed that when the boronic compound was used alone, it induced filamentation at concentrations corresponding to MIC, 0.5×MIC, 0.25×MIC, and 0.125×MIC. When combined with LVX, a reduction in filament length was observed only at the MIC value. For **D**, filamentation was again induced at MIC, 0.5×MIC, and 0.25×MIC concentrations, and a reduction in filamentation was observed at MIC and 0.5×MIC. In **E**, filamentation was caused by the boronic compound alone at MIC, 0.5×MIC, 0.25×MIC, and 0.125×MIC, and the combination with the inducer reduced filamentation only at MIC and 0.5×MIC. Finally, **J** exhibited behaviour similar to the previous compounds: it caused filamentation when used alone at four concentrations tested, 0.5×MIC, 0.25×MIC, and 0.125×MIC. When combined with LVX, the phenomenon was reduced at MIC and 0.5×MIC, although filamentation still occurred at this concentration. In general, a reduction in filamentation was observed for the other concentrations, but the compound could still activate the SOS response, although to a lesser extent. This is likely due to the molecular structure of the compounds: all of them feature a substituent at C3, the same for **C**, **D**, and **E**, while **J** contains a vinyl group at that position, but they share the same number of substituent atoms. The presence of this group at C3 may give the molecule properties that cause DNA damage, thus activating the SOS response. This is supported by filamentation being observed even at the highest concentrations (MIC values), where only about 20% of the cells remain viable, and the SOS response is still activated in the few surviving cells. As the concentration decreases, the number of viable cells increases, and so does the filament length. At very low concentrations, filamentation is not observed, and a higher number of viable cells are present in the sample, indicating that the molecule does not induce any effects that compromise cell viability, such as DNA damage, which would trigger the activation of the SOS response

CHAPTER VIII

Conclusions

The transcriptional repressor LexA is undoubtedly an excellent candidate for antimicrobial therapy, not only because of its essential role in the bacterial cell but also because it is a protein conserved across various microorganisms. The SOS response is a common system that, while exhibiting some minor differences, regulates the same processes across microbial species. Moreover, LexA is the ideal target from both an evolutionary and a bacterial uniqueness standpoint, as it lacks eukaryotic analogues, making it suitable for selective inhibitors. This specificity can potentially reduce the toxic effects that therapy might cause when targeting proteins with eukaryotic homologs. The fact that boron-based compounds can interfere with LexA activation further strengthens their appeal, given the safety and relatively low toxicity of boronic acids.

The results obtained confirm, first and foremost, the growing interest in boronic acid derivatives due to their low toxicity and versatility, making them well-suited for inhibiting LexA's self-cleavage. This positions them as a valuable tool in addressing antimicrobial resistance (AMR). Furthermore, these studies have identified an excellent scaffold, the benzoxaborole, demonstrating its ability to interact with the transcriptional repressor, with varying degrees of efficacy depending on the nature of the attached substituent. Notably, two of the compounds examined, Tavaborole and Crisaborole, not only confirmed our hypothesis that they could interact with LexA, but their existing approval status offers a significant advantage for drug repurposing. This approach bypasses major early-stage experimentation and pharmacovigilance challenges, as these compounds are already subjected to post-market monitoring.

It is also important to highlight that the activity of boronic acids extends to inhibiting biofilm formation, another critical aspect of AMR, further emphasizing their importance and versatility. This strengthens the case that interest in these molecules will continue to grow in the coming year.

References:

- Abraham EP, Chain E. An enzyme from bacteria able to destroy penicillin. 1940. Rev Infect Dis. 1988 Jul-Aug;10(4):677-8. PMID: 3055168.
- Adams, R.A., Leon, G., Miller, N.M. *et al*. Rifamycin antibiotics and the mechanisms of their failure. *J Antibiot* **74**, 786–798 (2021). https://doi.org/10.1038/s41429-021-00462-x.
- Alam MK, Alhhazmi A, DeCoteau JF, Luo Y, Geyer CR. RecA Inhibitors Potentiate Antibiotic Activity and Block Evolution of Antibiotic Resistance. Cell Chem Biol. 2016 Mar 17;23(3):381-91. doi: 10.1016/j.chembiol.2016.02.010. PMID: 26991103.
- Alexander Yakimov, Georgii Pobegalov, Irina Bakhlanova, Mikhail Khodorkovskii, Michael Petukhov, Dmitry Baitin, Blocco dell'attività RecA e della risposta SOS nei batteri con un peptide a breve elica α, *Nucleic Acids Research* , Volume 45, Numero 16, 19 settembre 2017, Pagine 9788–9796, https://doi.org/10.1093/nar/gkx687
- Allmeier H, Cresnar B, Greck M, Schmitt R. Complete nucleotide sequence of Tn1721: gene organization and a novel gene product with features of a chemotaxis protein. Gene. 1992 Feb 1;111(1):11-20.
- Ash C, Priest FG, Collins MD. Molecular identification of rRNA group 3 bacilli (Ash, Farrow, Wallbanks and Collins) using a PCR probe test. Proposal for the creation of a new genus Paenibacillus. Antonie Van Leeuwenhoek. 1993-1994;64(3-4):253-60. doi: 10.1007/BF00873085. PMID: 8085788.
- Bakker, E.P. (1979). Ionophore Antibiotics. In: Hahn, F.E. (eds) Mechanism of Action of Antibacterial Agents. Antibiotics, vol 5 / 1. Springer, Berlin, Heidelberg. https://doi.org/10.1007/978-3-642-46403-4_5.
- Banach-Orlowska M, Fijalkowska IJ, Schaaper RM, Jonczyk P. DNA polymerase II as a fidelity factor in chromosomal DNA synthesis in Escherichia coli. Mol Microbiol. 2005 Oct;58(1):61-70. doi: 10.1111/j.1365-2958.2005.04805.x. PMID: 16164549.
- Barreteau H, Kovac A, Boniface A, Sova M, Gobec S, Blanot D. Cytoplasmic steps of peptidoglycan biosynthesis. FEMS Microbiol Rev. 2008 Mar;32(2):168-207. doi: 10.1111/j.1574-6976.2008.00104.x. Epub 2008 Feb 11. PMID: 18266853.
- Beaber JW, Hochhut B, Waldor MK. SOS response promotes horizontal dissemination of antibiotic resistance genes. Nature. 2004 Jan 1;427(6969):72-4. doi: 10.1038/nature02241. Epub 2003 Dec 21. PMID: 14688795.
- Beattie JH, Peace HS. The influence of a low-boron diet and boron supplementation on bone, major mineral and sex steroid metabolism in

postmenopausal women. Br J Nutr. 1993 May;69(3):871-84. doi: 10.1079/bjn19930087. PMID: 8329361.

- Bellio P, Brisdelli F, Perilli M, Sabatini A, Bottoni C, Segatore B, Setacci D, Amicosante G, Celenza G. Curcumin inhibits the SOS response induced by levofloxacin in Escherichia coli. Phytomedicine. 2014 Mar 15;21(4):430-4. doi: 10.1016/j.phymed.2013.10.011. Epub 2013 Nov 17. PMID: 24252336.
- Bellio P, Di Pietro L, Mancini A, Piovano M, Nicoletti M, Brisdelli F, Tondi D, Cendron L, Franceschini N, Amicosante G, Perilli M, Celenza G. SOS response in bacteria: Inhibitory activity of lichen secondary metabolites against Escherichia coli RecA protein. Phytomedicine. 2017 Jun 15;29:11-18. doi: 10.1016/j.phymed.2017.04.001. Epub 2017 Apr 8. PMID: 28515022.
- Bellio P, Mancini A, Di Pietro L, Cracchiolo S, Franceschini N, Reale S, de Angelis F, Perilli M, Amicosante G, Spyrakis F, Tondi D, Cendron L, Celenza G. Inhibition of the transcriptional repressor LexA: Withstanding drug resistance by inhibiting the bacterial mechanisms of adaptation to antimicrobials. Life Sci. 2020 Jan 15;241:117116. doi: 10.1016/j.lfs.2019.117116. Epub 2019 Nov 29. PMID: 31790690.
- Berger, M., Aijaz, I., Berger, P. *et al*. Transcriptional and Translational Inhibitors Block SOS Response and Shiga Toxin Expression in Enterohemorrhagic *Escherichia coli*. *Sci Rep* **9**, 18777 (2019). https://doi.org/10.1038/s41598-019-55332-2
- Bernier SP, Lebeaux D, DeFrancesco AS, Valomon A, Soubigou G, Coppée JY, Ghigo JM, Beloin C. Starvation, together with the SOS response, mediates high biofilm-specific tolerance to the fluoroquinolone ofloxacin. PLoS Genet. 2013;9(1):e1003144. doi: 10.1371/journal.pgen.1003144. Epub 2013 Jan 3. PMID: 23300476; PMCID: PMC3536669.
- Bisognano C, Kelley WL, Estoppey T, Francois P, Schrenzel J, Li D, Lew DP, Hooper DC, Cheung AL, Vaudaux P. A recA-LexA-dependent pathway mediates ciprofloxacin-induced fibronectin binding in Staphylococcus aureus. J Biol Chem. 2004 Mar 5;279(10):9064-71. doi: 10.1074/jbc.M309836200. Epub 2003 Dec 29. PMID: 14699158.
- Biţă A, Scorei IR, Bălşeanu TA, Ciocîlteu MV, Bejenaru C, Radu A, Bejenaru LE, Rău G, Mogoşanu GD, Neamţu J, Benner SA. New Insights into Boron Essentiality in Humans and Animals. Int J Mol Sci. 2022 Aug 15;23(16):9147. doi: 10.3390/ijms23169147. PMID: 36012416; PMCID: PMC9409115.
- Blanco, P.; Hernando-Amado, S.; Reales-Calderon, J.A.; Corona, F.; Lira, F.; Alcalde-Rico, M.; Bernardini, A.; Sanchez, M.B.; Martinez, J.L. Bacterial Multidrug Efflux Pumps: Much More Than Antibiotic Resistance Determinants. *Microorganisms* **2016**, *4*, 14. https://doi.org/10.3390/microorganisms4010014.

- Börjesson S, Ny S, Egervärn M, Bergström J, Rosengren Å, Englund S, Löfmark S, Byfors S. Limited Dissemination of Extended-Spectrum β-Lactamase- and Plasmid-Encoded AmpC-Producing Escherichia coli from Food and Farm Animals, Sweden. Emerg Infect Dis. 2016 Apr;22(4):634-40. doi: 10.3201/eid2204.151142. PMID: 26982890; PMCID: PMC4806949.
- Bozdogan B, Appelbaum PC. Oxazolidinones: activity, mode of action, and mechanism of resistance. Int J Antimicrob Agents. 2004 Feb;23(2):113-9. doi: 10.1016/j.ijantimicag.2003.11.003. PMID: 15013035.
- Brandish PE, Kimura KI, Inukai M, Southgate R, Lonsdale JT, Bugg TD. Modes of action of tunicamycin, liposidomycin B, and mureidomycin A: inhibition of phospho-N-acetylmuramyl-pentapeptide translocase from Escherichia coli. Antimicrob Agents Chemother. 1996 Jul;40(7):1640-4. doi: 10.1128/AAC.40.7.1640. PMID: 8807054; PMCID: PMC163387.
- Brent R. Regulation and autoregulation by lexA protein. Biochimie. 1982 Aug-Sep;64(8-9):565-9. doi: 10.1016/s0300-9084(82)80088-6. PMID: 6814502.
- Brooks WL, Sumerlin BS. Synthesis and Applications of Boronic Acid-Containing Polymers: From Materials to Medicine. Chem Rev. 2016 Feb 10;116(3):1375-97. doi: 10.1021/acs.chemrev.5b00300. Epub 2015 Sep 14. PMID: 26367140.
- Burmeister AR. Horizontal Gene Transfer. Evol Med Public Health. 2015 Jul 29;2015(1):193-4. doi: 10.1093/emph/eov018. PMID: 26224621; PMCID: PMC4536854.
- Bush K, Bradford PA. β-Lactams and β-Lactamase Inhibitors: An Overview. Cold Spring Harb Perspect Med. 2016 Aug 1;6(8):a025247. doi: 10.1101/cshperspect.a025247. PMID: 27329032; PMCID: PMC4968164.
- Butala M, Zgur-Bertok D, Busby SJ. The bacterial LexA transcriptional repressor. Cell Mol Life Sci. 2009 Jan;66(1):82-93. doi: 10.1007/s00018-008-8378-6. PMID: 18726173; PMCID: PMC11131485.
- Campbell EA, Korzheva N, Mustaev A, Murakami K, Nair S, Goldfarb A, Darst SA. Structural mechanism for rifampicin inhibition of bacterial rna polymerase. Cell. 2001 Mar 23;104(6):901-12. doi: 10.1016/s0092-8674(01)00286-0. PMID: 11290327.
- Campoy S, Fontes M, Padmanabhan S, Cortés P, Llagostera M, Barbé J. LexA-independent DNA damage-mediated induction of gene expression in Myxococcus xanthus. Mol Microbiol. 2003 Aug;49(3):769-81. doi: 10.1046/j.1365-2958.2003.03592.x. PMID: 12864858.
- Campoy S, Mazón G, Fernández de Henestrosa AR, Llagostera M, Monteiro PB, Barbé J. A new regulatory DNA motif of the gamma subclass Proteobacteria: identification of the LexA protein binding site of the plant pathogen Xylella fastidiosa. Microbiology (Reading). 2002 Nov;148(Pt 11):3583-3597. doi: 10.1099/00221287-148-11-3583. PMID: 12427949.

- Cardoso, P., Glossop, H., Meikle, T.G. *et al*. Molecular engineering of antimicrobial peptides: microbial targets, peptide motifs and translation opportunities. *Biophys Rev* **13**, 35–69 (2021). https://doi.org/10.1007/s12551-021-00784-y.
- Carey D. Nadell, Joao B. Xavier, Kevin R. Foster, The sociobiology of biofilms, *FEMS Microbiology Reviews*, Volume 33, Issue 1, January 2009, Pages 206–224, https://doi.org/10.1111/j.1574-6976.2008.00150.x.
- Carrano CJ, Schellenberg S, Amin SA, Green DH, Küpper FC. Boron and marine life: a new look at an enigmatic bioelement. Mar Biotechnol (NY). 2009 Jul-Aug;11(4):431-40. doi: 10.1007/s10126-009-9191-4. Epub 2009 May 8. PMID: 19424754.
- Celebi O, Celebi D, Baser S, Aydın E, Rakıcı E, Uğraş S, Ağyar Yoldaş P, Baygutalp NK, Abd El-Aty AM. Antibacterial Activity of Boron Compounds Against Biofilm-Forming Pathogens. Biol Trace Elem Res. 2024 Jan;202(1):346-359. doi: 10.1007/s12011-023-03768-z. Epub 2023 Jul 18. PMID: 37464169.
- Cendron L, Quotadamo A, Maso L, Bellio P, Montanari M, Celenza G, Venturelli A, Costi MP, Tondi D. X-ray Crystallography Deciphers the Activity of Broad-Spectrum Boronic Acid β-Lactamase Inhibitors. ACS Med Chem Lett. 2019 Mar 27;10(4):650-655. doi: 10.1021/acsmedchemlett.8b00607. PMID: 30996812; PMCID: PMC6466825.
- Chalmers R, Sewitz S, Lipkow K, Crellin P. Complete nucleotide sequence of Tn10. J Bacteriol. 2000 May;182(10):2970-2. doi: 10.1128/JB.182.10.2970-2972.2000. PMID: 10781570; PMCID: PMC102010.
- Chaves J, Ladona MG, Segura C, Coira A, Reig R, Ampurdanés C. SHV-1 beta-lactamase is mainly a chromosomally encoded species-specific enzyme in Klebsiella pneumoniae. Antimicrob Agents Chemother. 2001 Oct;45(10):2856-61. doi: 10.1128/AAC.45.10.2856-2861.2001. PMID: 11557480; PMCID: PMC90742.
- Chen Z, Yang H, Pavletich NP. Mechanism of homologous recombination from the RecA-ssDNA/dsDNA structures. Nature. 2008 May 22;453(7194):489-4. doi: 10.1038/nature06971. PMID: 18497818.
- Chen, H.; Yan, C.-H.; Zhan, Y.-F.; Geng, L.-T.; Zhu, L.-L.; Gong, L.-C.; Wang, J. Boron Derivatives Accelerate Biofilm Formation of Recombinant *Escherichia coli* via Increasing Quorum Sensing System Autoinducer-2 Activity. *Int. J. Mol. Sci.* **2022**, *23*, 8059. https://doi.org/10.3390/ijms23158059
- Cheo DL, Bayles KW, Yasbin RE. Cloning and characterization of DNA damage-inducible promoter regions from Bacillus subtilis. J Bacteriol. 1991 Mar;173(5):1696-703. doi: 10.1128/jb.173.5.1696-1703.1991. PMID: 1847907; PMCID: PMC207320.

- Chitral Chatterjee, Gokul Raj Mohan, V.C Hariharan, Bhumika Biswas, Vidya Sundaram, Ashutosh Srivastava, Saravan Matheshwaran. Boronic acid derivative inhibits LexA mediated SOS response in Mycobacteria. bioRxiv 2023.11.15.567215; doi: https://doi.org/10.1101/2023.11.15.567215
- Chodisetti PK.Reddy M.2021.Peptidoglycan: Structure, Synthesis, and Regulation. 9:.https://doi.org/10.1128/ecosalplus.ESP-0010-2020).
- Chopra I, Roberts M 2001. Tetracycline Antibiotics: Mode of Action, Applications, Molecular Biology, and Epidemiology of Bacterial Resistance. Microbiol Mol Biol Rev 65:.https://doi.org/10.1128/mmbr.65.2.232-260.2001.
- Cooper RM, Tsimring L, Hasty J. Inter-species population dynamics enhance microbial horizontal gene transfer and spread of antibiotic resistance. Elife. 2017 Nov 1;6:e25950. doi: 10.7554/eLife.25950. PMID: 29091031; PMCID: PMC5701796.
- Cory MB, Li A, Hurley CM, Carman PJ, Pumroy RA, Hostetler ZM, Perez RM, Venkatesh Y, Li X, Gupta K, Petersson EJ, Kohli RM. The LexA-RecA* structure reveals a cryptic lock-and-key mechanism for SOS activation. Nat Struct Mol Biol. 2024 Oct;31(10):1522-1531. doi: 10.1038/s41594-024-01317-3. Epub 2024 May 16. PMID: 38755298; PMCID: PMC11521096.
- Cox, M. M. (2007)a. Regulation of Bacterial RecA Protein Function. *Critical Reviews in Biochemistry and Molecular Biology*, *42*(1), 41–63. https://doi.org/10.1080/10409230701260258.
- Cox, M.M. (2007)b. The bacterial RecA protein: structure, function, and regulation. In: Aguilera, A., Rothstein, R. (eds) Molecular Genetics of Recombination. Topics in Current Genetics, vol 17. Springer, Berlin, Heidelberg. https://doi.org/10.1007/978-3-540-71021-9_3.
- Cuñé J, Cullen P, Mazon G, Campoy S, Adler B, Barbe J. The Leptospira interrogans lexA gene is not autoregulated. J Bacteriol. 2005 Aug;187(16):5841-5. doi: 10.1128/JB.187.16.5841-5845.2005. PMID: 16077133; PMCID: PMC1196068.
- Curran MP, McKeage K. Bortezomib: a review of its use in patients with multiple myeloma. Drugs. 2009;69(7):859-88. doi: 10.2165/00003495-200969070-00006. PMID: 19441872.
- D.Y. Aksoy, S. Unal, New antimicrobial agents for the treatment of Gram-positive bacterial infections, Clinical Microbiology and Infection, Volume 14, Issue 5, 2008. Pages 411-420, ISSN 1198-743X, https://doi.org/10.1111/j.1469-0691.2007.01933.x.

- De Francesco H, Dudley J and Coca A. Boron Chemistry: An Overview. Boron reagents and in synthesis, Chapter 1, pp 1-25. ACS Symposium Series, Vol 1236. ISBN13: 9780841231832.
- Del Val E, Nasser W, Abaibou H, Reverchon S. RecA and DNA recombination: a review of molecular mechanisms. Biochem Soc Trans. 2019 Oct 31;47(5):1511-1531. doi: 10.1042/BST20190558. PMID: 31654073.
- Dewangan J, Srivastava S, Rath SK. Salinomycin: A new paradigm in cancer therapy. *Tumor Biology*. 2017;39(3). doi:10.1177/1010428317695035.
- Dönhöfer A, Franckenberg S, Wickles S, Berninghausen O, Beckmann R, Wilson DN. Structural basis for TetM-mediated tetracycline resistance. Proc Natl Acad Sci U S A. 2012 Oct 16;109(42):16900-5. doi: 10.1073/pnas.1208037109. Epub 2012 Oct 1. PMID: 23027944; PMCID: PMC3479509.
- Erill, I., Campoy, S., & Barbé, J. (2007). *Aeons of distress: an evolutionary perspective on the bacterial SOS response*. *FEMS Microbiology Reviews, 31(6), 637–656*. doi:10.1111/j.1574-6976.2007.00082.x.
- Escarceller M, Hicks J, Gudmundsson G, Trump G, Touati D, Lovett S, Foster PL, McEntee K, Goodman MF. Involvement of Escherichia coli DNA polymerase II in response to oxidative damage and adaptive mutation. J Bacteriol. 1994 Oct;176(20):6221-8. doi: 10.1128/jb.176.20.6221-6228.1994. PMID: 7928992; PMCID: PMC196962.
- Fagnani, L.; Nazzicone, L.; Brisdelli, F.; Giansanti, L.; Battista, S.; Iorio, R.; Petricca, S.; Amicosante, G.; Perilli, M.; Celenza, G.; et al. Cyclic and Acyclic Amine Oxide Alkyl Derivatives as Potential Adjuvants in Antimicrobial Chemotherapy against Methicillin-Resistant *Staphylococcus aureus* with an MDR Profile. *Antibiotics* **2021**, *10*, 952. https://doi.org/10.3390/antibiotics10080952.
- Falagas ME, Kasiakou SK. Toxicity of polymyxins: a systematic review of the evidence from old and recent studies. Crit Care. 2006 Feb;10(1):R27. doi: 10.1186/cc3995. PMID: 16507149; PMCID: PMC1550802.
- Fernandes, G. F. dos S., Salgado, H. R. N., & Santos, J. L. dos. (2017). *Isoniazid: A Review of Characteristics, Properties and Analytical Methods*. *Critical Reviews in Analytical Chemistry, 47(4), 298–308*. doi:10.1080/10408347.2017.1281098.
- Fernández de Henestrosa AR, Cuñé J, Mazón G, Dubbels BL, Bazylinski DA, Barbé J. Characterization of a new LexA binding motif in the marine magnetotactic bacterium strain MC-1. J Bacteriol. 2003 Aug;185(15):4471-82. doi: 10.1128/JB.185.15.4471-4482.2003. PMID: 12867456; PMCID: PMC165786.
- Fischer J, San José M, Roschanski N, Schmoger S, Baumann B, Irrgang A, Friese A, Roesler U, Helmuth R, Guerra B. Spread and persistence of VIM-1

Carbapenemase-producing Enterobacteriaceae in three German swine farms in 2011 and 2012. Vet Microbiol. 2017 Feb;200:118-123. doi: 10.1016/j.vetmic.2016.04.026. Epub 2016 May 7. PMID: 27234907.

- Fishovitz J, Hermoso JA, Chang M, Mobashery S. Penicillin-binding protein 2a of methicillin-resistant Staphylococcus aureus. IUBMB Life. 2014 Aug;66(8):572-7. doi: 10.1002/iub.1289. Epub 2014 Jul 14. PMID: 25044998; PMCID: PMC4236225.
- Flemming, Hans-Curt, Thomas R. Neu, and Daniel J. Wozniak. "The EPS matrix: the "house of biofilm cells"." *Journal of bacteriology* 189.22 (2007): 7945-7947.
- Floss HG, Yu TW. Rifamycin-mode of action, resistance, and biosynthesis. Chem Rev. 2005 Feb;105(2):621-32. doi: 10.1021/cr030112j. PMID: 15700959.
- Fontaine F, Héquet A, Voisin-Chiret AS, Bouillon A, Lesnard A, Cresteil T, Jolivalt C, Rault S. Boronic species as promising inhibitors of the Staphylococcus aureus NorA efflux pump: study of 6-substituted pyridine-3-boronic acid derivatives. Eur J Med Chem. 2015 May 5;95:185-98. doi: 10.1016/j.ejmech.2015.02.056. Epub 2015 Mar 2. PMID: 25817769.
- Foti, C.; Piperno, A.; Scala, A.; Giuffrè, O. Oxazolidinone Antibiotics: Chemical, Biological and Analytical Aspects. *Molecules* **2021**, *26*, 4280. https://doi.org/10.3390/molecules26144280.
- Frank EG, Ennis DG, Gonzalez M, Levine AS, Woodgate R. Regulation of SOS mutagenesis by proteolysis. Proc Natl Acad Sci U S A. 1996 Sep 17;93(19):10291-6. doi: 10.1073/pnas.93.19.10291. PMID: 8816793; PMCID: PMC38377.
- Freeman, C.D., Klutman, N.E. & Lamp, K.C. Metronidazole. *Drugs* **54**, 679–708 (1997). https://doi.org/10.2165/00003495-199754050-00003.
- Galimand M, Sabtcheva S, Courvalin P, Lambert T. Worldwide disseminated armA aminoglycoside resistance methylase gene is borne by composite transposon Tn1548. Antimicrob Agents Chemother. 2005 Jul;49(7):2949-53. doi: 10.1128/AAC.49.7.2949-2953.2005. PMID: 15980373; PMCID: PMC1168633.
- Gaynor, M., & Mankin, A. S. (2005). Macrolide Antibiotics: Binding Site, Mechanism of Action, Resistance. Frontiers in Medicinal Chemistry - Online, 2(1), 21–35. doi:10.2174/1567204052931113.
- Giese KC, Michalowski CB, Little JW. RecA-dependent cleavage of LexA dimers. J Mol Biol. 2008 Mar 14;377(1):148-61. doi: 10.1016/j.jmb.2007.12.025. Epub 2007 Dec 15. PMID: 18234215; PMCID: PMC2277360.
- Gorustovich AA, Steimetz T, Nielsen FH, Guglielmotti MB. A histomorphometric study of alveolar bone modelling and remodelling in

mice fed a boron-deficient diet. Arch Oral Biol. 2008 Jul;53(7):677-82. doi: 10.1016/j.archoralbio.2008.01.011. Epub 2008 Mar 3. PMID: 18313642.

- Gotoh H, Kasaraneni N, Devineni N, Dallo SF, Weitao T. SOS involvement in stress-inducible biofilm formation. Biofouling. 2010 Jul;26(5):603-11. doi: 10.1080/08927014.2010.501895. PMID: 20603726.
- Grossman TH. Tetracycline Antibiotics and Resistance. Cold Spring Harb Perspect Med. 2016 Apr 1;6(4):a025387. doi: 10.1101/cshperspect.a025387. PMID: 26989065; PMCID: PMC4817740.
- Gupta G, Foley KA, Gupta AK. Tavaborole 5% Solution: A Novel Topical Treatment for Toenail Onychomycosis. Skin Therapy Lett. 2015 Nov;20(6):6-9. PMID: 27224843.
- Hakki SS, Bozkurt BS, Hakki EE. Boron regulates mineralized tissue-associated proteins in osteoblasts (MC3T3-E1). J Trace Elem Med Biol. 2010 Oct;24(4):243-50. doi: 10.1016/j.jtemb.2010.03.003. Epub 2010 Aug 3. PMID: 20685097.
- Heeb S, Fletcher MP, Chhabra SR, Diggle SP, Williams P, Cámara M. Quinolones: from antibiotics to autoinducers. FEMS Microbiol Rev. 2011 Mar;35(2):247-74. doi: 10.1111/j.1574-6976.2010.00247.x. PMID: 20738404; PMCID: PMC3053476.
- Henrikus, S.S., van Oijen, A.M. & Robinson, A. Specialised DNA polymerases in *Escherichia coli*: roles within multiple pathways. *Curr Genet* **64**, 1189–1196 (2018). https://doi.org/10.1007/s00294-018-0840-x.
- Hiramatsu K, Katayama Y, Matsuo M, Sasaki T, Morimoto Y, Sekiguchi A, Baba T. Multi-drug-resistant Staphylococcus aureus and future chemotherapy. J Infect Chemother. 2014 Oct;20(10):593-601. doi: 10.1016/j.jiac.2014.08.001. Epub 2014 Aug 27. PMID: 25172776.
- Ho YI, Chan CY, Cheng AF. In-vitro activities of aminoglycoside-aminocyclitols against mycobacteria. J Antimicrob Chemother. 1997 Jul;40(1):27-32. doi: 10.1093/jac/40.1.27. PMID: 9249201.
- Hopkins KL, Davies RH, Threlfall EJ. Mechanisms of quinolone resistance in Escherichia coli and Salmonella: recent developments. Int J Antimicrob Agents. 2005 May;25(5):358-73. doi: 10.1016/j.ijantimicag.2005.02.006. PMID: 15848289.
- Hörtnagel K, Voloshin ON, Kinal HH, Ma N, Schaffer-Judge C, Camerini-Otero RD. Saturation mutagenesis of the E. coli RecA loop L2 homologous DNA pairing region reveals residues essential for recombination and recombinational repair. J Mol Biol. 1999 Mar 5;286(4):1097-106. doi: 10.1006/jmbi.1998.2515. PMID: 10047484.
- HOWARD-FLANDERS P, SIMSON E, THERIOT L. A LOCUS THAT CONTROLS FILAMENT FORMATION AND SENSITIVITY TO RADIATION IN ESCHERICHIA

COLI K-12. Genetics. 1964 Feb;49(2):237-46. doi: 10.1093/genetics/49.2.237. PMID: 14124942; PMCID: PMC1210565.

- https://go.drugbank.com/drugs/DB12810
- https://go.drugbank.com/drugs/DB16039
- Hunt CD, Shuler TR, Mullen LM. Concentration of boron and other elements in human foods and personal-care products. J Am Diet Assoc. 1991 May;91(5):558-68. PMID: 2019698.
- Huovinen P, Sundström L, Swedberg G, Sköld O. Trimethoprim and sulfonamide resistance. Antimicrob Agents Chemother. 1995 Feb;39(2):279-89. doi: 10.1128/AAC.39.2.279. PMID: 7726483; PMCID: PMC162528.
- Huovinen P. Trimethoprim resistance. Antimicrob Agents Chemother. 1987 Oct;31(10):1451-6. doi: 10.1128/AAC.31.10.1451. PMID: 3324955; PMCID: PMC174969.
- Jarnagin K, Chanda S, Coronado D, Ciaravino V, Zane LT, Guttman-Yassky E, Lebwohl MG. Crisaborole Topical Ointment, 2%: A Nonsteroidal, Topical, Anti-Inflammatory Phosphodiesterase 4 Inhibitor in Clinical Development for the Treatment of Atopic Dermatitis. J Drugs Dermatol. 2016 Apr;15(4):390-6. PMID: 27050693.
- Jaszczur MM, Vo DD, Stanciauskas R, Bertram JG, Sikand A, Cox MM, Woodgate R, Mak CH, Pinaud F, Goodman MF. Conformational regulation of Escherichia coli DNA polymerase V by RecA and ATP. PLoS Genet. 2019 Feb 4;15(2):e1007956. doi: 10.1371/journal.pgen.1007956. PMID: 30716079; PMCID: PMC6375631.
- Jensen GS, Cruickshank D, Hamilton DE. Disruption of Established Bacterial and Fungal Biofilms by a Blend of Enzymes and Botanical Extracts. J Microbiol Biotechnol. 2023 Jun 28;33(6):715-723. doi: 10.4014/jmb.2212.12010. Epub 2023 Mar 10. PMID: 37072676; PMCID: PMC10331947.
- Kadurugamuwa JL, Sin L, Albert E, Yu J, Francis K, DeBoer M, Rubin M, Bellinger-Kawahara C, Parr TR Jr, Contag PR. Direct continuous method for monitoring biofilm infection in a mouse model. Infect Immun. 2003 Feb;71(2):882-90. doi: 10.1128/IAI.71.2.882-890.2003. PMID: 12540570; PMCID: PMC145362.
- Kahan FM, Kahan JS, Cassidy PJ, Kropp H. The mechanism of action of fosfomycin (phosphonomycin). Ann N Y Acad Sci. 1974 May 10;235(0):364-86. doi: 10.1111/j.1749-6632.1974.tb43277.x. PMID: 4605290.
- Khaliq H, Juming Z, Ke-Mei P. The Physiological Role of Boron on Health. Biol Trace Elem Res. 2018 Nov;186(1):31-51. doi: 10.1007/s12011-018-1284-3. Epub 2018 Mar 15. PMID: 29546541.

- Kim B, Little JW. Dimerization of a specific DNA-binding protein on the DNA. Science. 1992 Jan 10;255(5041):203-6. doi: 10.1126/science.1553548. PMID: 1553548.
- Kim SR, Matsui K, Yamada M, Gruz P, Nohmi T. Roles of chromosomal and episomal dinB genes encoding DNA pol IV in targeted and untargeted mutagenesis in Escherichia coli. Mol Genet Genomics. 2001 Oct;266(2):207-15. doi: 10.1007/s004380100541. PMID: 11683261.
- Konaklieva, M.I.; Plotkin, B.J. Activity of Organoboron Compounds against Biofilm-Forming Pathogens. *Antibiotics* **2024**, *13*, 929. https://doi.org/10.3390/antibiotics13100929
- Kotra LP, Haddad J, Mobashery S. 2000. Aminoglycosides: Perspectives on mechanisms of action and resistance and strategies to counter resistance. Antimicrob Agents Chemother 44: 3249–3256.
- Krause KM, Serio AW, Kane TR, Connolly LE. Aminoglycosides: An Overview. Cold Spring Harb Perspect Med. 2016 Jun 1;6(6):a027029. doi: 10.1101/cshperspect.a027029. PMID: 27252397; PMCID: PMC4888811.
- Kraut J. Serine proteases: structure and mechanism of catalysis. Annu Rev Biochem. 1977;46:331-58. doi: 10.1146/annurev.bi.46.070177.001555. PMID: 332063.
- Kresge N, Simoni RD, Hill RL. Selman Waksman: the Father of Antibiotics. *J Biol Chem*. 2004;279(48):e7-e8. doi: 10.1016/S0021-9258(20)67861-9.
- Landman D, Babu E, Shah N, Kelly P, Bäcker M, Bratu S, Quale J. Activity of a novel aminoglycoside, ACHN-490, against clinical isolates of Escherichia coli and Klebsiella pneumoniae from New York City. J Antimicrob Chemother. 2010 Oct;65(10):2123-7. doi: 10.1093/jac/dkq278. Epub 2010 Jul 28. PMID: 20667885.
- Landman D, Kelly P, Bäcker M, Babu E, Shah N, Bratu S, Quale J. Antimicrobial activity of a novel aminoglycoside, ACHN-490, against Acinetobacter baumannii and Pseudomonas aeruginosa from New York City. J Antimicrob Chemother. 2011 Feb;66(2):332-4. doi: 10.1093/jac/dkq459. Epub 2010 Dec 3. PMID: 21131322.
- Lenz, K.D.; Klosterman, K.E.; Mukundan, H.; Kubicek-Sutherland, J.Z. Macrolides: From Toxins to Therapeutics. *Toxins* **2021**, *13*, 347. https://doi.org/10.3390/toxins13050347
- Little JW, Edmiston SH, Pacelli LZ, Mount DW. Cleavage of the Escherichia coli lexA protein by the recA protease. Proc Natl Acad Sci U S A. 1980 Jun;77(6):3225-9. doi: 10.1073/pnas.77.6.3225. PMID: 6447873; PMCID: PMC349587.
- Little JW. The SOS regulatory system: control of its state by the level of RecA protease. J Mol Biol. 1983 Jul 15;167(4):791-808. doi: 10.1016/s0022-2836(83)80111-9. PMID: 6410076.

- Luo Y, Pfuetzner RA, Mosimann S, Paetzel M, Frey EA, Cherney M, Kim B, Little JW, Strynadka NC. Crystal structure of LexA: a conformational switch for regulation of self-cleavage. Cell. 2001 Sep 7;106(5):585-94. doi: 10.1016/s0092-8674(01)00479-2. PMID: 11551506.
- Lupo A, Saras E, Madec JY, Haenni M. Emergence of blaCTX-M-55 associated with fosA, rmtB and mcr gene variants in Escherichia coli from various animal species in France. J Antimicrob Chemother. 2018 Apr 1;73(4):867-872. doi: 10.1093/jac/dkx489. PMID: 29340602.
- Maiques E, Úbeda C, Campoy S, Salvador N, Lasa Í, Novick RP, Barbé J, Pen adés JR 2006. β-Lactam Antibiotics Induce the SOS Response and Horizontal Transfer of Virulence Factors in *Staphylococcus aureus*. J Bacteriol 188:.https://doi.org/10.1128/jb.188.7.2726-2729.2006.
- Manyi-Loh C, Mamphweli S, Meyer E, Okoh A. Antibiotic Use in Agriculture and Its Consequential Resistance in Environmental Sources: Potential Public Health Implications. Molecules. 2018 Mar 30;23(4):795. doi: 10.3390/molecules23040795. PMID: 29601469; PMCID: PMC6017557.
- Marcellini L, Giammatteo M, Aimola P, Mangoni ML. Fluorescence and electron microscopy methods for exploring antimicrobial peptides mode(s) of action. Methods Mol Biol. 2010;618:249-66. doi: 10.1007/978-1-60761-594-1_16. PMID: 20094869.
- Markham A. Tavaborole: first global approval. Drugs. 2014 Sep;74(13):1555-8. doi: 10.1007/s40265-014-0276-7. PMID: 25118637.
- Masker W, Hanawalt P, Shizuya H. Role of DNA polymerase II in repair replication in Escherichia coli. Nat New Biol. 1973 Aug 22;244(138):242-3. doi: 10.1038/newbio244242a0. PMID: 4580165.
- Maslowska KH, Makiela-Dzbenska K, Fijalkowska IJ. The SOS system: A complex and tightly regulated response to DNA damage. Environ Mol Mutagen. 2019 May;60(4):368-384. doi: 10.1002/em.22267. Epub 2019 Jan 7. PMID: 30447030; PMCID: PMC6590174.
- Maso L, Vascon F, Chinellato M, Goormaghtigh F, Bellio P, Campagnaro E, Van Melderen L, Ruzzene M, Pardon E, Angelini A, Celenza G, Steyaert J, Tondi D, Cendron L. Nanobodies targeting LexA autocleavage disclose a novel suppression strategy of SOS-response pathway. Structure. 2022 Nov 3;30(11):1479-1493.e9. doi: 10.1016/j.str.2022.09.004. Epub 2022 Oct 13. PMID: 36240773.
- Mazón G, Campoy S, Fernández de Henestrosa AR, Barbé J. Insights into the LexA regulon of Thermotogales. Antonie Van Leeuwenhoek. 2006 Aug;90(2):123-37. doi: 10.1007/s10482-006-9066-x. Epub 2006 Aug 8. PMID: 16897562.
- Mazón G, Lucena JM, Campoy S, Fernández de Henestrosa AR, Candau P, Barbé J. LexA-binding sequences in Gram-positive and cyanobacteria are

closely related. Mol Genet Genomics. 2004 Feb;271(1):40-9. doi: 10.1007/s00438-003-0952-x. Epub 2003 Dec 2. PMID: 14652736.

- McCarty, S., Woods, E., & Percival, S. L. (2014). *Biofilms. Biofilms in Infection Prevention and Control, 143–163*. doi:10.1016/b978-0-12-397043-5.00009-8.
- McKenzie GJ, Harris RS, Lee PL, Rosenberg SM. The SOS response regulates adaptive mutation. Proc Natl Acad Sci U S A. 2000 Jun 6;97(12):6646-51. doi: 10.1073/pnas.120161797. PMID: 10829077; PMCID: PMC18688.story.
- McMurry L, Petrucci RE Jr, Levy SB. Active efflux of tetracycline encoded by four genetically different tetracycline resistance determinants in Escherichia coli. Proc Natl Acad Sci U S A. 1980 Jul;77(7):3974-7. doi: 10.1073/pnas.77.7.3974. PMID: 7001450; PMCID: PMC349750.
- Mégraud F, Doermann HP. Clinical relevance of resistant strains of Helicobacter pylori: a review of current data. Gut. 1998 Jul;43 Suppl 1(Suppl 1):S61-5. doi: 10.1136/gut.43.2008.s61. PMID: 9764043; PMCID: PMC1766605.
- Merrikh H, Kohli RM. Targeting evolution to inhibit antibiotic resistance. FEBS J. 2020 Oct;287(20):4341-4353. doi: 10.1111/febs.15370. Epub 2020 Jun 8. PMID: 32434280; PMCID: PMC7578009.
- Merritt JH, Kadouri DE, O'Toole GA. Growing and analysing static biofilms. Curr Protoc Microbiol. 2005 Jul;Chapter 1:Unit 1B.1. doi: 10.1002/9780471729259.mc01b01s00. PMID: 18770545; PMCID: PMC4568995.
- Millanao, A.R.; Mora, A.Y.; Villagra, N.A.; Bucarey, S.A.; Hidalgo, A.A. Biological Effects of Quinolones: A Family of Broad-Spectrum Antimicrobial Agents. *Molecules* **2021**, *26*, 7153. https://doi.org/10.3390/molecules26237153.
- Minozzi M, Lattanzi G, Benz R, Costi MP, Venturelli A, Carloni P. Permeation through the cell membrane of a boron-based β-lactamase inhibitor. PLoS One. 2011;6(8):e23187. doi: 10.1371/journal.pone.0023187. Epub 2011 Aug 17. PMID: 21858024; PMCID: PMC3157353.
- Miwa K, Fujiwara T. Boron transport in plants: co-ordinated regulation of transporters. Ann Bot. 2010 Jun;105(7):1103-8. doi: 10.1093/aob/mcq044. Epub 2010 Mar 12. PMID: 20228086; PMCID: PMC2887066.
- MIYAZAKI, Y., SHIBUYA, M., SUGAWARA, H., KAWAGUCHI, O., HIROSE, C., NAGATSU, J., & ESUMI, S. (1974). Salinomycin, a new polyether antibiotic. The Journal of Antibiotics, 27(11), 814–821. doi:10.7164/antibiotics.27.814.
- Mo CY, Birdwell LD, Kohli RM. Specificity determinants for autoproteolysis of LexA, a key regulator of bacterial SOS mutagenesis. Biochemistry. 2014 May 20;53(19):3158-68. doi: 10.1021/bi500026e. Epub 2014 May 8. PMID: 24779472; PMCID: PMC4030785.

- Mohana-Borges R, Pacheco AB, Sousa FJ, Foguel D, Almeida DF, Silva JL. LexA repressor forms stable dimers in solution. The role of specific dna in tightening protein-protein interactions. J Biol Chem. 2000 Feb 18;275(7):4708-12. doi: 10.1074/jbc.275.7.4708. PMID: 10671501.
- Molander GA, Trice SL, Kennedy SM. Scope of the two-step, one-pot palladium-catalyzed borylation/Suzuki cross-coupling reaction utilizing bis-boronic acid. J Org Chem. 2012 Oct 5;77(19):8678-88. doi: 10.1021/jo301642v. Epub 2012 Sep 20. PMID: 22994557; PMCID: PMC3465529.
- Morris, G. M., Huey, R., Lindstrom, W., Sanner, M. F., Belew, R. K., Goodsell, D. S. and Olson, A. J. (2009) Autodock4 and AutoDockTools4: automated docking with selective receptor flexiblity. *J. Computational Chemistry* 2009, **16**: 2785-91.
- Motta SS, Cluzel P, Aldana M. Adaptive resistance in bacteria requires epigenetic inheritance, genetic noise, and cost of efflux pumps. PLoS One. 2015 Mar 17;10(3):e0118464. doi: 10.1371/journal.pone.0118464. PMID: 25781931; PMCID: PMC4363326.
- Movahedzadeh F, Colston MJ & Davis EO (1997) Characterisation of *Mycobacterium tuberculosis* LexA: *recognition of a Cheo (Bacillus-type SOS) box*. Microbiology 143 (Part 3): 929– 936.
- Mulani MS, Kamble EE, Kumkar SN, Tawre MS, Pardesi KR. Emerging Strategies to Combat ESKAPE Pathogens in the Era of Antimicrobial Resistance: A Review. Front Microbiol. 2019 Apr 1;10:539. doi: 10.3389/fmicb.2019.00539. PMID: 30988669; PMCID: PMC6452778.
- Munita JM, Arias CA. Mechanisms of Antibiotic Resistance. Microbiol Spectr. 2016 Apr;4(2):10.1128/microbiolspec.VMBF-0016-2015. doi: 10.1128/microbiolspec.VMBF-0016-2015. PMID: 27227291; PMCID: PMC4888801.
- Munsiff SS, Kambili C, Ahuja SD. Rifapentine for the treatment of pulmonary tuberculosis. Clin Infect Dis. 2006 Dec 1;43(11):1468-75. doi: 10.1086/508278. Epub 2006 Oct 24. PMID: 17083024.
- Murrell DF, Gebauer K, Spelman L, Zane LT. Crisaborole Topical Ointment, 2% in Adults With Atopic Dermatitis: A Phase 2a, Vehicle-Controlled, Proof-of-Concept Study. J Drugs Dermatol. 2015 Oct;14(10):1108-12. PMID: 26461821.
- Narra K, Mullins SR, Lee HO, Strzemkowski-Brun B, Magalong K, Christiansen VJ, McKee PA, Egleston B, Cohen SJ, Weiner LM, Meropol NJ, Cheng JD. Phase II trial of single agent Val-boroPro (Talabostat) inhibiting Fibroblast Activation Protein in patients with metastatic colorectal cancer. Cancer Biol Ther. 2007 Nov;6(11):1691-9. doi: 10.4161/cbt.6.11.4874. Epub 2007 Aug 14. PMID: 18032930.

- Nation RL, Velkov T, Li J. Colistin and polymyxin B: peas in a pod, or chalk and cheese? Clin Infect Dis. 2014 Jul 1;59(1):88-94. doi: 10.1093/cid/ciu213. Epub 2014 Apr 3. PMID: 24700659; PMCID: PMC4305129.
- Newman H, Krajnc A, Bellini D, Eyermann CJ, Boyle GA, Paterson NG, McAuley KE, Lesniak R, Gangar M, von Delft F, Brem J, Chibale K, Schofield CJ, Dowson CG. High-Throughput Crystallography Reveals Boron-Containing Inhibitors of a Penicillin-Binding Protein with Di- and Tricovalent Binding Modes. J Med Chem. 2021 Aug 12;64(15):11379-11394. doi: 10.1021/acs.jmedchem.1c00717. Epub 2021 Jul 31. PMID: 34337941; PMCID: PMC9282634.
- NEWTON BA. The properties and mode of action of the polymyxins. Bacteriol Rev. 1956 Mar;20(1):14-27. doi: 10.1128/br.20.1.14-27.1956. PMID: 13303920; PMCID: PMC180843.
- Nikaido H. Molecular basis of bacterial outer membrane permeability revisited. Microbiol Mol Biol Rev. 2003 Dec;67(4):593-656. doi: 10.1128/MMBR.67.4.593-656.2003. PMID: 14665678; PMCID: PMC309051.
- Nuyts S, Van Mellaert L, Barbé S, Lammertyn E, Theys J, Landuyt W, Bosmans E, Lambin P, Anné J. Insertion or deletion of the Cheo box modifies radiation inducibility of Clostridium promoters. Appl Environ Microbiol. 2001 Oct;67(10):4464-70. doi: 10.1128/AEM.67.10.4464-4470.2001. PMID: 11571144; PMCID: PMC93191.
- Nzietchueng RM, Dousset B, Franck P, Benderdour M, Nabet P, Hess K. Mechanisms implicated in the effects of boron on wound healing. J Trace Elem Med Biol. 2002;16(4):239-44. doi: 10.1016/S0946-672X(02)80051-7. PMID: 12530586.
- O'Neill Jim (2016) tackling drug-resistance infections globally: final report and recommendations. The review on antimicrobial resistance.
- Oh TJ, Lee CW, Kim IG. The damage-inducible (din) genes of Escherichia coli are induced by various genotoxins in a different way. Microbiol Res. 1999 Sep;154(2):179-83. doi: 10.1016/S0944-5013(99)80012-3. PMID: 10522385.
- Osman K.T. 2010 Design and characterization of LexA dimer interface mutants.
- Ovung A, Bhattacharyya J. Sulfonamide drugs: structure, antibacterial property, toxicity, and biophysical interactions. Biophys Rev. 2021 Mar 29;13(2):259-272. doi: 10.1007/s12551-021-00795-9. PMID: 33936318; PMCID: PMC8046889.
- Pande S, Shitut S, Freund L, Westermann M, Bertels F, Colesie C, Bischofs IB, Kost C. Metabolic cross-feeding via intercellular nanotubes among bacteria. Nat Commun. 2015 Feb 23;6:6238. doi: 10.1038/ncomms7238. PMID: 25703793.

- Patel S, Saw S. Daptomycin. [Updated 2024 Aug 17]. In: StatPearls [Internet]. Treasure Island (FL): StatPearls Publishing; 2024 Jan-. Available from: https://www.ncbi.nlm.nih.gov/books/NBK470407/.
- Pattishall KH, Acar J, Burchall JJ, Goldstein FW, Harvey RJ. Two distinct types of trimethoprim-resistant dihydrofolate reductase specified by R-plasmids of different compatibility groups. J Biol Chem. 1977 Apr 10;252(7):2319-23. PMID: 14961.
- Peirano G, Pitout JD. 2010. Molecular epidemiology of Escherichia coli producing CTX-M beta lactamases: the worldwide emergence of clone ST131 O25:H4. Int J Antimicrob Agents 35:316–321 http://dx.doi .org/10.1016/j.ijantimicag.2009.11.003.
- Penland JG. The importance of boron nutrition for brain and psychological function. Biol Trace Elem Res. 1998 Winter;66(1-3):299-317. doi: 10.1007/BF02783144. PMID: 10050926.
- Pérez-Martín, J.M.; Esquivel-Martín, T. New Insights for Teaching the One Health Approach: Transformative Environmental Education for Sustainability. *Sustainability* **2024**, *16*, 7967. https://doi.org/10.3390/su16187967.
- Perry KL, Elledge SJ, Mitchell BB, Marsh L, Walker GC. umuDC and mucAB operons whose products are required for UV light- and chemical-induced mutagenesis: UmuD, MucA, and LexA proteins share homology. Proc Natl Acad Sci U S A. 1985 Jul;82(13):4331-5. doi: 10.1073/pnas.82.13.4331. PMID: 2989816; PMCID: PMC390407.
- Piddock LJ. Clinically relevant chromosomally encoded multidrug resistance efflux pumps in bacteria. Clin Microbiol Rev. 2006 Apr;19(2):382-402. doi: 10.1128/CMR.19.2.382-402.2006. PMID: 16614254; PMCID: PMC1471989.
- Pieren M, Tigges M. Adjuvant strategies for potentiation of antibiotics to overcome antimicrobial resistance. *Curr Opin Pharmacol*. 2012;12(5):551-555. doi: 10.1016/j.coph.2012.07.005.
- Pizzorno L. Nothing Boring About Boron. Integr Med (Encinitas). 2015 Aug;14(4):35-48. PMID: 26770156; PMCID: PMC4712861.
- Podlesek Zdravko, Žgur Bertok Darja. The DNA Damage Inducible SOS Response Is a Key Player in the Generation of Bacterial Persister Cells and Population Wide Tolerance. Frontiers in Microbiology, 2020, volume 11. https://www.frontiersin.org/article/10.3389/fmicb.2020.01785. doi:10.3389/fmicb.2020.01785. 1664-302X.
- Poirel L.Madec J.Lupo A.Schink A.Kieffer N.Nordmann P.Schwarz S. 2018. A ntimicrobial Resistance in *Escherichia coli*. Microbiol Spectr 6:10.1128/microbiolspec.arba-0026-2017. https://doi.org/10.1128/microbiolspec.arba-0026-2017.

- Poole K. Efflux-mediated antimicrobial resistance. J Antimicrob Chemother. 2005 Jul;56(1):20-51. doi: 10.1093/jac/dki171. Epub 2005 May 24. PMID: 15914491.
- Pospíšil J, Vítovská D, Kofroňová O, Muchová K, Šanderová H, Hubálek M, Šiková M, Modrák M, Benada O, Barák I, Krásný L. Bacterial nanotubes as a manifestation of cell death. Nat Commun. 2020 Oct 2;11(1):4963. doi: 10.1038/s41467-020-18800-2. Erratum in: Nat Commun. 2020 Nov 3;11(1):5672. doi: 10.1038/s41467-020-19618-8. PMID: 33009406; PMCID: PMC7532143.
- Preda VG, Săndulescu O. Communication is the key: biofilms, quorum sensing, formation and prevention. Discoveries (Craiova). 2019 Sep 30;7(3):e100. doi: 10.15190/d.2019.13. PMID: 32309618; PMCID: PMC7086079.
- Prosser GA, de Carvalho LP. Kinetic mechanism and inhibition of Mycobacterium tuberculosis D-alanine:D-alanine ligase by the antibiotic D-cycloserine. FEBS J. 2013 Feb;280(4):1150-66. doi: 10.1111/febs.12108. Epub 2013 Feb 1. PMID: 23286234).
- Purnima Kumar, 33 - Pharmacology of Specific Drug Groups: Antibiotic Therapy**The author wishes to recognize Dr. Thomas J. Pallasch for his past contributions to this chapter., Editor(s): Frank J. Dowd, Barton S. Johnson, Angelo J. Mariotti. Pharmacology and Therapeutics for Dentistry (Seventh Edition), Mosby, 2017, Pages 457-487, ISBN 9780323393072. https://doi.org/10.1016/B978-0-323-39307-2.00033-3.
- Radman, M. (1975). *SOS Repair Hypothesis: Phenomenology of an Inducible DNA Repair Which is Accompanied by Mutagenesis. Molecular Mechanisms for Repair of DNA, 355–367.* doi:10.1007/978-1-4684-2895-7_48.
- Raedler LA. Ninlaro (Ixazomib): First Oral Proteasome Inhibitor Approved for the Treatment of Patients with Relapsed or Refractory Multiple Myeloma. Am Health Drug Benefits. 2016 Mar;9(Spec Feature):102-5. PMID: 27668055; PMCID: PMC5013850.
- Ramirez MS, Tolmasky ME. Aminoglycoside modifying enzymes. Drug Resist Updat. 2010 Dec;13(6):151-71. doi: 10.1016/j.drup.2010.08.003. Epub 2010 Sep 15. PMID: 20833577; PMCID: PMC2992599.
- Recacha E, Machuca J, Díaz-Díaz S, García-Duque A, Ramos-Guelfo M, Docobo-Pérez F, Blázquez J, Pascual A, Rodríguez-Martínez JM. Suppression of the SOS response modifies spatiotemporal evolution, post-antibiotic effect, bacterial fitness and biofilm formation in quinolone-resistant Escherichia coli. J Antimicrob Chemother. 2019 Jan 1;74(1):66-73. doi: 10.1093/jac/dky407. PMID: 30329046.

- Recchia GD, Hall RM. Gene cassettes: a new class of mobile element. Microbiology (Reading). 1995 Dec;141 (Pt 12):3015-27. doi: 10.1099/13500872-141-12-3015. PMID: 8574395.
- Ristuccia AM, Cunha BA. An overview of amikacin. Ther Drug Monit. 1985;7(1):12-25. doi: 10.1097/00007691-198503000-00003. PMID: 3887667.
- Rodríguez-Martínez JM, Machuca J, Cano ME, Calvo J, Martínez-Martínez L, Pascual A. Plasmid-mediated quinolone resistance: Two decades on. Drug Resist Updat. 2016 Nov;29:13-29. doi: 10.1016/j.drup.2016.09.001. Epub 2016 Sep 13. PMID: 27912841.
- Rossolini GM, D'Andrea MM, Mugnaioli C. The spread of CTX-M-type extended-spectrum beta-lactamases. Clin Microbiol Infect. 2008 Jan;14 Suppl 1:33-41. doi: 10.1111/j.1469-0691.2007.01867.x. Erratum in: Clin Microbiol Infect. 2008 May;14 Suppl 5:21-4. PMID: 18154526.
- Salam, M.A.; Al-Amin, M.Y.; Salam, M.T.; Pawar, J.S.; Akhter, N.; Rabaan, A.A.; Alqumber, M.A.A. Antimicrobial Resistance: A Growing Serious Threat for Global Public Health. *Healthcare* **2023**, *11*, 1946. https://doi.org/10.3390/healthcare11131946.
- Salverda ML, De Visser JA, Barlow M. Natural evolution of TEM-1 β-lactamase: experimental reconstruction and clinical relevance. FEMS Microbiol Rev. 2010 Nov;34(6):1015-36. doi: 10.1111/j.1574-6976.2010.00222.x. PMID: 20412308.
- Săndulescu, O.; Viziteu, I.; Streinu-Cercel, A.; Miron, V.D.; Preoțescu, L.L.; Chirca, N.; Albu, S.E.; Craiu, M.; Streinu-Cercel, A. Novel Antimicrobials, Drug Delivery Systems and Antivirulence Targets in the Pipeline—From Bench to Bedside. *Appl. Sci.* **2022**, *12*, 11615. https://doi.org/10.3390/app122211615.
- Sarkar P, Yarlagadda V, Ghosh C, Haldar J. A review on cell wall synthesis inhibitors with an emphasis on glycopeptide antibiotics. Medchemcomm. 2017 Jan 26;8(3):516-533. doi: 10.1039/c6md00585c. PMID: 30108769; PMCID: PMC6072328.
- Sauer RT, Ross MJ, Ptashne M. Cleavage of the lambda and P22 repressors by recA protein. J Biol Chem. 1982 Apr 25;257(8):4458-62. PMID: 6461657.
- Sayin Z, Ucan US, Sakmanoglu A. Antibacterial and Antibiofilm Effects of Boron on Different Bacteria. Biol Trace Elem Res. 2016 Sep;173(1):241-6. doi: 10.1007/s12011-016-0637-z. Epub 2016 Feb 11. PMID: 26864941.
- Schnarr M, Granger-Schnarr M, Hurstel S, Pouyet J. The carboxy-terminal domain of the LexA repressor oligomerises essentially as the entire protein. FEBS Lett. 1988 Jul 4;234(1):56-60. doi: 10.1016/0014-5793(88)81302-4. PMID: 2968919.

- Schnarr M, Pouyet J, Granger-Schnarr M, Daune M. Large-scale purification, oligomerization equilibria, and specific interaction of the LexA repressor of Escherichia coli. Biochemistry. 1985 May 21;24(11):2812-8. doi: 10.1021/bi00332a032. PMID: 3896306.
- Schrödinger, L., & DeLano, W. (2020). *PyMOL*. Retrieved from http://www.pymol.org/pymol
- Schwarz S, Johnson AP. Transferable resistance to colistin: a new but old threat. J Antimicrob Chemother. 2016 Aug;71(8):2066-70. doi: 10.1093/jac/dkw274. Epub 2016 Jun 24. PMID: 27342545.
- Schwarz S, Shen J, Kadlec K, Wang Y, Brenner Michael G, Feßler AT, Vester B. Lincosamides, Streptogramins, Phenicols, and Pleuromutilins: Mode of Action and Mechanisms of Resistance. Cold Spring Harb Perspect Med. 2016 Nov 1;6(11):a027037. doi: 10.1101/cshperspect.a027037. PMID: 27549310; PMCID: PMC5088508.
- Scorei RI, Popa R Jr. Boron-containing compounds as preventive and chemotherapeutic agents for cancer. Anticancer Agents Med Chem. 2010 May;10(4):346-51. doi: 10.2174/1871520107911622289. PMID: 19912103.
- Scott D. Taylor, Michael Palmer,The action mechanism of daptomycin, Bioorganic & Medicinal Chemistry, Volume 24, Issue 24, 2016, Pages 6253-6268, ISSN 0968-0896, https://doi.org/10.1016/j.bmc.2016.05.052. (https://www.sciencedirect.com/science/article/pii/S0968089616303856.
- Shatha Rouf Moustafa. Clinical Association Between Alterations of Boron, Cesium, Rhenium and Rubidium with the Pathogenesis of Atherosclerosis. *Am. J. Clin. Exp. Med*. **2015**, *3*(5), 247-254. doi: 10.11648/j.ajcem.20150305.19.
- Sheu CC, Chang YT, Lin SY, Chen YH, Hsueh PR. Infections Caused by Carbapenem-Resistant *Enterobacteriaceae*: An Update on Therapeutic Options. Front Microbiol. 2019 Jan 30;10:80. doi: 10.3389/fmicb.2019.00080. PMID: 30761114; PMCID: PMC6363665.
- Shinohara A, Ogawa H, Ogawa T. Rad51 protein involved in repair and recombination in S. cerevisiae is a RecA-like protein. Cell. 1992 May 1;69(3):457-70. doi: 10.1016/0092-8674(92)90447-k. Erratum in: Cell 1992 Oct 2;71(1):following 180. PMID: 1581961.
- Silva MP, Saraiva L, Pinto M, Sousa ME. Boronic Acids and Their Derivatives in Medicinal Chemistry: Synthesis and Biological Applications. Molecules. 2020 Sep 21;25(18):4323. doi: 10.3390/molecules25184323. PMID: 32967170; PMCID: PMC7571202.
- Sköld, O. (2010). Sulfonamides and trimethoprim. *Expert Review of Anti-Infective Therapy*, *8*(1), 1–6. https://doi.org/10.1586/eri.09.117.
- Slilaty SN, Little JW. Lysine-156 and serine-119 are required for LexA repressor cleavage: a possible mechanism. Proc Natl Acad Sci U S A. 1987

Jun;84(12):3987-91. doi: 10.1073/pnas.84.12.3987. PMID: 3108885; PMCID: PMC305006.

- Smith MH, Cavenagh MM & Little JW (1991) *Mutant LexA Proteins with an Increased Rate of in vivo Cleavage*, Vol. 88, eds), pp. 7356– 7360.
- Smoum R, Rubinstein A, Dembitsky VM, Srebnik M. Boron containing compounds as protease inhibitors. Chem Rev. 2012 Jul 11;112(7):4156-220. doi: 10.1021/cr608202m. Epub 2012 Apr 20. PMID: 22519511.
- Sogut I, Paltun SO, Tuncdemir M, Ersoz M, Hurdag C. The antioxidant and antiapoptotic effect of boric acid on hepatoxicity in chronic alcohol-fed rats. Can J Physiol Pharmacol. 2018 Apr;96(4):404-411. doi: 10.1139/cjpp-2017-0487. Epub 2017 Sep 12. PMID: 28898587.
- Song S, Wood TK. The Primary Physiological Roles of Autoinducer 2 in *Escherichia coli* Are Chemotaxis and Biofilm Formation. Microorganisms. 2021 Feb 14;9(2):386. doi: 10.3390/microorganisms9020386. PMID: 33672862; PMCID: PMC7918475.
- Storm DR, Rosenthal KS, Swanson PE. Polymyxin and related peptide antibiotics. Annu Rev Biochem. 1977;46:723-63. doi: 10.1146/annurev.bi.46.070177.003451. PMID: 197881.
- Story, R., Weber, I. & Steitz, T. The structure of the *E. coli recA* protein monomer and polymer. *Nature* **355**, 318–325 (1992). https://doi.org/10.1038/355318a0.
- Sulfonamides, Trimethoprim-Sulfamethoxazole, Quinolones, and Agents for Urinary Tract Infections. In: Hilal-Dandan R, Brunton LL. eds. *Goodman and Gilman's Manual of Pharmacology and Therapeutics, 2e*. McGraw-Hill Education; 2016. Accessed November 03, 2024. https://accesspharmacy.mhmedical.com/content.aspx?bookid=1810&sectionid=124495758.
- Sun D, Jeannot K, Xiao Y, Knapp CW. Editorial: Horizontal Gene Transfer Mediated Bacterial Antibiotic Resistance. Front Microbiol. 2019 Aug 27;10:1933. doi: 10.3389/fmicb.2019.01933. PMID: 31507555; PMCID: PMC6718914.
- Tamma PD, Cosgrove SE, Maragakis LL. Combination therapy for treatment of infections with gram-negative bacteria. Clin Microbiol Rev. 2012 Jul;25(3):450-70. doi: 10.1128/CMR.05041-11. PMID: 22763634; PMCID: PMC3416487.
- Tan SY, Tatsumura Y. Alexander Fleming (1881-1955): Discoverer of penicillin. Singapore Med J. 2015 Jul;56(7):366-7. doi: 10.11622/smedj.2015105. PMID: 26243971; PMCID: PMC4520913.
- Tanel Tenson, Martin Lovmar, Måns Ehrenberg, The Mechanism of Action of Macrolides, Lincosamides and Streptogramin B Reveals the Nascent Peptide Exit Path in the Ribosome, Journal of Molecular Biology, Volume 330,

Issue 5, 2003, Pages 1005-1014, ISSN 0022-2836, https://doi.org/10.1016/S0022-2836(03)00662-4.

- Travers, Richard L., George C. Rennie, and Rex E. Newnham. "Boron and arthritis: the results of a double-blind pilot study." *Journal of Nutritional Medicine* 1.2 (1990): 127-132.
- Trimble MJ, Mlynárčik P, Kolář M, Hancock RE. Polymyxin: Alternative Mechanisms of Action and Resistance. Cold Spring Harb Perspect Med. 2016 Oct 3;6(10):a025288. doi: 10.1101/cshperspect.a025288. PMID: 27503996; PMCID: PMC5046685.
- Trusca D, Scott S, Thompson C, Bramhill D 1998. Bacterial SOS Checkpoint Protein SulA Inhibits Polymerization of Purified FtsZ Cell Division Protein. J Bacteriol 180:. https://doi.org/10.1128/jb.180.15.3946-3953.1998.
- Tsivkovski R, Lomovskaya O. Biochemical Activity of Vaborbactam. Antimicrob Agents Chemother. 2020 Jan 27;64(2):e01935-19. doi: 10.1128/AAC.01935-19. PMID: 31712199; PMCID: PMC6985712.
- Urban-Chmiel R, Marek A, Stępień-Pyśniak D, Wieczorek K, Dec M, Nowaczek A, Osek J. Antibiotic Resistance in Bacteria-A Review. Antibiotics (Basel). 2022 Aug 9;11(8):1079. doi: 10.3390/antibiotics11081079. PMID: 36009947; PMCID: PMC9404765.
- Valery M Dembitsky, Reem Smoum, Abed Aziz Al-Quntar, Hijazi Abu Ali, Inna Pergament, Morris Srebnik, Natural occurrence of boron-containing compounds in plants, algae and microorganisms. Plant Science, Volume 163, Issue 5, 2002, Pages 931-942, ISSN 0168-9452,https://doi.org/10.1016/S0168-9452(02)00174-7. (https://www.sciencedirect.com/science/article/pii/S0168945202001747).
- Van Houten B, Croteau DL, DellaVecchia MJ, Wang H, Kisker C. 'Close-fitting sleeves': DNA damage recognition by the UvrABC nuclease system. Mutat Res. 2005 Sep 4;577(1-2):92-117. doi: 10.1016/j.mrfmmm.2005.03.013. PMID: 15927210.
- Velazquez-Meza ME, Galarde-López M, Carrillo-Quiróz B, Alpuche-Aranda CM. Antimicrobial resistance: One Health approach. Vet World. 2022 Mar;15(3):743-749. doi: 10.14202/vetworld.2022.743-749. Epub 2022 Mar 28. PMID: 35497962; PMCID: PMC9047147.
- Vendeville A, Winzer K, Heurlier K, Tang CM, Hardie KR. Making 'sense' of metabolism: autoinducer-2, LuxS and pathogenic bacteria. Nat Rev Microbiol. 2005 May;3(5):383-96. doi: 10.1038/nrmicro1146. PMID: 15864263.
- Venkatraman S, Wu W, Prongay A, Girijavallabhan V, George Njoroge F. Potent inhibitors of HCV-NS3 protease derived from boronic acids. Bioorg Med Chem Lett. 2009 Jan 1;19(1):180-3. doi: 10.1016/j.bmcl.2008.10.124. Epub 2008 Nov 5. PMID: 19022670.

- Vera-Maldonado P, Aquea F, Reyes-Díaz M, Cárcamo-Fincheira P, Soto-Cerda B, Nunes-Nesi A, Inostroza-Blancheteau C. Role of boron and its interaction with other elements in plants. Front Plant Sci. 2024 Feb 12;15:1332459. doi: 10.3389/fpls.2024.1332459. Erratum in: Front Plant Sci. 2024 Jun 05;15:1425825. doi: 10.3389/fpls.2024.1425825. PMID: 38410729; PMCID: PMC10895714.
- Vierling S, Weber T, Wohlleben W, Muth G. Evidence that an additional mutation is required to tolerate insertional inactivation of the Streptomyces lividans recA gene. J Bacteriol. 2001 Jul;183(14):4374-81. doi: 10.1128/JB.183.14.4374-4381.2001. PMID: 11418579; PMCID: PMC95328.
- Vispé S, Defais M. Mammalian Rad51 protein: a RecA homologue with pleiotropic functions. Biochimie. 1997 Oct;79(9-10):587-92. doi: 10.1016/s0300-9084(97)82007-x. PMID: 9466696.
- von Hippel PH, Berg OG. On the specificity of DNA-protein interactions. Proc Natl Acad Sci U S A. 1986 Mar;83(6):1608-12. doi: 10.1073/pnas.83.6.1608. PMID: 3456604; PMCID: PMC323132.
- Wade JT, Reppas NB, Church GM, Struhl K. Genomic analysis of LexA binding reveals the permissive nature of the Escherichia coli genome and identifies unconventional target sites. Genes Dev. 2005 Nov 1;19(21):2619-30. doi: 10.1101/gad.1355605. PMID: 16264194; PMCID: PMC1276735.
- Walter BM, Cartman ST, Minton NP, Butala M, Rupnik M. The SOS Response Master Regulator LexA Is Associated with Sporulation, Motility and Biofilm Formation in Clostridium difficile. PLoS One. 2015 Dec 18;10(12):e0144763. doi: 10.1371/journal.pone.0144763. PMID: 26682547; PMCID: PMC4689574.
- Wang M, Liang L, Lu J, Yu Y, Zhao Y, Shi Z, Li H, Xu X, Yan Y, Niu Y, Liu Z, Shen L, Zhang H. Delanzomib, a novel proteasome inhibitor, sensitizes breast cancer cells to doxorubicin-induced apoptosis. Thorac Cancer. 2019 Apr;10(4):918-929. doi: 10.1111/1759-7714.13030. Epub 2019 Mar 18. PMID: 30883017; PMCID: PMC6449274.
- Wehrli W. Rifampin: mechanisms of action and resistance. Rev Infect Dis. 1983 Jul-Aug;5 Suppl 3:S407-11. doi: 10.1093/clinids/5.supplement_3.s407. PMID: 6356275.

  Weisblum B. 1995. Erythromycin resistance by ribosome modification. *Antimicrob Agents Chemother* 39:577–585.
- Wibowo JT, Kellermann MY, Köck M, Putra MY, Murniasih T, Mohr KI, Wink J, Praditya DF, Steinmann E, Schupp PJ. Anti-Infective and Antiviral Activity of Valinomycin and Its Analogues from a Sea Cucumber-Associated Bacterium, *Streptomyces* sp. SV 21. Mar Drugs. 2021 Feb 2;19(2):81. doi: 10.3390/md19020081. PMID: 33540548; PMCID: PMC7912928.

- Windsor IW, Palte MJ, Lukesh JC 3rd, Gold B, Forest KT, Raines RT. Sub-picomolar Inhibition of HIV-1 Protease with a Boronic Acid. J Am Chem Soc. 2018 Oct 31;140(43):14015-14018. doi: 10.1021/jacs.8b07366. Epub 2018 Oct 22. PMID: 30346745; PMCID: PMC6249028.
- Wojciechowski MF, Peterson KR & Love PE (1991) Regulation of the SOS response in *Bacillus subtilis*: *evidence for a LexA repressor homolog*. J Bacteriol 173: 6489– 6498.
- Wynn JE, Zhang W, Tebit DM, Gray LR, Hammarskjold ML, Rekosh D, Santos WL. Characterization and in vitro activity of a branched peptide boronic acid that interacts with HIV-1 RRE RNA. Bioorg Med Chem. 2016 Sep 1;24(17):3947-3952. doi: 10.1016/j.bmc.2016.04.009. Epub 2016 Apr 5. PMID: 27091070; PMCID: PMC4972714.
- Yang MK, Yang YC, Hsu CH. Characterization of Xanthomonas axonopodis pv. citri LexA: recognition of the LexA binding site. Mol Genet Genomics. 2002 Dec;268(4):477-87. doi: 10.1007/s00438-002-0754-6. Epub 2002 Nov 12. PMID: 12471445.
- Yang S, Li X, Cang W, Mu D, Ji S, An Y, Wu R, Wu J. Biofilm tolerance, resistance and infections increasing threat of public health. Microb Cell. 2023 Sep 26;10(11):233-247. doi: 10.15698/mic2023.11.807. PMID: 37933277; PMCID: PMC10625689.
- Zervosen A, Bouillez A, Herman A, Amoroso A, Joris B, Sauvage E, Charlier P, Luxen A. Synthesis and evaluation of boronic acids as inhibitors of Penicillin Binding Proteins of classes A, B and C. Bioorg Med Chem. 2012 Jun 15;20(12):3915-24. doi: 10.1016/j.bmc.2012.04.018. Epub 2012 Apr 16. PMID: 22579615.
- Zhanel, G.G., Dueck, M., Hoban, D.J. *et al*. Review of Macrolides and Ketolides. *Drugs* **61**, 443–498 (2001). https://doi.org/10.2165/00003495-200161040-00003.
- Zhang AP, Pigli YZ, Rice PA. Structure of the LexA-DNA complex and implications for SOS box measurement. Nature. 2010 Aug 12;466(7308):883-6. doi: 10.1038/nature09200. PMID: 20703307; PMCID: PMC2921665.
- Zhu X, Hong A, Sun X, Wang W, He G, Luo H, Wu Z, Xu Q, Hu Z, Wu X, Huang D, Li L, Zhao X, Deng X. Nigericin is effective against multidrug resistant gram-positive bacteria, persisters, and biofilms. Front Cell Infect Microbiol. 2022 Dec 20;12:1055929. doi: 10.3389/fcimb.2022.1055929. PMID: 36605124; PMCID: PMC9807916.
- Zhu YI, Stiller MJ. Dapsone and sulfones in dermatology: overview and update. J Am Acad Dermatol. 2001 Sep;45(3):420-34. doi: 10.1067/mjd.2001.114733. PMID: 11511841.
- Zimmerli W, Sendi P. Role of Rifampin against Staphylococcal Biofilm Infections In Vitro, in Animal Models, and in Orthopedic-Device-Related

Infections. Antimicrob Agents Chemother. 2019 Jan 29;63(2):e01746-18. doi: 10.1128/AAC.01746-18. PMID: 30455229; PMCID: PMC6355554.

- Zverlov VV & Schwarz WH (1999) Organisation of the chromosomal region containing the genes lexA and topA in *Thermotoga neapolitana*. Primary structure of LexA reveals phylogenetic relevance. *Syst Appl Microbiol* 22: 174– 178.
- Zygmunt DJ, Stratton CW, Kernodle DS. Characterization of four beta-lactamases produced by Staphylococcus aureus. Antimicrob Agents Chemother. 1992 Feb;36(2):440-5. doi: 10.1128/AAC.36.2.440. PMID: 1605608; PMCID: PMC188454.